MOLECULAR CHARACTERISTICS OF THE SCRAPIE AGENT

Patrick A. Lewis
MRC Prion Unit
Institute Of Neurology
University College London

ProQuest LLC
789 East Eisenhower Parkway
P.O. Box 1346
Ann Arbor, MI 48106-1346

MOLECULAR CHARACTERISTICS OF THE SCRAPIE AGENT

A thesis presented in partial fulfilment of the requirements for the degree of Doctor of Philosophy to the University of London

by

Patrick Alfryn Lewis BSc

Institute of Neurology, University College London

Supervisors: Dr Graham S. Jackson
Professor Anthony R. Clarke

ACKNOWLEDGEMENTS

The research contained within this thesis would not have been possible without the help and guidance of many people. The author wishes to thank his supervisors, Dr Jackson and Professor Clarke, for support and scholarly tutelage throughout the three and a half years of his postgraduate study. Special thanks are due to Professor John Collinge, director of the Medical Research Council Prion Unit, for providing the environment and securing the funding for prion research to flourish. Many thanks are also due to the members of the Prion Unit protein research group; Sam Jones, Mark Batchelor, Daljit Bhelt, Dr Howard Tattum and Dr Clare Trevitt; all of whom were generous in handing out advice with regards to techniques and experimental approaches. Their support and encouragement are gratefully acknowledged. Although many individuals in the Prion Unit have provided help and advice over the past forty months, the author would like to single out Dr Francesca Properzi for her help with the scrapie cell assay, Jackie Linehan and Professor Sebastian Brandner for histological examinations, Ray Young for assistance with figures and the technicians at the Prion Unit animal facility for help with the bioassay of C-terminally truncated PrP^{Sc}.

Without the tolerance and patience of the authors family; Rhys Thomas Lewis, Dr Peter Rhys Lewis, Shelagh Lewis, David Alistair, Fiona Elizabeth and Roger Oliver Lewis; the author would long ago have had a nervous breakdown and probably joined the Foreign Legion. The author is also indebted to (in no particular order): Captain Benjamin J. Stell KORBR (Retd.), Captain Benjamin Watts RDG, Captain Douglas Bartholemew BW, Lieutenant Samuel D. R. Steevenson D&D, Benjamin Quirk, Seamus O'Cleary, Dr Anna J. H. Malone and Matthew Kerruish-Jones, barrister-at-law. All of the above have provided valuable insight, solid support, enlightening perspective and interesting times for the last three years.

"It is one thing to show a man that he is in error, and another to put him in possession of the truth" (1)

This work is dedicated to the memory of Catherine Redmond

ABBREVIATIONS

TSE – Transmissible Spongiform Encephalopothy, TME – Transmissible Mink Encephalopathy, CWD – Chronic Wasting Disease, BSE – Bovine Spongiform Encephalopathy, CJD – Creutzfeldt Jakob Disease, FFI – Fatal Familial Insomnia, GSS – Gerstmann Sträussler Scheinker Syndrome, PrP – prion protein, PrP^{C} – cellular prion protein, PrP^{Sc} – scrapie prion protein, PrP^{RES} – protease resistant prion protein, RML – rocky mountain line, DNA – Deoxyribose Nucleic Acid, GuHCl – Guanidine Hydrochloride, NMR – Nuclear Magnetic Resonance, CD – circular dichroism, UV – ultra violet, SOD – super oxide dismutase, PK – Proteinase K, PMCA – protein misfolding cyclical amplification, GPI – glycosylphosphatidylinositol, PIPLC - phosphodiesterase phosphoinositide phospholipase C, CNS – central nervous system.

ABSTRACT

The prion diseases of humans and animals, including Creutzfeld-Jakob disease (CJD) and Kuru of humans, scrapie of sheep and Bovine Spongiform Encephalopothy (BSE), are a family of closely linked neurodegenerative disorders that have proved to be both heritable and transmittable. The aetiology of these disorders has been shown to be intrinsically linked to a novel infectious particle made up either solely or overwhelmingly of protein, the major component of which is the prion precursor protein (PrP). PrP is a 253 amino acid protein modified during synthesis by the addition of a glycophosphatidinol (GPI) anchor and either one or two N-linked sugar chains. PrP normally exists within the cell in a predominantly α-helical conformation (PrP^C), but can adopt an alternative, predominantly β-sheet structure closely linked to the disease state. In this thesis, investigations into two of the molecular characteristics of the scrapie agent are described: the impact of the GPI anchor on infectivity and the biochemical effect of the codon 129 M/V polymorphism.

The M/V polymorphism plays a major role in the disease process – with the codon 129 status of an individual modifying both susceptibility to disease and disease course. No alterations were observed in the stability, structure, protease resistance or copper binding properties of the α-helical form of PrP due to this polymorphism. Both forms had a similar propensity to form the β-rich isoform of PrP and, once in the β-rich conformation, no differences in structure, protease resistance or stability were observed between the two polymorphic variants. The codon 129 polymorphism was found, however, to have a dramatic impact on the ability of the prion protein to form ordered aggregates.

To investigate the contribution of the GPI anchor to the infectivity of PrP^{Sc}, a novel proteolytic treatment was used to remove the C-terminal and GPI from the prion protein. The infectious properties of PrP^{Sc} lacking the GPI were examined using *in vitro*, cell based and *in vivo* models of prion replication. No alteration in the ability of C-terminally truncated PrP^{Sc} to propagate was observed.

TABLE OF CONTENTS

Contents | Page No.

LIST OF TABLES AND ILLUSTRATIONS

MOLECULAR CHARACTERISTICS OF THE SCRAPIE AGENT

1.0 Introduction

The prion diseases of humans and animals, including Creutzfeld-Jakob disease (CJD) and kuru of humans, scrapie of sheep and Bovine Spongiform Encephalopothy (BSE) affecting cows, are a family of closely related neurodegenerative disorders that have proved to be both heritable and transmissible. The aetiology of these disorders has been shown to be intrinsically linked to a novel infectious particle made up either solely or overwhelmingly of protein, dubbed the prion. The concept of infectious proteins causing disease whilst acting independently of nucleic acids is a revolutionary one, and remains a subject of some debate and much research.

1.1 The Transmissible Spongiform Encephalopothies

The first documented description of what are now known as prion disorders (also known as Transmissible Spongiform Encephalopothies or TSEs) dates back to 1755, when a parliamentary enquiry was held into the incidence of a disease that led sheep to scrape themselves and eventually killed them (2). In 1772, a veterinarian called Comber described a disease of sheep that was characterised by a loss of co-ordination and an uncontrollable urge to itch, with the disease leading to collapse and death (3). This disease was originally described as cuddy trot or yeukie pine, but later became known as scrapie, due to the response of the sheep upon the urge to itch. Since the 18th century, TSEs have been described in many mammalian species and have exhibited the ability to

spread between species. They are all thought to share a common pathogenesis linked to accumulation of the Prion protein (PrP) and all exhibit related neuropathological alterations – most markedly spongiform degeneration. There are also shared symptomatic characteristics, with specific combinations of behavioural and movement disorders being indicative of TSE disease, although there is marked variation between TSEs in different species, between different TSEs within a species and even within a given TSE (4).

1.1.1 TSEs in Animals

Scrapie

Scrapie is a progressive degenerative disease of the nervous system affecting sheep. The initial presentation is often behavioural, such as apprehension, hypersensitivity or even dementia. This is followed by pruritus, resulting in the affected sheep scraping its body against objects (hence "scrapie"). The result of this is a loss of wool and damage to the skin that, combined with fatigue and weight loss associated with the disease process, yields a characteristic emaciated appearance. As the disease progresses, the sheep suffer from gait disorders, typically ataxia of the rear limbs and a high stepping movement of the forelimbs, often accompanied by tremor. These symptoms progressively worsen, eventually leading to collapse and incapacitation. Death invariably occurs 6 weeks to 6 months after the onset of symptoms, with rare cases surviving up to a year (5;6).

The neuropathological hallmarks of scrapie, upon which categorical diagnosis is heavily reliant, include global neuronal loss and cytoplasmic vacuolation; the spongiform

degeneration that characterizes the TSEs (7). The epidemiology of scrapie is complex and, after well over a century of intense scrutiny, still not fully understood. Throughout the 18th and 19th centuries the disease was thought to be hereditary in nature. Although this is now known not to be the case, there is a strong genetic element in the occurrence rate of scrapie: this is exemplified by the fact that the disease is not seen at all in some breeds and sheep can be selected for resistance to the disease (8;9). The first attempts to transmit scrapie experimentally were made by Besnoit and co-workers in the last years of the 19th century (10). Although unsuccessful, the transmission of scrapie was achieved in 1936 by Cuille *et al*, who also showed that infectivity could be removed from inocula by filtration (11). Scrapie has since been transmitted to several experimental animals, including mice (12).

Chronic Wasting Disease

First described in the 1960s, Chronic Wasting Disease (CWD) is a spongiform encephalopathy affecting elk, mule deer and white tail deer in the US and Canadian Rockies. CWD was originally identified in farmed mule deer and was thought to be caused by the increased stress of living in captive conditions as compared to the wild. It was, however, eventually shown to be a TSE and has subsequently been found in wild populations of deer and elk in the Rockies (13-15).

The cardinal symptom, as the epithet wasting would suggest, is progressive weight loss. The disease also shares many other symptoms with scrapie, including ataxia and behavioural alterations. The age of onset is normally between 3 and 5 years, with the disease course usually between several weeks and four months with an invariably fatal outcome. Following the advent of Bovine Spongiform Encephalopathy in the UK,

medical and veterinary authorities in America are increasingly concerned as to the possibility transmission of CWD to either cattle or humans (16).

Transmissible Mink Encephalopathy

Although first described in 1965, Transmissible Mink Encephalopathy (TME) is thought to have first occurred amongst farmed mink in Minnesota and Wisconsin during the 1940s and has since been observed in farmed mink from both America and Europe. The origin of TME is unknown, although the disease appears to be spread via contaminated food sources and there is the possibility that scrapie contamination may have a role in TME outbreaks. As with the other TSEs, the disease is uniformly fatal and shares the classic hallmarks of spongiform degeneration in the brain and transmissibility. The clinical progression is very similar to that of scrapie (17).

Bovine Spongiform Encephalopathy

Bovine Spongiform Encephalopathy, often described as "mad cow disease", is one of the most recent TSEs to emerge. The first case of BSE was described in the UK during 1985 although, in common with several other TSEs in animals, it is thought the disease had been present in the bovine population for several years before this (18-20). The origin of BSE remains elusive, with the likely cause being either passage of scrapie-infected tissue into bovine food or an initial, sporadic case of BSE entering the bovine food chain (21). The impact of this initial infection was magnified by the reprocessing of bovine carcases into cattle feed which resulted in a full-blown epidemic of the disease. This was brought under control only by radical alteration of cattle husbandry practice, including an overhaul of what could be used in cattle food, and the culling of affected and at risk herds on a huge scale. Over one hundred and seventy thousand cows were diagnosed with BSE

during the epidemic, and it is estimated that over a million were actually affected by the disease (although not all of those infected lived long enough to present symptoms) (22). Since it was initially described in the UK, BSE has been identified in cattle throughout Europe, in Japan, Canada and the USA (23-25).

In terms of human health concerns, the transmission of BSE to a number of other species, including cats, exotic ungulates and humans (see section 1.1.2, variant CJD) (26-29), has raised the possibility of an epidemic of transmitted prion disease within the human population of the UK, although estimates of how many may be affected vary from hundreds to tens of thousands (30;31).

1.1.2 Human TSEs

The human TSEs share many characteristics with their animal counterparts, including similar disease progression and pathological characteristics. The greater depths to which they have been studied, and the more complex neurological nature of those afflicted, have yielded a range of closely related, yet differentiated, disorders.

Creutzfeldt-Jakob disease

The most common of the human TSEs, Creutzfeldt-Jakob disease (CJD), takes it name from the two doctors who first described the disorder. Hans Gerhard Creutzfeldt documented a single case in 1920: a 22 year old who died after a six-year period of neurological degeneration (32). In 1921 Alfons Jakob described five cases with similar presentation and neuropathology to Creutzfeldts case (33;34). Ironically, recent analysis of the case histories and tissue has shown that only two of these initial cases would now

be defined as CJD (35). The disease, as recognised today, is characterised by rapid onset neurological degeneration. This initially presents as dementia, followed by the development of movement disorders such as tremor, spasticity and rigidity. A feature common to almost all cases of CJD is myoclonus, and most cases also display abnormal EEG recordings. Once symptoms are detected, the disease course is extremely aggressive, especially when compared to other neurodegenerative diseases such as Alzheimer's and Parkinson's. The average disease duration is 7.6 months, and the vast majority of patients die within 12 months (between 85% and 90%). By the end stage of the disease, patients sink into akinetic mutism, with death usually occurring due to systemic or pulmonary infection. In terms of neuropathology, CJD cases display extensive spongiform degeneration and neuronal loss, coupled with gliosis and deposits of the prion protein within the brain. In a small proportion of cases, the presence of amyloid plaques can also be demonstrated (36;37).

CJD presents a complex epidemiological picture. It has been described in three forms, each defined by their mode of emergence. The most common of these is sporadic CJD (sCJD), which constitutes approximately 85% of reported cases. This occurs at a remarkably uniform global rate of one case per million capita per annum. The disease appears to arise spontaneously, with a mean age of onset of 60 years and a mean duration of 8 months (37). With the exception of two polymorphisms in the prion gene at codons 129 and 219 where homozygosity is significantly over-represented, studies attempting to identify risk factors for sCJD have so far been unsuccessful (38-40).

CJD also occurs as a transmissible disease. This first came to light following the kuru epidemic in Papua New Guinea (*vide infra* kuru), which led Drs Gajdusek and

Gibbs to investigate whether CJD had similar infectious properties. This was demonstrated in 1967 by the passage of CJD to chimpanzees, indicating that inter-person spread of CJD was, in principle, a possibility (41;42). Thankfully, such transmission is rare and has, thus far, only been described in a small number of cases involving several modes of iatrogenic infection (iCJD). Transmission has been reported due to use of CJD contaminated batches of cadaveric human growth hormone or gonadotrophin, following dura mater grafts from diseased donors, due to corneal transplants from CJD patients or due to use of contaminated neurosurgical instruments (43-46).

The familial form of CJD (fCJD) is also rare, accounting for 14% of CJD cases. The disease phenotype has been found to segregate with mutations in the prion protein gene located on chromosome 20 (mutations in which also cause other inherited forms of prion disease). The first of these to be identified were an octapeptide repeat insertion (a peptide repeat of GGGWGQPH, four of which form part of the normal sequence of the prion protein) in the N terminal section of the protein and a lysine for glutamate substitution at codon 200. These have since been joined by several other mutations (e.g D178N, E196K, T183A). Compared to sCJD, fCJD tends to have an earlier onset and longer disease duration, although there is wide variation between the different causative mutations (47-49).

The incidence and phenotype of all three forms of CJD are altered by a methionine/valine polymorphism within the prion gene at position 129. As mentioned, heterozygosity at this codon has been shown to confer a protective effect against the incidence of sCJD (with heterozygotes being underrepresented) and has also been shown

to be protective against acquisition of iCJD (38;50). Within some fCJD kindreds, the M/V polymorphism influences both age of onset and disease duration (51;52).

Gerstmann-Sträussler-Scheinker disease

The familial TSE Gerstmann-Sträussler-Scheinker (GSS) syndrome was first described in the 1930s by the three doctors who gave the disease its name (53;54). It is differentiated from familial forms of CJD by the predominance of ataxia as its main symptom and by the large amyloid plaque burden within the brain. The original family in which GSS was described was subsequently found to harbour a mutation at codon 102 of the prion protein, and this mutation (proline to leucine) has been found to be the most common cause of GSS (48;52;55). There are, however, a number of mutations within the prion gene associated with this disease worldwide, and there is a significant amount of variation both in disease phenotype and in duration/age onset (Table 1.1).

Mutation	Age at onset (years)	Duration (months)	Phenotype
P102L	50	45	Ataxic
P105L	45	100	Paraspastic
A117V	40	40	Pyramidal/ Extrapyramidal
F198S	55	70	Extrapyramidal

Table 1.1 Gerstmann-Sträussler-Schienker mutations and phenotypes. Four of the inherited mutations that can cause GSS are shown, illustrating the range in age of onset, disease duration and phenotype. This underlines the heterogeneous nature of the syndrome.

As with fCJD, the M/V polymorphism has been shown to have an impact on the phenotype of GSS.

Kuru

Kuru, a fatal neurological disorder found amongst the Fore language group in the Eastern highlands of Papua New Guinea, was the first human TSE to be defined as such and was critical in establishing the common pathogenesis linking human and animal TSEs. Kuru was initially described during the 1950s, following the first contact between Europeans and the Stone Age culture of the Fore (56). The Fore used the word kuru, meaning shaking or trembling, to describe the disease. Indeed, tremor is usually both the first and most pronounced symptom. This progressively worsens, combining with ataxia, until the patient is incapacitated (Figure 1.1). Towards the final stages of the disease, dementia is common and incontinence is frequently present. Death occurs, often through starvation, after a disease course of between 6 to 9 months (57). The neuropathological hallmarks have many similarities to those of CJD, although there is the additional presence of "kuru-like" plaques within the brain (Figure 1.1) (58). It is thought that kuru emerged during the first few years of the 20th century. By the late 1950s, it had reached epidemic proportions, with over 100 deaths from the disease per year – the majority of those dying being either adult women or children – making it the leading cause of death among the Fore (59).

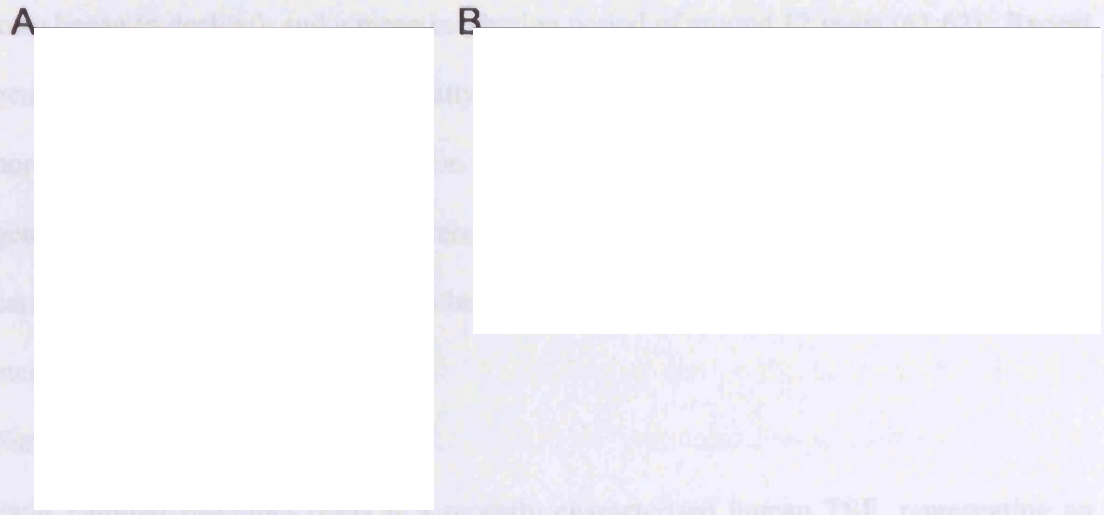

Figure 1.1 A kuru patient and kuru plaque. A) A young Fore boy in the final stages of kuru, photographed in the late 1960s. B) "kuru" plaques of deposited PrP in the brain of a patient who died of kuru. Hemotoxylin and Eosin stain on the right reveals ultrastructural cellular detail and immunohistochemical staining with ICSM 35 (D-Gen ltd., London) shows PrP deposits as areas of dark stain on the blue tissue backgrond. The spongiform degeneration characteristic of the TSEs is also clearly visible as vacuoles in the tissue.

The mode of transmission was eventually determined to be *via* the endocannibalism practised by the Fore. At mortuary feasts to commemorate the dead, women and children from the immediate family would eat tissue from their dead relative, including brain tissue. It has been suggested that the disease spread from an initial sporadic or familial CJD case that was subsequently cannibalised. The infectious nature of kuru was eventually confirmed by its transmission to various primates, all of which exhibited extended incubation periods of greater than 10 months (41;60). This mirrors the situation in the human population, with incubation periods in excess of 40 years being documented (cannibalism having been eradicated during the 1950s, following which the incidence of

kuru began to decline), and a mean incubation period of around 12 years (61;62). Recent genetic analysis has shown a greatly increased susceptibility to kuru in individuals homozygous for methionine at codon 129 in the prion protein, due to which the M/M genotype is now greatly underrepresented in the Fore (63-65). Both M/V and V/V carrying individuals have proved to be susceptible to infection, albeit with an increased incubation period (63).

Fatal Familial Insomnia

Fatal Familial Insomnia (FFI) is a recently characterised human TSE, representing an extreme of the phenotypic variance exhibited in these disorders. First described in 1986, FFI is a predominantly autosomal dominant inherited disorder, although there have been subsequent descriptions of sporadic cases (66-68). Insomnia is the initial presenting symptom, with sleep disturbance increasing as the disease progresses. The major disturbance appears to be loss of deep sleep due to alterations in, and loss of circadian rhythmic control of, body functions. This develops concurrently with gait disturbance and hallucinations, although these are thought to be linked to lack of sleep rather than with dementia *per se*. Eventually the patient enters a vegetative state and death results around a year after onset of symptoms, often from respiratory or systemic infection (although there is a wide variation in disease duration). Pathologically, FFI is distinct from other human TSEs in that its destructive impact is localised mainly in the thalamus, manifesting as neuronal loss. Spongiform degeneration is, on the whole, limited, as is PrP deposition. The classification of FFI as a TSE rests on its transmissibility and the fact that genetic analysis of the kindreds suffering from this disorder revealed a mutation in the prion protein gene that co-segregates with disease (69;70). Medori and co-workers

identified this mutation in 1992: an asparagine for aspartic acid substitution at codon 178 (D178N) (71). Several other FFI families were later shown to harbour the same mutation. Interestingly, D178N has also been documented in families suffering from fCJD – the modifying factor being the M/V codon 129 polymorphism. Carriers of the D178N mutation and methionine (on the same allele) developed FFI, whilst those carrying valine developed CJD (72;73). Of further note is the fact that the M/V 129 status on the none mutant allele affected the age of onset and disease duration in both FFI and CJD caused by the D178N mutation (74).

Variant CJD

The most recent TSE to be described, variant CJD (vCJD) emerged in the 1990s following the advent of the BSE epidemic (75). vCJD exhibits marked differences in disease profile to those associated with classical CJD or the other human TSEs. The age of onset varies greatly, with patients as young as 16 and as old as 51 being diagnosed (mean age of onset 29 years) (4). The initial symptoms are behavioural, with disorders of movement such as ataxia occurring weeks to months later. Dementia and myoclonus, usually the initial symptoms in classical CJD, occur towards the later stages of the disease and electroencephalogram (EEG) abnormalities, very common in CJD, are frequently absent in vCJD. The disease course is also longer than classic CJD, with a mean of 14 months as compared with 7.6 for sCJD (4). The neuropathology if vCJD is also in marked contrast to most other human TSEs, with spongiform degeneration concentrated in the basal ganglia and thalamus, allied with the presence of so called "florid" plaques (figure 1.2).

Figure 1.2 "Florid" Variant CJD plaques. Histological examination of variant CJD (bottom panel) compared with sporadic CJD (top panel). Hemotoxylin and Eosin stain on the right reveals ultrastructural cellular detail and immunohistochemical staining with ICSM 35 (D-Gen ltd., London) shows PrP deposits. The vCJD sample shows the "florid" plaques associated with this form of CJD (indicated by the area of intense dark staining), with the sporadic CJD case exhibiting a more diffuse pattern of PrP deposition.

These are similar to those found in kuru and scrapie. There is, in addition, widespread deposition of PrP throughout the cerebellum and cerebrum (76).

To date 154 people have been diagnosed with vCJD in the United Kingdom, with several cases identified overseas including France and the United States (figures from the CJD surveillance unit www.cjd.ed.ac.uk/figures.htm). The risk factors thus far identified are limited to residency in Britain during the height of the BSE epidemic and a genetic susceptibility based on methionine homozygosity at codon 129 in the prion protein (all patients so far diagnosed with vCJD have been M/M) (77). Several lines of evidence now support the causative link between vCJD and exposure to BSE-infected bovine

tissue. Transmission studies carried out using mice show a close correlation in disease clinicopathology between BSE and vCJD, and molecular studies of the prion protein found deposited in both bovine and human brains affected by these diseases have revealed similar biochemical characteristics (21;27-29;78;79).

The current state of the vCJD epidemic in the UK and across the world is one of uncertainty. Whilst the number of new cases each year has remained relatively constant since the late 1990s, there is a strong possibility that those succumbing to disease are an usual and highly susceptible subset of the population, and that a more general epidemic lies in the future. Certainly, using the parallel of the kuru epidemic where incubation periods greater than 40 years have been observed in a situation where there was no species barrier to infection, this does not bode well. Recent clinical research in the UK has uncovered a number of subclinical carriers, identified by screening of archived appendix tissue samples, and there has been a report of possible transmission via blood transfusion to an individual with heterozygosity at codon 129 (80;81). Epidemiological studies have estimated that the 95% confidence limit for vCJD deaths is between 50 and 50,000 future deaths, although due to the large number of unknown factors any such projections must be treated with caution (22;31). Given that human exposure to high infectious titre material from cattle during the BSE epidemic was on a massive scale (with anywhere up to 300,000 infected cattle potentially entering the human food chain), it is unlikely that vCJD is a disease that will disappear in the near future (4).

1.2 The Curious Nature of the Scrapie Agent

The nature of the causative agent of the TSEs is an issue that has perplexed scientists for over one hundred years, and the diseases defy placement into any of the established categories of human disease. As illustrated in the previous section, the TSEs present a complex disease pattern: the combination of inherited, sporadic and infectious forms of the same disease is almost without parallel in medical science. It is the last of these that most complicates the categorisation of the TSEs, as there are several other examples of slow-developing neurological disorders that occur in both familial and sporadic forms (for example Alzheimer's disease and Parkinson's disease) (82). Closer study of the infectious process reveals curious aspects of the active agent that cloud the issue even more. First, transmissible forms of the TSEs exhibit extended incubation periods as compared to the vast majority of described infectious diseases. In the extreme case of kuru, incubation periods in excess of 40 years have been described, followed by a rapid clinical course – which begs the question as to what the infectious agent is doing during this lag period, and where it is propagating. Secondly, several studies dating back to the 1960s showed that the scrapie agent could survive treatment that inactivated other infectious agents: it was resistant to heat treatment and could withstand high levels of formalin (83). Examination of the infected and infectious tissue, moreover, reveals no evidence of bacteria or virions. It was also proven that transmission could occur by inoculation with cell free isolates, indicative of a small active agent. Later work further investigating the size of the scrapie agent using ultraviolet and γ radiation treatment discovered that it was much smaller than bacteria and viruses, suggesting that the scrapie

agent might replicate without nucleic acid (84-86). In addition to this, there was also a species barrier preventing the passage of infection between certain species but not others (for example blocking infection of mice with goat scrapie, or of mice with hamster scrapie), and the existence of varied "strains" identified by incubation time and phenotype (87;88). This specificity was suggestive of a complex flow of phenotypic information during the infective process that did not derive from an agent-specific nucleic acid genome.

1.2.1 Early Theories

Several theories have been put forward to explain these data. Sigurdsson first proposed a viral origin for the disease in 1954 (89). After studying Rida (the Icelandic name for scrapie), he suggested that the causative agent was a virus, albeit a slow acting one, and used the term slow infection or slow virus. This did not explain the absence of a detectable virus particle and was not congruent with the ensuing discoveries of the resistance of the agent to treatments that inactivated all other known viruses. In the absence of a better explanation, however, the theory was accepted by many as a reflection of what was happening.

Several other theories were developed during the 1960s, when the profile of the TSEs was raised due to the demonstration that both kuru and CJD were transmissible (42;60;90) and the link with scrapie was suggested (91). Writing in 1967, Gibbons and Hunter summarised the possible mechanisms of transmission and proposed that the

disease could be associated with an aberrant steric rearrangement of the membrane (table 1.2) (92).

Hypothesis	Mechanism
Virus	Extremely small virus with unusual resistance to UV inactivation
Protein	Self replicating protein/nucleoprotein. Consistent with inactivation data but difficult to reconcile with central dogma of molecular biology (see figure 1.3 for possible mechanisms)
Carbohydrate	Poly/oligosaccharide acts as inducer or activator of a polysaccharase that synthesises further, identical oligosaccharides. Not consistent with lack of resistance to urea and phenol
Membrane	Properties of membrane lipids consistent with resistance data. Could self replicate in a similar fashion to oligosaccharide mechanism

Table 1.2 Theoretical mechanisms of scrapie replication. The four hypothetical mechanisms for scrapie replication proposed by Gibbons and Hunter in 1967, taking into account the unusual properties of the scrapie agent (92).

In the same issue of Nature, Griffith, a mathematician, further elaborated the hypothesis of a protein only mechanism of transmission and proposed three possible models for this to occur (figure 1.3) (93).

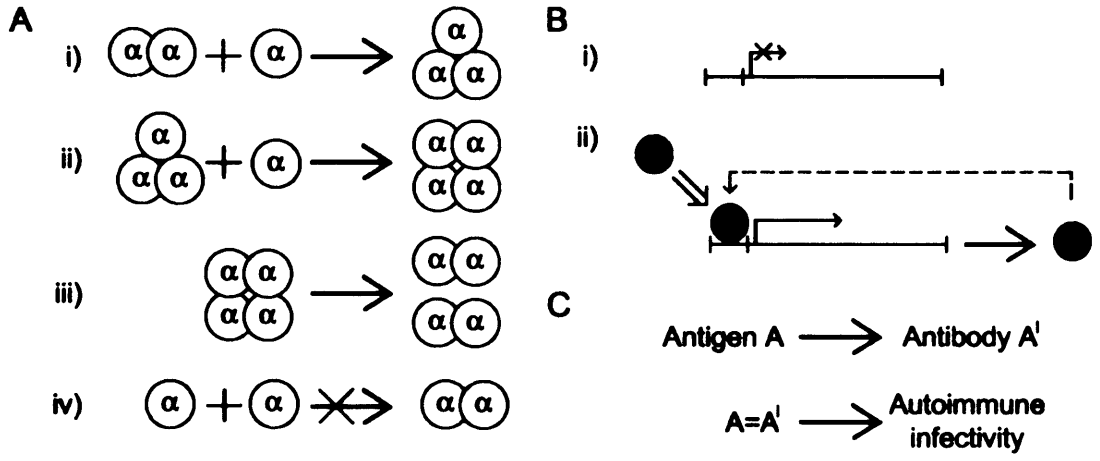

Figure 1.3 Griffiths models of protein only replication. The three models of protein only replication proposed by Griffith in 1967 (93). A) Addition of monomeric protein α to an α dimer leads to production of trimers (i) and tetramers (ii). Tetramers can then fracture to form dimers (iii), which can feed back into the process. If it is assumed that α exists in the cell as a monomer and monomers cannot associate to form dimers (iv) then only extrinsic addition of a dimer will result in self propagating behaviour. B) Protein S is required for transcription of gene G – the product of which is protein S. Introduction of S from an extrinsic source results in production of S from gene G, which leads to a positive feedback and infectious behaviour (ii). C) Autoimmune infectious process. Antigen A stimulates production of antibody A′. Where A is the same as A′ this would be an infectious, self propagating process.

These were, of course, theoretical mechanisms and Griffith did not pretend to have the hard scientific evidence to support them, although they could explain an intriguing number of the characteristics of the scrapie agent. What should be emphasised, however, is the fact that, at the time, these proposals were tantamount to heresy. The assertion that a protein was capable of some form of self-replication ran counter to the central dogma of molecular biology as proposed by Francis Crick following the elucidation of the structure of DNA (figure 1.4) (94).

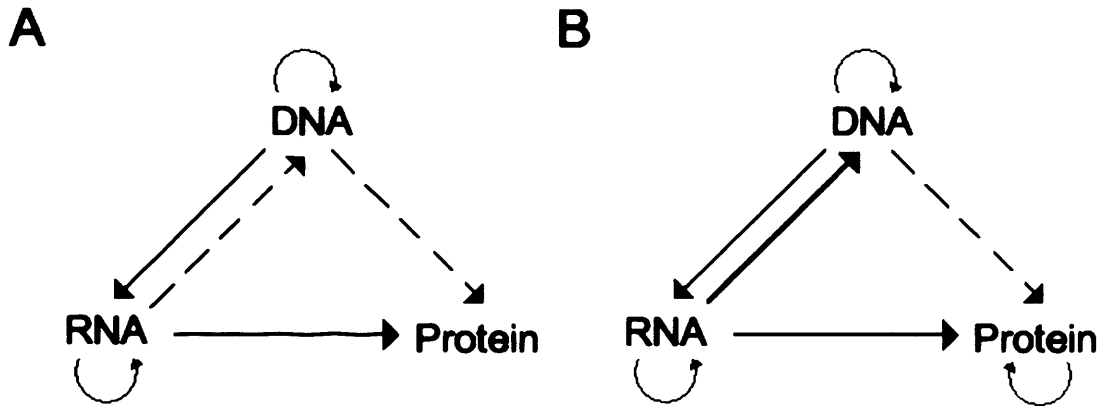

Figure 1.4 The central dogma of molecular biology. Proposed by Crick after the elucidation of the structure of DNA (94). A) The central dogma as it stood in 1970 showing transfer of information supported by scientific evidence (solid lines) and hypothetically possible (dashed lines). B) The central dogma following the discovery of reverse transcriptase (DNA produced from RNA) and prion behaviour (protein to protein replication), indicated by red arrows.

Indeed, the implication of a protein being capable of infectious properties, and therefore of self-replication, was that proteins were capable of acting as heritable agents. This possibility had been dismissed by Crick himself as being intrinsically impossible, and has proved highly controversial ever since (95). It is interesting to note, however, that prior to the discovery of the structure of DNA and the proof that it acted as the purveyor of inheritance within the cell, polypeptides had been looked on as a favourable candidate for this role due to the greater number of possible combinations provided by 20 amino acids as compared to 4 nucleic acid bases (96).

Proof of the Griffith hypothesis was not, however, forthcoming. When Carleton Gjadusek received the 1978 Nobel Prize in physiology or medicine for his work on the

transmissibility of CJD and kuru, he acknowledged that the slow virus theory, whilst not ideal, was still the most likely basis for the infectious properties of the scrapie/CJD agent (57).

1.2.2 The Prion Hypothesis

Several developments led to the slow acceptance that the causative agents of the TSEs were indeed protein based. The first of these was the development of a sensitive and rapid animal assay for infectivity. Using Syrian Golden hamsters and hamster adapted scrapie homogenate, Stanley Prusiner and colleagues working at the University California, San Francisco, established an accurate incubation time assay for infectivity (97). Prior to this, animal assays for infectivity were severely limited by the length of time required for a result to be achieved and the number of animals required for a final titre of infectivity to be arrived at. The newly developed assay provided Prusiner and his co-workers with a nearly ideal tool for probing the nature of the scrapie agent. In a seminal paper published in 1982, Prusiner set forth the prion (derived from *pro*teinaceous *in*fectious particle) hypothesis, essentially an extension of the theory propounded by Griffith over a decade earlier (83). It stated, in necessarily caged terms, that a protein, possibly acting with a small nucleic acid accomplice, was capable of self-replication within vulnerable host cells and that this protein was the causative agent of scrapie. Using the hamster scrapie assay, Prusiner was able to support his hypothesis with evidence that this was indeed the nature of the scrapie agent (table 1.3).

Properties of the Scrapie Agent

Resistant to treatment with ribonucleases and deoxyribonucleases, UV at 254nm (8 times more resitant than most resistant virus), Zn^{2+} catalysed hydrolysis, psorelen photoadduct formation and NaOH chemical modification

Susceptible to protein denaturants and proteolysis

Stable at 90°C for 30 minutes

Molecular mass < 50,000 daltons

Hydrophobic protein required for infectivity

Table 1.3 Evidence supporting the prion hypothesis. Characteristics of the scrapie agent listed by Prusiner in his seminal 1982 paper as evidence supporting a protein only basis for the TSEs (83). Stability at high temperature, low molecular mass, resistance to nucleases, sodium hydroxide and zinc hydrolysis all weigh heavily against the scrapie agent being nucleic acid based, whilst the lack of resistance to protein denaturants, proteolysis and the requirement for a hydrophobic protein point towards a protein based agent.

Swiftly following this work, the UCSF group isolated a scrapie associated protein rich fraction using a sucrose column purification protocol (98). The major constituent of this fraction was a proteinase resistant protein of molecular mass 27-30 KDa, the presence of which in isolated fractions correlated with infectivity (98). The fraction contained almost no nucleic acid, and the concomitant infectivity was resistant to nuclease treatment. Based upon the prion hypothesis, it was proposed that this protein was the major structural constituent of the scrapie agent and was dubbed the prion precursor protein, or PrP.

All of this evidence supported the prion hypothesis, but categorical proof that infectious proteins were causing scrapie was still lacking and there was an understandable resistance to a theory that ran counter to some of the most basic principles of molecular biology (although it should be noted that, in 1970, the discovery of retroviruses and reverse transcriptase had resulted in a major modification of the central dogma of molecular biology by introducing the possibility of RNA acting as a template for DNA) (99;100). The essential issue was that, with the purification techniques available, it was impossible to prove that it was PrP alone that was acting as the infectious agent, and there was as yet no detailed molecular mechanism demonstrating how this could occur.

Genetic Evidence

More evidence supporting the prion hypothesis was soon uncovered. A Zurich-based group led by Charles Weissmann identified, in collaboration with Prusiner, a cellular gene in hamsters that shared the amino acid sequence of the 27-30 protease resistant scrapie associated protein (101). The protein was coded for in a single exon of 254 amino acids, with predicted characteristics correlating with those found in the infectious form: the two shared similar molecular masses of 27 KDa and an isoelectric focussing point of 9 to 9.4. Furthermore, it was shown that the cellular form was present in both infected and uninfected hamsters, and that antibodies raised against epitopes within the protein reacted with both the purified scrapie 27-30 protein and cellular prion protein (102). The discovery of the PrP gene provided a potential substrate for an infectious protein to act upon, hinting at a molecular basis for the disease. Interestingly, the cellular form of the protein did not exhibit the protease resistance that had been demonstrated with the infectious form. This raised the possibility that there was a conformational

difference between the two at a tertiary or quaternary level resulting in increased protease resistance for the scrapie associated form. This also provided a method whereby the infectious and cellular forms could be differentiated. It was impossible, however, to exclude that alterations in the post-translational modification of the protein (for example glycosylation or phosphorylation) were responsible for the different behaviour of the two forms.

Further evidence that the cellular PrP gene was central to the process of infection was the establishment that the PrP locus was a crucial determinant in the length of scrapie incubation following inoculation (103;104). It was also shown that by expressing the hamster prion gene in mice, the species barrier between hamster and mouse could be breached and the mice became susceptible to hamster scrapie. This underlined the role of the cellular gene, but did not necessarily equate to a protein based infectious agent: these data could also be reconciled with a viral model, with cellular PrP acting as a receptor for a putative scrapie virus. It could also be postulated that the accumulation of protease resistant PrP was a product of the viral infective process, perhaps as a response to cell stress, and so was merely a marker for disease rather than a fundamental aspect of prion aetiology (105).

A year after the discovery of the hamster cellular prion protein, a homologous human gene was located on chromosome 20 (106). The presence of a cellular gene that encoded the prion protein in scrapie suggested that this might provide a locus for the familial TSEs, and this indeed proved to be the case. In 1989, a missense mutation in the prion gene was found to co-segregate with GSS in two pedigrees (48). A cytosine to thymine substitution was discovered resulting in a proline to leucine change at codon 102

in the open reading frame of PrP. Importantly, affected members of the families were found to have protease resistant material in their brains and horizontal transmission of GSS to animal models had previously been demonstrated. The implication of this discovery was that a mutation in the prion gene could alter the structure of the cellular prion protein causing it to adopt an infectious, disease causing form – although this was by no means proven. Subsequent to the discovery of the P102L substitution, further mutations were found in the familial forms of CJD and FFI, lending weight to the argument that mutations in PrP were causally linked to prion disease. A major advance was the production of transgenic mice expressing the mouse homologue of the P102L mutation (P101L). These mice developed spontaneous neurodegeneration with spongiosis and gliosis, mimicking the progression seen in the human form of the disease. Although the transgene was expressed at extremely high levels (eight times higher than endogenous levels), and there was an absence both of amyloid plaques within the brain and of infectivity, this model provided evidence of the pathogenicity of the mutation (107;108).

A model was thus emerging of a protein with altered conformation (now dubbed PrP scrapie or PrP^{Sc}) acting as an infectious agent, converting a normal, cellular substrate (dubbed PrP^{C}) into a conformational replicate of the scrapie form. How exactly this occurred was still a mystery, and the thermodynamic issues associated with a single protein with unchanged amino acid sequence occupying two different three dimensional conformations, especially *in vivo*, was the cause of much anxiety in the protein chemistry field. This ran contrary to the hypothesis that the tertiary fold of a protein was coded for

by its primary sequence alone, a hypothesis accepted as fact by protein scientists in a similar fashion to the acceptance of the central dogma of molecular biology.

Animal Models

In addition to the animal models that had been used to assay scrapie infectivity for several decades, and the P102L GSS mutation model, several novel animal models have leant weight to the Prion hypothesis. Approaching the problem of proving the prion hypothesis from the reverse angle, Weissmann and colleagues set out to falsify the theory. They produced a PrP knockout ($PrP^{0/0}$) mouse, which was both viable and showed a remarkable absence of phenotype (which, in itself, had major implications for the cellular role of the prion protein – see section 1.3) and reasoned that, if the conversion of PrP^{C} to PrP^{Sc} was the central aspect of the infectious process, a knockout mouse not expressing PrP^{C} should be resistant to infection – if mice were still susceptible this would disprove the hypothesis (109;110). The mice were indeed resistant, and there was a direct correlation with the amount of PrP present and infectivity: heterozygous knockouts ($PrP^{0/+}$) exhibited a longer incubation period and extended disease course as compared to mice carrying two copies of the *Prn-p* gene (111). In addition to this, $PrP^{0/0}$ mice expressing a copy of the Syrian hamster PrP gene allowed the reconstitution of susceptibility. Yet again, these experiments did not provide conclusive proof of the hypothesis, but were a major factor in swinging the balance of probability towards a protein only basis for the TSEs. Most recently, work by Prusiner and his group have successfully transmitted prion disease to a transgenic mouse producing a shortened prion protein construct (covering residues 89-230 of the mouse prion protein) at a level 16 times greater than endogenous expression. The inoculum was comprised entirely of

recombinant PrP assembled *in vitro* into amyloid fibrils in the absence of any nucleic acid (112;113).

Molecular Studies

Molecular studies of both PrP^{C} and PrP^{Sc} also yielded important information as to the nature of the infective process, and several major advances were made during the early 1990s. The cloning of the prion gene opened the possibility of recombinant studies of PrP^{C}, resulting in the determination of structures for hamster, mouse and human PrP using nuclear magnetic resonance (NMR) (114-119). The recombinant protein was determined to consist of a structured C terminal domain, with three alpha helices and two short beta anti-parallel sheets, and an unstructured N terminus. Cellular studies confirmed that the protein could be modified by the addition of N-linked glycosylation at two locations (N181 and N197) and contains an internal disulphide bond between C179 and C214 (120;121). The protein was found to be located at the cell surface and was anchored to the cell membrane via a GPI anchor attached to the serine at codon 231 (122). The scrapie form has proved more difficult to define. Studies of purified scrapie material using Fourier transform infrared spectroscopy and circular dichroism suggested that PrP^{Sc} contained an increased proportion of beta sheet, leading to the suggestion that the infective process resulted in a switch from the predominantly alpha helical PrP^{C} to the predominantly beta sheet PrP^{Sc} (123-125). The hydrophobic nature of PrP^{Sc} is not, however, conducive to structural studies and little progress has been made towards elucidation of its atomic structure. The importance of an atomic level model for PrP^{Sc} cannot be underestimated, as, if the prion hypothesis holds true, it is the three-

dimensional structure of the protein that contains the information required for self-replication.

Using recombinant PrP expressed in, and purified from, prokaryotes such as *Escherischia coli*, several experimental systems have been established to convert globular α-PrP, thought to be representative of the cellular form of PrP, into conformations resembling the scrapie isoform. These rely for the most part on adjusting the solvent conditions that the recombinant prion protein is exposed to. At a neutral pH and in none reducing conditions, PrP adopts the predominantly α-helical structure that has been extensively studied using NMR. By denaturing the PrP and refolding it at lower pH and in reducing conditions, recombinant PrP can be forced to adopt a predominantly β-sheet conformation (126;127). How this conformation relates to the scrapie isoform is a matter of debate, although this β-PrP certainly possesses some of the characteristics of PrP^{Sc}, such as an increased predilection for aggregation and increased resistance to digestion by proteinase K. Another system, developed by Baskakov and colleagues, uses the presence of denaturants to allow the generation of amyloid fibrils at pH 6 in a nucleation dependant reaction (128;129).

Ex Vivo Analyses

A number of cell models of prion infection and propagation have been developed. Attempts to generate such lines date back to the discovery of the transmissibility of CJD and kuru in the 1960s, although these attempts met with limited success (130-132). During the 1980s, however, a number of cell lines were developed that could stably propagate a limited range of prion strains (e.g. Rat PC12 cells, Murine N2a neuroblastoma cells, GT1 cells) (133;134). These cell lines have proved extremely useful

for studying the cellular pathogenesis of prion diseases, and have been extensively used for identification of compounds with an anti-prion activity (135-137). It should be noted, however, that cell models of prion replication do not provide a complete recapitulation of the *in vivo* situation. A good example of this is the fact that many of the compounds identified using cell models have no impact in animal models of disease (138). Recently, work has been carried out by several groups to produce highly susceptible sub-clones of the N2a cell line (139;140). This has facilitated the development of cell based assays for infectivity that are at least as sensitive as *in vivo* models, but require far shorter incubation times (140). It has been suggested that the reason that these cell lines are capable of sustaining prion replication is because their cellular environment is such that the kinetics of PrP^{Sc} propagation are above the threshold for its continued presence but does not reach a level that would be toxic to the cells (the dynamic susceptibility model) (141).

In addition to cell models of propagation, numerous cell based studies have been carried out using cell lines studying the biology of endogenous PrP or transfected with prion protein constructs expressed from viral or episomal vectors. These have been widely used to probe the normal role of PrP and to analyse the behaviour of mutant forms of the protein (142-145).

In Vitro Analyses

The importance of *in vitro* techniques to both the study of TSEs and the prion hypothesis was recognised by Prusiner and by other groups, leading to several attempts to establish an *in vitro* conversion of PrP^{C} to PrP^{Sc} (146). The reduced complexity and increased malleability of an *in vitro* system, as compared to an *in vivo* model, would, it was hoped,

lend itself to a dissection of the infectious process and facilitate the definition of what was required for the conversion to take place. Such a system would thus make proving, or falsifying, the premise that a purely protein agent was leading to infection and disease much easier. It was certainly possible that *in vitro* techniques would open the door to the ultimate proof of the prion hypothesis: the constitution of protein-based genuine *de novo* infectivity in the absence of animal derived disease material.

In 1994 Caughey and co-workers developed the first in vitro model of PrP^{Sc} formation. They utilised a cell free system where PrP^{Sc} isolated from infected hamster brains was mixed with PrP^{C} material isolated from uninfected cultured cells partially denatured in 3M Guanidine Hydrochloride (GuHCl), with a ratio of 50 volumes of infected material to 1 volume of uninfected material. Radiolabelling of the PrP^{C} material using ^{35}S methionine allowed discrimination between the infectious seed and any *de novo* PrP^{Sc}, as identified by protease resistance. They found that under these conditions new protease resistant material could be formed (figure 1.5) (147). Furthermore, the system could be used to model some aspects of *in vivo* prion disease, for instance the species barrier: hamster PrP^{C} could be converted to a protease resistant form by mouse PrP^{Sc}; but the reverse, with hamster PrP^{Sc} converting mouse PrP^{C}, could not occur (148). This mirrored data from animal models of the species barrier. Mutational studies of the PrP^{C} substrate for the reaction, creating mouse/hamster chimeras, also allowed the identification of which regions of the prion protein were required for the species barrier to operate. Later work demonstrated that the cell-free conversion system could be used to assay compounds with anti-prion activity and, importantly, that certain structural characteristics of distinct prion strains could be propagated in the system (149-151).

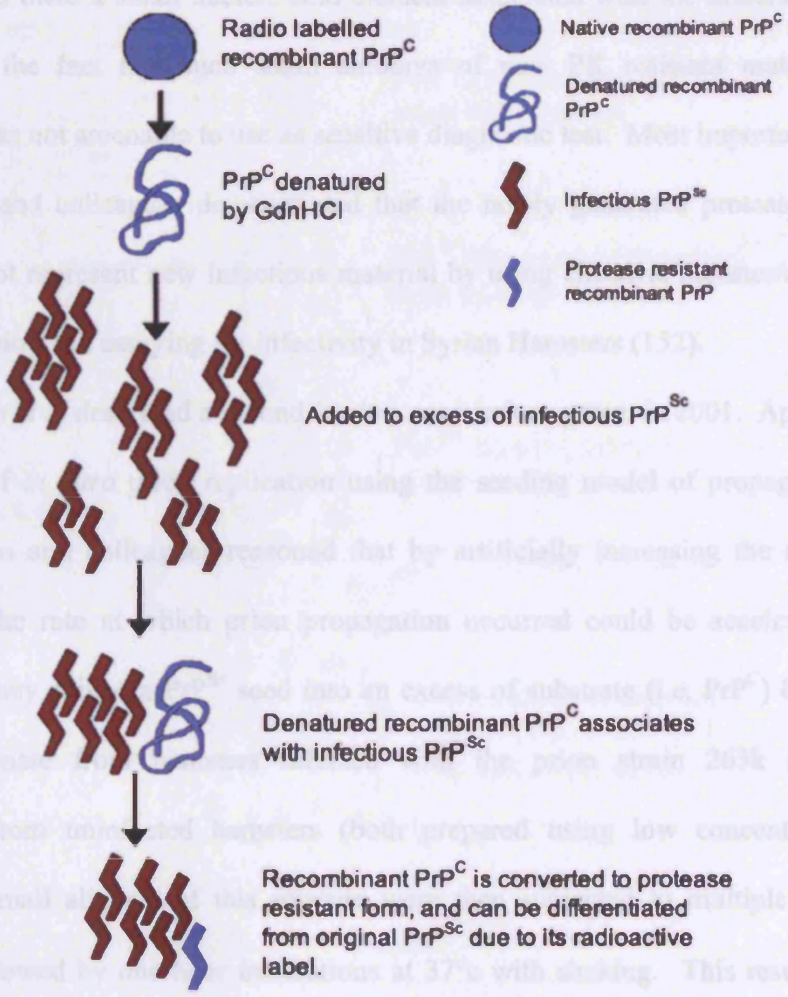

Figure 1.5 Cell free replication of PrP^{RES}. Conversion of denatured, radiolabelled PrP^{C} *in vitro* to a protease resistant state by incubation with an excess of PrP^{Sc} (147).

The development of the cell free conversion system represented a substantial advance in the prion research field, and proved that interaction between PrP^{C} and PrP^{Sc} could result in the production of protease resistant material. It could not, however, answer several questions. Why was such a vast excess of infectious material required for the conversion? What were the specific co-factors needed for the conformational change

to occur? Was there a small nucleic acid element associated with the infectious agent? Also, due to the fact that such small amounts of new PK resistant material were produced, it was not amenable to use as sensitive diagnostic test. Most importantly of all, work by Hill and colleagues demonstrated that the newly generated protease resistant material did not represent new infectious material by using chimeric hamster/mouse PrP for the conversion and assaying for infectivity in Syrian Hamsters (152).

Saborio *et al* described a second *in vitro* conversion system in 2001. Approaching the problem of *in vitro* prion replication using the seeding model of propagation as a model, Saborio and colleagues reasoned that by artificially increasing the number of small seeds, the rate at which prion propagation occurred could be accelerated. To achieve this, they spiked a PrP^{Sc} seed into an excess of substrate (i.e. PrP^{C}) by diluting brain homogenate from hamsters infected with the prion strain 263k into brain homogenate from uninfected hamsters (both prepared using low concentrations of detergent). Small aliquots of this mixture were then subjected to multiple cycles of sonication followed by one-hour incubations at 37°c with shaking. This resulted in an apparent amplification of protease resistant PrP as analysed by western blotting with anti-PrP antibodies (figure 1.6) (153). Indeed, the results of this technique, dubbed protein misfolding by cyclical amplification or PMCA, were quite spectacular - allowing detection of PrP^{Sc} at 1000 fold dilution. But, as with other *in vitro* models of prion replication, several questions still remain. First, the amplification that results from PMCA has only been quantified by analysing band intensities from western blots.

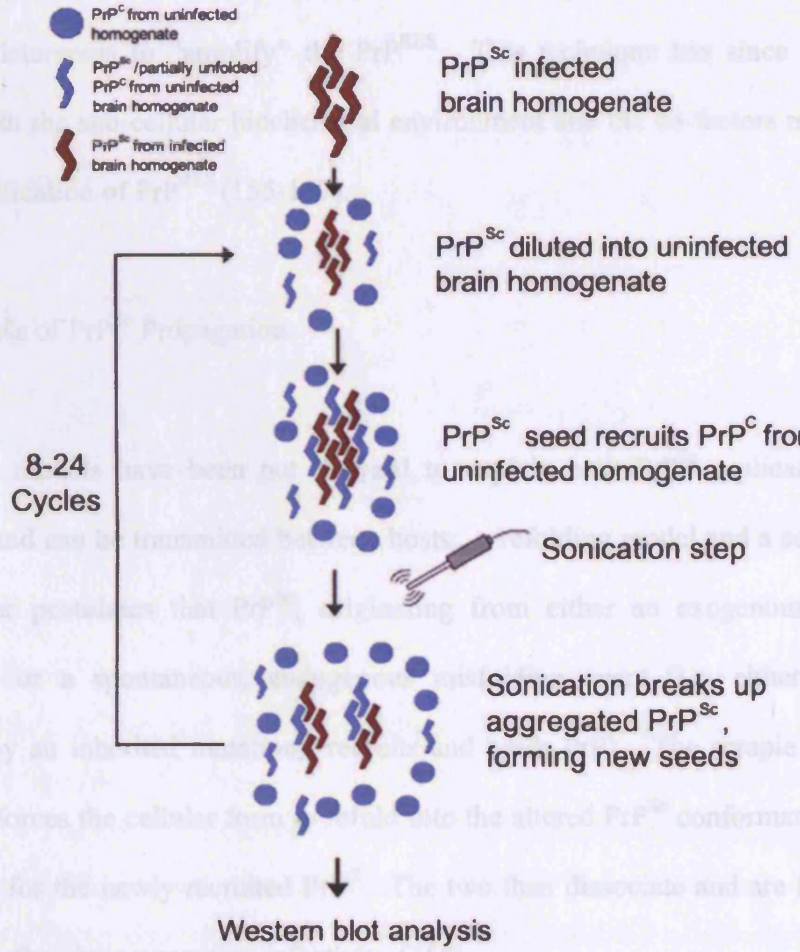

Figure 1.6 Protein misfolding by cyclical amplification. Developed by Saborio and colleagues, protein misfolding by cyclical amplification uses mild denaturants and repeated sonication steps to accelerate fragmentation of PrP^{Sc} and conversion of PrP^{C} to the protease resistant state.

Whether this represents an increase in PrP^{RES}, let alone genuine *de novo* infectious PrP^{Sc}, is still a matter of debate. Recent work by Bieschke and colleagues has suggested that PMCA does not result in any amplification of infectivity (154). The PMCA technique

was subsequently adapted by Suppatapone and colleagues, who relied purely on the action of detergents to "amplify" the PrP^{RES}. This technique has since been used to analyse both the sub-cellular biochemical environment and the co-factors required for *in vitro* amplification of PrP^{RES} (155-157).

1.2.3 Models of PrP^{Sc} Propagation

Two main models have been put forward to explain how PrP^{Sc} replicates within an organism and can be transmitted between hosts: a refolding model and a seeding model. The former postulates that PrP^{Sc}, originating from either an exogenous source (i.e. infectious) or a spontaneous, endogenous misfolding event (i.e. either sporadic or favoured by an inherited mutation), recruits and binds PrP^{C}. The scrapie isoform then somehow forces the cellular form to refold into the altered PrP^{Sc} conformation, acting as a template for the newly recruited PrP^{C}. The two then dissociate and are free to recruit more PrP^{C}, thereby propagating infectivity (158).

The alternative, seeding model of scrapie replication states that equilibrium exists between the two alternate folded conformers of the prion protein. This equilibrium is normally skewed in favour of the cellular form of the protein but can be disrupted either by mutations that shift the equilibrium in favour of PrP^{Sc} or by the presence of stable, aggregated seed material. Such seeds act as nodes that can lock misfolded PrP in the scrapie form, producing oligomers that aggregate to form amyloid fibrils in a nucleation dependant polymerisation reaction. At some point these polymers will fracture to form

multiple new seeds that can go on to propagate more misfolded PrP (figure 1.7) (159-161).

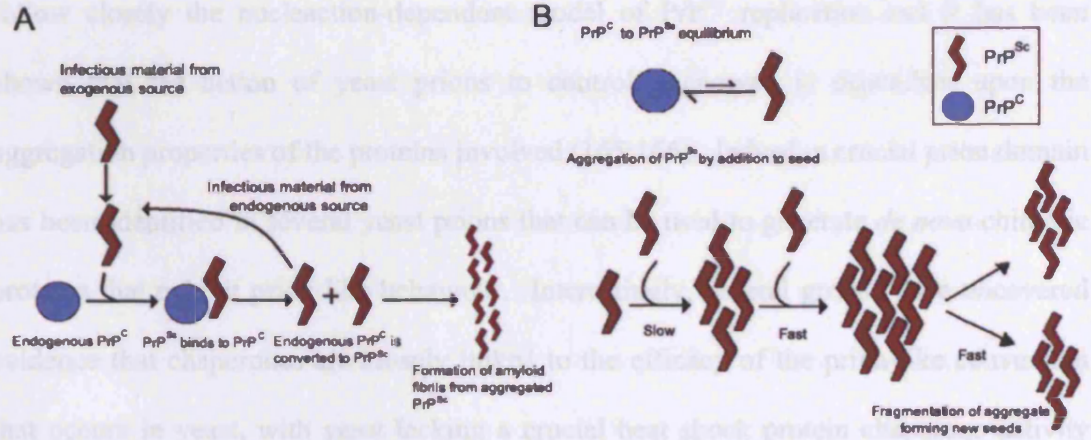

Figure 1.7 Refolding and seeding models of prion replication. The refolding model (A) proposes that PrP^{Sc} recruits PrP^{C} and converts it to the scrapie isoform by an as yet unidentified mechanism. Newly converted PrP^{Sc} is then free to recruit and convert further PrP^{C}. The increased concentration of the scrapie form results in aggregation. The seeding model (B) suggests that PrP^{C} and PrP^{Sc} exist in an equilibrium that normally favours the cellular form. Mutations in PrP or the presence of extrinsic aggregated PrP^{Sc} shifts the equilibrium towards the scrapie form, favouring accumulation and aggregation of the scrapie isoform.

1.2.4 A Yeast Paradigm

Some of the most convincing evidence that some proteins may have the ability to act as heritable elements comes not from the field of mammalian prion disease, where the possibility was first recognised, but from the field of yeast genetics. During the 1970s, several enigmatic non-mendelian epigenetic inherited traits were described in fungi. In 1994, Reed Wickner suggested that prion-like behaviour could explain this epigenetic

behaviour and there is now a substantial portfolio of evidence supporting this for a number of yeast proteins (162-164). The emerging science of yeast prions seems to follow closely the nucleaction-dependent model of PrP^{Sc} replication and it has been shown that the action of yeast prions to control phenotype is dependent upon the aggregation properties of the proteins involved (165;166). Indeed, a crucial prion domain has been identified in several yeast prions that can be used to generate *de novo* chimeric proteins that exhibit prion like behaviour. Interestingly, several groups have uncovered evidence that chaperones are closely linked to the efficacy of the prion-like conversion that occurs in yeast, with yeast lacking a crucial heat shock protein chaperone activity (HSP104) being unable to propagate the [PSI^{+}] prion (167;168). This reinforces the crucial role of protein folding in the process of prion propagation, and may have important ramifications for mammalian prions, as there is evidence that PrP interacts with cellular chaperones (169-171). Recent publications by the groups of Weissman in California and King in Florida have shown that *in vitro* produced amyloid fibrils can replicate the infective properties of *in vivo* derived yeast prions, experimental evidence central to the tenets of the prion hypothesis (172;173). Crucially, both groups reported that they were able to generate and propagate strain specific characteristics.

1.2.5 The Prion Hypothesis Today

In the quarter of a century since the origination of the prion hypothesis, much progress has been made towards its ultimate proof. In terms of the principle of protein only inheritance, the yeast prion field has provided close to conclusive evidence that this

occurs in nature (172;173). The fact that strain specific characteristics, albeit characteristics very different to those observed in the TSEs, could be propagated *in vitro* in the absence of nucleic acid has gone some way to countering one of the major arguments against the prion hypothesis: that, even if protein only replication was possible, it was not possible for one protein to encode the spectrum of TSE phenotypes. An emerging possibility is that the three dimensional structure of the ordered aggregates produced by prions facilitates the phenotypic diversity observed in both yeast prions and prion disease. This may well be a function of the differing kinetics of formation and degradation which fibrils constructed from different prion strains display, coupled to variations in the tissue specific expression of both degradation specific machinery and protein folding apparatus. Interestingly, work in the field of protein folding has shown that many proteins, under the right conditions, can be forced to adopt an amyloidogenic conformation and form fibrils (174). What may make the yeast prions and PrP exceptional is that their rate of folding or formation of critical nuclei is such that propagation of this generic amyloidogenic conformation can occur between cells, yielding an infectious process (175). This correlates well with data indicating that PrP folds and unfolds at an unusually rapid rate (176). One implication of this is that the basic disease mechanism in prion disorders and other diseases of protein aggregation, such as Alzheimer's disease and Parkinson's disease, may well be very closely related.

The advances in our understanding of protein-only inheritance in yeast have not yet been wholly translated to the field of mammalian prions, and it is important to note that the relationship between the mechanisms observed in the yeast prion field and those in infectious mammalian disease remains unclear. The recent work by Legname and

colleagues, inducing prion disease in a transgenic model using amyloid fibrils produced *in vitro* from recombinant PrP, makes progress towards establishing such a link. Their results suggest, albeit with many experimental caveats, that *in vitro* production of mammalian proteins capable of prion behaviour in a similar way to the experiments carried out in yeast is achievable (112). Extension of this work, and detailed analysis of control experiments, is extremely important.

There remain, however, many questions regarding the exact nature of the scrapie agent and our knowledge of the critical steps leading to conversion of PrP form the cellular to the scrapie isoform is limited. It is still not clear which of the models of prion replication best reflects the disease process, although the evidence from recombinant PrP fibril formation and from yeast studies suggests that the seeding model of replication may be closest to the *in vivo* situation. From a pathological point of view, there is still a great deal of argument as to what is actually causing cell death in the prion diseases. There is increasing evidence that amyloid protein deposits that are common to so many protein folding disorders are not the actual toxic species, and that it is the small oligomeric aggregates that lead to cellular loss, increasing the need to define the chemistry of oligimer formation and the structures that these form (177;178).

1.3 The Molecular Characteristics of the Cellular Prion Protein

Structure

The human cellular prion protein – all subsequent numbering refers to human PrP - is produced from a 253 amino acid single exon open reading frame located on the short arm

of chromosome 20 (179). PrP is highly conserved throughout mammals and birds and is widely expressed in adult tissues (180;181). Following translation, an N terminal signal peptide of 22 residues is removed, as is a C terminal peptide which is replaced with a GPI anchor (figure 1.8) (122).

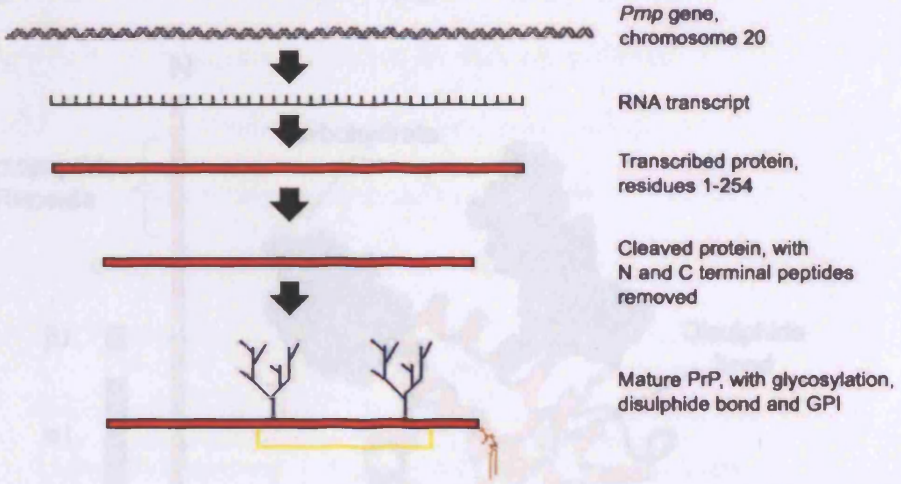

Figure 1.8 Processing of the prion protein. Following transcription and translation, N and C terminal peptides are removed. Asparagine residues at positions 181 and 197 are glycosylated, a GPI anchor is added to residue 231 and a disulphide bond is formed between cysteines at 179 and 214.

The remaining polypeptide consists of an unstructured N terminus from residue 23 to 124 and a structured, globular C terminus from residue 125 to residue 228 with a short unstructured tail attached to the GPI anchor (182). PrP can be glycosylated at two residues, asparigine 181 and 197, and exists *in vivo* as a mix of unglycosylated, monoglycosylated and diglycosylated moieties (121). The unstructured N terminus of the human prion protein contains 5 octopeptide repeats (four repeats of GGGWGQPH and a pseudo repeat of GGGWGQGG) (183). These repeats bind copper with a femtomolar efficiency, a fact that indicates copper binding plays an important part in the prion

proteins normal, physiological role(183-185). Away from the flexible N terminus, the structured C terminal domain of the prion protein contains 3 regions of α-helix (residues 144-154, 173-194 and 200-228) and a short antiparallel β-sheet (residues 128-131 and 161-164) (116;119). Within the structured domain, an internal disulphide bond is formed between cysteines at residue 179 and 214 (figure 1.9) (120).

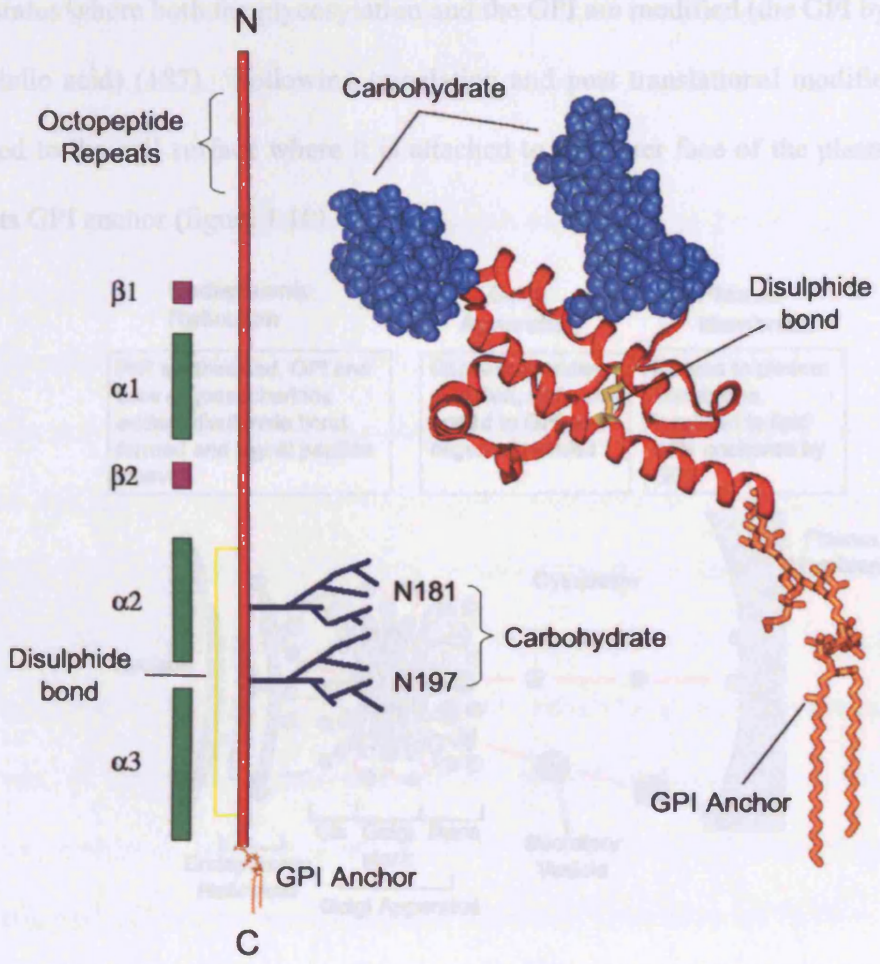

Figure 1.9 Linear and three dimensional structures of the cellular prion protein. The structured C-terminus consists of three α-helices and two short stretches of anti-parallel β-sheet. The unstructured N-terminus shows the octopeptide repeat region. Adapted from Jackson and Collinge (186).

Cell Biology

The cell biology of PrP has been studied in a great deal of detail since the cellular form of the protein was discovered in the 1980s. PrP is translated in the rough endoplasmic reticulum, where the signal peptides within it are cleaved off, the central cores of the oligosaccharides are attached and the GPI anchor added. It is then trafficked to the Golgi apparatus where both the glycosylation and the GPI are modified (the GPI by the addition of Sialic acid) (187). Following translation and post translational modification, PrP is passed to the cell surface where it is attached to the outer face of the plasma membrane via its GPI anchor (figure 1.10).

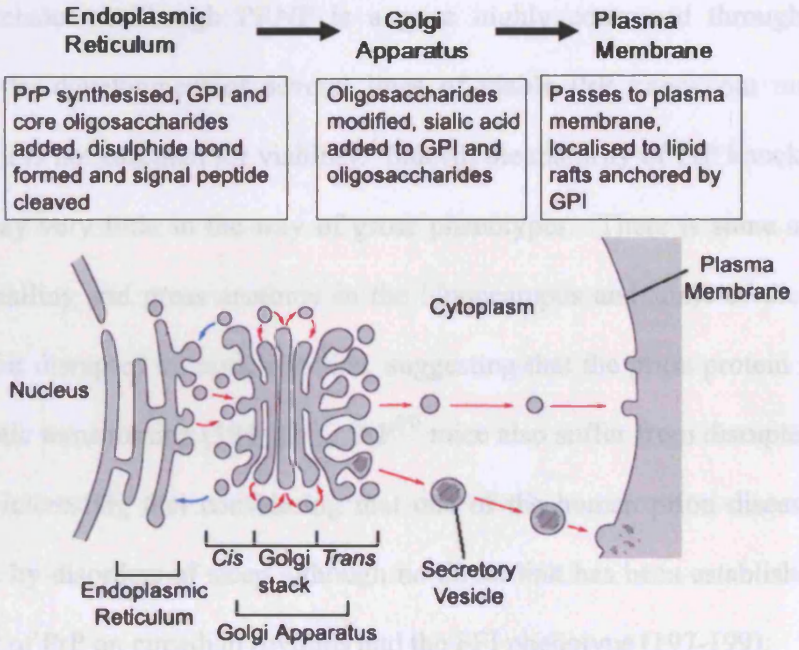

Figure 1.10 Trafficking of the prion protein. Following translation, PrP is modified by glycosylation, disulphide bond formation and addition of a GPI in the endoplasmic reticulum. It then passes to the Golgi where further modifications occur and thence to the plasma membrane where it is attached to the extracellular face of the bilayer via the GPI anchor. Adapted from Alberts *et al* and Caughey (144;188).

In common with many other GPI-anchored proteins, PrP is localised to cholesterol rich areas of the plasma membrane called lipid rafts or detergent resistant membranes, although the functional reason for this is not clear (189-191). PrP is continually recycled from the cell surface through the endocytic pathway into the endosomes, an aspect of its cell biology that lends credence to the idea of PrP acting as a receptor of some kind (192). This recycling occurs through association of PrP with Clathrin coated pits, invaginations of the cell membrane that bud off into the cytoplasm to form the endosomes (193).

Function

Despite 20 years of research, the normal physiological role of the prion protein remains a subject of debate. Although PRNP is a gene highly conserved throughout higher Eukaryotes, the development of several lines of viable PrP knock out mice ($PrP^{0/0}$) indicate that it is not essential for viability. Indeed, the majority of PrP knock out mouse models display very little in the way of gross phenotypes. There is some alteration in Calcium signalling and gross anatomy in the hippocampus and some of the knock out models exhibit disrupted synaptic function, suggesting that the prion protein may play a role in synaptic transmission (194-196). $PrP^{0/0}$ mice also suffer from disrupted circadian rhythms, an interesting fact considering that one of the human prion diseases (FFI) is characterised by disorders of sleep although no direct link has been established in terms of the impact of PrP on circadian rhythms and the FFI phenotype (197-199).

As noted, PrP binds copper with high affinity, and it has been suggested that the prion protein acts in some way as a copper transporter within the brain (200;201). This is supported by the report that neuronal copper levels being decreased in PrP knockout mice, although the viability of these mice argue against PrP being a central player in

copper transport (202). It has also been reported that PrP displays an activity similar to that of Super Oxide Dismutase (SOD), providing a link between neuronal survival in the face of apoptotic stress and PrP – which would have ramifications for the mechanism of PrP^{Sc} induced cell death (203-205). This agrees with work by Kuwahara *et al* describing the protective effect of PrP against neuronal apoptosis, although it is by no means clear that this is directly linked to any putative SOD activity (206). It should be noted, however, that work by several groups have found no SOD activity associated with the prion protein (207).

Given the location of the prion protein on the cell surface and evidence that it cycles between the surface and the endosomes, there has been much speculation as to whether the prion protein is involved in cell adhesion or cell signalling. Interaction between PrP and neuronal cell adhesion molecules, and the fact that overexpression of PrP increases cell aggregation in a neuronal cell line, tend to support a role in cell adhesion (208;209). In terms of cell signalling, direct evidence has not been forthcoming although several proteins (including the laminin receptor) have been described as interacting with PrP – it is whether these interactions have a functional basis that remains unclear (210-212). These is also evidence from antibody mediated cross linking studies in cell culture that PrP may act as part of a signal transduction cascade, although the physiological relevance of this has yet to be discerned (213).

1.4 The Molecular Characteristics of the Scrapie Agent

Structure

The structure of the scrapie agent has been a major stumbling block to TSE research since its earliest days. Whilst major advances have occurred – notably the isolation of PrP in the early 1980s – our knowledge of the atomic level structure of the scrapie agent remains scanty. PrP^{Sc} retains the primary sequence of its cellular counterpart and is not differentiated from it by covalent modification (102). The acquisition of resistance to both proteolysis and proteasomal degradation by PrP^{Sc} is suggestive of an alteration in secondary and tertiary structure (98;214-216). PrP^{Sc} also acquires resistance to PIPLC cleavage of its GPI anchor, again suggesting that there has a structural re-arrangement occurs that results in steric inhibition of the digesting enzyme (217;218). Structural studies of purified PrP^{Sc} using circular dichroism and infrared spectroscopy have indicated that it adopts a predominantly β sheet conformation (the isolation of β rich fibrils from TSE infected patients and animals supports this) (20;125;219). Unfortunately, atomic resolution structures for either PrP^{Sc} or recombinant β-PrP have, to date, proved unobtainable for a variety of technical reasons. Most importantly, the intrinsic insolubility of the protein to be studied makes it difficult to generate accurate structures using NMR or X-ray crystallography. Despite this, models of PrP^{Sc}, featuring extensive β-sheet or β-helix, have been produced but, whilst fitting the meagre data that is available, remain hypothetical (160;220;221).

A fascinating aspect of prion structural biology is the existence of structural variations in PrP^{Sc} that correlate with the pathological variation found in the prion

disorders (222). These structural strains are associated with specific patterns of protease resistant fragments of different sizes and glycoform ratios (between di-, mono- and un-glycosylated forms of the prion protein) following proteinase K digestion. Specific strains, defined by phenotype and incubation time, and capable of propagating both phenotype and structural aspects upon transmission, have been described in both animal models and human disease (figure 1.11) (223;224).

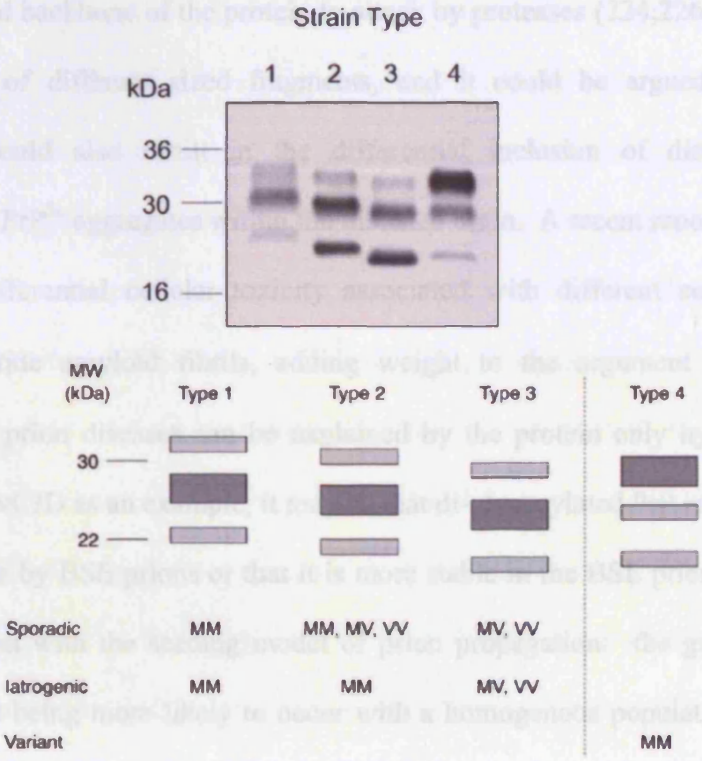

Figure 1.11 Human molecular strain types. A western blot (upper panel) and schematic (bottom panel) of human molecular strain types. This illustrates alterations in fragment size following proteinase K digestion and altered glycoform ratios (as indicated by different intensities for the di-, mono- and unglycosylated PrP fragments – upper, middle and lower bands respectively). Type 4, predominantly diglycosylated, is associated exclusively with variant CJD. Adapted from Jackson and Collinge (225).

One of the key pieces of evidence supporting the aetiological link between BSE and vCJD is the continuity of strain type between the two diseases – both marked by a predomination of diglycosylated PrP^{Sc} (27). Indeed, as noted earlier (section 1.2), the existence of such strains was initially a major weakness of the prion hypothesis. In terms of the structural origin of these strains, it has been proposed that they originate from subtle alterations in the three dimensional structure of PrP^{Sc}, exposing different residues in the amino acid backbone of the protein to attack by proteases (224;226). This leads to the production of different sized fragments, and it could be argued that such re-arrangements could also result in the differential inclusion of discrete ratios of glycoforms into PrP^{Sc} aggregates within the diseased brain. A recent report by Petkova *et al* described differential cellular toxicity associated with different conformations of amyloid β peptide amyloid fibrils, adding weight to the argument that the strain phenomenon in prion diseases can be explained by the protein only hypothesis (227). Using BSE and vCJD as an example, it may be that di-glycosylated PrP is either recruited with greater ease by BSE prions or that it is more stable in the BSE prion conformation. This is congruent with the seeding model of prion propagation: the growth of highly ordered amyloid being more likely to occur with a homogenous population of available subunits. In the case of BSE transmission to humans, bovine PrP^{C} is predominantly di-glycosylated, and the BSE agent reflects this bias in its substrate. Upon transmission to a human host, the BSE prion would be more likely to recruit and propagate with the di-glycosylated subpopulation of human PrP^{C} rather than the structurally dissimilar mono- and un-glycosylated forms, and this is then reproduced in the strain profile of vCJD PrP^{Sc}.

Cell Biology

Defining the cell biology of PrP^{Sc} has proved nearly as difficult as defining its structure. Several cellular models of prion propagation exist; including mouse N2a cells, rat PC12 cells and hympothalamic GT1 cells (133;134;228;229). Exposure of these cell lines to infectious brain homogenate results in the stable propagation of infectious PrP^{Sc}. The susceptibility of these lines is, however, severely limited to certain strains and the factors that make these cell lines susceptible are not well understood. In addition to models of propagation, mutant forms of PrP overexpressed in a variety of cell lines acquire some of the characteristics of PrP^{Sc} (for example protease and phospholipase resistance) and have been used to investigate the cell biology of the scrapie agent (145;218;230).

In terms of what cell types can propagate PrP^{Sc}, the *in vivo* situation is complex. Central nervous system (CNS) tissue is both able to propagate prions and, as witnessed by the neuronal death concomitant with prion disease, susceptible to prion mediated toxicity in all prion diseases. The pattern of tissue distribution outside the CNS varies between the different prion diseases. In most sporadic disease, for example, it is primarily the CNS that is affected (4). In vCJD and in experimentally transmitted forms of the prion diseases, the lymphoreticular system is intimately involved in the spread of infection from the initial site of infection (for example the digestive system) to the CNS, although the greatest concentration of infectivity is still located in CNS tissue (231;232). Worryingly, small quantities of PrP^{Sc} have also been documented in muscle tissue, raising the possibility of transmission from ingestion of muscle (233). The reason for these differences in tissue pathogenesis between prion diseases is unknown.

Even given the availability of cell models of prion propagation, the actual cellular location of the PrP^{C} to PrP^{Sc} conversion remains a mystery. Research by Millson and colleagues in the 1960s and 70s applying cell fractionation to cells isolated from infected mice showed that the majority of scrapie infectivity was associated with the plasma membrane (234;235). More recently, work by Susan Lindquist and colleagues at the Whitehead institute showed that, in uninfected cells, PrP could be forced to adopt a self perpetuating protease resistant form following accumulation in the cytosol, suggesting that this could be the genesis site of PrP^{Sc} (143). How relevant this observation is to true infectious propagation is not yet clear, although it has been noted that PrP^{Sc} accumulates in the cytosol of infected N2a cells (236). There is also evidence that conversion may occur in the endosomes and the lysosomal pathway (237). Indeed, based upon studies of the recombinant β-PrP, the low pH of these cellular compartments would favour the formation of a β-sheet rich isoform, and endocytosis would provide an entry route for PrP^{Sc} into the cell. Evidence from cell lines expressing disease associated mutant PrP indicates that such proteins are retained in the endoplasmic reticulum, raising the possibility that some element of conversion (perhaps limited to the inherited prion diseases) may be located in the endoplasmic reticulum (238). It may be that PrP^{Sc} is gregarious, and is capable of recruiting PrP^{C} and converting it to the scrapie form in several cellular locations. The current data are inconclusive.

Toxicity

In terms of the pathogenesis of prion disease, a central question is how prion replication and the accumulation of PrP^{Sc} leads to cellular toxicity, neuronal loss and, eventually, host death. Again, this has been the subject of a great deal of research but remains

unresolved (239). It was originally proposed that PrP^{Sc} in its aggregated form was the toxic agent, but studies by Brandner and co-workers showed that PrP^{Sc} on its own was not enough to cause cell death and that the presence of cellular PrP was required for the toxic effect (240). This has been reinforced by recent work indicating that, following removal of PrP expression in transgenic mice infected with RML, PrP^{Sc} persists and yet there is a reversal of spongiosis (241). Both models suggest that it may be an aspect of the prion replication process itself that induces toxicity rather than the end product PrP^{Sc}. Indeed, in a cell model of Huntington's disease (where protein aggregation is a neuropathological hallmark), there is evidence that there is a protective effect upon formation of aggregated protein deposits within cells (242). There does, however, appear to be intrinsic cytotoxicity of at least a fragment of the prion protein, covering residues 106 to 126, although the mechanism of this toxicity is unclear and how relevant such a small fragment has to *in vivo* pathogenesis is open to debate (243-245). There is increasing evidence that the mechanism of prion toxicity is not limited to PrP, but is common to several disorders of protein aggregation (178). This work suggests that it is the small oligomeric species formed prior to the generation of large protein aggregates that are the cause of cytotoxicity, and that these oligomers share a certain level of structural similarity in prion disease, Alzheimer's disease and Huntington's disease (177;178). This leads to the possibility that it is the "sticky", none-polymerised growing ends of amyloid fibrils that are causing the damage in affected cells, as the absolute number of these is higher in a population of oligomers as opposed to mature fibrils given the same concentration of subunits. The formation of fibrillar deposits then begins to look like a self defence mechanism by the cell to try to limit the number of growing fibril

seeds, an idea supported by the studies of huntingtin aggregation in cell culture. Another possible mechanism of toxicity has been described by Lansbury and co-workers at Harvard University. They presented evidence from microscopy studies that oligomeric amyloid can form pore like complexes, and it has been suggested that amyloid pores could play a role in the cytotoxicity of amyloidogenic protein disorders, inserting into membranes within the cell and altering the osmotic balance, leading to cell death (246;247).

1.5 The Molecular Characteristics of the Prion Protein Codon 129 Polymorphism

The codon 129 polymorphism of the prion protein coding for either a methionine or a valine was first described by Goldfarb and colleagues in 1989 and was originally mistaken for a pathogenic mutation (248). It was soon discovered, however, that variation at codon 129 was not causally linked to disease and was present in the general population (249;250). The allelic distribution in Caucasian populations is approximately 62.5% methionine and 37.5% valine (51% of Caucasian populations are MV heterozygotes, 37% MM homozygotes and 12% are valine homozygotes) (251). This rate varies around the world, and the codon 129 polymorphism is not found in East Asian populations where a lysine or glutamine polymorphism at codon 219 is present (E219K) and appears to confer the same advantage as a polymorphic codon 129 (39;40;64;252).

It was soon apparent that the codon 129 polymorphism status in an individual, although not pathogenic, was a major modifier of the aetiology of prion disease. This first came to light with the discovery that homozygosity at this codon predisposed

carriers to iatrogenic and sporadic CJD (38;50). Although homozygotes make up 49% of Caucasian populations, they represent 84% of sporadic CJD cases and 77% of iatrogenic cases (figure 1.12) (38;50;253)*. Later studies also showed that methionine homozygotes were more susceptible to transmission of kuru and, thus far, all clinically affected vCJD patients have also been methionine homozygotes (63;77;254).

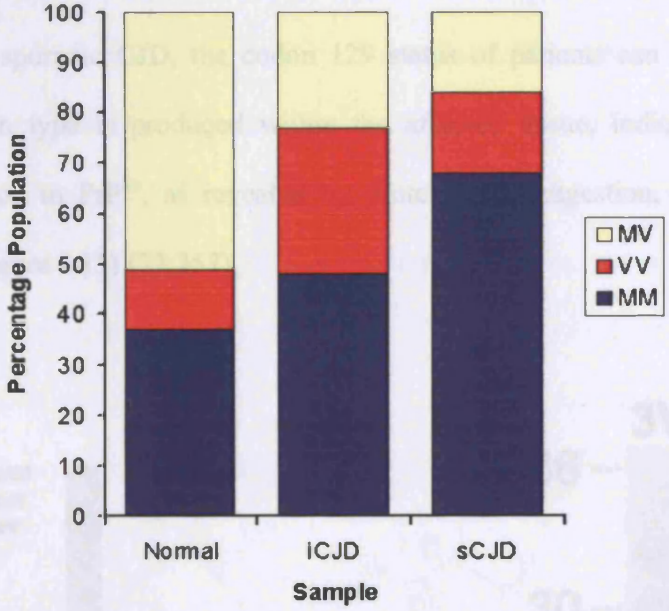

Figure 1.12 Population distribution of codon 129 polymorphic variants. The distribution in the population as a whole shows a 51:49 split between heterozygotes and homozygotes. In the disease state, this shifts dramatically to a ratio of 23:77 heterozygotes to homozygotes for iatrogenic CJD and 16:84 for sporadic CJD. The underlying mechanism causing this predisposition of homozygotes to disease is unclear.

Furthermore, the codon 129 status plays a significant role in duration, age at onset and even phenotype of prion disease caused by inherited mutations, with homozygotes having

* The E219K polymorphism seems to have the same effect, with heterozygotes protected against sporadic disease (39).

younger age at onset and shorter disease course than heterozygotes in large pedigrees with pathogenic PrP mutations (51;255). In several families carrying the D178N mutation of PrP, the 129 codon on the affected allele even defined whether the patients developed CJD (D178N, V129) or FFI (D178N, M129) (72;73). A phenotypic alteration based on codon 129 status is also witnessed in some families carrying the E200K mutation, although not as marked as that found with the D178N mutation (256). In these kindreds, and in sporadic CJD, the codon 129 status of patients can also affect what biochemical strain type is produced within the affected tissue, indicating a possible structural alteration in PrP^{Sc}, as revealed by proteinase K digestion, based upon this polymorphism (figure 1.13) (73;257).

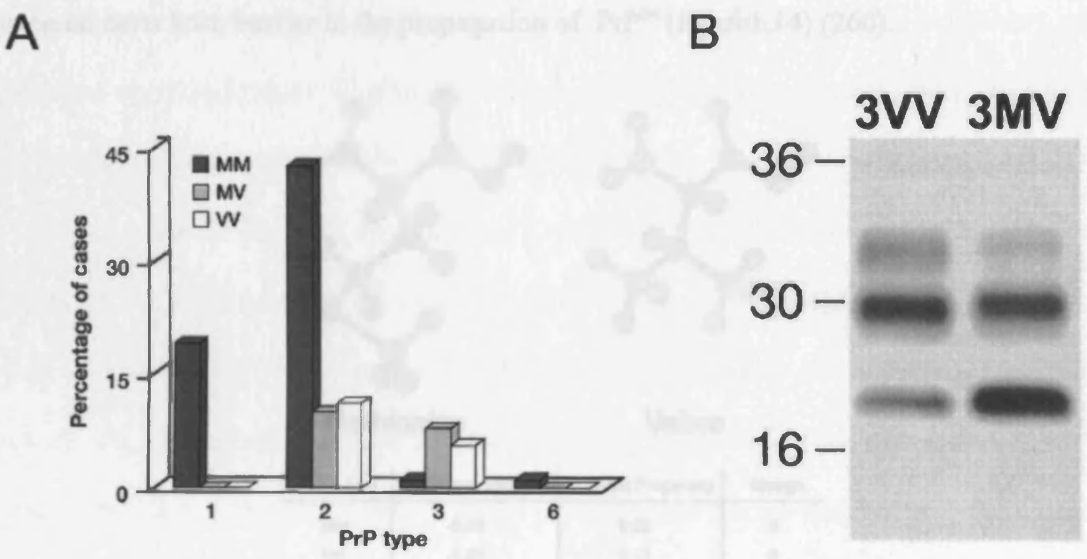

Figure 1.13 Codon 129 molecular strain type variation. A) Distribution of codon 129 genotypes across the different molecular strain types, illustrating the uneven distribution of MM and VV homozygotes. B) Alterations in glycoform ratio in type 3 human PrP^{Sc} due to codon 129 genotype. Type 3 PrP^{Sc} from heterozygote patients exhibits a greater proportion of unglycosylated PrP. Taken from reference 257.

What then is the biochemical basis of the codon 129 phenotypic effects? There are several ways in which heterozygosity could potentially act to affect the aetiology of prion disease. As detailed in section 1.4, there is a wealth of evidence supporting the need for sequence homology as an important factor in the transmissibility of the scrapie agent, with the species barrier being a prime example of this (258). Of particular relevance to the codon 129 polymorphism question is that bovine PrP encodes a methionine at the homologous amino acid to codon 129 in humans, immediately suggesting a possible basis for the occurrence of vCJD in methionine homozygotes (180;259). Although the methionine to valine polymorphism is a relatively conservative one, it could be that this provides enough of difference to cause an *intra* species, maybe even an *intra* host, barrier to the propagation of PrP^{Sc} (figure1.14) (260).

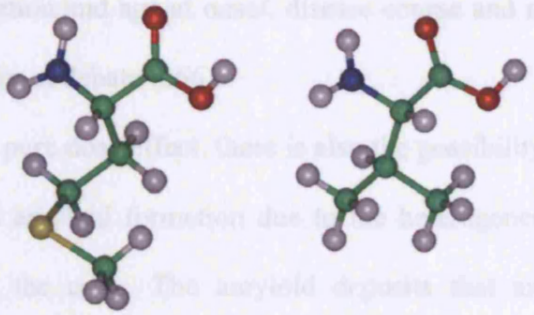

Methionine Valine

Amino Acid	Hydrophobicity	β Sheet Propensity	Charge
Met	-0.96	0.26	0
Val	-1.30	0.13	0
Gly	0.00	0.60	0
Asp	3.81	0.72	-1

Figure 1.14 Methionine and valine atomic structures and properties. Three dimensional structures of methionine and valine (upper panel) and molecular characteristics (lower panel) compared to glycine and asparagine. This illustrates the similarities in the properties of the two amino acids.

Based upon the seeding model of prion propagation, the immediate impact of heterozygosity within an individual host, assuming that there was a kinetic barrier of some kind introduced by the polymorphism, would be a halving of the substrate available for conversion and propagation of the amyloid conformation (261;262). There is increasing evidence that there is a dose effect in the propagation of amyloid in disease, as witnessed by the pathogenic effect of gene triplication of Amyloid β in downs syndrome and α-Synuclein in some cases of inherited Parkinson's disease (263;264). Increasing the concentration of available substrate would increase the rate of amyloid formation (as in Down's syndrome and α-Synuclein triplication) and, conversely, halving the available concentration of substrate (the case in M/V heterozygotes) would decrease the rate of amyloid is a matter of simple physical chemistry (265). Whether there is a direct link between amyloid formation and age at onset, disease course and maybe even phenotype is, however, still a matter of debate (266).

In addition to a pure dose effect, there is also the possibility that the heterozygote status actively disrupts amyloid formation due to the heterogeneous population of PrP that is present within the cell. The amyloid deposits that are formed in diseases associated with protein misfolding are remarkably uniform in structure within a given individual fibril, although there is marked variation between fibrils (267;268). If there is intrinsic variation in the subunits, introduced for example by a polymorphism, available for a growing fibril to recruit, this may act to terminate any polymerisation that is occurring.

Biochemical Studies of the Codon 129 Polymorphism

Because of the obvious importance of the 129 polymorphism in the aetiology of the human prion disorders, the biochemical properties of the two variants have come under significant scientific scrutiny. Some structural differences were uncovered by Wong and colleagues, who looked at the effect of copper upon mouse recombinant prion protein residues 23-231, with either methionine at codon 128 (homologous to codon 129 in huPrP) or an artificial valine 128 construct, although it should be noted that moPrP is not naturally polymorphic at this codon. They found no differences in copper binding, protease resistance or SOD activity between the two forms, however they did find that there were structural alterations differentiating the two polymorphs upon binding of copper (269). These were revealed by CD spectroscopy and antibody binding using a panel of antibodies to different regions of the prion protein. A major problem with this study is that, in addition to the fact that the codon 129 polymorphism does not occur in mice, there is a further 12% variation in sequence homology between mouse and human prion proteins (180). Thus, whilst this study sheds light on the effects of the codon 129 polymorphism and copper on moPrP, its conclusions are not necessarily transferable to human PrP. This limitation is further highlighted by a synthetic mutation (changing phenylalanine at residue 175 to a tryptophan) introduced into mouse PrP to act as an optical probe of conformational change by Glockshuber and co-workers (176). In mouse PrP, this had no observable impact on structure or stability of the protein. When this mutation was created on a human PrP background, however, it resulted in massive destabilisation of the polypeptide, preventing it from achieving its native conformation (270). This result is a dramatic example of the drawbacks of modelling human mutations

on a mouse framework, drawbacks which act as a caveat to the work of Wong and colleagues with regard to the copper binding properties of the codon 129 variants.

Using a shortened PrP synthetic peptide covering residues 109-136, Petchanikow *et al* studied the biochemical characteristics of the methionine and valine 129 polymorphs under a variety of conditions. They found that the methionine form of the peptide had a greater propensity to adopt a β-sheet conformation (as analysed by CD) and to form amyloid like fibrils (examined by electron microscopy) (271). The fact that this study was carried out on a 27 amino acid peptide rather than either full length PrP or the structured C-terminal domain (roughly residue 90 onwards), calls into question whether this truly reflects the behaviour of the mature protein, although it is certainly suggestive of a biochemical basis for the phenotypic differences observed in prion disease associated with the M/V polymorphism. The propensity of the M and V variants of human PrP 91-231 to aggregate and form oligomers was examined by Tahari-Alaoui *et al.* They put both forms of the protein into conditions that favoured the formation of oligomeric aggregates (128). Under these conditions, they found that the methionine form formed such aggregates more rapidly then the valine form, again suggesting that the aggregation properties of the M and V variants may play an important part in the phenotypic differences between the two forms (272). Fibrillisation studies carried out using a short peptide sequence (residues 118-133 of human PrP) by Come and Lansbury also revealed differences in the behaviour of the two polymorphic variants (262). Studying the nucleation dependent polymerisation of these short peptides, they showed that methionine forms fibrils faster than valine, and both undergo polymerisation more rapidly

than a "heterozygous" mixture*. This led to the production of a nucleation model for the formation of amyloid by the two polymorphs (figure 1.15). As discussed above, there are problems associated with extrapolating results gained with short peptides to the situation in the full length or the structured C-terminus of the prion protein.

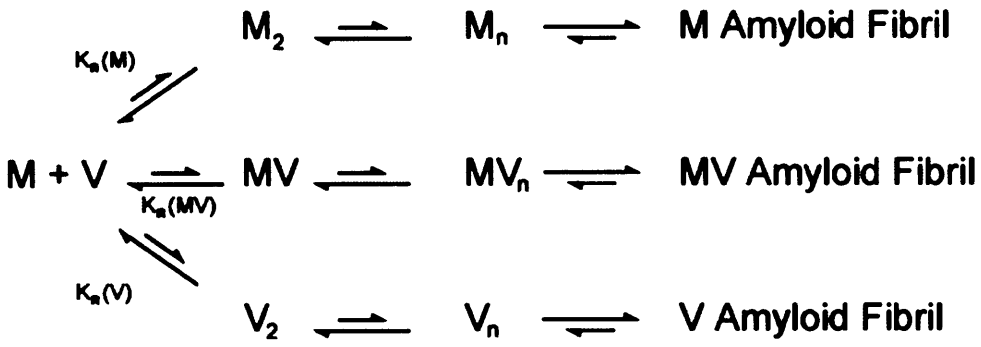

Figure 1.15 Nucleation model of the codon 129 impact on prion replication. This model proposes that the formation of dimers (M_2, V_2 and MV) is energetically unfavourable, as is the formation of a nucleating critical mass (M_n, V_n and MV_n). Once a nucleus is formed, the growth of amyloid fibrils becomes energetically favoured. If the dissociation constants for M and V (K_nM and K_nV) are lower than that for MV (K_nMV), then the formation of aggregates in homozygotes would have a lower energy barrier to overcome than in heterozygotes. Adapted from Come and Lansbury (262).

This study does, again, suggest that there may be a biochemical difference between the two forms based upon their aggregation/polymerisation properties. Most recently, however, work by Tahiri-Alaoui and James has suggested that the interaction between the

* Nucleation time (defined as the time point at which fibril concentration reaches 20% of maximum) of 48±11 minutes for M129, 78±18 minutes for V129 and 107±14 minutes for an M/V mixture.

two polymorphic variants in the formation of fibrils is more complex. A recently published paper from them shows no difference in amyloid formation (measured by thioflavin T binding) from the native α-helical rich monomeric conformer between the two variants. Referred to in the paper, however, is data in preparation that suggests that there is a large impact of the polymorphism on amyloid formation from the partially or fully denatured state, although full details are not given. Their hypothesis is that there are several pathways leading to either amyloid or oligomer formation, with the codon 129 polymorphism differentially impacting on amyloid formation from the denatured form and oligomer formation, but not on amyloid formation from the PrP in a fully natured state (273).

One obvious possibility for a biochemical difference between the two forms is a simple alteration in the secondary or tertiary structure. Although little progress has been made in elucidating the structures of either methionine or valine PrP^{Sc}, the NMR solution structures of M and V polymorphs of α-PrP have been determined (115;116;274). No significant difference was observed in structure, stability or amide protection, indicating that it is unlikely that the phenotypic differences between the variants originate from effects upon cellular PrP (figure 1.16).

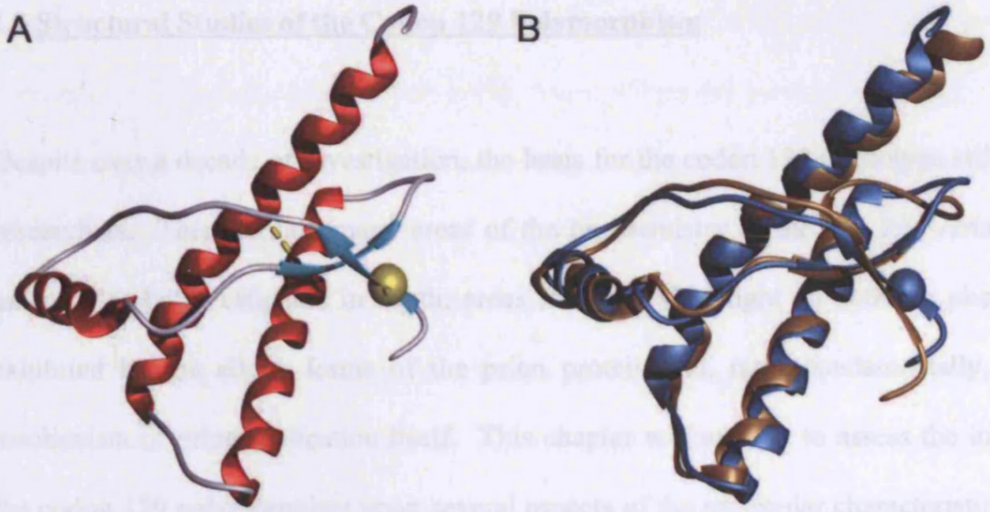

Figure 1.16 Atomic resolution structures of M129 and V129 prion protein variants. Panel (A) shows the three dimensional structure of valine 129 α-PrP with alpha helices highlighted in red, beta sheet structures highlighted in turquoise, the disulphide bridge indicated by a dashed yellow line and residue 129 depicted as a yellow sphere. Panel (B) shows structures for V129 α-PrP (gold) and M129 α-PrP (blue). There is no significant difference between the structures detectable at this level of resolution. Taken from Hosszu *et al* (275).

Liemann and Glockshuber also examined the stability of the two polymorphic variants of PrP, using recombinant α-PrP covering residues 121-231. They found no significant difference in the stabilities of the two forms as revealed by urea denaturation (276). In summary, there are some intriguing (and, based upon the conservative nature of the polymorphism, somewhat unexpected) biochemical data suggesting differences between the codon 129 polymorphic variants in terms of their aggregation properties, balanced by evidence showing very little alteration in the basic structure of α PrP. Much of the biochemistry of the M/V polymorphism, however, remains to be investigated. There is a strong possibility, based upon the absence of alterations in the α-conformation, that the polymorphism may be exerting its impact via an altered conformational state.

2.0 Structural Studies of the Codon 129 Polymorphism

Despite over a decade of investigation, the basis for the codon 129 phenotype still eludes researchers. There remain many areas of the biochemistry of the two PrP variants that have yet to be investigated in depth; areas that may shed light on both the phenotypes exhibited by the allelic forms of the prion protein and, more fundamentally, on the mechanism of prion replication itself. This chapter will attempt to assess the impact of the codon 129 polymorphism upon several aspects of the molecular characteristics of the scrapie agent, comparing and contrasting the basic structural properties of the two codon 129 variants. The investigation of the biochemistry and structure of the codon 129 polymorphism presents several unique problems. The greatest of these are the problems associated with modelling a protein that can adopt two radically different conformations with the same primary sequence and the intractable issue of dealing with the inherent insolubility of the scrapie isoform. In the absence of PrP^{Sc} purified to a level that would allow accurate structural studies, most biophysical and structural studies have been carried out using recombinant PrP expressed in bacteria or yeast. When purified and initially folded under neutral pH conditions, recombinant PrP adopts a predominantly α-helical conformation – representative of the normal cellular conformation of PrP. Several systems have been developed to refold recombinant PrP into a predominantly β-sheet conformation (127;277;278). Whilst these do not exactly replicate the scrapie isoform, they do recapitulate several of its properties (such as the β-sheet structure, partial proteinase K resistance and propensity to form amyloid fibrils). The major drawback with these systems is that, with the possible exception of a protocol producing amyloid

fibrils from recombinant PrP developed by Baskakov *et al*, it has not yet been possible to demonstrate infectivity generated *in vitro*. Since within the protein only hypothesis this is the defining characteristic of PrP^{Sc}, recombinant forms of β PrP are, at best, incomplete models of the scrapie agent. Despite this, the amenability of recombinant PrP to structural analyses makes it the best available model at present and recombinant protein was used in this study. Using recombinant PrP as a model, the structure, stability, protease resistance and copper binding properties of M129 and V129 PrP were examined using a range of techniques in an attempt to uncover a biochemical basis for the codon 129 phenotype. Due to the problems associated with modelling human mutations or polymorphisms on a mouse protein background (see section 1.5), all studies were carried out using recombinant human prion protein. There are several alternatives as regards the size of the recombinant prion protein to be used in such studies, with a range of different length constructs having been used in previous studies. As described in section 1.4, the prion protein consists of an unstructured N-terminal region and a structured C-terminal region, comprising approximately residues 124 to 231. Most studies have been carried out using full-length prion protein, residues 23-231 (residues 1-22 being removed *in vivo* as a signal peptide), or the structured C-terminal region plus a copper binding domain, residues 91-231. In terms of structural properties, several studies have shown that the C-terminal ordered domains have broadly similar properties to the full length protein and so, for the purposes of this study, recombinant human protein covering the structured region of residues 91-231 will be used (276).

2.1 Purification of Recombinant PrP

In order to carry out these investigations, recombinant human prion protein covering residues 91-231 and encoding either a methionine or a valine at codon 129 had to be produced and purified from bacteria.

2.1.1 Production of α PrP

All work with recombinant prion protein was carried out in a class III laboratory following strict biosafety protocols. Decontamination of equipment and materials was carried out as per institutional guidelines using either Sodium Hypochlorite (at greater than 20,000 parts per million available chlorine) or 2M Sodium Hydroxide.

A human prion protein construct coding for residues 91 to 231 was amplified from the open reading frame of huPrP M129 and inserted into the expression vector pTrcHisB (Invitrogen). Residue 90 was converted to a methionine in order to insert a thrombin cleavage site into the protein and a His tag was added to the N terminal of the protein. Using site directed mutagenesis, a duplicate construct containing valine at codon 129 was created. Both constructs were transformed into *Escherichia coli* strain BL21 (DE3) (Novagen) and the bacteria then grown on agar plates containing 100μg/ml carbenicillin to facilitate selection of transfected clones. Following selection, constructs were sequenced to confirm the presence of the correct PrP variant. To grow bacteria sufficient for purification of protein, a clone of each construct was inoculated into 100mls of LB

growth media containing 100μg/ml carbenicillin and grown overnight at 37°C with shaking. 10mls of this overnight growth was then placed into 1 litre flasks of LB media (total volume 9 litres), also containing carbenicillin, and grown until the optical density at 600nm reached 0.6. Induction of prion protein expression was achieved by the addition of IPTG to a final concentration of 1mM. The bacteria were then grown for 16 hours and harvested by centrifugation at 9,600 rpm for 10 minutes.

Harvested cells were then resuspended in 50ml extraction buffer (50mM TRIS.Cl pH 8.0, 200mM NaCl, 0.1% Tween-20, 50U/ml Benzonase, 10ug/ml Lysozyme) and sonicated with a 15 second burst at 25% power 5 times. The resulting suspension was centrifuged for 30 minutes at 9,600 rpm, the supernatant discarded and the process repeated. 50ml of solubilisation buffer (6M GuHCl, 50mM TRIS.Cl pH8.0, 0.8% v/v beta-mercaptoethanol) was then added to the pellet and the protein resuspended by sonication for 30 seconds at 25% power 4 times. The suspension was then centrifuged at 14,000 rpm for 45 mins and the supernatant removed. The process was repeated with the resulting pellet and the supernatants pooled. The protein concentration was then determined by measurement at λ280nm and the solution diluted to ≈ 5mg/ml protein.

To remove contaminating endogenous bacterial proteins, the crude solubilised protein was then purified using metal chelate affinity chromatography. A nitrilotriacetic acid sepharose matrix loaded with nickel ions was used and the recombinant prion protein bound *via* the His tag at its N terminus. The column was washed with 6M GuHCl, 50mM TrisCl pH 8.0 to remove any non-specifically bound proteins and the PrP eluted using a gradient of the wash buffer with the addition of 1M Imidazole, which competes with the histidines for binding to the nickel. The flow through from the initial

loading was reloaded onto the column and eluted prion protein fractions pooled. The pooled fractions were diluted to ≈ 1mg/ml protein, and 1μM copper sulphate added to the mix. The protein was then allowed to oxidise for 16 hours by vigorous stirring in the presence of atmospheric oxygen. The resulting oxidised protein was then dialysed four times against 25mM TRIS.Cl pH 8.4, 0.02% Na azide to remove the GuHCl, with the final dialysis against 25mM Tris.Cl pH8.4, 150mM NaCl, 2.5mM CaCl and 0.02% azide to facilitate thrombin cleavage. To remove the poly-histidine tag, the protein was then treated with 0.1 units of Thrombin per milligram of protein for 16 hours at room temperature, with the digest terminated by the addition of 4-(2-aminoethyl)-benzene sulfonyl fluoride (AEBSF) to a final concentration of 5mM (figure 2.1).

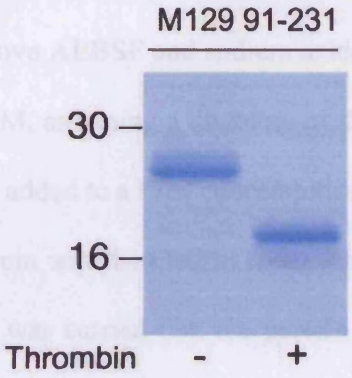

Figure 2.1 Thrombin cleavage of recombinant prion protein. Coomassie blue stained M129 91-231 PrP separated by SDS gel electrophoresis before and after incubation with thombin. This shows the decrease in relative molecular mass following removal of the polyhistidine purification tag.

The pH of the buffer was reduced to 7 by the addition of dilute hydrochloric acid. In order to remove the cleaved His tag from the protein solution, the protein was then run over a nickel column, to which the His tag bound tightly but the protein did not. The protein was eluted by a wash with 20mM TrisCl pH 7.5 containing 25mM imidazole, a concentration of imidazole high enough to release the PrP but not high enough to disrupt the binding of the His tag to the nickel. The eluted protein was dialysed against 10mM TRIS.Cl, 10mM Na.acetate and 0.02% NaN_3 pH 8.0 prior to quantification of protein

concentration, analysis of purity by SDS polyacrylamide gel electrophoresis and staining with Coomassie blue, and analysis of conformation by circular diochroism spectropolarimetry. The protein was then stored at 4°C in the presence of 1mM AEBSF and 0.02% sodium azide until required for use.

2.1.2 Conversion of α-PrP to β-PrP

Conversion to the β-PrP conformation was carried out using a protocol adapted from Jackson *et al* (127). α-PrP comprising residues 91 to 231 containing either M or V at codon 129 was concentrated to 2 mg/ml and dialysed against 10mM NaAcetate pH 7 to remove AEBSF and sodium azide. Solid GuHCl was then added to a final concentration of 6M, assuming a doubling of the initial volume, to denature the protein and solid DTT was added to a final concentration of 100mM in order to reduce the disulphide bond. The protein was then left at room temperature for 2 hours. Refolding of denatured, reduced PrP was carried out: the protein was dialysed against 50 volumes of 10mM NaAcetate pH4.0, 100mM DTT for 6 hours and then transferred to 50 volumes of 10mM NaAcetate pH4.0, 10mM DTT for 16 hours. This last step was repeated for a 6 hour dialysis against fresh buffer and final dialysis was carried out against 10mM NaAcetate pH4.0, 2mM DTT, 0.02% w/v NaAzide for 16 hours. The protein was concentrated to 2mg/ml and spun at 150,000g for 4 hours in Beckmann Optima XL-100k preparative ultracentrifuge to remove any aggregated protein. The supernatant was removed, assayed for protein concentration by measuring absorbance at λ280nm, and analysed for secondary structure conformation using circular dichroism spectropolarimetry (see below, section 2.2).

2.2 Structural and Stability of the codon 129 polymorphs

There are several techniques that can be used to analyse the structural characteristics and properties of recombinant protein. These vary in the level of detail they reveal and the complexity of the technique and preparation required for analysis. In terms of structural detail, NMR and X-ray crystallography reveal the highest level of atomic detail. Unfortunately, both require carefully prepared material, free in solution in the case of NMR and in the form of crystal lattices in the case of x-ray determination. NMR has been successfully applied to the α-helical form of recombinant PrP (both M and V forms), but has not yet yielded results for the β-rich form. To date, no crystal structure has been elucidated for β-PrP, although several exist for the α-helical form (279;280). Far cruder in terms of the detail they reveal, but simpler to use, are infrared and circular dichroism (CD) spectropolarimetry. Both can be used to examine the global folding of proteins, yielding information about the proportion of alpha helical and beta sheet structure to be found within a given polypeptide. These techniques also have the advantage that they can be used to follow folding as conditions change, for example as temperature, pH or the concentration of denaturants alters.

Analysis by Circular Dichroism

Analysis of recombinant PrP secondary structure was carried out using a Jasco J-715 circular dichroism spectropolarimeter (figure 2.2). Circular dichroism relies on the interaction of optically active molecules (those with a chiral centre) with left and right handed circularly polarised light.

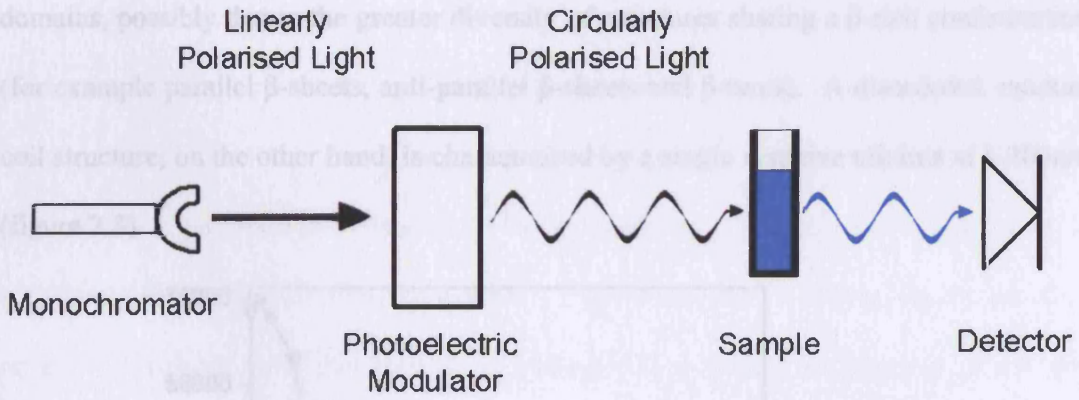

Figure 2.2 Circular dichroism spectropolarimeter setup. Linearly polarised light is produced in a monochromator. This light is then circularised by a photoelectric modulator and passed through the sample of interest. Any alterations in molecular ellipticity at different wavelengths due to the sample are recorded by the detector.

Such light interacts differently with L and D enantomers of a given chiral molecule, producing different absorbances (A_L and A_R) at different wavelengths. In addition to allowing determination of chirality in a non-racemic mixture, CD is highly sensitive to conformational alterations in complex biomolecules (composed, as most of them are, of optically active subunits) (281;282). From the standpoint of protein chemistry, the fact that α-helical and β-sheet conformations interact with circularly polarised light at different wavelengths in different ways provides a useful, if somewhat crude, tool for the estimation of protein structure (283;284). The distinctive CD spectra in the far UV region for α-helical, β-sheet and random coil structures adopted by polypeptide chains have been defined experimentally (285). Predominantly α-helical structures exhibit 2 negative minima at λ 208 and λ 222nm, with a positive maximum at 190nm. Predominantly β-sheet polypeptides exhibit a single negative minimum at 217nm, with a

positive maximum at 195nm. There are a greater variety of spectra recorded for β-sheet domains, possibly due to the greater diversity of structures sharing a β-rich conformation (for example parallel β-sheets, anti-parallel β-sheets and β-turns). A disordered, random coil structure, on the other hand, is characterised by a single negative minima at λ 200nm (figure 2.3).

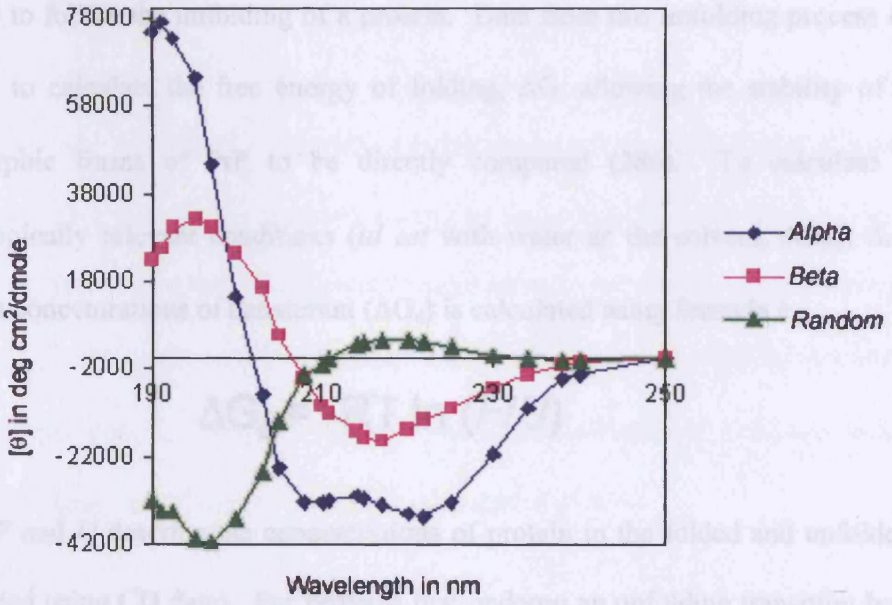

Figure 2.3 Experimentally determined circular dichroism spectra for α-helical, β-sheet and random coil protein structures. α-helical polypeptides exhibit double minima at 208nm and 222nm, β-sheet polypeptides a single minimum at 217nm and polypeptides in random coil conformation a minimum around 200nm. Data taken from Greenfield and Fasman (285).

In addition to global folding information, CD can also be used to examine the stability of proteins upon either heat or chemical denaturation. As the minima observed between 222nm and 208nm are indicative of 2° structural organisation, changes in this region can be used as a guide to the proportion of folded molecules present in solution. Upon the

application of denaturing conditions (for example increased heat or increased concentrations of chemical denaturants such as Guanidine Hydrochloride), absorption values in this region will become less negative as the protein loses 2° structure and becomes more random coil like. By increasing the temperature or denaturant concentration stepwise and measuring the concomitant alteration in CD signal, it is possible to follow the unfolding of a protein. Data from this unfolding process can then be used to calculate the free energy of folding, ΔG, allowing the stability of the two polymorphic forms of PrP to be directly compared (286). To calculate ΔG for physiologically relevant conditions (*id est* with water as the solvent, ΔG_w), the ΔG at different concentrations of denaturant (ΔG_d) is calculated using formula *i*:

$$\Delta G_d = -RT \ln (F/U)$$

Where *F* and *U* describe the concentrations of protein in the folded and unfolded states (calculated using CD data). For proteins that undergo an unfolding transition between 0 and 1M GuHCl, these data can be extrapolated in a linear fashion using equation *ii*:

$$\Delta G_d = \Delta G_w + m\,[\text{denaturant}]$$

Where *m* is the gradient of the data in the linear plot. By extrapolating to a denaturant concentration of zero, the ΔG_w can be derived. For proteins that undergo an unfolding transition at concentrations of GuHCl between 1 and 4M, however, a simple linear extrapolation does not result in an accurate value for ΔG_w. In these conditions, the

solvation energy of the side chains involved in the unfolding process must be taken into consideration using formula *iii*:

$$\Delta G_d = \frac{\Delta G_w + n_{wr}\Delta G_{s,m}[\text{denaturant}]}{(K_{den} + [\text{denaturant}])}$$

Where n_{wr} is the number of completely buried residues in the fully folded protein, $\Delta G_{s,m}$ is the maximum change in solvation energy at an infinite concentration of denaturant, K_{den} is the dissociation constant for the denaturant concentration required to achieve half of $\Delta G_{s,m}$. These values can be calculated from the atomic resolution structure of the protein in question. Using this formula, an accurate estimation of ΔG_w can be achieved, allowing comparison of protein stability in the folded state.

Methods

For collection of CD spectra in the far UV range, protein was diluted to 1mg/ml, spun for 20 mins at 15,000 rpm and placed in a 0.01cm path length cuvette. Absorption values were recorded using a Jasco J-715 CD spectropolarimeter at 20°C from λ 250 to λ 190 nm with a 1nm pitch and a band width of 10nm. Scanning speed was set at 200nm/min and the final spectra were averages from 40 individual scans. In parallel to sample CD spectra, scans were recorded under the same conditions for buffer alone – values for which were subtracted from sample readings to remove any background absorption.

For stability analysis, protein was diluted to 0.1mg/ml, spun for 20 mins at 15,000 rpm and placed in a 1cm path length, 3ml cuvette with a minimum initial volume of

1.5ml. To ascertain the starting folded population, an initial reading was taken with a 10nm bandwidth around λ 220nm. A set volume of denaturant was then added to the fully natured protein and mixed well, with the absorption reading allowed to settle to a flat line before subsequent additions were made. Absorption values were recorded for each stepwise addition of denaturant. Taking the initial reading as being representative of 100% of molecules in the native state, these were then converted to a percentage of molecules folded – taking into account the dilution effect of denaturant addition. These values were then plotted against denaturant concentration and/or denaturant activity (calculated using formula *iv*), again taking into account any dilution effect.

$$\text{Denaturant activity} = \frac{[\text{GuHCl}] \times 7.5}{[\text{GuHCl}] + 7.5}$$

$$= \frac{[\text{Urea}] \times 22}{[\text{Urea}] + 22}$$

2.2.1 Alpha PrP Studies

As an initial investigation, the structure of αPrP residues 91-231 containing valine or methionine at codon 129 were examined by CD spectroscopy. Spectra in the far UV range (λ 190-230nm – containing information about 2° structure) were recorded for both variants. As one would expect based upon previous studies, both methionine and valine forms exhibited spectra characteristic of a predominantly α-helical conformation, with minima at 208 and 222 nm (figure 2.4).

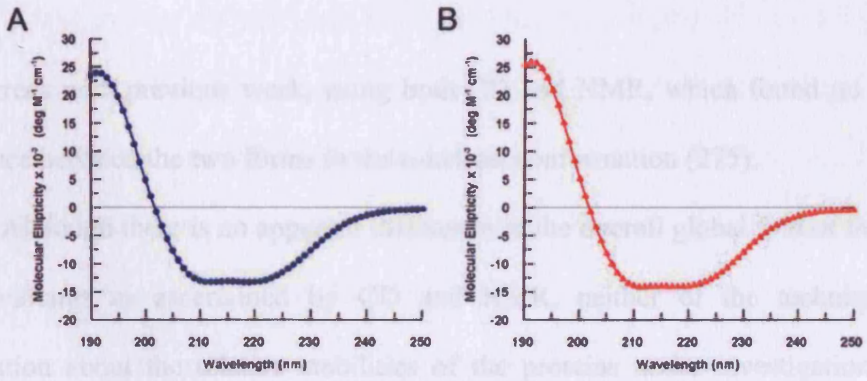

Figure 2.4 α-PrP 91-231 M129 and V129 circular dichroism spectra. Far UV circular dichroism spectra for M129 α-PrP (A) and V129 α-PrP (B). Spectra were recorded using a Jasco J-715 spectropolarimeter at a protein concentration of 1mg/ml and over a pathlength of 0.01cm. Final spectra represent an average of 40 individual scans. Both M129 α-PrP and V129 α-PrP display spectra characteristic of a predominantly α-helical conformation, with minima at 208nm and 222nm.

When overlaid, the spectra were not significantly different, with slight differences in intensity across the spectra reflecting small differences in protein concentration (figure 2.5).

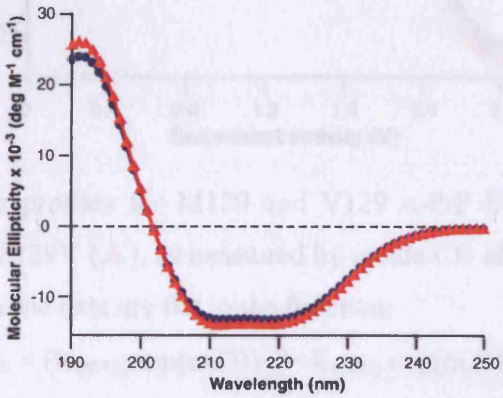

Figure 2.5 Overlaid M129 (●) and V129 (▲) α-PrP circular dichroism spectra. No significant difference was observed between the polymorphs. Collection details are as for figure 2.4.

This agrees with previous work, using both CD and NMR, which found no significant difference between the two forms in the α-helical conformation (275).

Although there is no apparent difference in the overall global fold of the M and V α-PrP variants as ascertained by CD and NMR, neither of the techniques reveal information about the relative stabilities of the proteins under investigation. Despite having very similar folded structures, it may be that the differences in the M and V side chains at residue 129 results in different protein stabilities for the two forms. To examine this, M and V recombinant prion proteins were subjected to equilibrium unfolding by addition of the denaturant guanidine hydrochloride (figure 2.6).

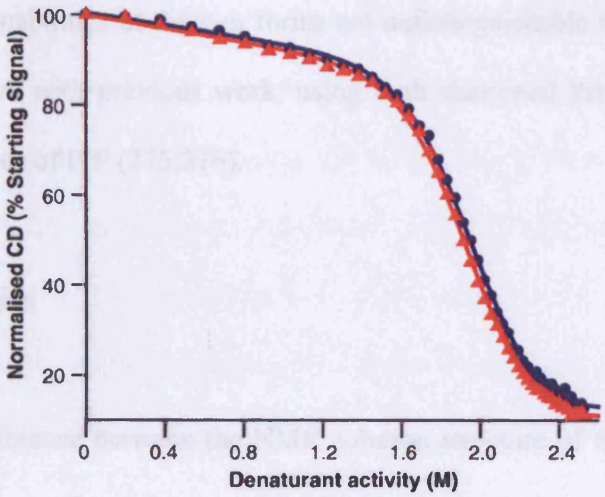

Figure 2.6 Denaturation profiles for M129 and V129 α-PrP Equilibrium denaturation curves of 129M (●) and 129V (▲), as measured by amide CD absorption at 222nm. The lines superimposed upon the data are fits to the function:

$$\alpha_N = (K_{(N/U)}.\exp(m.D))/(1+K_{(N/U)}.\exp(m.D))$$

The free energy of unfolding in water was calculated to be 6.62 kcal mol^{-1} for M129 α-PrP and 6.52 kcal mol^{-1} for V129 α-PrP.

The unfolding process was followed using circular dichroism to measure the percentage of molecules present in solution in a folded state, and is displayed in figure 2.6 as a percentage of folded molecules (taking the measurement in the presence of no denaturant as 100%) plotted against denaturant concentration. As the concentration of denaturant increase, both forms initially unfold slowly until a GuHCl concentration of 2M is reached, when both undergo a cooperative unfolding transition, characteristic of a compacted single folded domain. Importantly, both forms undergo this transition at equivalent GuHCl concentrations – showing that their relative stabilities in the presence of guanidine are very similar. When the ΔG of unfolding was calculated for M129 and V129 91-231 α-PrP, there was no significant difference in the values for the two proteins, indicating that the stabilities of the two forms are indistinguishable using this technique. This is in agreement with previous work, using both shortened PrP constructs and the structured C-terminus of PrP (275;276).

2.2.2 Beta PrP Studies

The absence of difference between the NMR solution structure of the two polymorphic variants in the alpha conformation, combined with biophysical data using several other techniques, suggests that, if a structural difference between the two forms exists, it lies either in partly folded intermediates or in the β-rich state (274). This is supported by the results from CD and unfolding studies described in the previous section. If there is a difference between the structures of the codon 129 polymorphic variants in the β-rich conformation, this poses the question as to how to uncover such a difference. As noted in

section 1.4, a great deal of effort has been dedicated by researchers across the globe in an attempt to elucidate the atomic resolution structure of the β-form of PrP. At present, these efforts remain unrewarded. Low resolution techniques, such as CD spectroscopy, have been used to investigate within the limits of their sensitivity the structure of β-PrP. Approaches such as CD, and indirect methods that reveal aspects of protein structure such as partial proteolytic digestion, offer the best routes currently available towards determining if there is a difference in the structures of M and V forms of β-PrP.

As a first step towards investigating the M and V polymorphs in the beta conformation, the conversion from the α to the β-state was examined. This was carried out using the protocol of Jackson *et al* (127). Briefly, equal volumes and concentrations of each variant were unfolded in 10M GuHCl in reducing conditions and then refolded by dialysis into sodium acetate buffer at low pH. After confirming that the protein had converted to a predominantly β-fold using CD (see below), the percentage yield was calculated by comparing the amount of β-folded protein left in solution to the initial amount of protein. By comparing the percentage yields from multiple conversion experiments, the relative propensities of the two forms to undergo the conversion to the β conformation could be compared (figure 2.7).

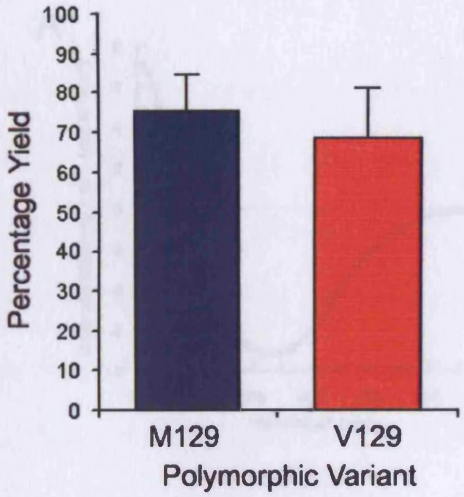

Figure 2.7 Yield for conversion of α-PrP M129 and V129 variants to β-PrP form. The yield of folded soluble, monomeric protein in a beta-sheet conformation is shown for for M129 (blue) and V129 (red) polymorphs of human PrP91-231. Black bars indicate the standard deviation from an average of 5 independent experiments.

Although there was a certain degree of variation in the yields of the β-conversion (as indicated by standard deviations of ±9.6% for methionine and ±12.4% for valine), there was no obvious or significant difference between M129 and V129 PrP ($p > 0.1$, paired T-test). From this it can be concluded that, in this refolding system at least, both M and V forms of PrP have an equal propensity to form the β-isoform.

Once in the β-rich state, the structures of the two variants were compared using CD spectroscopy in an attempt to uncover any gross differences in structure between M and V PrP. Using the same protocol applied to PrP in the α-helical conformation, far UV (between 190nm and 230nm) circular dichroism spectra for β-PrP M129 and β-PrP V129 at the same concentration (1mg/ml) were recorded. Both forms exhibited spectra characteristic of a predominantly β-sheet fold with a single minimum at λ 216nm, as compared to the double minima (208 and 222) recorded for α-PrP (figure 2.8).

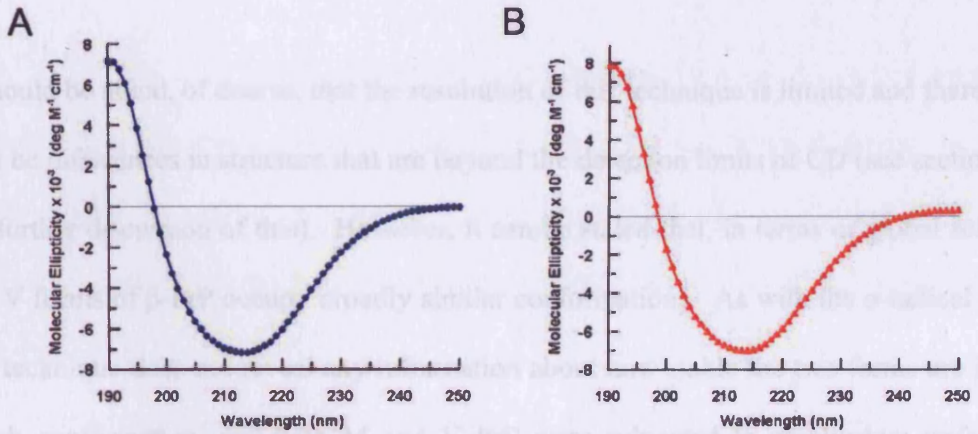

Figure 2.8 β-PrP M129 and V129 circular dichroism spectra. Far UV circular dichroism spectra for M129 β-PrP (A) and V129 β-PrP (B). Spectra were recorded as for figure 2.4. Both M129 β-PrP and V129 β-PrP display spectra characteristic of a predominantly β-sheet conformation, with a single minimum at 212nm.

These spectra were overlaid and there was no observable difference between the two forms (figure 2.9).

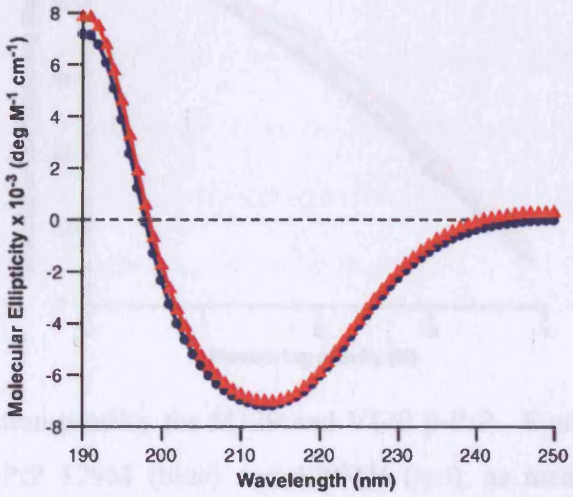

Figure 2.9 Overlaid M129 (●) and V129 (▲) β-PrP circular dichroism spectra. No significant difference was observed between the polymorphs. Collection details are as for figure 2.4.

It should be noted, of course, that the resolution of this technique is limited and there may well be differences in structure that are beyond the detection limits of CD (see section 2.5 for further discussion of this). However, it can be stated that, in terms of global fold, M and V forms of β-PrP occupy broadly similar conformations. As with the α-helical state, this technique does not reveal any information about how stable the two forms are in the β-rich conformation, and both M and V PrP were subjected to equilibrium unfolding using urea as a denaturant. Previous experiments have demonstrated that β-PrP is prone to aggregation at high ionic strength and therefore urea was used as an alternative to GuHCl in order to avoid any precipitation of β-PrP (126). In contrast to the α-helical form, the denaturing of both forms of β-PrP demonstrated little evidence of cooperative unfolding (figure 2.10).

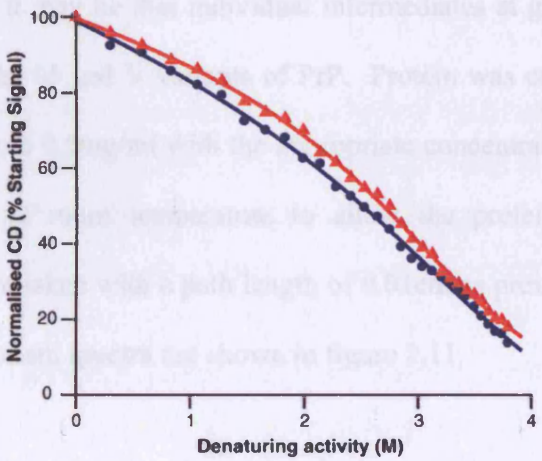

Figure 2.10 Denaturation profiles for M129 and V129 β-PrP. Equilibrium denaturation curves of human β-PrP 129M (blue) and 129MV (red), as measured by amide CD absorption at 222nm. The lines superimposed upon the data are fits to the function:

$$\alpha_N = (K_{(N/U)}.\exp(m.D))/(1+K_{(N/U)}.\exp(m.D))$$

The free energy of unfolding in water was calculated to be 2.36 kcal mol^{-1} for M129 β-PrP and 2.73 kcal mol^{-1} for V129 β-PrP

Both M129 and V129 PrP exhibited a gradual decrease in secondary structure proportional to the concentration of denaturant, with no significant difference between the two forms. The lack of a cooperative unfolding transition is in keeping with the idea that β-PrP represents a molten globule type of organisation that lacks significant tertiary organisation (127).

To further investigate the unfolding of M and V β-PrP using chemical denaturant, spectra from λ 190 to 230nm were recorded in the presence of varying concentrations of urea. The rationale behind this was to attempt to reveal any differences between putative folding intermediates that may be populated by the two codon 129 polymorphs. As the concentration of denaturant increases, the tertiary and secondary structure of the protein is destabilised. Whilst the β-PrP spectra for the two forms under fully natured conditions are undistinguishable, it may be that individual intermediates at given concentrations of denaturant differ for the M and V variants of PrP. Protein was concentrated to 1mg/ml and then diluted down to 0.5mg/ml with the appropriate concentration of Urea. Samples were then incubated at room temperature to allow the protein to reach a folding equilibrium and spectra taken with a path length of 0.01cm as previously described. The resulting circular dichroism spectra are shown in figure 2.11.

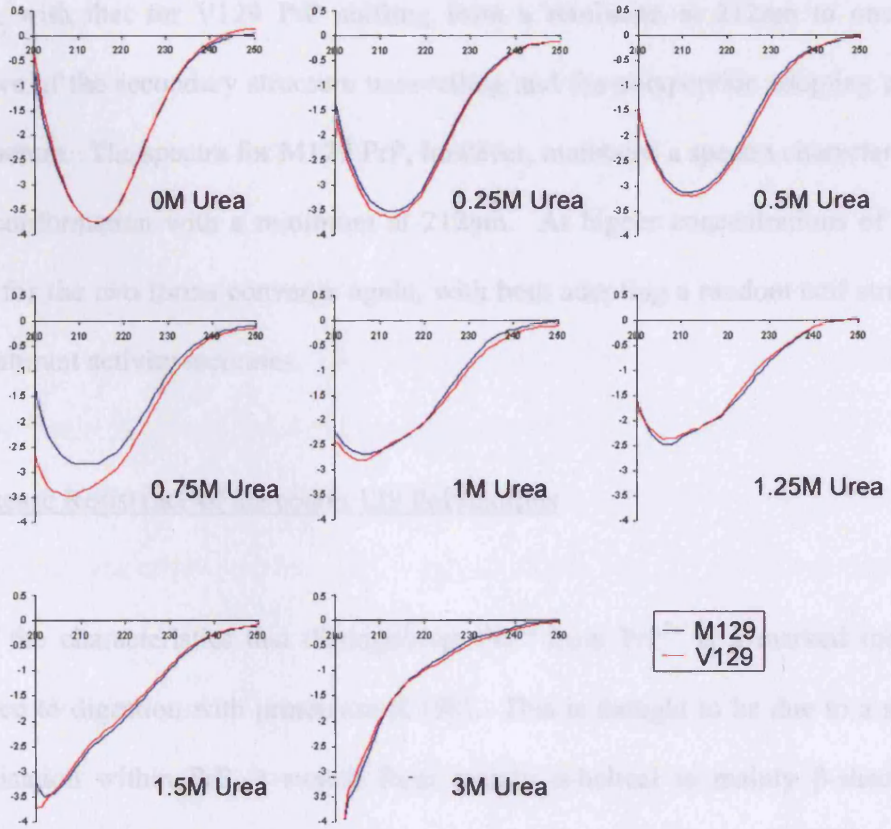

Figure 2.11 Partially denatured circular dichroism spectra for M and V129 β-PrP. M129 (blue) and V129 (red) β-PrPs at a final concentration of 0.5mg/ml were incubated in the presence of the appropriate concentration of urea. CD spectra were recorded as for figure 2.4. Between 0 and 0.5M urea, there was no observable difference between the two polymorphs. At a urea concentration of 0.75M, the spectra for the two forms diverge with M129 exhibiting a greater retention of β-sheet structure. At higher concentrations of urea, spectra for M129 and V129 converge again as both adopt random coil structures.

Between 0M and 0.5M urea there is no observable difference between the spectra for the two polymorphs, with both forms exhibiting spectra characteristic of a predominantly β-sheet conformation. At a urea concentration of 0.75M the CD spectra for the forms

diverge, with that for V129 PrP shifting from a minimum at 212nm to one at 208, indicative of the secondary structure unravelling and the polypeptide adopting a random coil structure. The spectra for M129 PrP, however, maintains a spectra characteristic of a β-rich conformation with a minimum at 212nm. At higher concentrations of urea the spectra for the two forms converge again, with both adopting a random coil structure as the denaturant activity increases.

2.3 Protease Resistance of the codon 129 Polymorphs

One of the characteristics that distinguishes PrP^{C} from PrP^{Sc} is a marked increase in resistance to digestion with proteinase K (98). This is thought to be due to a structural reorganisation within PrP, a switch from mainly α-helical to mainly β-sheet, which results in decreased availability of peptide bonds within the structure of PrP to cleavage by the protease. When infectious homogenates containing different prion strains are subjected to proteinase K digestion, different sized protease resistant fragments are produced which can be distinguished by western blot analysis. Alterations in fragment size resulting from digestion are representative of subtle alterations in three dimensional conformation exposing different residues within PrP to cleavage (224). Based upon this, therefore, proteinase K digestion can be used as a crude tool to probe alterations in secondary and tertiary conformation – with such changes being visualised by the detection of different sized fragments (representative of different cleavage points and, therefore, conformations) separated by SDS PAGE. This method has been applied to recombinant PrP expressed in both prokaryotic and eukaryotic cells, with PrP in the β-

sheet conformation purified from prokaryotic cells and PrP engineered to contain pathogenic mutations in eukaryotic cells both displaying enhanced resistance to proteolytic digestion compared to α-PrP (127;287).

Methods

To investigate whether the codon 129 polymorphism has any effect on protease resistance, recombinant human PrP residues 91-231 containing either methionine or valine at codon 129 were exposed to a range of proteinase K concentrations over a one hour time course. Both α and β-forms of the two polymorphic variants were examined. To control for alterations in proteinase K activity due to low pH, α-PrP was digested at a pH equivalent to β-PrP conditions, allowing a direct comparison between the protease resistance characteristics of the two conformations. Results were examined both for protease resistance and for the production of different sized fragments. 10μl aliquots of 1mg/ml protein of the appropriate codon 129 status and predominant fold (either α or β) were digested with proteinase K at 0.1, 1, 10 or 100 μg/ml final concentration. Reactions were terminated by the addition of 2x SDS loading buffer containing DME and 5mM AEBSF. Samples were heated to 100°C for 10mins and then centrifuged (15,000 g) for 1 minute. 20μl of each supernatant was applied to a 16% Tris-glycine gel (Novex; Life Technologies, Paisley, UK) according to the manufacturer's instructions. Gels were washed with distilled water and then stained with Coomassie blue (Coomassie brilliant blue 0.025%, methanol 40% and acetic acid 7%) for 1 hour followed by destaining with 40% methanol, 7% acetic acid.

Results

In the α-helical conformation, M129 and V129 PrP treated with proteinase K concentrations from 0 to 10μg/ml displayed similar levels of proteinase resistance, being completely degraded by digestion with 10μg/ml for 1 hour (figure 2.12).

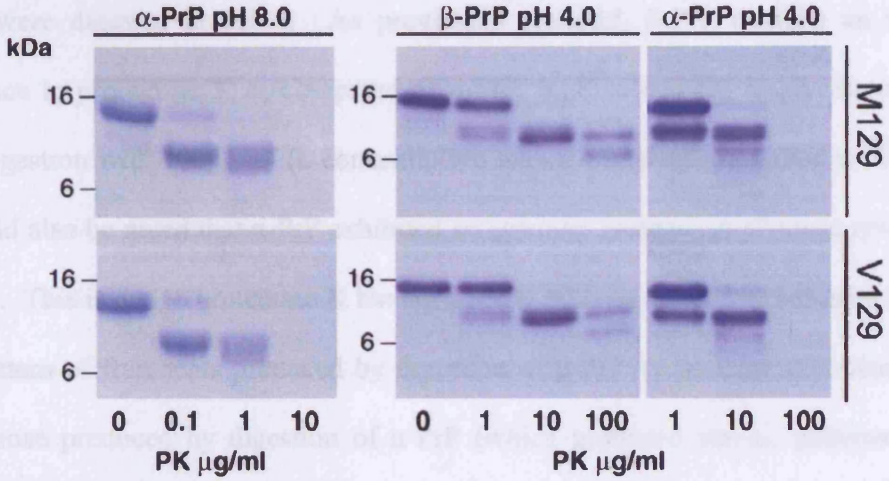

Figure 2.12 Protease resistance of α and β-PrP codon 129 variants. Using identical conditions for digestion, soluble β-PrP has increased resistance to proteinase K when compared to α-PrP. The M and V polymorphs have identical levels of resistance and display similar patterns of cleavage products. The concentrations of PK indicated are the final concentrations in the digestion reactions.

The fragments produced by incomplete digestion with < 10μg/ml PK were similar for both polymorphs – indicating that, within the limits of this technique, there is no observable difference between either the absolute resistance to proteolysis, or the location of proteinase K cleavage sites in the two codon 129 variants. This is what would be expected based upon the structural studies of the α-conformation, considering the close

coincidence of the α-structures of M and V PrP, and agrees with work carried out by Wong *et al* using codon 129 variants on a mouse background (269).

Due to the absence of an atomic resolution structure of the β-sheet rich conformer of PrP, the impact of the codon 129 polymorphism on the protease resistance of PrP is more difficult to predict. Using proteinase K concentrations up to 100μg/ml, both α and β-PrP were digested at pH 4. As previously reported, β-PrP exhibits an increased resistance to proteinase K as compared to α-PrP, with substantial fragments remaining after digestion with 100μg/ml (a concentration which completely digested α-PrP) (127). It should also be noted that α-PrP exhibited an apparent increase in protease resistance at this pH. This is due to proteinase K having a lower activity at pH 4 as compared to pH 8. The pattern of fragments produced by digestion of β-PrP by proteinase K also differed from those produced by digestion of α-PrP (which produced similar patterns whether digested at pH 4 or 8, although at different concentrations of proteinase K), again agreeing with previous work (127). Comparing the two polymorphic variants, both M and V PrP proteins exhibited similar levels of protease resistance at pH 4, whether in the α-helical or β-sheet rich conformation, and no difference could be observed in the fragment patterns produced by the two forms after protease digestion. With special regard to the β-sheet conformation, this suggests that similar cleavage sites are available to proteinase K that, in turn, is suggestive of structural similarities between the two forms. Beyond this, due to the crudity of proteinase digestion as a determinant of structural characteristics, further conclusions are difficult to draw. However, due to the absence of data using more refined techniques, this does supply evidence that there is no gross alteration in structure of β-PrP due to the codon 129 polymorphism.

2.4 Copper Binding Properties of the codon 129 Polymorphs

As previously described (section 1.3), the prion protein binds copper with femtomolar efficiency. It is possible that the polymorphism at codon 129 has an impact on the ability of PrP to bind copper, a subject that was investigated by Wong *et al*, who used mouse PrP with an artificial variation introduced at codon 129 to model the binding of copper ions to PrP (269). They found no alteration in copper binding, but did find evidence for different conformations in M and V forms of the protein that they used upon binding of copper. To investigate whether there are any differences in copper binding between the human codon 129 variants, as opposed to this polymorphism on an artificial mouse background (see section 1.5), and to establish if this resulted in alterations in structure, recombinant prion proteins containing methionine and valine at codon 129 were subjected to metal binding analysis in an attempt to uncover any differential binding ability.

Methods

To analyse the copper binding properties of M129 and V129 recombinant human α-PrP comprising residues 91-231, both forms were dialysed into 5mM MOPS at pH 8 and diluted to a final concentration of 1μM. Copper binding was carried out as described by Jackson *et al* (183). Briefly, 2.5ml of protein in solution was aliquoted into a quartz cuvette and the intrinsic fluorescence of the protein (based upon the presence of a tryptophan at codon 99) was measured using a Jasco Fp-750 Spectrofluorimeter at 20°C. The excitation wavelength was set at 285nm, with emission recorded at 350nm. Once a baseline was set, 25μM Cu^{2+} ($CuSO_4$ in solution) was added 20μl at a time using a glass

syringe, followed immediately by thorough mixing. The decrease in the fluorescence was measured and the process repeated until the curve was saturated. This was then carried out in the presence of increasing concentrations of glycine (200μM and 1mM), which acted as a mild chelator to mitigate the effect of the copper on the fluorescence of the protein and to suppress any weak binding effects, allowing an accurate estimation of copper binding. Fluorescence was then plotted against copper concentration for each condition and data fitted using the equation:

$$F_L = F_0 - (F_{AMP} \times [L]/(K_{d(App)}+[L]))$$

Where F_L is the fluorescence at a concentration of ligand, L; F_0 is the starting fluorescence; F_{AMP} is the flouresence amplitude and $K_{d(app)}$ is the apparent dissociation constant. This allowed the determination of apparent dissociation constants for the two forms. These data were then corrected using the equation below to take into consideration the presence of glycine as a chelator, allowing the real dissociation constant - $k_{d(real)}$ - to be calculated.

$$K_{d(real)} = K_{d(App)} \times (K_{d1}/[G]) \times (K_{d2}/[G])$$

Results

The binding of copper to the two polymorphic variants of PrP was examined at glycine concentrations of 200μM and 1mM (figure 2.13).

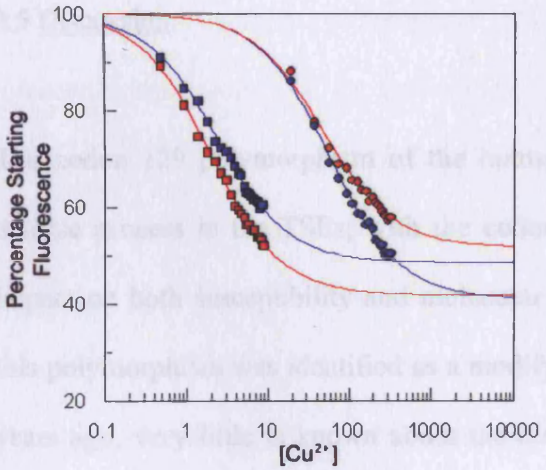

Figure 2.13 Affinity of Cu^{2+} for M and V α-PrP. Copper binding to 1μM M and V α-PrP was calculated by measuring quenching of intrinsic fluorescence from Trp 99 concomitant with addition of Cu^{2+}. Results are shown for M129 and V129 in the presence of 200μM glycine (squares; blue for M129, red for V129) and 1000mM glycine (circles; blue for M129, red for V129) The lines superimposed represent an optimal fit with the equation:

$$F_L = F_o - (F_{Amp} x\ [L]/(K_{d(App)} + [L]))$$

At 200μM glycine, the apparent dissociation constant was 2.0×10^{-6} for V129 PrP and 2.5×10^{-6} for V129 PrP. These increased to 48×10^{-6} and 58×10^{-6} for M and V respectively at 1mM glycine. Once the presence of glycine had been accounted for, the K_d values observed for both binding conditions were equivalent (table 2.1).

	v200	m200	v1000	m1000
% Quench	58	51	49	59
$k_{d(app)}$	2.0×10^{-6}	2.5×10^{-6}	48×10^{-6}	58×10^{-6}
k_d	3×10^{-14}	4×10^{-14}	3×10^{-14}	4×10^{-14}
k_d pH 7.5	7.5×10^{-10}	9.0×10^{-10}	7.5×10^{-10}	8.5×10^{-10}

Table 2.1 Dissociation constants for binding of Cu^{2+} to M129 and V129 α-PrP

In neither case was there an observable difference between the two polymorphic variants, indicating that codon 129 does not affect the binding of copper to the structured C-terminus of human PrP in the α-helical conformation.

2.5 Discussion

The codon 129 polymorphism of the human prion protein is intimately linked to the disease process in the TSEs, with the codon 129 status of individuals having a major impact on both susceptibility and molecular pathogenesis of these disorders. Although this polymorphism was identified as a modifying factor in the prion diseases over fifteen years ago, very little is known about the biochemical mechanism whereby it exerts its influence. This is partly a reflection of our lack of knowledge about all aspects of the prion replication process, but the codon 129 issue has certainly proved to be one of the more enigmatic of the molecular characteristics of the scrapie agent. In this study, recombinant human PrP protein encoding either methionine or valine at codon 129 was examined using a variety of molecular techniques in an attempt to establish a biochemical basis for the effect of this polymorphism.

The starting point for this investigation was to examine whether the codon 129 polymorphism has any impact on the α-helical form of recombinant human PrP, thought to best reflect the cellular isoform of the prion protein. In agreement with previous work, both M and V forms of recombinant human PrP exhibited similar CD spectra and stabilities (as evaluated by equilibrium unfolding in the presence of Guanidine Hydrochloride) (274). Several studies have now indicated that it is unlikely that pathological differences between the two forms of the prion protein originate in the native α-helical state.

The conversion from a mainly α-helical form to a predominantly beta form is central to the pathogenic process in the prion diseases. The equal proclivity of M and V

recombinant PrP to form a predominantly β-fold by refolding at low pH and in reducing conditions was examined by calculating the percentage yield from the conversion process. There was no significant difference between the ability of the two polymorphs to undergo this conversion, indicating that (in this system at least) the ability to convert to the β-rich form is not involved in the pathological differences between the polymorphs. It is, however, difficult to generalise based upon this result as there is much debate as to the exact relationship between the recombinant β-rich form and infectious PrP^{Sc} *in vivo*.

Once in the β-rich form, CD spectra were taken of both M129 and V129 PrP – again with no significant differences observed between the spectra. This indicates that the overall global folds of the two polymorphs coincide closely once in the β-sheet conformation, although circular dichroism is too blunt a determinant of protein structure to elucidate the finer details of their molecular structure. It is therefore impossible, based upon these data, to exclude the possibility that there are significant differences between the secondary and/or tertiary structures of M and V β-rich forms of PrP that are below the threshold of CD detection, and that these result in the phenotypic impact of the polymorphism. Here, the stumbling block of structural determination of the β-rich form appears. As previously discussed in section 1.4, attempts to define the structure of the scrapie agent have, thus far, proved futile. Confirmation of whether there are structural differences between the M and V forms of β-PrP will have to await the development of atomic resolution structures of the two codon 129 variants. Although equilibrium unfolding failed to reveal any difference between the two polymorphs, it is intriguing that the CD spectra of partially denatured M and V PrP in the β-rich conformation revealed different structures at a concentration of 0.75M urea. This suggests that there may be an

underlying difference in the stability and the structure of the two polymorphs, a possibility that requires further investigation.

Another technique used to investigate any structural differences between the two polymorphs was resistance to the action of the proteolytic enzyme proteinase K. Although, again, a very crude guide to the structure of PrP, for the purposes of this study (the uncovering of any biochemical characteristics that differ between the M and V forms of the human prion protein), resistance and proteolytic degradation patterns can be used as a pointer to underlying structural variation. For PrP^{Sc} associated with sporadic and familial CJD, alterations in glycoform ratio following PK digestion have previously been described (see section 1.5). Unfortunately, due to the complex nature of the *in vivo* situation, it is technically very difficult to compare absolute resistance of PrP^{Sc} between cases. This is mainly due to the fact that it is very difficult to calculate the exact starting quantity of resistant material as a percentage of total PrP using existing techniques. This percentage will vary based upon genetic factors, disease progression at time of death, regional PrP^{Sc} deposition patterns within the brain and *post-mortem* delays. With recombinant protein in the β-rich conformation, however, the initial concentrations of protein can be carefully controlled and so any differences in protease resistance can be revealed. Using this approach, and studying recombinant PrP in both α-helical and β-sheet rich conformations, no difference in either protease resistance or fragment pattern was observed between the M and V polymorphic variants. Again, this technique is far too crude to exclude the possibility that there are structural differences between the two forms – but it does suggest that any differences that are present are not gross, major alterations in conformation. It is of interest that, in contrast to these results with

recombinant PrP, the codon 129 polymorphism *in vivo* does seem to have an impact on the protease resistant strain profile. This illustrates the limitations of the existing recombinant models of PrP^{Sc}, as these are as yet unable to fully or accurately replicate the range of conformations occupied by different naturally occurring and experimental strains of infectious prions.

The prion protein binds copper with a femtomolar affinity, although the exact nature of this interaction is still a matter of debate with regard to how many copper atoms PrP binds, and the manner and locations in which this occurs. Using recombinant PrP in the α-helical conformation, the copper binding characteristics of the M and V forms of the human prion protein were examined. As noted in section 2, Wong and colleagues had previously investigated the ability of M and V containing mouse PrP recombinant protein to bind copper, although the relationship between humanised mouse prion protein and the *in vivo* situation in humans is difficult to determine (269). Using human prion protein constructs covering residues 91-231, no significant difference in the copper binding characteristics of M and V forms were observed, agreeing with the results published by Wong *et al.* Based upon examination of 91-231 recombinant prion protein, it seems unlikely that differences in the copper binding abilities (or alterations in structure upon binding of Cu^{2+}) of the M and V forms of the human prion protein plays a significant role in the phenotypic impact this polymorphism has. The possibility cannot be excluded, however, that there is a difference in copper binding between these two forms, but that it would only be revealed by examining copper co-ordination in full length PrP in the β-sheet rich conformation. Although this is not likely, as it would require intimate

cooperation between the unstructured N terminus and residue 129, further studies would be required, using full length (23-231) M and V protein, to resolve this issue.

3.0 Aggregation Properties of the Codon 129 Polymorphs

One of the hallmarks of prion disease, along with other neurodegenerative disorders such as Alzheimer's disease and Parkinson's disease, is the deposition of aggregated protein in the brain. These deposits are often in the form of amyloid, distinguished neuropathologically by its ability to bind Congo red (288). The formation of small aggregates and the deposition of larger, ordered species in the form of amyloid fibrils play an important part in the pathogenesis of the prion diseases, and in the wider field of protein folding disorders, although the exact nature of this role is unclear. One possible mechanism for the codon 129 polymorphism to affect the phenotype of prion disease is by altering the aggregation properties of the prion protein and impacting on the formation of oligomers and larger aggregates. Several studies looking at the formation of oligomers and aggregates by the codon 129 variants have been carried out (see section 1.5), with some evidence that the methionine form has a greater propensity to form oligomers and aggregates than the valine form (262;272;273). There are, however, several areas of the aggregation properties of the two polymorphs that have not yet been investigated in depth, meriting further examination.

Methods

To further investigate the aggregation properties of the M and V codon 129 variants, two approaches were used. First, the properties of both the alpha and beta forms of the two polymorphs were analysed using analytical ultracentrifugation (AUC). AUC is a technique that uses analysis of the sedimentation properties of macromolecules in

solution to examine their hydrodynamics and self-association properties. If one starts with a protein in solution, equally distributed, and place it under a centrifugal force the rate at which the protein sediments (once the solvent and centrifuge conditions have been taken into consideration) is a function of its molecular mass and its partial specific volume, described in the Svedberg equation:

$$S = \frac{u}{\omega^2 r} = \frac{M(1-\bar{v}\rho)}{N_A f} = \frac{MD(1-\bar{v}\rho)}{RT}$$

Where S is the sedimentation velocity, u is the observed radial velocity of the protein, ω is the angular velocity of the rotor, $\omega^2 r$ is the centrifugal field, v is the partial specific volume, M is the relative molecular mass in Daltons, N_A is Avogadro's number, f is the frictional coefficient, D is the diffusion coefficient and R is the gas constant (289). S values are given in Svedbergs, equivalent to 10^{-13} seconds (a none SI unit). An analytical ultracentrifuge measures the radial velocity (u) of a given protein in solution by either ultraviolet absorption or visible absorption relying on alterations to the refractive index as the protein concentration changes (figure 3.1) (290).

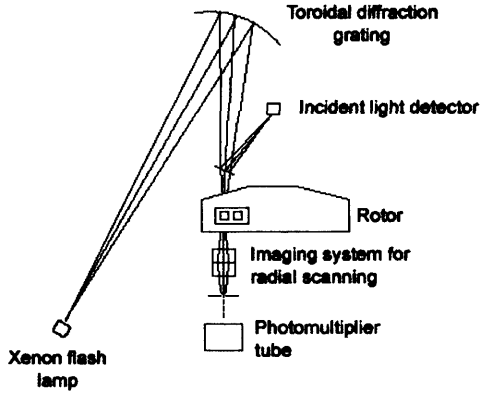

Figure 3.1 Analytical ultracentrifugation setup. Sedimentation in the sample of interest is measured by monitoring changes in absorbtion whilst under a centrifugal field.

This allows the velocity of sedimentation to be calculated. Stokes law, which describes the frictional coefficient for a perfect sphere, can be combined with the Svedberg equation to produce an equation that allows you to predict the S value assuming that the protein is perfectly spherical, taking into account the viscosity of water (291;292).

$$f_0 = 6\pi\eta R_0$$

$$S_{sphere} = 0.012 \frac{M^{2/3}(1-\bar{v}\rho)}{\bar{v}^{1/3}}$$

Where f_0 is the frictional coefficient for a perfect sphere, η is the viscosity of solvent and R_0 is the radius of the sphere in question. Using this information, it is possible to compare actual data to the predicted properties assuming a perfectly spherical structure and thus uncover any deviations due to asymmetry or elongation of the protein structure. With more advanced hydrodynamic modelling, accurate values for molecular mass and important structural information can be gleaned (293). Data captured from sedimentation analysis of a protein in an analytical ultracentrifuge also yields information about the self association properties of that protein. If a population of protein in solution is undergoing sedimentation as an aggregate, be that dimer, trimer or larger association, this will be detected and represented by higher order peaks in the sedimentation profile of the protein (294). This has been used within the field of neurodegenerative disease to examine, for

example, the aggregation properties of wild type α-Synuclein and disease associated mutants (295). Within the remit of this investigation AUC is being used as a tool for probing differences between two proteins: PrP containing methionine at codon 129, and PrP with valine at this position. Any difference in the Svedberg values for the monomeric forms of the protein will be due to altered partial specific volume that is in turn representative of differing three-dimensional structures. In addition to this, the presence of self-associated aggregates (and the ratio of these to the monomeric forms) will also be revealed, with any differences between the two polymorphs being highlighted.

AUC was carried out using a Beckman Optima XL-1 analytical ultracentrifuge. The protein to be analysed was concentrated to 1mg/ml and then three aliquots of 400µl of each were loaded into sample cells, with 400µl of buffer (exactly matched to sample) loaded into reference cells. The rotor was then put under vacuum and spun at 50,000 rpm for 16 hours. During this period, 990 scans were collected. These scans were then analysed using the SEDFIT analysis program (National Institutes of Health, MD, USA), which derives Svedberg values from the sedimentation profile. Both the alpha and beta forms of the two polymorphs were analysed.

Secondly, the ability of the two variants to form ordered aggregates or amyloid fibrils was analysed using a protocol adapted from that used by Baskakov and colleagues (128). This protocol allows real time analysis of amyloid growth by taking advantage of the increase in fluorescence associated with the binding of the dye thioflavin T to amyloid fibrils. Thioflavin T discriminates between disordered aggregates and highly regular amyloid formations, facilitating a specific assay for amyloid growth – a process

also confirmed by analysis of aggregated material using electron microscopy (128). The stimulation of amyloid growth from recombinant prion protein is carried out by agitating the protein in the presence of denaturants, acting to unfolding PrP to an extent that favours its polymerisation*. This has been used by Baskakov and colleagues to analyse the kinetics of amyloid formation by recombinant prion protein from several species, including mouse and human (129). The kinetics of amyloid growth observed with this protocol are consistent with the nucleated seeding model of amyloid generation, showing a lag phase prior to exponential growth of fibrils. Crucially, this lag phase is significantly reduced by the addition of preformed fibrils to the initial starting mixture, again agreeing well with the seeding model. The ability of preformed fibrils to reduce the lag phase prior to amyloid growth has been used by Baskakov to examine the species barrier, using preformed mouse fibrils to seed human growth and *vice versa*. He found that a species barrier does operate in this system, recommending it for use in analysis of any possible differences in amyloid formation between the M and V forms of the human prion protein, and any barrier that may operate between the two polymorphs (129). Crucially, as regards the relevance of this protocol to the *in vivo* situation, mouse PrP fibrils produced using this protocol initiated prion disease when introduced into highly susceptible transgenic mice over-expressing a homologous mouse prion protein construct at a level 16 times greater than wild type (112). The proteinase K resistance of fibril material, and ability of proteinase K treated seeds to stimulate fibril growth, have also been investigated with the evidence suggesting that this model recapitulates many of the structural features of PrP^{Sc} (277). This suggests that the there is a relationship between

* If the protein is shaken at low pH (<pH 4), PrP forms oligomeric species. At higher pH (around pH 6), the formation of amyloid fibrils is favoured.

fibrils formed using this protocol and the *in vivo* infectious process. In order to examine the aggregation properties of the two codon 129 variants PrP, fibril formation was analysed using a protocol adapted from that of Baskakov *et al* (128;129). Recombinant α-PrP of both M and V codon 129 variants were transferred by dialysis into 20mM Sodium Acetate pH 3.7 and denatured by the addition of 10M Urea. The protein was then refolded by dialysis into 1.3M Urea, 1M GuHCl pH 6. A sample of each was taken and analysed by CD as described in section 3.2. To stimulate assembly of monomeric PrP into fibrils, 800μl of 0.8mg/ml protein was aliquoted into 1.5ml eppendorfs and shaken at 37°C and 600rpm. The formation of amyloid fibrils was determined by monitoring of thioflavin T fluorescence. 10μl of sample was removed from the shaking aliquots and diluted 1 in 200 into 5mM Sodium Acetate pH 5.5. Thioflavin T was then added to a final concentration of 50μM and fluorescence measured on a Jasco Fp-750 Spectrofluorimeter (excitation 450nm, emission 485nm) with 5nm band widths.

3.1 Analytical Ultracentrifugation

To examine the self association properties of the two polymorphic variants, and as an additional method of structural comparison, the sedimentation properties of V129 and M129 human PrP were examined by analytical ultracentrifugation. Protein samples were examined in the absence of denaturants (that is, in their native folded conformation). Methionine and valine PrP in a predominantly α-helical conformation were present as monomeric species under these conditions with Svedberg coefficients of 1.74 and 1.80 respectively (figure 3.2).

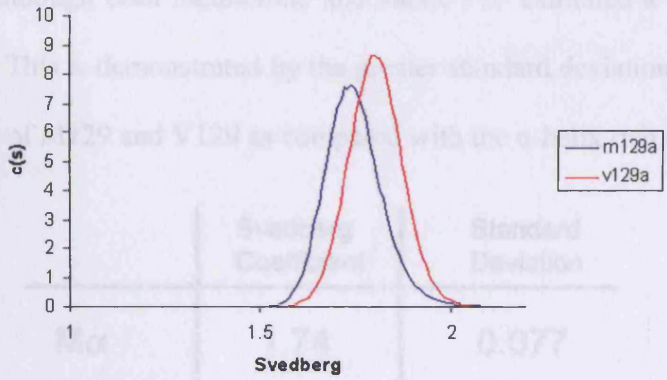

Figure 3.2 AUC profile of M and V129 α-PrP. Protein at a concentration of 1mg/ml was centrifuged at 50,000rpm for 16hrs in a Beckman Optima XL-1 centrifuge. 990 scans were collected and analysed using SEDFIT software. Profiles for M129 (blue) and V129 (red) are shown.

Protein folded into the β-rich conformation was also examined by the same method, with M129 PrP exhibiting a Svedberg coefficient of 1.53, V129 PrP a Svedberg coefficient of 1.81 (figure 3.3).

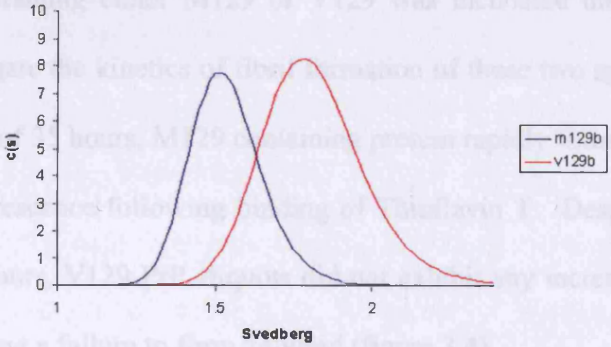

Figure 3.3 AUC profile of M and V129 β-PrP. Protein was analysed as for figure 3.2, with profiles for M129 (blue) and V129 (red) shown.

Both were present as monomeric species, with only one peak Svedberg value identified by this process, although both methionine and valine PrP exhibited a broader range of Svedberg values. This is demonstrated by the greater standard deviation exhibited by the β-rich conformers of M129 and V129 as compared with the α-helix rich form (table 3.1).

	Svedberg Coefficient	Standard Deviation
Mα	1.74	0.077
Vα	1.80	0.068
Mβ	1.53	0.116
Vβ	1.81	0.167

Table 3.1 Svedberg coefficients for α-PrP and β-PrP, M129 and V129 variants.

3.2 Amyloid Formation

Initially, protein containing either M129 or V129 was incubated under the described conditions to investigate the kinetics of fibril formation of these two species. Following an incubation period of 35 hours, M129 containing protein rapidly formed amyloid fibrils as measured by fluorescence following binding of Thioflavin T. Despite an incubation period of over 200 hours, V129 PrP aliquots did not exhibit any increase in thioflavin T fluorescence, indicating a failure to form amyloid (figure 3.4).

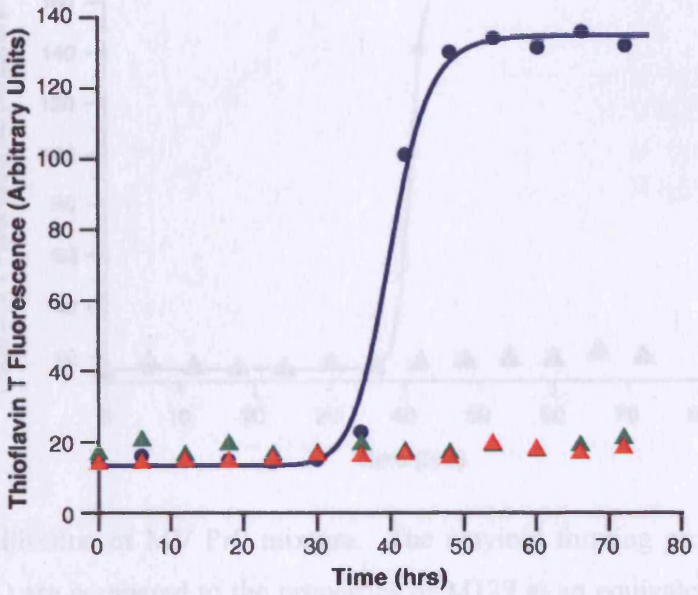

Figure 3.4 Fibrillisation of M129 and V129 PrP. The formation of amyloid fibrils as determined by Thioflavin T fluorescence is shown as a function of time. Fibrillogenesis of M129 PrP (blue, ●) occurs after a lag time of 35 hours, whereas V129 PrP at the same concentration (red, ▲), and twice the concentration (green, ▲) shows no evidence of fibril formation. Data were fitted using the equation $F=F_i+F_f/(1+\exp(-(t-t_m/\tau))$

In order to model the heterozygous state, M129 and V129 in equal proportions (but with a final concentration equal to that used in single species experiments) were incubated under the same conditions. Interestingly, this did not exhibit any amyloid growth, suggesting that there may be a dominant negative impact as methionine protein on its own at an equivalent concentration to the M129 PrP in the 1:1 mixture did form amyloid deposits (figure 3.5).

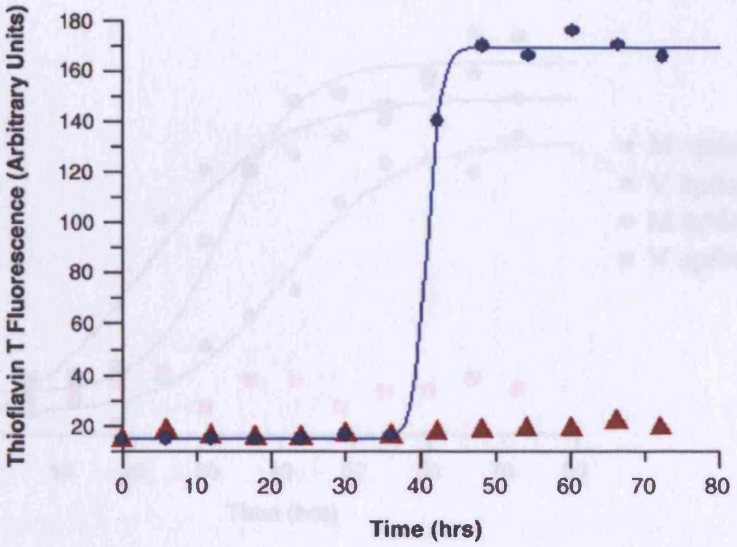

Figure 3.5 Fibrillisation of MV PrP mixture. The amyloid forming properties of a 1:1 MV mixture (▲) are compared to the properties of M129 at an equivalent concentration (●) with a lag time of 37 hours. Measurements were carried out as for figure 3.4.

To investigate the potential for mature fibrils to seed amyloid formation, preformed fibrils made up of PrP containing methionine at codon 129 were spiked at a level of 1% w/w total protein into monomeric V and M huPrP in solution. Spiking of M129 fibrils into M129 monomeric PrP resulted in a rapid seeding process with a significantly reduced lag phase, as would be expected based upon the seeding model of prion propagation and upon previous work carried out using this system (129;262). Introduction of M129 PrP into V129 monomeric PrP also resulted in formation of amyloid fibrils, although after a significantly extended lag phase (figure 3.6).

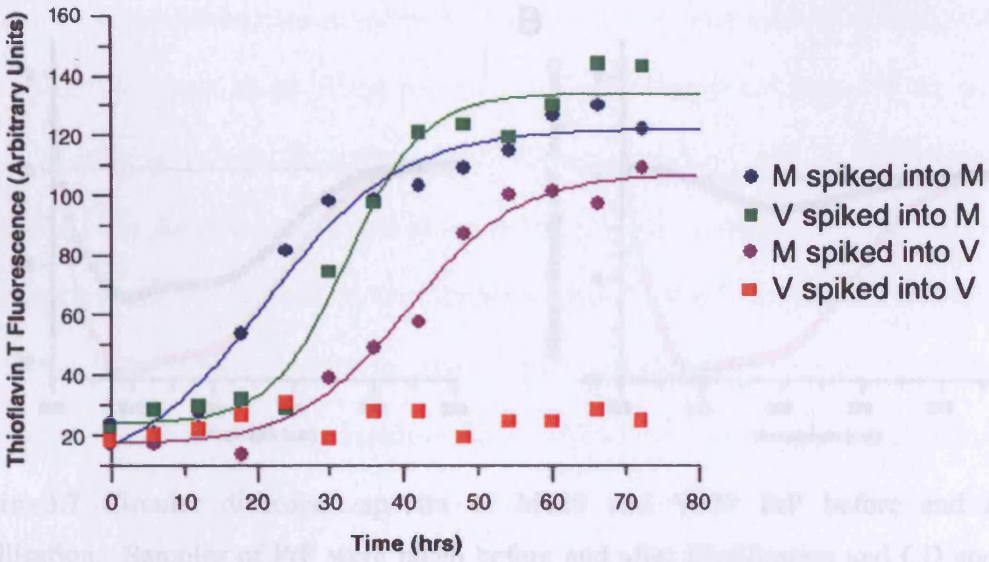

Figure 3.6 Seeding of M129 and V129 fibrillisation. 1% w/w protein (either preformed methionine fibrils or valine 129 incubated in parallel) was spiked into M129 or V129 PrP and incubated at 37°C with shaking. Measurements were taken as for figure 3.4.

This indicates that V129 protein is capable of amyloid formation in suitable conditions (in this case, the presence of a preformed amyloidogenic seed). It is unfortunate that biosafety protocols preclude the analysis of fibrils produced in these experiments by electron microscopy: our group does not have access to an electron microscope in containment level III conditions, required for experiments involving human recombinant PrP. It is possible that important information regarding structural diversity between fibrils made up of methionine and valine could be uncovered using this technique. To gain some insight into any structural alterations that may have occurred, M129 and V129 PrP was analysed using circular dichroism before and after fibrillisation (figure 3.7).

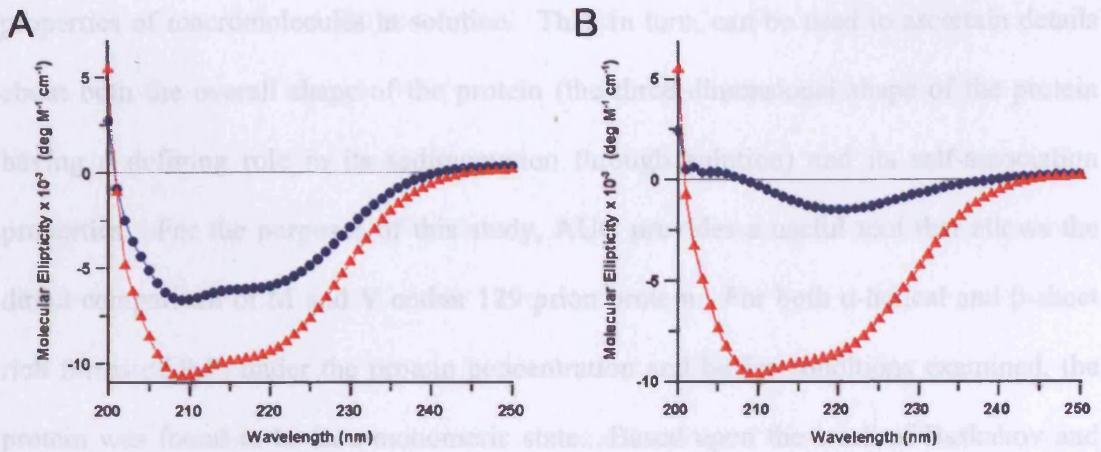

Figure 3.7 Circular dichroism spectra of M129 and V129 PrP before and after fibrillisation. Samples of PrP were taken before and after fibrillisation and CD spectra collected for both M and V codon 129 variants. A) PrP refolded into 1M GuHCl and 1.3M urea prior to incubation in fibril stimulating conditions (37°C and agitation), M129 PrP (blue,●) and V129 PrP (red,▲). B) PrP after incubation in fibril stimulating conditions, M129 PrP in blue (●) and V129 PrP in red (▲).

CD analysis revealed both forms in a predominantly α-helical conformation prior to fibrillisation, although with different molecular ellipticity absorption values with M129 exhibiting a less structured conformation. Following incubation in conditions conducive to fibril formation, V129 PrP maintained a predominantly α-helical conformation, whilst M129 PrP exhibited dramatically reduced absorption and a single minimum around 220nm.

3.3 Discussion

Using analytical ultracentrifugation, several biophysical characteristics of the two codon 129 forms were examined. AUC studies reveal information about the sedimentation

properties of macromolecules in solution. This, in turn, can be used to ascertain details about both the overall shape of the protein (the three dimensional shape of the protein having a defining role in its sedimentation through solution) and its self-association properties For the purposes of this study, AUC provides a useful tool that allows the direct comparison of M and V codon 129 prion protein. For both α-helical and β-sheet rich forms of PrP, under the protein concentration and buffer conditions examined, the protein was found to be in a monomeric state. Based upon the work of Baskakov and colleagues, it may well be of interest to investigate the sedimentation properties of PrP under mildly denaturing conditions, since it is these that are used (in combination with agitation) to stimulate the formation of oligomers and amyloid fibrils. It may be that some measure of self association can be stimulated by the presence of partly folded intermediates. With regard to the Svedberg coefficients, describing the sedimentation properties of the proteins, the α-helical folded M and V PrP variants exhibited very similar S values of 1.74 and 1.80 respectively, with standard deviations of 0.074 for M and 0.068 for V. This is in agreement with work using a wide variety of techniques suggesting that there is no major structural difference between the α-PrP codon 129 polymorphs – as, if there were a structural difference that altered the overall space filling shape of the protein then, this would result in a greater difference in Svedberg values. Both of the β-PrP forms exhibited Svedberg values with a broader distribution, suggesting greater structural heterogeneity (that is, a heterogeneous population of species with very similar structures but with slight variations resulting in subtly altered sedimentation characteristics), reflected in a higher standard deviation from the mean than those exhibited by the α-PrP forms – 0.116 and 0.167 β-PrP SD versus 0.074 and

0.067 α-PrP for M and V respectively. The Svedberg coefficients for the two polymorphs were qualitatively different (M129 1.52S, V129 1.78S). This is evidence, albeit inconclusive, of structural differences between the two forms in the β-conformation, with the suggestion that M129 β-PrP occupies a more spherical conformation than V129 β-PrP, reflected in the lower S value for M129. With regard to both the sedimentation properties of the monomeric species and the possibility of stimulating self association, it would be of great interest to examine the sedimentation properties of β-PrP in mildly denaturing conditions.

Finally, the amyloid fibril forming characteristics of the M and V variants of the prion protein were investigated using the technique developed by Baskakov and co-workers (128). First, the spontaneous formation of amyloid fibrils by methionine and valine recombinant PrP was examined. Surprisingly, it was found that only the protein encoding methionine at residue 129 formed fibrils, as measured by thioflavin T binding, with a lag phase of 35 hours. In contrast, V129 PrP did not form fibrils after a period in excess of 250 hours. This is in disagreement with the results gained by Come and Lansbury, who observed amyloid formation by a 16 amino acid peptide covering residues 118 to 133 of PrP, including both valine and methionine at codon 129 (262). It should be noted, however, that the 91-231 residue polypeptide in semi-denaturing conditions used in the current investigation provides a very different model system to the short peptide in non-denaturing conditions used by Come and Lansbury, and so this result does not contradict their work as much as it might at first appear. This is also the case for the work of Tahiri-Alaoui and James, who observed no difference in amyloid formation between the two forms under native conditions using recombinant protein covering

residues 91-231 (273). They note that they observe differences in amyloid formation under denaturing conditions similar to those used in this investigation, but do not describe these.

The inability of valine 129 PrP to form amyloid fibrils in this model system certainly represents a tangible biochemical difference between the two polymorphic variants, but how does this relate to the phenotypic differences observed in the prion diseases based upon this polymorphism? As with any *in vitro* model of disease, the extrapolation or relation of results to the *in vivo* situation must be made with caution. Although there is some evidence that the Baskakov system can generate infectivity in a transgenic mouse model, it is not yet known what molecular species may be acting to stimulate this (*id est* small oligomeric aggregates, mature amyloid fibrils or an as yet unidentified species) or by what mechanism this may occur, calling into question whether the generation of fibrils has relevance for the infectious process. This is in addition to the issue of what species is actually causing cell death in both the prion diseases and amyloidopothies in general, a matter that is still very much a matter of debate (see section 1.4). With regard to the link between amyloid and the prion diseases, it is noteworthy that, for many prion disorders, amyloid pathology is either not present or not the primary presenting neuropathological feature – again raising questions about the role of mature amyloid fibrils in prion pathogenesis (296). It is also important to take into consideration the conditions under which the fibril formation occurs: in an entirely cell free environment and under partially denaturing conditions. These are artificial conditions, and are not representative of those that would occur in the cellular environment. This may be critical with regard to the interaction of PrP with other cofactors important for the

infectious process (for example protein X, implicated in the replication of PrP^{Sc} by transgenic studies), which may be altered by the codon 129 polymorphism (297;298). It should also be noted that, with respect to the formation of amyloid material from other polypeptides, the conditions under which this can occur vary greatly from protein to protein – for example the formation of amyloid from the SH3 domain occurs at low pH and in native conditions, in contrast to the pH 5.5 denaturing conditions used in the Baskakov protocol (299). The inability of V129 PrP to form fibrils could, therefore, represent behaviour in none ideal conditions, with amyloid formation occurring at a different pH or under slightly different denaturing conditions. This would still be indicative of a biochemical impact of the codon 129 polymorphism, but perhaps a more subtle alteration in structure or stability favouring the formation of amyloid in different conditions than such a stark difference in amyloid forming ability in this system would suggest.

It is, however, of interest that methionine homozygotes are significantly overrepresented in transmissible and sporadic human prion disease, most obviously in the case of vCJD (valine homozygotes are also overrepresented, although not to the same extent – see section 1.5). Making the assumption that mature amyloid fibrils are directly involved in the disease cascade (as indicated above, not necessarily warranted), the high numbers of methionine homozygotes afflicted by these diseases would be congruent with the fibril forming data. This would not, however, explain why valine homozygotes are also more likely to develop disease than heterozygotes, which suggests that the situation is more complex than methionine 129 PrP forming amyloid and valine 129 PrP not doing so.

Thus far, only the homozygote condition had been examined. In order to further investigate the amyloid forming properties of huPrP in this system, a 1:1 mix of methionine and valine was incubated under standard conditions, modelling the situation in heterozygotes. In addition to this, methionine fibrils, and valine protein incubated in parallel to the fibrils, were spiked into methionine and valine protein samples which were then incubated using the standard protocol. This had the dual aim of providing more information about the mechanism of growth in heterozygote conditions as well as acting as a simple model of transmissible disease. Under these conditions, the 1:1 M/V mix did not exhibit fibril growth, suggesting the possibility of a dominant negative effect of valine on the growth of methionine fibrils. In the spiking experiments, methionine fibrils spiked into a methionine substrate resulted in a decrease of the lag phase prior to fibril formation from 35 hours to 15 hours, as one would expect based upon the work of Baskakov and colleagues. Valine spiked into valine had no impact, with no stimulation of fibril growth. When methionine fibrils were spiked into a V129 substrate population, however, fibrils were generated, albeit with an extended lag phase as compared to methionine only growth. When valine was spiked into a methionine substrate, fibril growth did occur with a reduced lag phase as compared to *ab initio* methionine growth – although not as rapidly as induced methionine fibril growth due to introduction of a preformed methionine fibril spike.

These data reveal a complex picture of amyloid fibril growth on a methionine/valine background in this *in vitro* system, perhaps only to be expected given the complexities of the *in vivo* situation. The decrease in lag phase seen with the methionine fibrils spiked into a methionine substrate certainly supports the supposition

that this echoes the work carried out by Baskakov and colleagues, and is consistent with the seeded nucleation model of prion - and amyloid – replication (see section 1.2.3). The spiking of valine into valine did not result in any fibril growth – since no fibrils were detectable in the material acting as a spike despite incubation in conditions favourable for amyloid formation this was only to be expected. Intriguingly, when preformed methionine fibrils were spiked into a valine substrate population, fibril growth was stimulated – although both less rapidly and after a longer lag phase than either methionine 129 PrP alone or seeded methionine PrP. This provides evidence that valine is capable of forming fibrils in this model system and under these conditions if the kinetic barrier to the formation of nuclei capable of stimulating fibril growth is overcome in some way (either through the addition of preformed nuclei or possibly by the manipulation of conditions to favour nuclei formation *ab initio*). This, again, supports the hypothesis that the difference between the two forms is more subtle than initial results would indicate. It is of interest that valine spiked into a methionine substrate appears to slightly decrease the lag phase prior to exponential growth, especially in the light of the fact that no growth was observed in a 1:1 mix of M and V. This suggests the possibility that although valine 129 PrP is not capable of forming fibrils on its own, there may be disordered oligomers present that are capable of stimulating the growth of methionine fibrils – again suggestive of a mechanism dependent upon subtle differences in secondary/tertiary structure or in stability for initiation of fibril growth in a strain dependent manner (were there no strain barrier operating, one would expect reciprocal growth with identical reductions in lag phases). This is supported by the CD spectra recorded for the pre-fibrillisation experiment, which suggested that M129 retains less

secondary structure in the conditions used in these experiments. The increased flexibility in the peptide backbone of PrP that this may represent might favour the formation of amyloid seeding nuclei.

The fact that no growth was observed in the MV 1:1 mix is particularly interesting from the point of view of the *in vivo* heterozygote condition. It provides evidence, although by no means conclusive, that in addition to a strain barrier of some kind operating between the two codon 129 variants (as suggested by the spiking experiments), that there may be an antagonistic aspect to the relationship between the variants: with valine having a dominant negative impact on the growth of methionine fibrils. Since the methionine PrP was present in conditions and at a concentration that had been shown to favour the formation of fibrils, the only possible conclusion is that the presence of valine PrP is in someway inhibiting the growth of amyloid consisting of M129. There are several mechanisms whereby this could occur. It is possible that the kinetics of formation for MV heterodimers/oligomers are more favourable than those for methionine alone or valine alone, and so recruit more of the monomers available in free solution. If it is then assumed that small MV aggregates do not favour the formation of nuclei capable of seeding amyloid fibril growth, or that the MV heterodimer itself is a kinetic dead end, a dominant negative affect would result. It is also possible that the addition of a monomeric species not related to a nascent fibril has a chain terminating impact (*exempli gratia* V129 PrP "capping" M129 PrP fibrils) similar to that of dideoxynucleotides in the process of DNA replication (300;301). This is unlikely, however, due to the positive growth results of the spiking experiments – where a methionine seed could stimulate valine fibril growth and *vice versa*. This must have the

proviso, however, that there is not a critical threshold operating below which heterologous monomer addition terminates growth, perhaps below the nucleation point, and above which the maturing fibril can tolerate such addition, a possibility that requires investigation. If the results of the MV growth experiments are bourn out by examination of the behaviour of MV 1:1 mixed populations in a range of conditions, they may have important ramifications for our understanding of the heterozygote situation *in vivo*. If there is some form of dominant negative impact by V129 containing protein on the aggregation properties of the M129 form, this may go some way towards explaining the resistance of heterozygotes to transmissible prion disease, and their low frequency in sporadic prion disease. Again, this requires much in the way of further investigation, but is certainly an intriguing possibility.

These data, taking into consideration M and V individually, spiking experiments and the MV mix results, suggest a model for this system (utilising recombinant PrP covering the structured domain of PrP, at pH 5.5 and in partly denaturing conditions) that differs from the model proposed by Come and Lansbury (section 1.5). This model excludes growth in the MV heterozygote situation, although the mechanism of this is not yet clear, and assumes that the kinetic barrier for formation of MV oligomers is lower than that for M129 fibrils, which is turn is lower than that for V129 fibrils (figure 3.8).

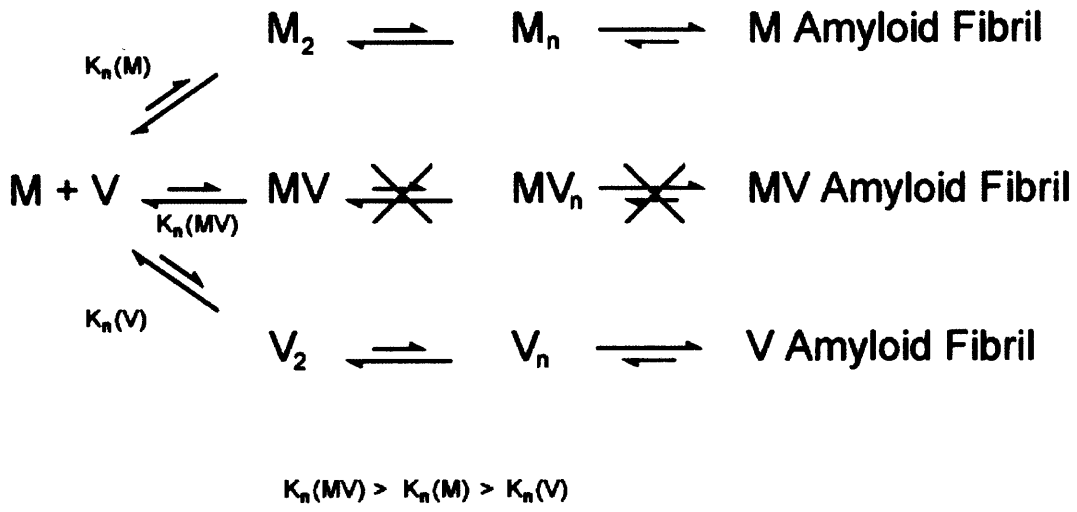

Figure 3.8 Nucleation model of codon 129 polymorphism variation. Based upon the model proposed by Come and Lansbury (figure 1.15), this model takes into account the dominant negative affect witnessed with the MV 1:1 mixture and the inability of valine 129 PrP to form fibrils (262).

In the current conditions, the barrier preventing formation of V129 nuclei (and thence fibrils) is high enough to prevent amyloid growth unless it is circumvented, for example, by the addition of preformed M129 fibril nuclei. This is not to say that, in conditions perhaps more favourable to the development of valine 129 fibrils, the reverse situation is possible with valine growth favoured over methionine or that MV amyloid fibril growth may occur. There is obviously much that remains to be investigated regarding the behaviour of PrP in this system, and any model based on this work must be considered incomplete at best. The *in vitro* techniques used in this investigation do, however, provide a powerful tool for the dissection of the basic mechanisms of aggregation involved in the prion diseases, in particular for the molecular properties that result in the species barrier and the phenotypic variation associated with the codon 129 variants. In

regard to this, the experiments described herein have identified the molecular aggregation properties of the two codon 129 variants as an area that merits further investigation, and potentially a molecular characteristic that may provide a biochemical basis for the phenotypic impact of this polymorphism.

4.0 Characterisation of the Cathepsin D Proteolytic Cleavage of PrP

4.0.1 PrP and its GPI Anchor

The attachment of a glycosylphosphatidylinositol (GPI) anchor to the prion protein was first described in 1987 (122). GPI anchors are glycolipid moieties that are covalently linked to polypeptides and facilitate their attachment to the plasma membrane (302). They are found throughout the eukaryotes, and can be found attached to a range of proteins with differing functions (303). The main theme uniting GPI anchored proteins in terms of their biology is their attachment to the plasma membrane, and their localisation to cholesterol-rich regions in the membrane (known as lipid rafts) (191). As post translational modifications, GPI anchors are added to nascent proteins upon translation in the ER, and are often themselves modified as they pass through the Golgi apparatus (304). Although the structures of several GPIs have been elucidated, there is marked heterogeneity in the exact chemical composition of GPIs attached to specific proteins and much remains to be uncovered about the biochemistry of these lipid tails (figure 4.1) (305).

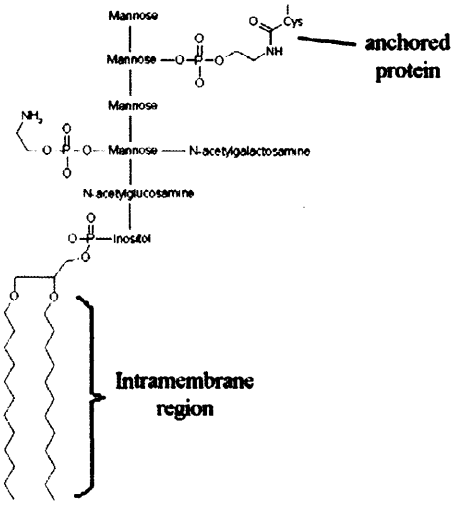

Figure 4.1 Glycosylphosphatidylinositol anchor structure. This shows the fatty acid moeities that sit within the membrane to anchor the GPI to the cell surface, with the sugars and phosphate groups that link the intramembrane region to the protein to be anchored.

Since the cellular role of the prion protein *per se* is somewhat enigmatic, it is not surprising that the role of the GPI in the function of PrP is unknown. It has been suggested, however, that the localisation of PrP to lipids rafts on the cell surface (due to its GPI attachment) is indicative of a role in either copper transport or signal transduction, although this is still very much a matter of debate (see section 1.3).

A useful tool in the study of GPI anchors and their role in the biochemistry of the proteins to which they are attached is the enzyme phosphodiesterase phosphoinositide phospholipase C (PIPLC). This enzyme acts to cleave the polar head group from inositide residues (306). In the case of GPI anchored proteins, this has the effect of separating the membrane imbedded lipid tail from the protein linked polar head group(figure 4.2).

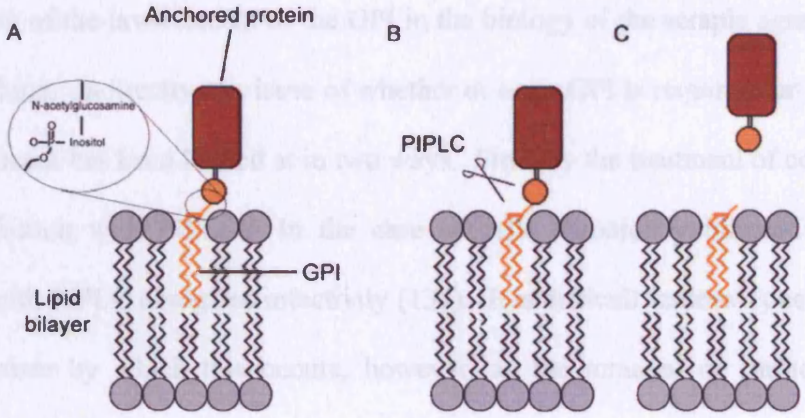

Figure 4.2 Phospholipase cleavage of GPI anchor. A) A GPI anchored protein sits on the cell membrane attached by the hydrophobic fatty acid tail of the GPI. B) PIPLC attaches to the inositol link between the fatty acid tail and the anchored protein, and breaks this link C) the anchored protein is released from the cell membrane, whilst the fatty acid tail remains inserted into the bilayer

In most cases this results in the release of the protein from the cell membrane, although some proteins maintain association with the extracellular face of the membrane via hydrophobic interactions or transmembrane domains. In the case of cells in culture, treatment with PIPLC results in the release of anchored proteins into the cell medium, leaving the GPI anchor attached to the cells. This is the case with PrP^{C}, and treatment with PIPLC has been used to investigate the cell biology of the prion protein (307). Interestingly, in addition to increasing the protease resistance of PrP, conversion to the scrapie isoform also results in resistance of the GPI anchor to cleavage by PIPLC (217;308). It has also been noted that PrP containing pathogenic mutations expressed in cell culture acquires resistance to PIPLC cleavage of its GPI (218).

The resistance of PrP^{Sc} to PIPLC has precluded the use of this enzyme in the investigation of the involvement of the GPI in the biology of the scrapie agent, at least in a direct fashion. Indirectly, the issue of whether or not a GPI is required for the infective process to occur has been looked at in two ways. First, by the treatment of cell models of scrapie infection with PIPLC. In the case of cells chronically infected with PrP^{Sc}, treatment with PIPLC abrogates infectivity (137). It is difficult to draw conclusions as to the mechanism by which this occurs, however, as the removal of surface PrP^{C}, the consequence of treatment of these cells with PIPLC, would act to decrease the concentration of cellular PrP available for propagation of the scrapie isoform. The treatment of cells prior to their infection has also been investigated, with the same affect (137). This could suggest that the loss of surface PrP^{C} prevents infection, although a mechanism involving a decrease in the absolute quantity of PrP^{C} cannot be excluded.

Secondly, PrP constructs with a stop codon at position 231 rather than a GPI attachment peptide sequence have been produced in cell culture (309). These cells have then been exposed to infectious agents and it has been shown that they are capable of propagating PrP^{RES}, although with decreased efficiency as compared to wild type protein. It should be noted that the infectivity of this protease resistant PrP without the GPI anchor has not been examined, and the cell culture system in which this was carried out (N2a cells over-expressing a truncated mouse/hamster chimeric PrP) could produce confounding conditions due to the presence of a heterologous population of PrP^{C} – the endogenous wild type mouse PrP and the chimeric fusion interfering with each others propagation. Work has also been carried out to examine whether the localisation of PrP to lipid rafts is essential for the conversion of PrP^{C} to PrP^{Sc}, examined by depleting the cholesterol levels of cells in culture using Lovastatin (310). Cholesterol is an essential component of lipid rafts, and GPI anchored proteins cannot be inserted into rafts without it (311;312). The impact of this was to prevent infection with scrapie, although whether this is specifically due to loss of lipid raft domains or due to increased cell stress *per se* as a result of cholesterol depletion is difficult to assess. In the same study, chimeric PrP with a transmembrane domain replacing the GPI was also produced in cells – resulting in the protein locating away from lipid rafts in the lipid bilayer. This construct did not convert to the protease resistant state, suggesting that either the GPI or the association of PrP with lipid rafts is important in the conversion process. Intriguingly, a recent report from the group of Bruce Chesebro at the Rocky Mountain Laboratories described transgenic mice expressing moPrP 23-231stop on a mouse PrP knockout background (thereby avoiding the problem of a heterogeneous population of PrP). These mice did not

develop disease when exposed to mouse adapted scrapie strains, but neuropathological examination revealed extensive extracellular deposits of protease resistant prion protein. This would suggest that the location of PrP at the cell surface due to its anchor is important in the toxicity of PrP^{Sc} but not necessarily in its generation. Again, this experiment does not directly examine the role of the GPI in infectivity. Rather it looks at the importance of cellular location (since much of the PrP is secreted from the cells) in the toxicity of the infective process, and the requirement of the GPI dependent location in *susceptibility* to infection (313).

A recent study by Kishida *et al* examined the introduction C-terminally truncated recombinant PrP as an antagonist of the replicative process in cell culture (314). By exposing chronically infected N2a cells to recombinant human PrP containing a Q218K mutation, the cells were cured of infection. The authors suggested that this was indicative of PrP lacking a GPI anchor inhibiting the process of replication, although again it is difficult to extricate the absence of a GPI from the impact of the mutation at codon 218 and the absence of glycosylation. It should also be noted that many compounds have been shown to be efficacious in curing cells in culture of "infection" without replicating such affects in infected animals, calling into question the relevance of this to the *in vivo* situation (138).

Of greater relevance to the disease situation is a familial GSS mutation reported by Kitamoto and colleagues in 1993. They described a GSS patient with an amber Y145Stop mutation in the *Prnp* gene, which results in a C-terminally truncated form of the prion protein (315). The patient in question had a large number of kuru-like plaques and, unusually, deposition of PrP as amyloid in the cerebral vascular system (316). This

was coupled with accumulation of the microtubule associated protein τ as paired helical filaments, indistinguishable from those found in Alzheimer's disease. Analysis of the deposited PrP revealed that only C-terminally truncated protein had been laid down, a finding that has been replicated in some amyloid plaque bearing cases of GSS without truncating mutations (317). This suggests the possibility that C-terminal truncation may play a role in deposition of PrP as an amyloid species. Unfortunately, this mutation has only been described in one patient and has not been proven to segregate with disease, making categorical statements about its disease causing nature impossible. It should also be noted that attempts to transmit experimentally this case of GSS proved unsuccessful, calling into question whether this case represents genuine prion disease (where the presence of infective material can be established) or a rare case of PrP amyloidosis (318;319).

As PrP^{Sc} is resistant to the action of PIPLC, this enzyme cannot be used to investigate the role of the GPI in the biology of the scrapie agent. An alternate approach to the use of PIPLC is to use a proteolytic activity that can remove a small C-terminal fragment of PrP, and thereby the GPI anchor, whilst leaving the core of PrP^{27-30} intact. Following a screen of proteases for the generation of novel cleavage patterns of type 4 human PrP^{Sc} such an activity was identified. During this screen, treatment of type 4 vCJD homogenate with the enzyme cathepsin D was discovered to result in an anomalous apparent increase in relative molecular mass. This is counter to what one would expect following treatment of a protein with a protease, as this should result in a decrease in molecular mass following cleavage of the protein and loss of amino acids. This apparent increase in molecular mass is analogous to that seen when PrP^{C} is treated with PIPLC to remove the

GPI anchor (218). The band shift upward that occurs with the loss of the GPI is essentially an artefact of SDS polyacrilamide gel electrophoresis (303). As the GPI is highly hydrophobic, it binds SDS with high affinity and its acyl chains attract more SDS molecules per unit mass than the polypeptide backbone of the protein (which binds approximately 1 molecule of SDS for every 2 amino acid residues) (320). This results in the GPI having a high negative charge following boiling in SDS as preparation for running on an acrilamide denaturing gel, yielding a faster rate of migration through the gel towards the cathode than would be expected for a protein of a given size. When the GPI is removed, this decreases the overall negative charge of the denatured protein more than the proportional loss of mass, resulting in an apparent retardation of the protein when analysed by SDS PAGE (figure 4.3).

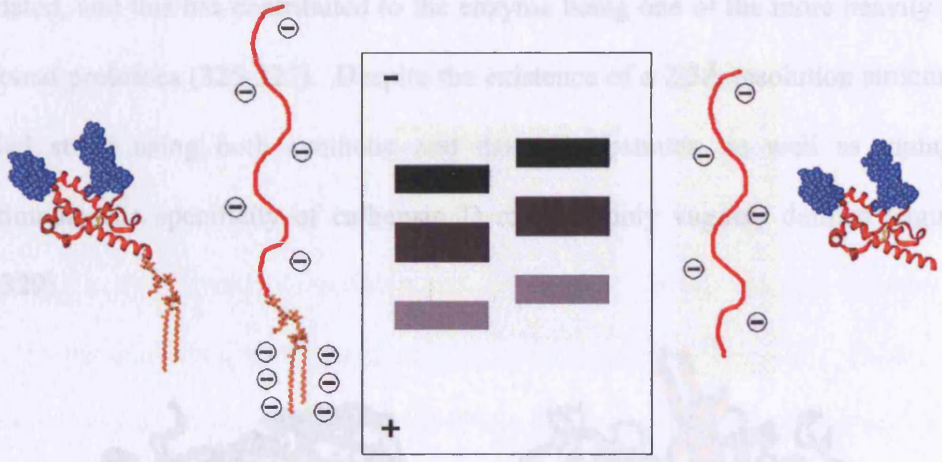

Figure 4.3 Polypeptide gel retardation due to loss of GPI anchor. Protein with a GPI attached (left hand panel) binds a disproportionately large amount of SDS when denatured prior to SDS gel electrophoresis due to the extremely hydrophobic nature of the GPI. With the GPI removed (right hand panel), the protein has a lower net negative charge. This results in decreased migration under electrophoretic field as compared to a protein with an intact GPI (central panel).

In order to examine the impact of GPI removal on the molecular characteristics of the scrapie agent, this study has two parts. First, an investigation of the cleavage event itself to characterise the nature of the interaction between cathepsin D and the scrapie agent. Secondly, to use the C-terminal truncation of PrP^{Sc} by cathepsin D to examine the impact, if any, that removal of the GPI anchor has on the infectivity of the scrapie agent.

4.0.2 Cathepsin D

Cathepsin D is an aspartic endoprotease located in the lysosomal degradation pathway (321;322). As would be expected for a protein involved in such a pervasive cellular pathway, cathepsin D is expressed ubiquitously and indeed constitutes up to 10% of lysosomal liver proteins (323;324). The NMR solution structure of cathepsin D has been elucidated, and this has contributed to the enzyme being one of the more heavily studied lysosomal proteases (325-327). Despite the existence of a 2.5Å resolution structure, and detailed study using both synthetic and natural substrates, as well as mutagenesis experiments, the specificity of cathepsin D remains only vaguely defined (figure 4.4) (328;329).

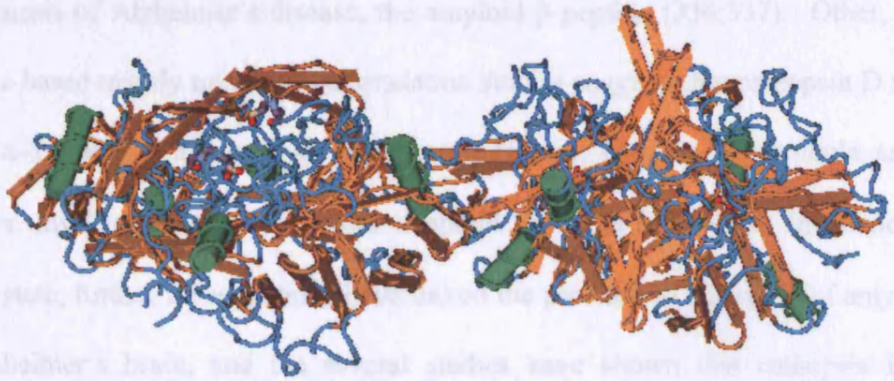

Figure 4.4 Atomic resolution structure of cathepsin D. Taken from reference (327).

Such specificity as exists is limited to a preference for cleavage between two hydrophobic residues (330-332). The protein itself is produced as *circa* 400 residue precursor (412 in the case of human cathepsin D, from a gene located on chromosome 11) termed procathepsin D (333). Following translation, the protein can undergo cleavage to form heavy and light chains which then associate to form an active protease, although the uncleaved form also has proteolytic activity (334). In terms of the cell biology of cathepsin D, it is found in an active form in the lysosomes and endosomes, where it plays an active role in the degradation of proteins targeted to these organelles (326).

Cathepsin D has been implicated in several diseases. The enzyme is over-expressed in breast tumours and is sometimes used as a biochemical marker for breast cancer, although whether it is involved in the aetiology of the disease is a matter of debate (335). Of greater relevance to this investigation, cathepsin D has been linked to several neurodegenerative diseases, most notably Alzheimer's disease. At a biochemical level, evidence from both *in vitro* and *in vivo* studies has shown cathepsin D to be involved in the normal degradation of the amyloidogenic protein central to the pathogenesis of Alzheimer's disease, the amyloid β peptide (336;337). Other, scantier, evidence based mainly on *in vitro* degradation studies suggests that cathepsin D may also act on α-Synuclein, involved in Parkinson's disease, and the microtubule associated protein τ, involved in AD and frontal temporal dementia (338;339). In relation to the disease state, further investigations have linked the protease to clearance of amyloid β in the Alzheimer's brain, and the several studies have shown that cathepsin D is up-regulated in brain tissue from Alzheimer's patients (340-342). It is, however, unclear as

to whether this is specific for cathepsin D or a more general up-regulation of the lysosomal degradation pathway (343). Providing an interesting genetic parallel for the biochemical interactions of cathepsin D and amyloid β is evidence that a polymorphism in the human form of cathepsin D, a C ⇒ T transition (resulting in a switch from alanine to valine) in codon 224, is a risk factor for late onset Alzheimer's disease (344;345). Researchers have found that the valine form of this allele was significantly over-represented in patients affected by Alzheimer's disease, with carriers of this allele having a 3.1 fold increased risk of developing disease as compared to non-carriers. The association is, however, controversial, as a subsequent attempt at verification in another population has returned a negative result (346).

There is also evidence that cathepsin D has some links to the disease process in the prion disorders. A study by Diedrich *et al* looking at neuropathology in scrapie and Alzheimer's disease showed that changes associated with disease were also associated with increased levels of cathepsin D (347). Cathepsin D has been identified in microarray screens looking for up-regulated proteins in scrapie infected mouse brains (348). Whether there is a link between upregulated cathepsin D and the fact that the endosomes and lysosomes have been linked with the replication of PrP has not been examined. A caveat to these studies is that, as in Alzheimer's disease, it remains unclear as to whether this is representative of a cathepsin D specific affect or whether this is representative of a more general up-regulation of lysosomal degradation in the diseased brain as would be expected to be concomitant with the deposition of abnormally folded protein.

Methods

Whole mouse brains from normal and RML-infected CD-1 mice were homogenised as a 10% w/v preparation in Dulbecco's phosphate-buffered saline (PBS) without calcium and magnesium ions using a Dounce homogeniser. Homogenates were split into aliquots and stored at -80°C. Mouse recombinant protein comprising residues 91-231 was produced as described in section 3.1.

Protease Treatment

Cathepsin D digests were carried out using bovine spleen cathepsin D (Merck), freshly made up in 1x PBS. Standard digest conditions were as follows: 10% w/v infectious brain homogenates were thawed and centrifuged at 100g for 1 minute to remove gross cellular debris. 10µl aliquots of 10% w/v homogenate supernatant were then digested with 100 units of cathepsin D for 4 hours at 37°C with shaking at 450rpm. Following this, samples were digested with Proteinase K (Sigma) at a final concentration of 50µg/ml for 1 hour at 37°C (232;349). Digests were terminated by the addition of 2x SDS sample buffer buffer [125 mM Tris.HCl (pH 6.8), 20% v/v glycerol, 4% w/v sodium dodecyl sulphate, 4% v/v 2-mercaptoethanol, 0.02% (w/v) bromophenol blue] containing 8 mM 4-(2-aminoethyl)-benzene sulfonyl fluoride (AEBSF; Pefabloc SC, Roche, Lewes, UK). In the case of cathepsin D digests carried out in the presence of ethylenediaminetetracetic acid (EDTA), 20mM EDTA (Sigma) was added to the reaction mixture and RML control samples.

Western Blot Analysis

Following the addition of 20µl of 2 x SDS-loading buffer, samples were heated to 100°C for 10mins and then subjected to centrifugation in a microfuge (15,000 g) for 1 minute. 20µl of each supernatant was applied to a 16% Tris-glycine gel (Novex; Life Technologies, Paisley, UK) according to the manufacturer's instructions. Gels were electrophoresed at 200 volts for 80 minutes and electroblotted onto PVDF membrane at 35 volts for 90 minutes (Immobilon-P; Millipore, Watford, UK). The resulting membrane with bound protein was then blocked in PBS containing 0.05% (v/v) Tween-20 (PBST) and 5% (w/v) non-fat milk powder for 60 min. After washing in PBST, the membranes were incubated with anti-PrP monoclonal antibody ICSM35 (D-Gen Ltd, London) diluted to 0.2µg/ml in PBST for at least 60 min before washing in PBST (30 min) and incubation with an alkaline phosphatase-conjugated goat anti-mouse antibody (Sigma, Dorset, UK) diluted 1:10,000 in PBST for 60 min. Following washing in PBST (30 min), the membranes were developed using AttoPhos reagent (Promega Corp., USA) and visualized on a Molecular Dynamics Storm 840 (Amersham, UK).

Cell Culture

The murine neuroblastoma cell line, N2a, was used throughout. Cells were cultured in OPTI-MEM with 10% fetal calf serum (OFCS) and 100U/ml of both penicillin and streptomycin (Invitrogen Corp.). PIPLC treatment of cells was carried out by removal of

growth media from confluent cells in a 10cm dish and addition of PBS containing either 200mUnits PIPLC (Sigma) or 100Units cathepsin D. Cells were incubated for 3hrs and the culture supernatant harvested. 300µl of culture supernatant was mixed with 4 volumes of ice-cold methanol and centrifuged for 30 minutes at 25,000g and 4°C. The precipitated protein was then re-suspended in 20 µl of PBS and analysed by western blot as described above.

Phase Separation

Phase separation was carried out based upon the protocol of Parkin *et al* (350). Prior to phase separation, 25µl RML samples were incubated with either 25µl of 20U/µl cathepsin D or with an equivalent volume of PBS as a control for 2hrs at 37°C with shaking at 450rpm. Both samples were then digested with proteinase K at a final concentration of 50µg/ml for 1hr at 37°C. Digests were terminated by the addition of AEBSF to a final concentration of 5mM. The samples were then mixed with 150µl of 10mM TrisCl pH 7.4, 150mM NaCl, 2% Triton X-114 and incubated at 4°C for 10mins, followed by a 3 min incubation at 30°C. Both aliquots were then layered onto a 300µl 6% w/v sucrose cushion and spun for 3mins at 3000g. Aqueous and detergent phases were separated and volumes made equivalent using 10mM TrisCl pH 7.4, 150mM NaCl. 20µl of each phase was then taken and western blotted using standard protocols.

Solubility Analysis

20µl of 10% w/v brain homogenate from RML infected mice were treated for 2hrs with 20µl of 20U/µl cathepsin D or an equivalent volume of PBS as a control. Both were then digested with proteinase K under standard conditions, with the digest terminated by the addition of AEBSF to a final concentration of 5 mM. Following this, 2% sarkosyl was added to the samples. These were then layered onto a 10%⇒60% w/v discontinuous sucrose gradient and centrifuged at 100,000g for 1hr at 4°C in an Optima XL 100K ultracentrifuge (Beckman) using a swing bucket rotor (SW 60Ti). Gradient fractions were then collected, with the interface between each discontinuous step in the middle of each fraction. 250µl of each fraction was then subjected to methanol precipitation: 4 volumes of ice cold methanol was added to each sample and mixed thoroughly prior to centrifugation at 15,000g, 4°C. The methanol was then aspirated and the pellets air dried for 30mins. Following this, the protein pellets were re-suspended in 20µl of PBS and western blotted using standard protocols.

4.1 Species Specificity

The initial observation of gel retardation following cathepsin D treatment was made during a screen of proteases looking for differential impact on type 4 human PrP^{Sc}, associated exclusively with vCJD. To investigate the strain and species specificity of this phenomenon further, infectious brain homogenates from two other human strain types, type 2 and type 3 (associated with sporadic and hereditary forms of the disease), and from

a selection of animal models of prion disease (the mouse adapted scrapie strain RML, mouse adapted BSE strains MRC1 and MRC2, and the hamster adapted scrapie strain 263K) were taken and treated with cathepsin D under standardised conditions. The human strains type 2, 3 and 4, RML and MRC strains 1 and 2 all exhibited marked gel retardation upon treatment with cathepsin D (figure 4.5).

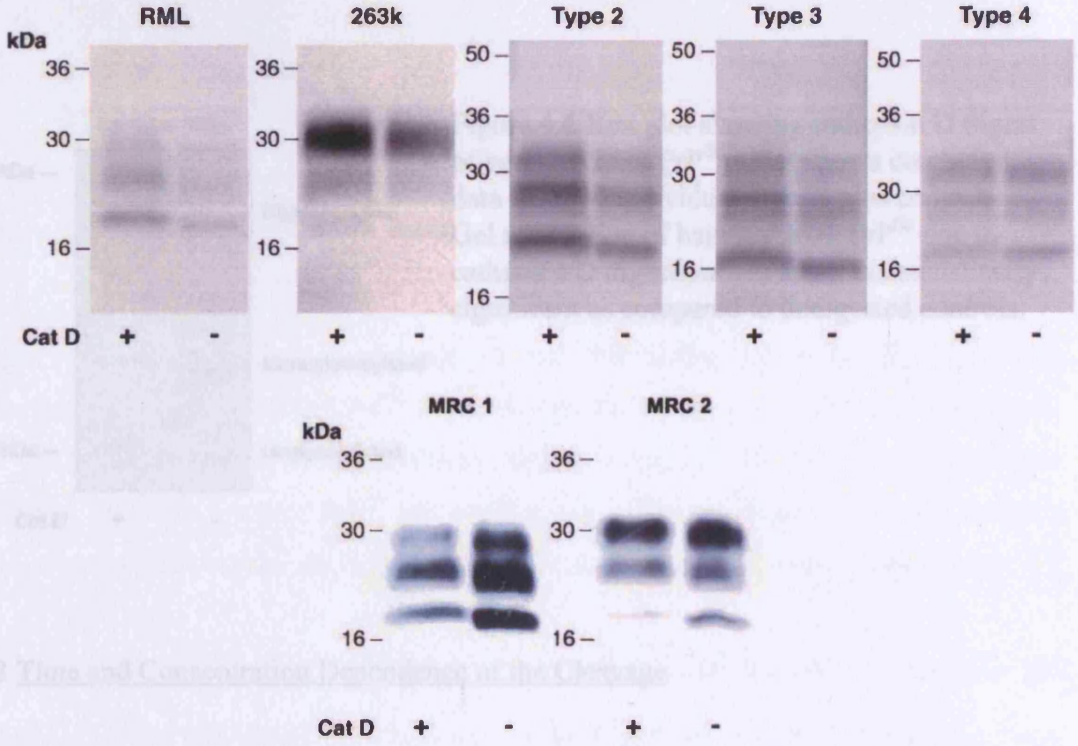

Figure 4.5 Gel retardation of PrP^{Sc} due to C-terminal truncation by cathepsin D. Cathepsin D digestion of mouse RML, hamster 263K, human types 2, 3 and 4 PrP^{Sc} and mouse MRC strains 1 and 2 visualised by western blot. Samples were digested with 20U cathepsin D per µl of 10% w/v brain homogenate and exhibit retarded migration in SDS PAGE as compared to untreated controls, indicative of C-terminal truncation and loss of GPI

Hamster strain 263K, although not exhibiting the same degree of retardation, did show a small but significant band shift upward upon digestion with cathepsin D. To assess this, samples from multiple independent digests were western blotted and the resulting band images quantified for migration retardation using Imagequant software (Amersham biotech). The migration for digested versus undigested material was compared using an unpaired two-tailed t-test, $p < 0.005$ (figure 4.6).

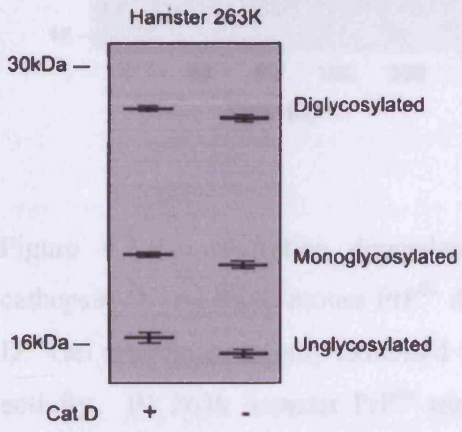

Figure 4.6 Box plot showing cathepsin D digest of hamster 263k PrP^{Sc}. Plot shows combined data from 10 individual digests plus controls. Gel retardation of hamster 263k PrP^{Sc} due to cathepsin D digestion was small but statistically significant as compared to undigested controls.

4.2 Time and Concentration Dependence of the Cleavage

If the gel retardation of PrP^{Sc} after treatment with cathepsin D is indeed due to an enzymatic cleavage event, one would expect the phenomena to exhibit both concentration and time dependence. These were examined primarily using RML mouse adapted scrapie as a model system, which provides a well studied strain type amenable to both laboratory manipulation and studies of infectivity. Initially, digests were carried out using different concentrations of cathepsin D over a set time course (2 hours) and under standardised conditions. Gel retardation of PrP was not observed until the concentration of cathepsin

D exceeded 50 units. This was repeated with the hamster prion strain 263K and similar results were recorded (figure 4.7).

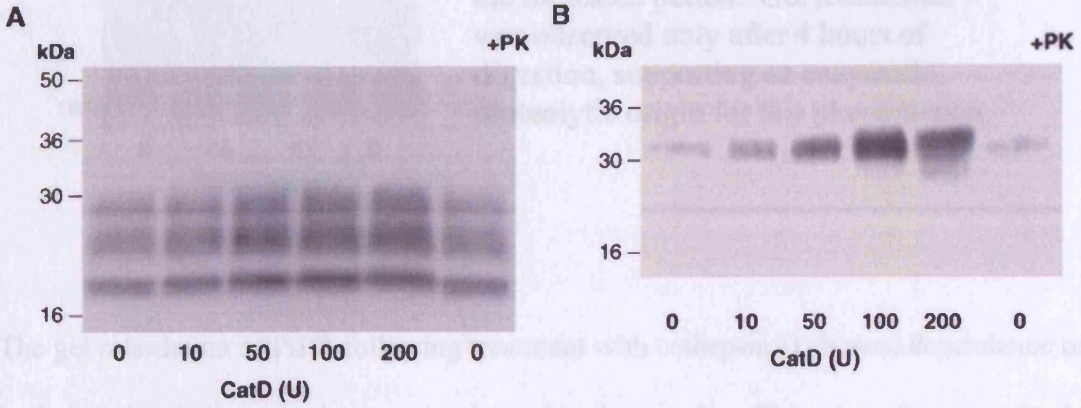

Figure 4.7 Concentration dependence of gel retardation following digestion with cathepsin D. A) RML mouse PrP^{Sc} digested with increasing concentrations of cathepsin D. Gel retardation is only exhibited when digestion occurs with 50U or greater enzyme activity. B) 263k hamster PrP^{Sc} treated likewise. The gel retardation again exhibits concentration dependence, strongly suggesting that this is an enzymatic phenomenon.

Following this, and using a concentration of cathepsin D that did not result in gel retardation after two hours of digestion, the time dependence of PrP^{Sc} cleavage was examined. Samples were removed at the start of the digest and at two-hour time points during its progression. Gel retardation occurred only after a period of 4 hours using this concentration, with no band shift in evidence at the two-hour time point, demonstrating the time dependence of this phenomenon (figure 4.8).

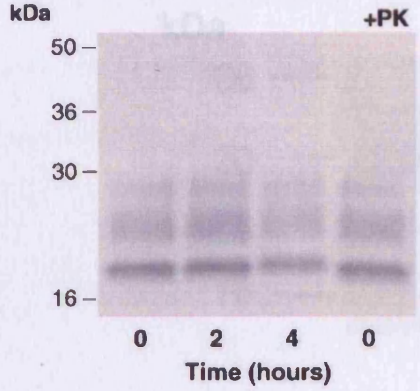

Figure 4.8 Time dependence of gel retardation following digestion with cathepsin D. Mouse RML PrP^{Sc} was incubated with 10U of cathepsin D for the indicated period. Gel retardation was observed only after 4 hours of digestion, supporting an enzymatic, proteolytic origin for this phenomenon.

The gel retardation of PrP^{Sc} following treatment with cathepsin D showed dependence on both length of digest and concentration of cathepsin D. This strongly supports the argument that this is an enzymatic phenomenon, and one mediated by the proteolytic action of cathepsin D upon the scrapie isoform of PrP.

4.3 Investigation of Glycoform Ratio Alteration

An observation made in the case of several cathepsin D digested samples of PrP^{Sc} was that there appeared to be alterations in the glycoform ratio presented by western blotted prion protein before and after cathepsin D digestion. The glycoform ratio exists between the three possible glycosylation states of the prion protein – di-glycosylated, mono-glycosylated or with no glycosylation. This is reflected by the presence of three immunoreactive bands for PrP (for both the cellular and the scrapie isoform), with the highest molecular mass band having two glycosylated sites, the middle band one and the lowest band none (figure 4.9).

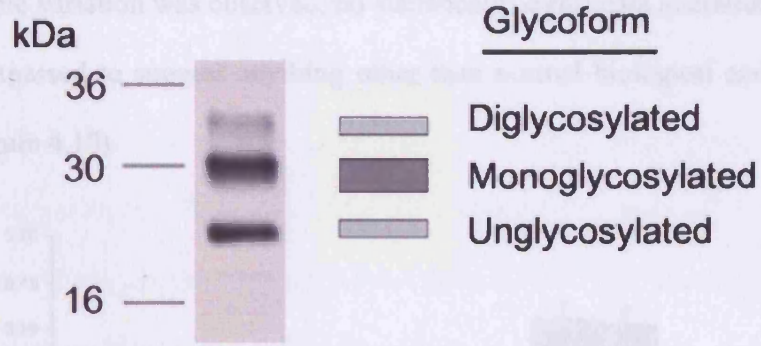

Figure 4.9 Prion protein glycoforms. Western blot (left hand panel), schematic (central panel) and glycoform status (right hand panel) for Type 2 human PrP^{Sc}. This illustrates the three different possible glycosylation states that PrP^{Sc} can occupy – diglycosylated with the largest relative molecular mass, monoglycosylated running as the middle band and unglycosylated with the lowest relative molecular mass.

For reasons not well understood, the predominance of the glycoforms varies widely between the different strain types found in natural and experimental prion disease, resulting in significantly different ratios between the three glycoforms. In the case of some, but not all, cathepsin D digests of PrP^{Sc}, a decrease in the unglycosylated species of PrP was witnessed (see figure 4.5 – strains MRC 1 and 2 as an example). To investigate this, multiple independent digests were carried out in parallel under identical conditions. These were then western blotted and imaged on a Storm 840 scanner (Molecular Dynamics corp), facilitating analysis of band intensity using the Imagemaster 1D software program (Amersham biotech). This allowed relative densities of bands from individual blots to be calculated and glycoform ratios established. The data from these multiple digests were then pooled and statistically compared using a T test. Analyses were carried out of human types 2 and 3, and mouse RML. These lend themselves to such strain analysis due to their relatively even distribution of glycoforms (257;351).

Although some variation was observed, no statistically significant alteration in glycoform ratio was witnessed to suggest anything other than normal biological and experimental variation (figure 4.10).

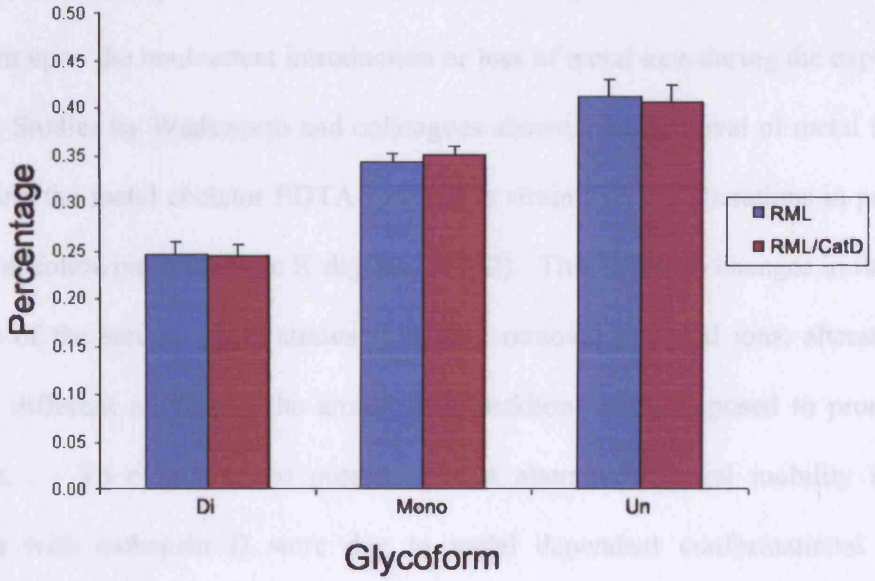

Figure 4.10 Glycoform analysis of RML PrP^{Sc} following digestion with cathepsin D and proteinase K. The percentage of the total PrP represented by each glycoform is shown for RML (blue) and for RML digested with cathepsin D (purple). Data was compiled from 10 independent digests with controls, with standard deviation indicated by error bars. No significant difference in the glycoform ratio was observed following cathepsin D digestion.

It is possible that the removal of the GPI anchor has a disproportionate impact on the ability of unglycosylated PrP to transfer from gel to membrane in a western blotting system; an impact mitigated by the presence of sugar chains on the di- and mono-glycosylated species. If this were the case, the differences between individual blots and digests could be due to slight variations in transfer conditions.

4.4 Metal Ion Independence of Cleavage

An alternative explanation for this alteration in electrophoretic properties following digestion with cathepsin D is that there is a change in conformation of the PrP^{Sc} dependent upon the inadvertent introduction or loss of metal ions during the experimental process. Studies by Wadsworth and colleagues showed that removal of metal ions from PrP^{Sc} using the metal chelator EDTA resulted in strain specific alterations in proteolytic fingerprint following proteinase K digestion (352). This is due to changes in the tertiary structure of the scrapie agent strains following removal of metal ions, alterations that result in different regions of the amino acid backbone being exposed to proteinase K digestion. To eliminate the possibility that alterations in gel mobility following digestion with cathepsin D were due to metal dependent conformational changes, cathepsin D digests were carried out in the presence and absence of the metal chelating agent EDTA and the affect of increasing concentrations of Cu^{2+} upon the strain profile of RML were investigated (figure 4.11).

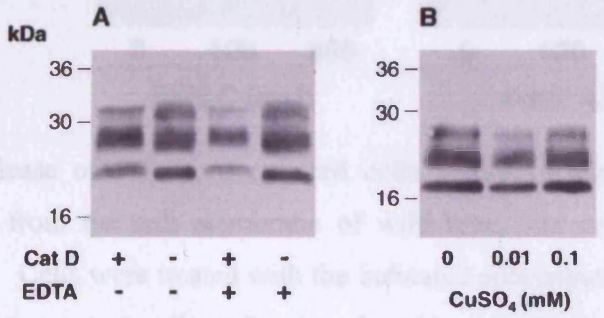

Figure 4.11 Metal ion independence of gel retardation following cathepsin D digestion. A) Cathepsin D digestion of mouse RML carried out in the presence of the metal chelating agent EDTA. No impact on gel retardation was observed. B) Impact of Cu^{2+} ions on RML strain profile. No alteration was observed.

The presence of EDTA did not affect the apparent increase in relative molecular mass of PrP in SDS gel electrophoresis following cathepsin D digestion, not did the addition of copper to RML result in any strain specific alteration - indicating that the phenomenon is not dependent on the metal ion status of PrP^{Sc}.

4.5 Cathepsin D Catalysed Release of PrP from Cell Membranes

If treatment with cathepsin D removes the GPI anchor, it would be expected that treatment of intact cells in culture with the enzyme would result in release of membrane anchored PrP into the cell media. To examine this, wild type N2a cells were treated with either cathepsin D or PIPLC, with the incubation media subsequently analysed for the presence of released PrP^{C} (figure 4.12).

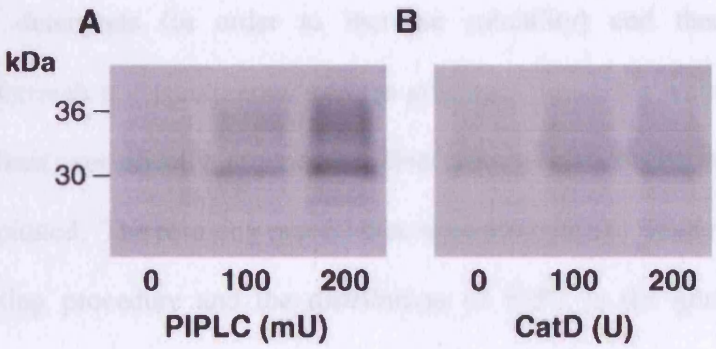

Figure 4.12 Release of PrP from cultured cells following exposure to cathepsin D. Release of PrP from the cell membrane of wild type N2a cells by PIPLC (A) and cathepsin D (B). Cells were treated with the indicated concentration of enzyme for three hours, with the supernatant collected and analysed by western blotting. The presence of PrP^{C} in the supernatant, recognised by ICSM 35, signifies release of the protein from the cell membrane upon either GPI cleavage (PIPLC) or C-terminal truncation (cathepsin D)

Under these conditions, treatment with both cathepsin D and PIPLC resulted in the release of PrP^C, as measured by an increase in the PrP^C collected from the media. This, again, supports the c-terminal truncation of PrP by cathepsin D, with the removal of the GPI anchor concomitant with release from the cell membrane.

4.6 Solubility of Cathespin D Treated PrP^{Sc}

The scrapie isoform of PrP is, by definition, highly insoluble. It is characterised by its ability to aggregate and, indeed, many of the problems in defining the molecular properties of PrP^{Sc} can be traced back to its poor solubility. To investigate whether C-terminal truncation of PrP^{Sc} has any impact upon its solubility, RML infected mouse brain homogenates were treated with cathepsin D, digested with proteinase K, exposed to low levels of detergents (in order to increase solubility) and then subjected to centrifugation through a discontinuous sucrose gradient. Fractions were then collected from this gradient, specifically around the discontinuous interfaces, and the protein methanol precipitated. The resulting precipitates were subjected to western blotting using standard operating procedure and the distribution of PrP^{Sc} in the gradient compared between cathepsin D treated and untreated material (figure 4.13).

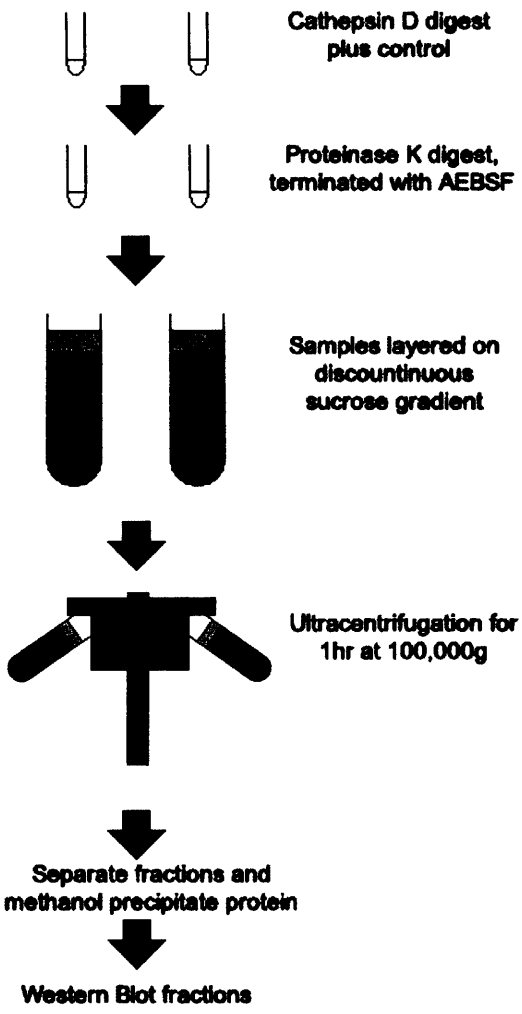

Figure 4.13 Protocol for solubility analysis. RML samples were treated with proteases and then subjected to centrifugation at 100,000g for 1hr through a sucrose gradient. Fractions were then collected, methanol precipitated and then analysed by western blot using standard procedures. Cathepsin D digested RML and an undigested control were compared.

Analysis of mouse RML PrP^{Sc} and cathepsin D treated mouse RML revealed alterations in the solubility of the scrapie isoform following C-terminal truncation with cathepsin D. C-terminally truncated RML exhibited a loss of solubility in lower concentrations of sucrose, with more of the PrP migrating to form a pellet at the bottom of the gradient (figure 4.14).

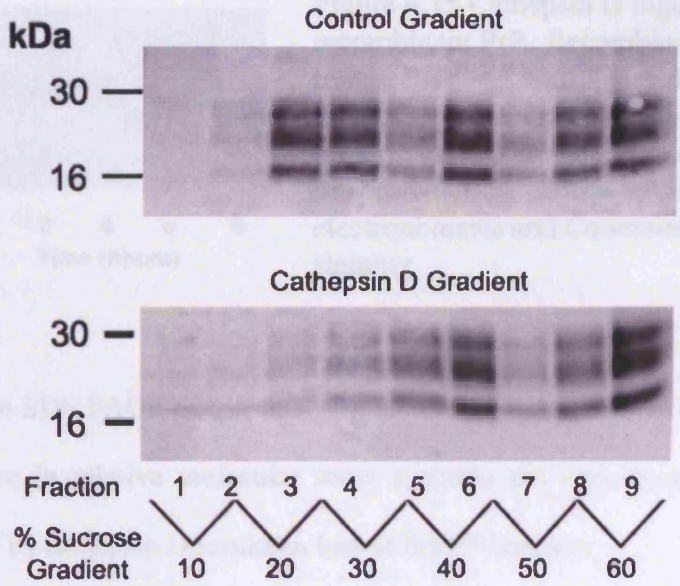

Figure 4.14 Solubility analysis of PrP^{Sc} and C-terminally truncated PrP^{Sc}. Samples were subjected protease digestion and separation on a sucrose gradient as described in figure 4.13. Upper panel shows mouse RML PrP^{Sc} digested with proteinase K as a control, lower panel shows mouse RML digested with cathepsin D and proteinase K.

4.7 Cathepsin D digest of recombinant PrP

As an alternate approach to investigating the digestion of PrP with cathepsin D, recombinant moPrP residues 91-231 was exposed to the enzyme. Using a fixed concentration of cathepsin D, a decrease in the relative molecular mass of recombinant mouse PrP 91-231 (as measured using SDS PAGE) was observed after 8 hours (figure 4.15). Since bacterially produced moPrP does not have post translational modifications (i.e. glycosylation or GPI anchor) the loss of the C-terminus of PrP would not result in

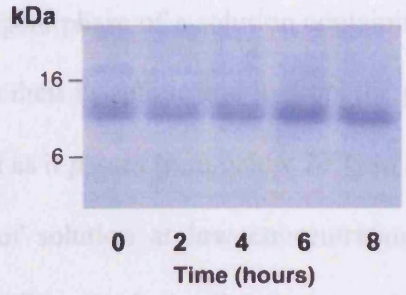

Figure 4.15 Cathepsin D digest of recombinant PrP. Recombinant mouse PrP^{91-231} was digested with 10U of cathepsin D for indicated time periods. Samples were assessed for proteolytic cleavage by SDS gel electrophoresis and Coomassie blue staining

gel retardation in SDS PAGE due to this. Again, the time dependence of this interaction and the decrease in relative molecular mass supports the hypothesis that proteolytic digestion of PrP by cathepsin D results in loss of the GPI anchor.

4.8 Ascertainment of GPI Loss

Several techniques were used to attempt to ascertain the loss of the GPI from PrP, in addition to gel retardation as a biophysical marker of this loss. In the first instance, an antibody specific residue left after for the PIPLC cleavage of the GPI anchor, the cross reacting determinate, was used. PrP^{Sc} was treated with cathepsin D and then proteinase K digested. Following this, the digested PrP was partially denatured by the addition of SDS and heating to 100°C for 10 mins. The detergent was then diluted out and PIPLC digestion carried out. The resulting homogenate was then western blotted and probed with the cross reacting determinant antibody. With PrP^{C} digested directly with PIPLC or PrP^{Sc} digested with cathepsin D and/or PIPLC following denaturation, no positive immunoreactivity was revealed.

The second technique used to examine the presence of absence of the GPI was phase separation. Phase separation refers to the transfer of proteins from the aqueous to the

detergent phase of a solution containing non-ionic detergents such as triton X-114 based upon their lipophilic and hydrophilic properties (353). Triton X-114 undergoes a cloud point as it passes from below 20°C to above this temperature (354). The detergent comes out of solution at low concentration and can be centrifuged into a pellet. Highly lipophilic proteins will associate with the pellet, with hydrophilic proteins staying in solution (figure 4.16).

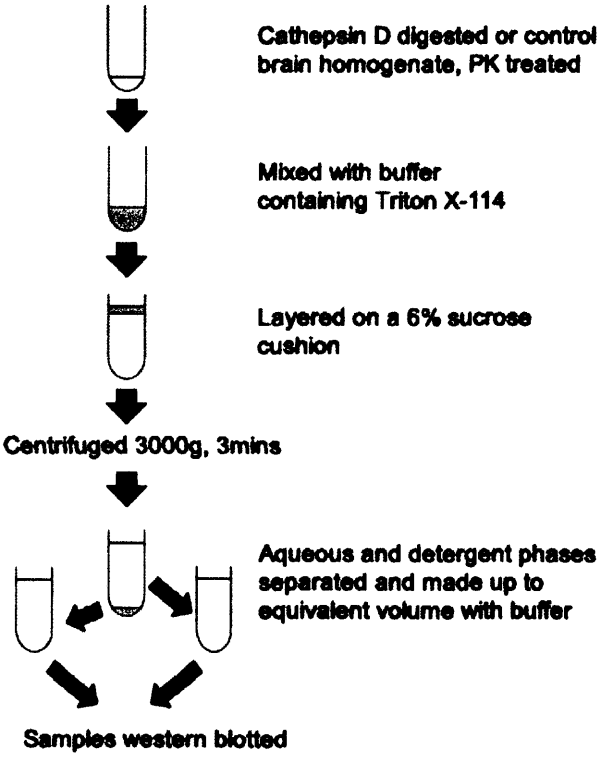

Figure 4.16 Phase separation protocol. Mouse RML PrP^{Sc} subjected to C-terminal truncation with cathepsin D and then digested with proteinase K underwent phase separation using Triton X-114. Untreated RML was used as a control and both samples analysed by western blot for partition of PrP into the aqueous and detergent phases.

This technique has been used to successfully evaluate the presence of the GPI anchor on PrP^{C}, but has not been applied to scrapie isoform. With PrP^{C}, GPI anchored protein

partitions exclusively to the lipid phase. After PIPLC treatment, all PrP localizes to the aqueous phase. With PrP^{Sc}, however, PrP could be found in both phases (figure 4.17).

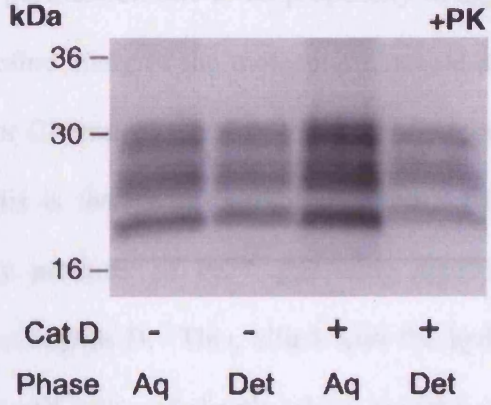

Figure 4.17 Phase separation analysis of C-terminally truncated PrP^{Sc}. RML and C-terminally truncated RML were subjected to phase separation as described in figure 4.16. Control (cathepsin D minus) and C-terminally truncated PrP^{Sc} are shown in aqueous phase (Aq) and detergent phase (Det).

After treatment with cathepsin D, there was an alteration in the distribution of PrP between the two phases, but not enough to provide conclusive evidence of GPI loss. It is likely that the hydrophobic nature of aggregated PrP^{Sc} interferes with the use of this technique as a means to evaluate the presence of the GPI, altering the solubility of the protein in the lipid and aqueous phases.

4.9 Discussion

In this study, cathepsin D has been used to remove a short carboxyl terminal peptide fragment from infectious PrP^{Sc}, removing at the same time the GPI anchor attached to the

C-terminus of PrP. In doing so, several major technical difficulties prevented the precise characterisation of the nature and location of the cleavage event. The scrapie-associated isoform of PrP resists purification due to its propensity to aggregate. This has severely hampered efforts to define many of the molecular characteristics of PrP^{Sc} *per se* in the past, and is the case for C-terminally truncated PrP^{Sc} following treatment with cathepsin D. The impact of this is that, with current protocols, it is not possible to directly sequence the cleavage products of PrP^{Sc} following digestion, whether that is with proteinase K or with cathepsin D. This, allied with the hydrophobicity of the scrapie agent, precludes the identification of exactly which residues in the C-terminus cathepsin D cleaves between. Unfortunately, this is coupled to the fact that cathepsin D has a poorly defined cleavage consensus sequence (characterised only as a preference to cleave between two hydrophobic residues – see section 5.2), increasing the difficulty of even putatively locating the cleavage site.

The conclusion that treatment of PrP^{Sc} with cathepsin D results in cleavage at the C-terminal is, therefore, based on several indirect lines of evidence. First and foremost is the gel retardation observed upon treatment of several strains of scrapie, from multiple species, with cathepsin D. This is analogous to the retardation observed upon treatment of PrP^{C} with PIPLC, which also results in the removal of the GPI anchor (described in section 5.1). Importantly, cathepsin D mediated retardation displays both time and concentration dependence, strongly supporting the hypothesis that this is indeed an enzymatic event, rather than a none-specific interaction with PrP^{Sc}. An alternative explanation for this phenomenon, alteration of PrP^{Sc} metal occupancy due to the addition of cathepsin D resulting in modification of the three dimensional structure of the protein

and an altered proteinase K digestion pattern, was excluded by investigation of this in the RML model system. Gel retardation was not affected by removal of metal ions with EDTA, and the fragmentation pattern of RML was not altered by the addition of excess Cu^{2+} ions.

Further support for the C-terminal truncation of PrP along with removal of the GPI anchor due to cathepsin D treatment comes from the cell release studies carried out using N2a mouse neuroblastoma cells, where increased levels of PrP were detected in the media following treatment of cells with either PIPLC or with cathepsin D (as compared to untreated cells). The simplest explanation for this is that cathepsin D removes the GPI anchor from PrP, thereby releasing the protein into the cell media. This is also backed up by studies of recombinant mouse PrP, which exhibits a loss in molecular mass following treatment with cathepsin D (also in a time dependent manner). As stated in section 6.7, this is as one would expect if cathepsin D is cleaving PrP, since recombinant PrP has no post translational modifications and so would not exhibit gel retardation as there is no GPI anchor to be removed.

Several other techniques were used in an attempt to confirm that the GPI anchor was being removed from PrP^{Sc}, however these were severely hampered by the aforementioned problems raised by the nature of the scrapie agent: its hydrophobicity and tendency to aggregate. This prevented the generation of clear results using either the cross reacting determinant antibody to recognise the presence or absence of the remnant of the GPI anchor, or the use of phase separation to identify PrP species with or without a GPI anchor.

5.0 Investigation of the Impact of GPI Removal on the infectivity of PrP^{Sc}

The C-terminal truncation of PrP^{Sc} by cathepsin D, removing the GPI anchor, provides an alternative to PIPLC treatment as a method to investigate the impact of GPI loss on the biology of the scrapie agent. As PIPLC cannot be used to remove the GPI from infectious PrP^{Sc}, this opens up the possibility of examining whether the GPI anchor is required for the infectivity of PrP^{Sc}. To analyse the impact of C-terminal truncation, including the removal of its GPI anchor, on the ability of PrP^{Sc} to propagate and initiate infection, three separate models of prion replication was used. Mouse models of prion replication are well characterised, and have the advantage that *in vitro*, *ex vivo* and *in vivo* systems exist allowing a broad approach to analysis of scrapie replication. A mouse based analysis also allows continuity of strain type across all forms of analysis (in this case the Rocky Mountain Line strain of mouse-adapted scrapie), which eliminates variability originating from strain specific characteristics from the experimental process. In terms of the mechanism of prion replication, carrying out analysis under cell free, cell culture and whole animal conditions may be useful in revealing a possible differential impact of C-terminal truncation on infectivity. For example, it is plausible to hypothesise that C-terminal truncation would have no impact on infectivity in cell free conditions, but would decrease infectivity when assayed using cells in culture due to a decreased ability to reach the site of conversion following removal of the GPI. It is important to note, however, that *in vivo* analysis of scrapie infectivity remains the ultimate test of PrP^{Sc} associated infectivity, with the *in vitro* and cell culture approaches complementing this study.

Methods

In vitro Amplification

Analysis of *in vitro* amplification of PrP^{Sc} was carried out using a modification of the protocol developed by Lucassen *et al* (156). 10% w/v homogenates were produced in PBS from RML infected CD-1, wild type CD-1 and FVB/$PrnP^{0/0}$ ablate mouse brains. RML homogenates were produced in the presence of 1% v/v Triton X-100 (Sigma), with the wild type and ablate homogenates containing 1x Complete protease inhibitors (Roche). 20µl of RML homogenate was digested with 200Units of cathepsin D for 2 hours and then, in parallel with undigested RML control, diluted 1 in 25 into 1x PBS with 1% v/v Triton X-100. These were then diluted 1:1 with CD-1 wild type or ablate brain homogenate and incubated for 16 hours at 37°C with shaking at 450 rpm. Following incubation, homogenates were digested with proteinase K at a final concentration of 50µg/ml for 1 hour at 37°C. The digest was terminated by the addition of 2x SDS loading buffer containing AEBSF at a final concentration of 5mM and analysed by western blotting. Each condition was repeated in triplicate.

Scrapie Cell Assay

Assay for prion infectivity was carried out as described by Klöhn *et al* (140). Briefly, N2a murine neuroblastoma cells were cultured in OPTI-MEM with 10% v/v fetal calf

serum (OFCS) and 100Units/ml of both penicillin and streptomycin (Invitrogen Corp.). PK1 cells, a subcloned N2a line highly susceptible to infection with the RML strain of mouse adapted scrapie, were used to assay the infectivity of cathepsin D treated, C-terminally truncated RML. Cells were plated out at a density of 20,000 cells per well in 96 well plates (cells were resuspended from stock flasks and counted using a haemocytometer prior to plating) in 200µl of OFCS. Plates were incubated at 37°C for 16hrs. RML homogenates thawed from frozen samples were prepared for assay by treatment with cathepsin D (20µl of cathepsin D was added to 20µl of 10% w/v RML homogenate) or an equivalent volume of PBS as a control. These were incubated for 2hrs at 37°C with shaking at 450rpm. In parallel with this, PBS alone, cathepsin D at an equivalent concentration to treated samples, cathepsin D treated mouse CD1 brain homogenate and RML thawed directly from stocks immediately prior to dilution were prepared as controls. All samples were diluted to a range of concentrations (from 10^{-4} to 10^{-7}). To achieve this, they were first diluted into 10% w/v mouse CD1 brain homogenate and then into OFCS at a concentration appropriate to ensure that a final concentration of brain homogenate (infectious and wild type) of 10^{-4}. 300µl of diluted sample was added to each well, with 8 wells used for each dilution of each condition in triplicate. Controls were included on each plate to allow plate to plate variation following development to be taken into consideration.

The initial diluted inocula were aspirated after 3 days and the confluent cells resuspended by pipetting up and down 40 times in 300µl of OFCS. 30µl of resuspended cells were transferred into sterile 96 well plates and diluted 1:10 into fresh OFCS. This was carried out three times, with the cells being grown to confluence after the final split.

The cells were then transferred to ELISPOT plates (Enzyme Linked Immunospot multiscreen immobilon P 96 well format filtration plates, Millopore), activated prior to addition of cells by washing with 50µl of 70% ethanol. To ensure an equal number of cells per well, confluent monolayers were resuspended in 200µl of OFCS and representative samples from each experimental condition were counted using a haemocytometer. 25,000 cells per well were than added to the prepared ELISPOT plate. Vacuum was applied to the plates, pulling the cells onto the membrane, and the plates were then dried in a 50°C oven for 1hr. 50µl of 0.5µg/ml proteinase K in lysis buffer (50mM TrisCl pH 8.0, 150mM NaCl, 0.5% Deoxycholate, 0.5% Triton X-100) was then added per well, incubated at 37°C for 90mins and removed by vacuum. Wells were washed twice with 160µl of PBS, and 160µl of 1mM PMSF was added to each well for 10mins then aspirated. To denature cellular proteins attached to the membrane, 160µl of Guanidine Isothiocyanate (3M GSCN, 10mM TrisCl, pH 8.0) was added to each well, incubated for 10mins at room temperature and discarded into 2M NaOH. The wells were then washed 4 times with 160µl of PBS.

Plates were then immunoprobed: 160µl of superblock (Pierce) was added to the cells for 1hr, removed by vacuum, followed by the addition of 50µl of anti-moPrP ICSM 18 antibody (D-Gen ltd., London) at a 1:5000 dilution in TBST with 1% milk powder. These were incubated for 1 hr at room temperature, the antibody discarded and the plate washed seven times with 160µ TBST (10 mM TrisCl pH 8.0, 150 mM NaCl, 0.1% v/v Tween 20). 50µl of secondary antibody (anti-IgG1 alkaline phosphatase conjugated, Sigma) was added to the wells at a dilution of 1:4500, again in TBST with 1% w/v milk powder, and incubated for 1hr at room temperature. This was then discarded and the

wells washed seven times with 160µl of TBST. The underdrains of the plates were then removed and the plates dried under airflow. To develop the plates, 50µl of Alkaline Phosphotase reactive development reagent was added to each well and incubated at room temperature for 16mins. The supernatant was discarded and the plates washed twice with 160µl of de-ionised H_20 before being dried under airflow. To quantify the PrP^{Sc} positive cells in each well, Zeiss KS ELISPOT system was used. Plates were read using a Stemi 2000c stereo microscope with a Hitachi HV-C20A color camera. Positive spots were detected using well scan software (Imaging Associates, Bicester UK), trained to detect appropriate colonies.

In vivo Bio-assay of Cathepsin D Treated PrP^{Sc}

Cathepsin D treated RML was subjected to conventional bio-assay using Tg20 transgenic mice (355). 10% w/v RML was treated with 20U/µl cathepsin D or mixed with an equivalent volume of PBS and incubated for 2hrs at 37°C. The treated and control RML were then diluted with PBS to a final concentration of 0.1% w/v in parallel with cathepsin D alone and PBS as control conditions. RML, cathepsin D treated RML, PBS and cathepsin D only controls were then inoculated (30µl) intra-cerebrally into anaesthetised Tg20 transgenic mice over expressing the murine *Prn-p* gene (20 mice each for RML and cathepsin D treated RML experimental conditions, 10 mice each for PBS and cathepsin D alone control conditions). Animal husbandry adhered to institutional and Home Office guidelines and animals were examined daily for signs of clinical prion disease. Brain samples were taken from all groups following death, analysed by western blot for the

presence of PrP^{Sc} and histologically for neuropathological evidence of prion disease. For western blots, 20µl of brain homogenate was taken from each experimental condition and digested with proteinase K for 1 hour at 37°C at a final concentration of 50µg/ml. SDS PAGE and transfer to PVDF were carried out as described in section 6.0, with brain homogenate not treated with proteinase K run in parallel with each digested sample. Immunoprobing was carried out using ICSM 35 primary antibody (D-Gen Ltd., London) and anti-IgG1 alkaline phosphatase conjugated secondary antibody (Sigma) and blots scanned using a Molecular Dynamics Storm 840 imaging machine. Neuropathological examination was also carried out to ascertain the presence of scrapie pathology. Brain tissue was fixed in 10% buffered formal saline and prion infectivity abolished by boiling in 98% formic acid for one hour. The samples were then washed for 24 hours in 10% formal saline prior to embedding in paraffin wax. Sections were cut from the fixed brains to a thickness of 4µm and treated with formic acid for 5 minutes. These sections were then boiled in EDTA-TRIS-citrate buffer (pH 7.8) for 20 minutes before immunohistochemical staining was carried out. The anti-PrP monoclonal antibody ICSM 35 (D-Gen Ltd., London) was used for this, applied using a Ventana automated immunohistochemical staining machine with a basic diaminobenzidine detection system according to the manufacturers instructions (Ventana medical systems, Tucson Arizona).

5.1 *In vitro* amplification of PrP^{Sc}

As noted in section 1.2.3, several *in vitro* models of scrapie replication exist. For the purposes of this investigation, a protocol adapted from that described by Lucassen *et al*

was adopted. This relies on incubation of infectious homogenate with either wild type or knock out brain homogenate in the presence of mild detergents and protease inhibitors and has been widely used to investigate the biochemical requirements and environment of the prion conversion process (155;157;356). The detergents act to break up PrP^{Sc} into multiple seeds, which can then recruit PrP^{C} for conversion. When PrP^{Sc} is spiked into wild type homogenate in this way, amplification of protease resistant PrP signal is observed. This is compared to PrP^{Sc} incubated with homogenate from $PrP^{0/0}$ mice not containing PrP^{C}, where amplification of signal is not observed (figure 5.1).

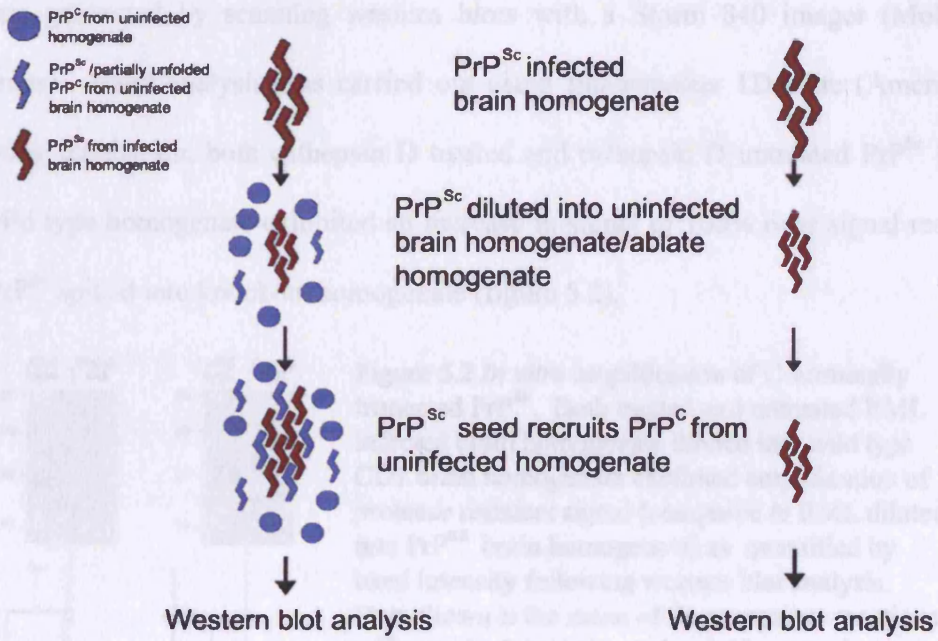

Figure 5.1 *In vitro* amplification protocol. PrP^{Sc} is diluted into wild type and ablate brain homogenate in the presence of protease inhibitors and 1% v/v Triton X-100. After incubation for 16hrs, PrP^{Sc} diluted into wild type homogenate exhibits an increase in protease resistant signal as compared to PrP^{Sc} diluted into ablate homogenate as analysed by western blot. Adapted from the protocol of Lucassen *et al* (156)

Although the exact nature of the amplification is not yet clear, for example as to whether or not the resulting increase correlates with an increase in infectivity*, the technique is more robust than the PMCA technique described by Saborio *et al* and does not require the use of radiolabelled PrP, as the cell free conversion process originated by Caughey and colleagues does, therefore making it both cheaper and safer to replicate (147;153).

To investigate the *in vitro* replication of C-terminally truncated PrP^{Sc}, RML was either treated with cathepsin D for two hours or diluted with PBS as a control and incubated in parallel. These were then subjected to the amplification protocol as described. Each condition was repeated in triplicate, and signal intensity data for each replicate generated by scanning western blots with a Storm 840 imager (Molecular Dynamics). Band analysis was carried out using Imagemaster 1D Elite (Amersham). Following incubation, both cathepsin D treated and cathepsin D untreated PrP^{Sc} spiked into wild type homogenate exhibited an increase in signal of 100% over signal recorded with PrP^{Sc} spiked into knockout homogenate (figure 5.2).

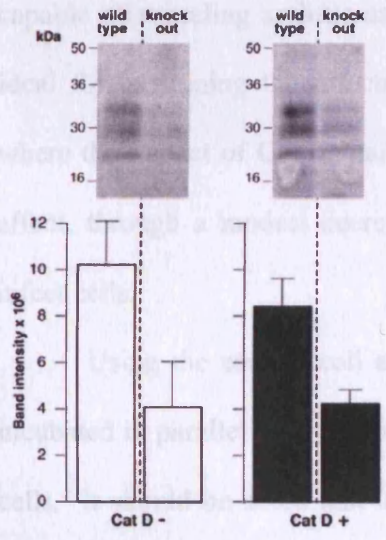

Figure 5.2 *In vitro* amplification of C-terminally truncated PrP^{Sc}. Both treated and untreated RML infected brain homogenate diluted into wild type CD1 brain homogenate exhibited amplification of protease resistant signal (compared to RML diluted into $PrP^{0/0}$ brain homogenate) as quantified by band intensity following western blot analysis. Data shown is the mean of three separate reactions with standard deviation indicated by error bars. No significant difference was observed between treated and untreated samples.

* Although recent work by Suppatapone and colleagues suggests that there is a least a transient increase in the infectivity of amplified samples (357).

There was no significant difference in amplification of signal between treated and untreated samples ($p > 0.35$, paired T-test), indicating that C-terminal truncation with cathepsin D does not affect *in vitro* amplification in this system.

5.2 Scrapie Cell Assay of PrP^{Sc}

Several cell lines that are capable of propagating PrP^{Sc} have been characterised. The most widely used, and most intensely studied, is the murine neuroblastoma cell line N2a. N2a cells are susceptible to infection with the RML strain of mouse adapted scrapie, and can be used to assay for infectivity. By subcloning N2a cells, it is possible to select clonal lines with heightened susceptibility to RML. Such a line, the PK1 subclone, was used in the scrapie cell assay developed by Peter Kloehn and Charles Weissmann at the MRC Prion unit (140). By using a range of dilutions, this system allows highly sensitive detection and titration of the number of infectious units in RML homogenate, and is capable of revealing as little as a two fold alteration in infectious titre. This makes it ideal for examining the infectivity of RML homogenates digested with cathepsin D, where the impact of C-terminal truncation is not known and could be anything from no affect, through a modest decrease in infectivity to complete ablation of the ability to infect cells.

Using the scrapie cell assay, cathepsin D treated RML was compared to RML incubated in parallel with the digest, and with RML thawed directly prior to exposure to cells. It should be noted that incubation at 37°C for two hours results in a decrease in infectivity, hence the introduction of two RML controls (F. Properzi, unpublished

observations). In addition to these two controls, cells were also exposed to cathepsin D at an equivalent concentration to that used in the digest, CD1 wild type homogenate exposed to cathepsin D, CD1 wild type homogenate alone and PBS. These were used to control for any cytotoxic affect that cathepsin D may have, either intrinsically (cathepsin D alone) or through toxic intermediates generated through the digestion of mouse brain homogenate. In both cases, no cytotoxic impact was revealed as measured by cell counts of treated wells compared to other controls. PBS and CD1 wild type controls were used to provide uninfected controls, thereby yielding a background level as a control for the rest of the experimental conditions. This is illustrated in figure 5.3.

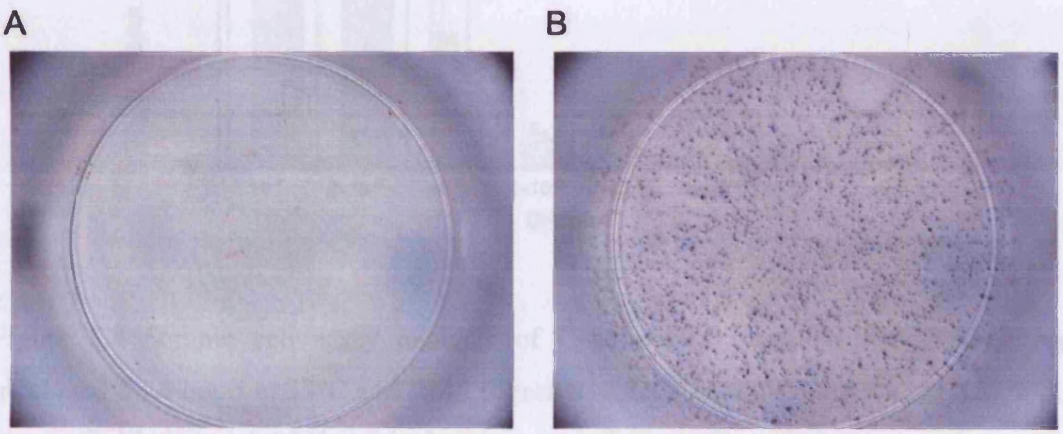

Figure 5.3. Positive and negative scrapie cell assay samples. 96 well plate individual wells showing cells exposed to wild type CD1 brain homogenate (A) and mouse RML PrP^{Sc} brain homogenate (B). The cells exposed to scrapie infected brain homogenate propagate PrP^{Sc}, detected by immunoprobing with anti-PrP antibodies following exposure of cells to proteinase K. Control cells exposed to CD1 brain homogenate show no evidence of protease resistant PrP.

With the experimental conditions themselves, cathepsin D treated RML did show a decrease in infectivity as compared to RML diluted on to cells directly after thawing. However, when compared to RML incubated in parallel with the digest for two hours at 35°C, there was no significant difference between the two (figure 5.4).

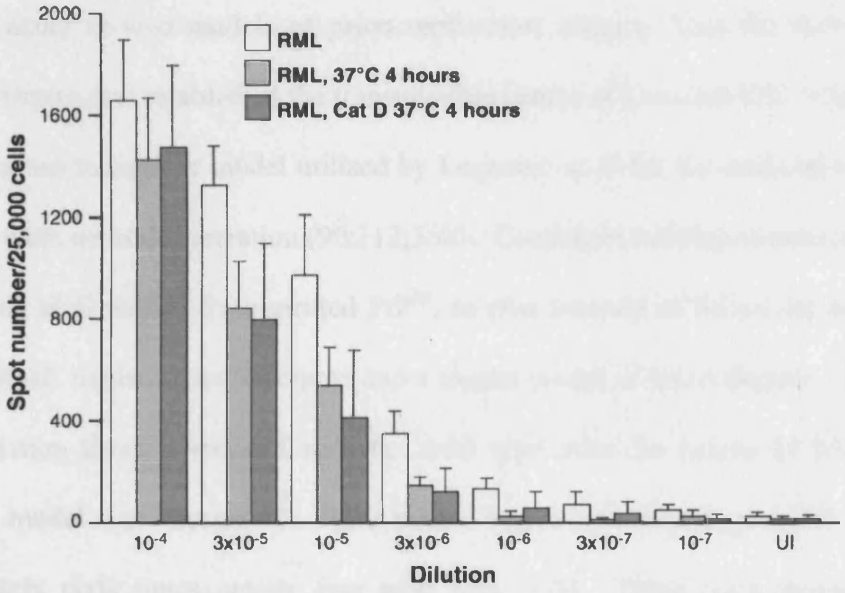

Figure 5.4 Scrapie cell assay analysis of C-terminally truncated PrP^{Sc}. RML was incubated for 4 hours at 37°C and RML digested with cathepsin D for 4 hours at 37°C. A range of dilutions of RML brain homogenates from 10^{-4} to 10^{-7} were used to allow estimation of any impact of cathepsin D digestion on the infectivity of RML, with no significant difference between digested and undigested samples. Data shown is the mean number of cells that contain detectable PrP^{RES} per 25,000 viable cells from 3 independent experiments with standard deviations as indicated.

Using the scrapie cell assay model of RML prion infection and propagation, there was no significant difference between wild type and C-terminally truncated, GPI minus cathepsin D treated RML. As was mentioned above, the scrapie cell assay is capable of detecting

alterations in titre of approximately 2 fold, making it a highly sensitive technique even compared to titrated animal assay.

5.3 *In vivo* Analysis of PrP^{Sc} Infectivity

There are many *in vivo* models of prion replication, ranging from the experimentally infected primates that established the transmissible nature of kuru and CJD through to the Tg 9949 mouse transgenic model utilised by Legname *et al* for the artificial stimulation of prion protein neurodegeneration (90;112;358). Consistent with the *in vitro* and *ex vivo* investigation of C-terminally truncated PrP^{Sc}, *in vivo* analysis of infectivity was carried out using RML mouse adapted scrapie and a mouse model of prion disease. Due to the long incubation times associated with the wild type mice (in excess of 150 days), a transgenic model was chosen: the Tg20 mouse line over-expressing MoPrP at a level approximately eight times greater than wild type (355). These mice develop scrapie sickness between 60 and 120 days post *intra* cerebral inoculation with RML infected mouse brain homogenate, allowing far more rapid appraisal of infectivity.

To examine the infectivity of C-terminally truncated PrP^{Sc} lacking the GPI anchor, 10% w/v RML infected brain homogenate was treated with cathepsin D using a standardised protocol. In parallel, RML was diluted to an equivalent concentration to the experimental group for use as a positive control and cathepsin D was diluted likewise to control for the possibility of toxicity and/or neurodegeneration (however unlikely) due to the presence of the enzyme. PBS was included as a negative control. All of these samples were then examined for infectivity by *intra* cerebral inoculation into Tg20

transgenic mice. These mice were examined on a daily basis for any evidence of the symptoms of scrapie, with the incubation period between inoculation and onset of symptoms noted. Following death or culling, brain samples were taken and examined for the presence of PrP^{Sc}, to confirm the diagnosis of prion disease and to examine any possible molecular alterations upon transmission due to C-terminal truncation. Samples were also taken for examination by immunohistochemistry, again to confirm the diagnosis of prion disease by revealing the presence or absence of pathology characteristic of infection.

Following inoculation, one hundred percent of both RML and C-terminally truncated RML treated animals developed the symptoms of scrapie (table 5.1).

Treatment	Clinically affected	Average incubation (SE)
RML	17/17	67.5 (±2.2)
Cathepsin D treated RML	17/17	67.4 (±2.5)
Cathepsin D	0/10	>200
PBS	0/10	>200

Table 5.1 *In vivo* bioassay of C-terminally truncated PrP^{Sc}. TG20 transgenic mice were inoculated *intra* cerebrally with 0.1% w/v RML brain homogenate and monitored for clinical signs of prion disease. Groups of mice inoculated with either cathepsin D treated RML or native RML exhibited similar incubation times shown in days post-inoculation. The presence of protease resistant material in the brains of both experimental groups was confirmed by western blotting. Control groups (PBS and cathepsin D alone) showed no evidence of prion disease.

After death, brain samples from each affected mouse were examined by western blot for the presence of PrP^{Sc}. All animals diagnosed with scrapie also had protease resistant PrP within their brains, with a protease resistant fragment profile and glycoform ratio characteristic of the RML strain of mouse adapted scrapie (figure 5.5).

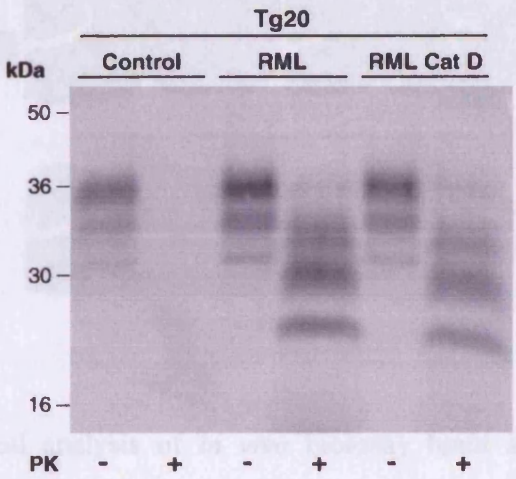

Figure 5.5 Protease resistant prion protein from *in vivo* bioassay. Brain samples were taken from PBS inoculated animals, RML inoculated animals and C-terminally truncated RML inoculated animals. 10% w/v homogenates were prepared and analysed by proteinase K digestion and western blot as described. RML and cathepsin D treated RML inoculated mouse brain homogenates contain protease resistant prion protein, whereas PBS inoculated brain homogenate does not.

Neuropathological examination of experimental and control animals were also carried out. No evidence of scrapie pathology was revealed in the control cases, with pathology typical of RML strain prion disease being found in both the RML and C-terminally truncated RML inoculated animals (figure 5.6).

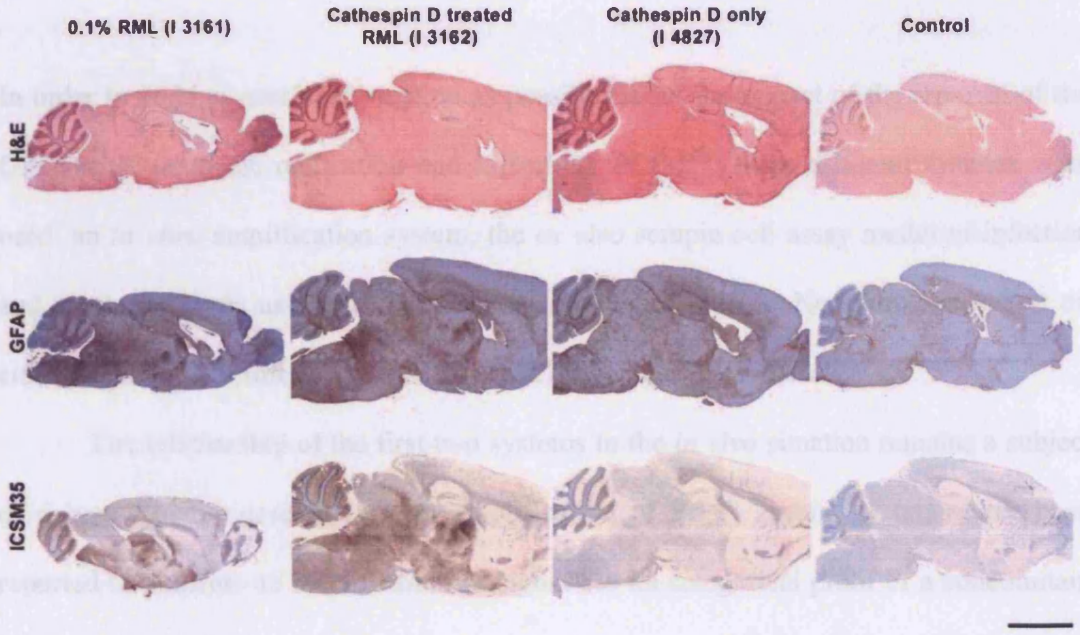

Figure 5.6 Histological analysis of *in vivo* bioassay brain sections. Samples were prepared by fixation in formalin and boiling in formic acid. Immunhistochemistry reveals widespread gliosis (using GFAP as a marker) in RML and cathepsin D treated RML brain slices. Analysis using anti-PrP antibody ICSM 35 reveals deposition of protease resistant PrP in the brains of animals inoculated with RML and cathepsin D treated RML, correlating with the western blot analysis of homogenates and symptomatic diagnosis of scrapie. Control samples show no evidence of PrP^{Sc} accumulation.

To summarise the *in vivo* infectivity analysis of C-terminally truncated RML, no significant difference in mortality, incubation period, strain type or neuropathology was revealed following inoculation of Tg20 mice with RML and with C-terminally truncated RML lacking the GPI anchor. Subject to certain caveats (see discussion) this suggests that removing the GPI anchor from PrP^{Sc} does not reduce infectivity.

5.4 Discussion

In order to yield as much information as possible about the impact of the removal of the GPI anchor upon the replication and infectivity of PrP^{Sc}, three different systems were used: an *in vitro* amplification system, the *ex vivo* scrapie cell assay model of infection and *in vivo* analysis using the Tg20 transgenic mouse model. No significant effect on either replication or infectivity was observed with any of these techniques.

The relationship of the first two systems to the *in vivo* situation remains a subject of debate. In the case of *in vitro* amplification of PrP^{Sc}, several systems have been reported to generate an amplification of signal but no categorical proof of a concomitant increase in infectivity has been produced and so these systems may reflect an increase in protease resistant PrP rather than a genuine amplification of infectivity. Despite these drawbacks, such systems offer a window on a specific aspect of prion replication – in isolation from issues of cell entry and tissue tropism. From this point of view, unimpaired *in vitro* replication of PrP^{Sc} lacking the GPI anchor is informative. It suggests that at the basic level of prion replication, be it a template assisted enzymatic process or a seeded polymerisation event, the GPI anchor is not required. This is in agreement with *in vitro* work utilising recombinant prion protein lacking a GPI anchor by several groups, showing that recombinant protein can adopt a β-sheet conformation and undergo amyloid polymerisation under suitable conditions (127;277).

N2a models of scrapie cellular infection, whilst exhibiting demonstrable propagation of infectivity, are limited by the fact that they are sensitive to infection by only a small range of prion strains, notably RML, and are easily cured of the infection as

compared to experimental *in vivo* prion disease (138). As neuroblastoma cells, N2a are also continually replicating, in contrast to the situation in the brain where prion infections propagate within a static neuronal population (359). It is also important to note that the mechanisms whereby N2a cells are capable of propagating scrapie, where so many other cell lines cannot, have not been identified (360). The central features of the model, in terms of the replication of PrP^{Sc}, remain unknown. N2a cells recapitulate, therefore, only certain aspects of the cellular pathology of the prion disorders and are not, of themselves, a complete model of the disease process. The high sensitivity of the scrapie cell assay does, however, lend itself to evaluation of infectivity. The lack of any significant difference in infectivity as measured by this assay suggests that, if there is an impact on infectivity due to the removal of the GPI anchor, it results in less than a two fold reduction (*id est*, below the detection levels of the assay). This is an important finding as the dynamic range of western blot detection of PrP does not exclude the possibility that less than one percent of PrP^{Sc} molecules retain their GPI anchor. A contamination with one percent uncleaved material might be sufficient to produce similar patterns of prion infection in a conventional bio-assay, but would be detected by the scrapie cell assay. As a cellular model, the scrapie cell assay also simulates prion replication at a higher order of complexity to *in vitro* systems, and suggests that (in addition to not impacting on the replication of PrP^{Sc}) loss of the GPI anchor does not result in a decrease in the ability of RML to infect cells.

In vivo models of prion disease remain the most complete system within which to study the TSEs, mirroring many of the features of the naturally occurring disorders. They provide a model of prion propagation, of the infection process and, as indicated by the

terminal nature of the disease generated, of the toxicity and cell death associated with prion replication. The fact that no significant difference between cathepsin D treated and untreated RML was observed using the Tg20 transgenic mouse line indicates that C-terminal truncation does not interfere (within the limits of this model) with these processes. A major problem with *in vivo* analysis of infectivity such as that used here is that only large alterations in infectivity would be detected, highlighting the importance of using *in vivo* analysis in parallel with other techniques such as the scrapie cell assay.

Taken individually, each of the three systems used to investigate the infective and replicative properties of C-terminally truncated PrP^{Sc} suggest that the removal of the GPI does not result in a reduced ability to replicate, infect cells or cause disease. Although each system carries with it different drawbacks, taken cumulatively this body of work argues strongly that removal of the GPI by C-terminal truncation does not affect the infectious properties of the scrapie agent. This is particularly well demonstrated by the scrapie cell assay which is capable of detecting just a two-fold change in titre. This finding has several implications. First, it demonstrates that the GPI does not play a central role in the process of infection and replication of PrP^{Sc}, and is not a required molecular characteristic of the scrapie agent. It follows that membrane insertion of the disease associated form of PrP via the GPI anchor is not part of the process of infection, suggesting that the initial infection either occurs at the cell surface via a direct interaction with exogenous PrP^{Sc} or following internalisation of the scrapie agent. This does not necessarily contradict work carried out *in vivo* and in cell culture using PrP constructs lacking the GPI attachment sequence, resulting in a loss of the symptomatic prion disease although not a loss of protease resistant prion protein (309;313). As noted in section 5.1,

these studies significantly alter the location of PrP as well as its molecular characteristics. Secondly, since endogenous proteolytic release of PrP^{C} has been reported, this may provide a mechanism whereby infectious PrP^{Sc} could spread from cell to cell (350). Infectious PrP could be released from the cell in a c-terminally truncated form following endogenous proteolytic digest. This study demonstrates that, were this to occur, then such PrP could go on to infect further cells. Thirdly, the absence of decreased infectivity following removal of the GPI from PrP^{Sc} means that this is not a factor preventing the production of *de novo* prion infectivity using recombinant protein. This is in agreement with the recent work by Legname *et al* which showed that PrP generated in E. coli cells by recombinant expression (lacking both glycosylation and a GPI) is capable of stimulating prion associated neurodegenerative disease in a transgenic mouse model (112).

6.0 Conclusions

It is only by defining the molecular characteristics of the scrapie agent that an understanding can be gained as to the mechanism of replication and of cell death in the prion diseases. The clarification of how these occur will, in turn, shed light both on methods of intervening and halting the progression of devastating disorders such as scrapie and CJD and upon a fascinating novel area of basic biology – that of protein only replication. It is unfortunate that the very nature of the scrapie agent has made the task of investigating and defining these characteristics an arduous one. The research contained within this thesis has concentrated on two of the molecular characteristics of the scrapie agent: the impact of the codon 129 polymorphism on the biochemistry of the prion protein, and thence the scrapie agent; and the role of the Gycosylphophatidylinositol anchor on the infectious capabilities of PrP^{Sc}.

As discussed in the introduction, the codon 129 polymorphism of the prion protein has a surprisingly large impact on several aspects of the pathogenesis of the prion diseases, affecting susceptibility, disease progression, phenotype and pathology. To date, a biochemical basis for this impact has not been identified. In this thesis, a range of biochemical properties were investigated for both the methionine and valine prion protein codon 129 variants using recombinant PrP in the α-helical and β-sheet rich conformations to model the behaviour of PrP^{C} and PrP^{Sc} respectively. The structure of the α-helical rich form of PrP was investigated using circular dichroism, proteolytic degradation and analytical ultracentrifugation, with no significant difference between the two polymorphs being observed. The ability of both forms of α-PrP to bind copper was also investigated,

again with no significant difference observed. These data are in agreement with previous research into the biochemical characteristics of the codon 129 variants of α-PrP and suggest that, if there is an alteration in the properties of the prion protein based upon variation at codon 129, then this difference must be expressed in the β-sheet rich form or an intermediate in the formation of the β-rich isoform (269;271;275). Due to the difficulties in elucidating a detailed atomic level structure for β-PrP using high resolution techniques such as NMR or X-ray crystallography, several indirect or low resolution techniques were used to investigate the structural characteristics of the codon 129 variants folded into a predominantly β-sheet conformation. No significant difference was observed in the ability of the two polymorphs to convert from the α-helical to the β-sheet state *in vitro* and, once in the β-rich conformation, there was no observable difference in the CD spectra or proteolytic resistance of the two polymorphs. Using urea as a denaturant, the stabilities of the β-rich M and V polymorphs were examined. Although no obvious difference between the two polymorphs was observed with equilibrium unfolding (using molecular ellipticity at λ220nm as a marker for secondary structure), when spectra covering λ200 to 220nm were collected for the two forms a difference was uncovered between the two forms in the presence of 0.75M urea. At this concentration of denaturant, M129 PrP exhibited a greater retention of β-sheet structure. The lack of resolution provided by CD makes it difficult to define the exact difference in structure between the two polymorphs in these conditions, and further study of this phenomenon using higher resolution techniques is required. This apparent difference in structure in the presence of mild denaturants is especially interesting when taken in tandem with the

result from fibrillisation experiments carried out in similar conditions with the two codon 129 variants (see below).

Analysis of the sedimentation behaviour of M and V β-PrP revealed that methionine β-Prp has a lower Svedberg coefficient than valine β-PrP. Taken together with CD analysis of the two variants, this suggests that although the two polymorphs share a common β-sheet structure, M129 occupies a more compact three-dimensional conformation than V129. It is possible that this more compact structure favours the ordered self-association of M129 over V129 – an intriguing possibility when considered in the light of fibril forming experiments with the two variants. It should be noted that, in the conditions examined using AUC in these experiments, no significant self-association of either form into dimers, trimers or higher order oligomers was observed. However, given the long lag phase for fibril formation it is possible that ordered polymerisation initiates from a very small population of self associated molecules.

Using the model of PrP fibrillisation developed by Baskakov and co-workers, the formation of amyloid by the two codon 129 polymorphs was examined. In mild denaturing conditions (1M GuHCl, 1.3M urea), M129 PrP formed fibrils after a lag phase of 35hrs, whilst V129 PrP did not form fibrils after a lag phase in excess of 200hrs. Results from seeding experiments, where valine PrP amyloid growth could be stimulated by the addition of preformed methionine fibril seeds, suggest that V129 is capable of forming fibrils in energetically favourable conditions (provided here by seeding). It is of interest that a 1:1 mix of M and V PrP did not form fibrils – indicating that V129 PrP may have a dominant negative effect on the fibrillisation of M129 PrP. AUC experiments and CD analysis of partially denatured β-PrP may suggest a reason for the

differing fibril forming properties of the two polymorphs. Data from these investigations suggest M129 β-PrP has a more compact structure than V129 β-PrP, and is also slightly more resistant to denaturation. It is possible that the combination of these factors is the reason why PrP containing methionine at codon 129 forms amyloid in these specific conditions whilst PrP with valine at the same residue does not. How this biochemical difference relates to the disease state is difficult to assess. As discussed in chapter 3, the link between amyloid and disease in neurological disorders of protein misfolding where amyloid deposits are described is unclear. There is still a great deal of argument as to whether amyloid is on the disease pathway itself, if it is merely a marker for the end stage of disease or perhaps even a protective mechanism to minimise toxicity (174). With the prion diseases in particular, the lack of amyloid pathology in the majority of cases blurs the link between the amyloid forming properties of PrP and disease. A counter to this is the evidence from *in vivo* bioassay that suggests that fibril mixtures formed from recombinant mouse PrP can stimulate disease in a transgenic mouse model (112). It should be noted that it is not yet clear what species within the fibril mixture acts to stimulate disease and, therefore, the amyloid generated in the Baskakov system may yet represent an extraneous by-product of a disease process that occurs *via* small toxic oligomers. Regardless of this issue, evidence is accruing that suggests that it is some aspect of the aggregation or fibrillisation properties of the two polymorphs that results in the phenotypic impact of this polymorphism – both from the work contained in this thesis and through the efforts of other researchers (272). It is important to remember when considering this that any alteration in oligomerisation or fibrillisation dependent upon codon 129 status is but a marker for an alteration in a more fundamental aspect of the

biochemistry of β-PrP. This emphasises once again the importance of high resolution structures of the two codon 129 variants in the β-rich conformation.

The codon 129 polymorphism of PrP is one of the most fascinating of the molecular characteristics of the scrapie agent. Recent genetic evidence suggests that the continued presence of this polymorphism (or similar polymorphisms such as the E219K variant) in human populations may be a protective mechanism resulting from multiple historic or prehistoric exposures to epidemic prion disease. As a natural defence mechanism against these diseases, an increased comprehension of the molecular basis for the protective effect of this polymorphism may lead to both a greater understanding of the infectious behaviour and replication of the scrapie agent and the development of effective interventional strategies as therapy for diseases such as CJD.

The second molecular characteristic to be investigated in this thesis was the Glycosylphosphatidylinositol anchor attached to the C-terminus of mature PrP. Although the role of the GPI in the biology of the cellular prion protein has been well documented, the technical difficulties associated with investigating PrP^{Sc} (especially the resistance of PrP^{Sc} to treatment with phospholipase C) have hampered any examination of the role of the GPI in the biology of the scrapie agent. The research in this thesis presents treatment of PrP^{Sc} with the aspartic endoprotease cathepsin D as an alternative to PIPLC treatment for removal of the GPI anchor. This activity was identified by retardation of PrP^{Sc} in SDS gel electrophoresis following treatment with cathepsin D, analogous to the retardation observed when PIPLC is used to remove the GPI anchor from PrP^{C}. The initial part of this work concentrated on the characterisation of the interaction between PrP^{Sc} and cathepsin D, showing that the gel retardation was dependent on the time of

incubation with and the concentration of cathepsin D. This strongly supported the idea that this was an enzymatic phenomenon, and that treatment with cathepsin D was resulting in the loss of C-terminal peptides and the GPI anchor. Further evidence to support this was provided by the release of PrP^{C} from cells in culture following treatment with cathepsin D and the decrease in molecular mass exhibited by recombinant PrP upon treatment with cathepsin D – no gel retardation would be expected since recombinant PrP lacks a GPI anchor. Unfortunately, direct sequencing of the cleavage products was not possible due to the hydrophobic, aggregation prone nature of PrP^{Sc}.

Following investigation of the cleavage of PrP^{Sc} by cathepsin D, the impact of GPI loss on the infectivity of PrP^{Sc} was examined. To achieve this, cathepsin D treated PrP^{Sc} was compared to untreated PrP^{Sc} in three different models of prion replication and infectivity. There was no alteration in the ability of PrP^{Sc} to replicate in an *in vitro* model of prion propagation after C-terminal truncation by treatment with cathepsin D, a result echoed by *ex vivo* examination using a cell assay of infectivity. The third model used to investigate infectivity following C-terminal truncation was a transgenic mouse model of prion disease utilising Tg20 mice overexpressing mouse PrP. Again, no difference in infectivity was observed between PrP^{Sc} and C-terminal truncated PrP^{Sc} lacking the GPI anchor. Although each of these models have drawbacks, as discussed in chapter 5, taken *in toto* these data strongly support the argument that removing the GPI from PrP^{Sc} does not decrease its infectivity.

The absence of any impact on the infectivity of PrP^{Sc} due to loss of the GPI anchor has several implications. First, these data make it highly unlikely that the GPI plays a direct role in the replication of the scrapie agent. From a mechanistic point of

view, it is also less likely that the GPI plays a role in the process of cell infection, for example by aiding the insertion of the scrapie agent into the cell membrane. It is important to stress that the results presented in this thesis with regard to loss of the GPI are focussed on C-terminal truncation of the infectious agent and these data do not exclude the possibility that loss of the GPI from the cellular form of PrP has a major impact on the pathogenesis of prion disease. Indeed, there is some evidence that this may be the case (313). The lack of any decrease in the infectivity of PrP^{Sc} due to GPI loss does, however, suggest that any alteration in pathogenesis would be due to changes in the spatial location of PrP^{C} within the cell concomitant with GPI loss rather than an intrinsic change in the mechanism of prion replication.

The essential conclusion of these investigations into the removal of the GPI anchor from PrP^{Sc} is a negative one – that removal of the GPI has no impact on the infectivity of the scrapie agent. The importance of this finding is that it takes a step, however small, towards narrowing the definition of prion infectivity. By excluding the GPI as a requirement for the infectious process, the minimum molecular infectious unit (with PrP at its heart) is closer to comprehensive characterisation. Approaching this from the reverse standpoint, the work of Legname and colleagues supports these findings by suggesting that recombinant PrP, lacking both GPI and glycosylation, can stimulate prion disease in a transgenic mouse model (112). By extending our knowledge of the minimum prerequisites for the infectious process to occur, a greater understanding of the mechanisms of prion replication can be gleaned – with ramifications for therapeutic development.

7.0 Future Work

There are several avenues of investigation that the work contained within this thesis highlights for further examination. In terms of the codon 129 polymorphism, major questions remain as to the basis of the phenotypic variance witnessed between the two allelic forms. It has become increasingly apparent that the origin of the codon 129 affect is likely to reside in the structure and properties of the β-form, a statement supported by the work in this thesis. The most important gap in our knowledge regarding this is, of course, an atomic resolution structure of the β-form. As noted (section 1.4), this has long been the focus of much of the biochemical investigations into prion biology. For the codon 129 polymorphism, a true understanding of the mechanism whereby it exerts its affect is unlikely to be arrived until atomic resolution structures of the β-rich conformation of both M129 and V129 forms of the prion protein are elucidated. With regard to this, it is of interest that some evidence for differential unfolding pathways followed by the M and V forms of recombinant prion protein in the presence of urea have been revealed (see section 2.2.2). It may be that more detailed examination of these partially unfolded states using higher resolution techniques will yield important information as to any molecular level conformational differences in the β-rich form due to the codon 129 polymorphism.

In addition to structural determination, there are several aspects of the biochemistry of M and V PrP investigated in this body of work that merit further investigation. In terms of the binding of Cu^{2+} to the prion protein, only interactions with 91-231 α-PrP were investigated. Whilst the amino acids covered by this recombinant

protein represent the structured domains of PrP, it is impossible to exclude (except by experimentation) that there may be differential copper binding to full length M and V forms. It is also important to exclude differential copper binding to the β-rich conformation as a possible molecular characteristic that varies between the two polymorphs – although there are technical difficulties associated with carrying out the copper binding in the low pH conditions that favour the β-rich isoform. It would also be of interest to revisit the super oxide dismutase properties of the M and V forms of the human prion protein, examined by Wong and colleagues using mouse PrP with an anthropomorphous codon 129 polymorphism (269). As has been discussed (section 1.5), a mouse PrP peptide sequence background does not present the best model in which to investigate human polymorphisms or mutations, and would not necessarily reveal alterations that may be present in the human *in vivo* system. This suggests the investigation of SOD-1 activity using human PrP may be worthwhile. Any such investigation should be qualified, however, by increasing evidence that PrP may lack a physiologically relevant SOD-1 activity (207).

Whilst the fibrillisation experiments described herein provide provocative evidence of a biochemical difference between the two polymorphs, there are many aspects of the aggregation properties of human M129 and V129 PrP that merit further investigation. Only a very small selection of possible fibrillisation conditions, in terms of pH, temperature, denaturant concentration and substrate concentration, were examined in this investigation for the M and V codon 129 variants. To fully understand the interaction of the two codon 129 polymorphs in the model system developed by Baskakov *et al*, a wider range of conditions needs to be investigated. As discussed in

section 3.3, it is possible that there are conditions that would favour the fibrillisation of valine 129 PrP over methionine 129 PrP (that is, the reverse of what was observed with the conditions used in the current experiments). There are also several other investigative techniques that could be applied to this system in order to shed light on the nature of the biochemical difference that is leading to this divergence in aggregation properties. Electron microscopy has been applied to several types of amyloid deposits, including PrP amyloid, yielding much important structural data (268;361;362). Due to the potentially infectious nature of the fibrils generated using the Baskakov protocol from recombinant human prion protein, it has not been possible under local biosafety rules to examine the fibrils formed from methionine or valine seeded by methionine by electron microscopy. This technique does, however, have the potential to reveal much information about any structural variation in fibrils due to the codon 129 polymorphism. Were the correct facilities to become available, electron microscopy should be applied to the amyloid generated in this study. Another technique that has the potential to reveal information about the fibril forming characteristics of M129 and V129 PrP is total internal reflection fluorescence microscopy (TIRFM). This technique allows direct observation of fibril growth by exploiting the fluorescent properties of thioflavin T bound to amyloid deposits. TIRFM has been successfully used to visualise amyloid generation by β2-microglobulin, revealing information about the kinetics and directionality of amyloid growth (363).

The codon 129 polymorphism has received a considerable amount of scientific scrutiny due to its role in the pathogenesis of the prion diseases, and especially its importance in susceptibility to vCJD. In contrast, the E219K polymorphism found in Asian populations has received very little attention in regards to its role in the

epidemiology of prion diseases, or in terms of any structural or biochemical impact it may have on the biology of PrP (39). Since it has been suggested that the E219K polymorphism plays essentially the same protective role fulfilled by the codon 129 polymorphism in other populations, further studies of the structural and biophysical characteristics of the codon 219 polymorphism may prove illuminating to the biology of codon 129 and its interaction with the disease process, as well as the pathogenesis of the prion diseases *per se* (64).

There are several questions surrounding the C-terminal truncation of PrP^{Sc} by cathepsin D that remain to be answered. The central issue that remains to be resolved is exactly where in the primary C-terminal sequence of PrP cathepsin D is cleaving. As noted in chapter 4, there are several technical difficulties that must be overcome before this can be achieved. Techniques for the purification of PrP^{Sc} are improving, but are not yet at the point where reliable peptide mapping, and therefore identification of the cleavage point, is attainable (232). An alternative approach to this would be the sequencing of recombinant PrP digested with cathepsin D, which might reveal information about which residues in the C-terminus of PrP are susceptible to cleavage by the enzyme. A major criticism of this approach, however, is that digestion of recombinant PrP, whether this be α-rich or β-rich, does not necessarily recapitulate the situation with PrP^{Sc} *in vivo* and so, at best, could only be used as indirect evidence of cleavage.

An interesting possible application of cathepsin D would be to use the enzyme to treat scrapie infected cell lines in an attempt to release PrP^{Sc} from the cell surface. In the course of the current research, it was shown that treatment of non-scrapie infected cells

with cathepsin D resulted in the release of PrP^C from the plasma membrane – but the impact on infected cells was not investigated. This approach may settle the question as to whether or not the scrapie agent is intracellular or membrane associated in cell lines propagating PrP^{Sc}, still a matter of some debate.

A final future area of investigation that is suggested by this body of work is to examine both a possible physiological interaction between either PrP^C or PrP^{Sc} and cathepsin D, and whether cathepsin D is involved in susceptibility to the prion diseases. In the first case, work carried out by Parkin *et al* suggests that endogenous PrP^C undergoes proteolytic release from cells (350). Although this study has not uncovered any direct evidence of an *in vivo* interaction between cathepsin D and PrP, it is intriguing to speculate as to whether this enzyme plays a role in proteolytic shedding or degradation of either the cellular or scrapie associated form of PrP – a possibility that warrants further investigation. As regards cathepsin D and susceptibility to the prion diseases, it would be of interest to investigate whether polymorphisms in the cathepsin D gene are risk factors for prion disease – as may be the case with the A224V polymorphism in cathepsin D and Alzheimer's disease (344). It would also be informative to investigate using western and northern blots any up or down regulation of cathepsin D associated with prion disease – again with the aim of identifying any link between the disease state and this proteolytic enzyme.

Reference List

1. Locke, J. (1690) Of Knowledge and Opinion. *An Essay Concerning Human Understanding,*

2. (1755) *Journal of the House of Commons* **27,** 87-88

3. Comber (1772) *Crit.Rev.London* **32,** 72-73

4. Collinge, J. (2001) *Annu.Rev Neurosci.* **24,** 519-550

5. Brugere-Picoux, J., Combrisson, H., Robain, G., Chatelain, J., Laplanche, J.-L., and Brugere, H. (1996) Clinical aspects of scrapie in sheep. In Court, L. and Dodet, B., editors. *Transmissible Subacute Spongiform Encephalopathies: Prion Diseases*, Elsevier, Paris

6. Parry, H. (1962) *Heredity (Edinburgh).* **17,** 75-105

7. Foster, J. D., Parnham, D., Chong, A., Goldmann, W., and Hunter, N. (2001) *Veterinary Record* **148,** 165-171

8. Parry, H. (1979) *Nature* **277,** 127-129

9. Draper, GJ. and Parry, H. (1962) *Nature* **195,** 670-672

10. Besnoit, C. (1899) *Rev.Vet.Toulouse* **24,** 265-343

11. Cuillé, J. and Chelle, P. L. (1936) *C.R.Acad.Sci.* **203,** 1552-1554

12. Chandler, R. L. (1961) *Lancet* 1378-1379

13. Guiroy, D. C., Williams, E. S., Song, K.-J., Yanagihara, R., and Gajdusek, D. C. (1993) *Acta Neuropathol (Berl)* **86,** 77-80

14. Miller, M. W. and Williams, E. S. (2004) *Curr.Top.Microbiol.Immunol.* **284,** 193-214

15. Williams, E. S. and Young, S. (1980) *J Wildl.Dis.* **16,** 89-98

16. (2003) *MMWR Morb.Mortal.Wkly.Rep.* **52,** 125-127

17. Marsh, R. F. (1992) Transmissible Mink Encephalopathy. In Prusiner, S. B., Collinge, J., Powell, J., and Anderton, B., editors. *Prion Diseases of Humans and Animals*, Ellis Horwood, London

18. Wells, G. A. H., Scott, A. C., Johnson, C. T., Gunning, R. F., Hancock, R. D., Jeffrey, M., Dawson, M., and Bradley, R. (1987) *Vet.Rec.* **Oct 31,** 419-420

19. Anderson, R. M., Donnelly, C. A., Ferguson, N. M., Woolhouse, M. E. J., Watt, C. J., Udy, H. J., MaWhinney, S., Dunstan, S. P., Southwood, T. R. E., Wilesmith, J. W., Ryan, J. B. M., Hoinville, L. J., Hillerton, J. E., Austin, A. R., and Wells, G. A. H. (1996) *Nature* **382,** 779-788

20. Hope, J., Reekie, L. J., Hunter, N., Multhaup, G., Beyreuther, K., White, H., Scott, A. C., Stack, M. J., Dawson, M., and Wells, G. A. (1988) *Nature* **336,** 390-392

21. Prusiner, S. B. (1997) *Science* **278,** 245-251

22. Ferguson, N. M., Ghani, A. C., Donnelly, C. A., Hagenaars, T. J., and Anderson, R. M. (2002) *Nature* **415,** 420-424

23. Sugiura, K., Ito, K., Yokoyama, R., Kumagai, S., and Onodera, T. (2003) *Rev.Sci Tech.* **22,** 777-794

24. (2004) *MMWR Morb.Mortal.Wkly.Rep.* **52,** 1280-1285

25. Coulthart, M. B., Mogk, R., Rancourt, J. M., Godal, D. L., and Czub, S. (2003) *Genome* **46,** 1005-1009

26. Kirkwood, J. K., Wells, G. A., Wilesmith, J. W., Cunningham, A. A., and Jackson, S. I. (1990) *Vet.Rec.* **127,** 418-420

27. Hill, A. F., Desbruslais, M., Joiner, S., Sidle, K. C. L., Gowland, I., and Collinge, J. (1997) *Nature* **389,** 448-450

28. Raymond, G. J., Hope, J., Kocisko, D. A., Priola, S. A., Raymond, L. D., Bossers, A., Ironside, J., Will, R. G., Chen, S. G., Petersen, R. B., Gambetti, P., Rubenstein, R., Smits, M. A., Lansbury, P. T. Jr., and Caughey, B. (1997) *Nature* **388,** 285-288

29. Manuelidis, L., Fritch, W., and Xi, Y.-G. (1997) *Science* **277,** 94-98

30. Cousens, S. N., Zeidler, M., Esmonde, T. F., De Silva, R., Wilesmith, J. W., Smith, P. G., and Will, R. G. (1997) *BMJ* **315,** 389-395

31. Ghani, A. C., Ferguson, N. M., Donnelly, C. A., and Anderson, R. M. (2000) *Nature* **406,** 583-584

32. Creutzfeld H (1920) *Zeitschrift für die gesamte Neurologie und Psychiatrie* **57,** 1-18

33. Jakob, A. (1921) *Z.Gesamte Neurol..psychiatry.* **64,** 147-228

34. Jakob, A. (1921) *Med.Klin.* **13,** 372-376

35. Masters, C. L. and Richardson, E. P., Jr. (1978) *Brain* **101,** 333-344

36. Brown, P., Cathala, F., Castaigne, P., and Gajdusek, D. C. (1986) *Ann Neurol* **20,** 597-602

37. Brown, P., Gibbs, C. J. Jr., Rodgers Johnson, P., Asher, D. M., Sulima, M. P., Bacote, A., Goldfarb, L. G., and Gajdusek, D. C. (1994) *Ann Neurol* **35,** 513-529

38. Palmer, M. S., Dryden, A. J., Hughes, J. T., and Collinge, J. (1991) *Nature* **352,** 340-342

39. Shibuya, S., Higuchi, J., Shin, R. W., Tateishi, J., and Kitamoto, T. (1998) *Ann.Neurol.* **43,** 826-828

40. Shibuya, S., Higuchi, J., Shin, R. W., Tateishi, J., and Kitamoto, T. (1998) *Lancet* **351,** 419

41. Gajdusek, D. C. and Gibbs, C. J. Jr. (1971) *Nature* **230,** 588-591

42. Gibbs, C. J. Jr., Gajdusek, D. C., Asher, D. M., Alpers, M. P., Beck, E., Daniel, P. M., and Matthews, W. B. (1968) *Science* **161,** 388-389

43. Billette de Villemeur, T. B., Beauvais, P., Gourmelen, M., and Richardet, J. M. (1991) *Lancet* **337,** 864-865

44. Brown, P., Gajdusek, D. C., Gibbs, C. J. Jr., and Asher, D. M. (1985) *New Eng J Med* **313,** 728-731

45. Cavanagh, H. D. and Hogan, R. N. (1999) *Journal of the American Medical Association* **282,** 2211

46. Martinez-Lage, J. F., Poza, M., Sola, J., Tortosa, J. G., Brown, P., Cervenakova, L., Esteban, J. A., and Mendoza, A. (1994) *J Neurol Neurosurg.Psychiatry* **57,** 1091-1094

47. Owen, F., Poulter, M., Lofthouse, R., Collinge, J., Crow, T. J., Risby, D., Baker, H. F., Ridley, R. M., Hsiao, K., and Prusiner, S. B. (1989) *Lancet* **1,** 51-52

48. Hsiao, K., Baker, H. F., Crow, T. J., Poulter, M., Owen, F., Terwilliger, J. D., Westaway, D., Ott, J., and Prusiner, S. B. (1989) *Nature* **338,** 342-345

49. Prusiner, S. B. (1994) *Annu.Rev.Microbiol.* **48,** 655-686

50. Collinge, J., Palmer, M. S., and Dryden, A. J. (1991) *Lancet* **337,** 1441-1442

51. Baker, H. E., Poulter, M., Crow, T. J., Frith, C. D., Lofthouse, R., Ridley, R. M., and Collinge, J. (1991) *Lancet* **337,** 1286

52. Kovacs, G. G., Trabattoni, G., Hainfellner, J. A., Ironside, J. W., Knight, R. S., and Budka, H. (2002) *J.Neurol.* **249,** 1567-1582

53. Gerstmann, J., Sträussler, E., and Scheinker, I. (1936) *Z.Neurol.* **154,** 736-762

54. Gerstmann, J., Straussler, E., and Scheinker, I. (1935) *Verein fur Psychiatrie und Neurologie* 736-762

55. Kretzschmar, H. A., Honold, G., Seitelberger, F., Feucht, M., Wessely, P., Mehraein, P., and Budka, H. (1991) *Lancet* **337,** 1160

56. Gajdusek, D. C. and Zigas, V. (1957) *New Eng J Med* **257,** 974-978

57. Gajdusek, D. C. (1977) *Science* **197,** 943-960

58. Kretzschmar, H. A. (1993) *Dev.Biol.Stand.* **80,** 71-90

59. Goldfarb, L. (2002) *Microbes.Infect.* **4,** 875

60. Gajdusek, D. C., Gibbs, C. J. Jr., and Alpers, M. P. (1966) *Nature* **209,** 794-796

61. Huillard d'Aignaux, J. N., Cousens, S. N., Maccario, J., Costagliola, D., Alpers, M. P., Smith, P. G., and Alperovitch, A. (2002) *Epidemiology* **13,** 402-408

62. Prusiner, S. B., Gajdusek, D. C., and Alpers, M. P. (1982) *Ann Neurol* **12,** 1-9.

63. Lee, H. S., Brown, P., Cervenáková, L., Garruto, R. M., Alpers, M. P., Gajdusek, D. C., and Goldfarb, L. G. (2001) *Journal of Infectious Diseases* **183,** 192-196

64. Mead, S., Stumpf, M. P., Whitfield, J., Beck, J. A., Poulter, M., Campbell, T., Uphill, J., Goldstein, D., Alpers, M., Fisher, E. M., and Collinge, J. (2003) *Science*

65. Cervenakova, L., Goldfarb, L., Garruto, R., Lee, H. S., Gajdusek, C. D., and Brown, P. (1999) *Proc Natl Acad Sci USA* **95,** 13239-13241

66. Lugaresi, E., Medori, R., Baruzzi, P. M., Cortelli, P., Lugaresi, A., Tinuper, P., Zucconi, M., and Gambetti, P. (1986) *N.Engl.J Med.* **315,** 997-1003

67. Montagna, P., Gambetti, P., Cortelli, P., and Lugaresi, E. (2003) *Lancet Neurol.* **2,** 167-176

68. Mastrianni, J. A., Nixon, R., Layzer, R., DeArmond, S. J., and Prusiner, S. B. (1997) *Neurology* **48,** A296

69. Tateishi, J., Brown, P., Kitamoto, T., Hoque, Z. M., Roos, R., Wollman, R., Cervenakova, L., and Gajdusek, D. C. (1995) *Nature* **376,** 434-435

70. Collinge, J., Palmer, M. S., Sidle, K. C. L., Gowland, I., Medori, R., Ironside, J., and Lantos, P. L. (1995) *Lancet* **346,** 569-570

71. Medori, R., Tritschler, H. J., LeBlanc, A., Villare, F., Manetto, V., Chen, H. Y., Xue, R., Leal, S., Montagna, P., Cortelli, P., Tinuper, P., Avoni, P., Mochi, M., Baruzzi, Q., Hauw, J. J., Ott, J., Lugaresi, E., Autilio-Gambetti, L., and Gambetti, P. (1992) *N.Engl.J Med* **326,** 444-449

72. Monari, L., Chen, S. G., Brown, P., Parchi, P., Petersen, R. B., Mikol, J., Gray, F., Cortelli, P., Montagna, P., Ghetti, B., Goldfarb, L. G., Gajdusek, D. C., Lugaresi, E., Gambetti, P., and Autilio-Gambetti, L. (1994) *Proc.Natl.Acad.Sci.USA* **91,** 2839-2842

73. Goldfarb, L. G., Petersen, R. B., Tabaton, M., Brown, P., LeBlanc, A. C., Montagna, P., Cortelli, P., Julien, J., Vital, C., Pendelbury, W. W., Haltia, M., Wills, P. R., Hauw, J. J., McKeever, P. E., Monari, L., Schrank, B., Swergold, G. D., Autilio-Gambetti, L., Gajdusek, D. C., Lugaresi, E., and Gambetti, P. (1992) *Science* **258,** 806-808

74. Medori, R. and Tritschler, H. J. (1993) *Am J Hum.Genet.* **53,** 822-827

75. Will, R. G., Ironside, J. W., Zeidler, M., Cousens, S. N., Estibeiro, K., Alperovitch, A., Poser, S., Pocchiari, M., Hofman, A., and Smith, P. G. (1996) *Lancet* **347,** 921-925

76. Peden, A. H. and Ironside, J. W. (2004) *Folia Neuropathol.* **42 Suppl A,** 85-91

77. Zeidler, M., Stewart, G., Cousens, S. N., Estebeiro, K., and Will, R. G. (1997) *Lancet* **350,** 668

78. Scott, M. R., Will, R., Ironside, J., Nguyen, H. O. B., Tremblay, P., DeArmond, S. J., and Prusiner, S. B. (1999) *Proc.Natl.Acad.Sci.USA* **96,** 15137-15142

79. Lasmézas, C. I., Deslys, J.-P., Demaimay, R., Adjou, K. T., Lamoury, F., Dormont, D., Robain, O., Ironside, J., and Hauw, J.-J. (1996) *Nature* **381,** 743-744

80. Peden, A. H., Head, M. W., Ritchie, D. L., Bell, J. E., and Ironside, J. W. (2004) *Lancet* **364,** 527-529

81. Hilton, D. A., Ghani, A. C., Conyers, L., Edwards, P., McCardle, L., Ritchie, D., Penney, M., Hegazy, D., and Ironside, J. W. (2004) *J Pathol.* **203,** 733-739

82. Ross, C. A. and Poirier, M. A. (2004) *Nat Med* **10 Suppl 1,** S10-S17

83. Prusiner, S. B. (1982) *Science* **216,** 136-144

84. Alper, T., Haig, D. A., and Clarke, M. C. (1966) *Biochem.Biophys.Res.Commun.* **22,** 278-284

85. Alper, T., Cramp, W. A., Haig, D. A., and Clarke, M. C. (1967) *Nature* **214,** 764-766

86. Gibbs-CJ, J., Gajdusek, C. D., and Latarjet, R. (1978) *PNAS* **75,** 6268-6270

87. Dickinson, A. G. and Meikle, V. M. H. (1971) *Molec.Gen.Genetics* **112,** 73-79

88. Dickinson, A. G., Fraser, H., Meikle, V. M., and Outram, G. W. (1972) *Nature New Biol* **237,** 244-245

89. Sigurdsson, B. (1954) *Br.Vet.J* **110,** 341-354

90. Gajdusek, D. C., Gibbs, C. J. Jr., and Alpers, M. (1967) *Science* **155,** 212-214

91. Hadlow, W. J. (1959) *Lancet* **ii,** 289-290

92. Gibbons, R. A. and Hunter, G. D. (1967) *Nature* **215,** 1041-1043

93. Griffith, J. S. (1967) *Nature* **215,** 1043-1044

94. Crick, F. (1970) *Nature* **227,** 561-563

95. Crick, F. (1964) *Intern.Union Biochem.* **33,** 109

96. Crick, F. (1989) The Baffling Problem. *What Mad Pursuit*, Penguin,

97. Prusiner, S. B., Cochran, S. P., Groth, D. F., Downey, D. E., Bowman, K., and Martinez, H. M. (1982) *Ann Neurol* **11,** 353-38.

98. McKinley, M. P., Bolton, D. C., and Prusiner, S. B. (1983) *Cell* **35,** 57-62

99. Baltimore, D. (1970) *Nature* **226,** 1209-1211

100. Temin, H. M. and Mizutani, S. (1970) *Nature* **226,** 1211-1213

101. Oesch, B., Westaway, D., Walchli, M., McKinley, M. P., Kent, S. B., Aebersold, R., Barry, R. A., Tempst, P., Teplow, D. B., Hood, L. E., and Raeber, A. J. (1985) *Cell* **40,** 735-746

102. Basler, K., Oesch, B., Scott, M., Westaway, D., Walchli, M., Groth, D. F., McKinley, M. P., Prusiner, S. B., and Weissmann, C. (1986) *Cell* **46,** 417-428

103. Bossers, A., Schreuder, B. E. C., Muileman, I. H., Belt, P. B. G. M., and Smits, M. A. (1996) *J Gen Virol* **77,** 2669-2673

104. Carlson, G. A., Goodman, P. A., Lovett, M., Taylor, B. A., Marshall, S. T., Peterson Torchia, M., Westaway, D., and Prusiner, S. B. (1988) *Mol.Cell Biol.* **8,** 5528-5540

105. Manuelidis, L. (1994) *Ann.NY Acad.Sci.* **724,** 259-281

106. Liao, Y. C., Lebo, R. V., Clawson, G. A., and Smuckler, E. A. (1986) *Science* **233,** 364-367

107. Hsiao, K. K., Scott, M., Foster, D., Groth, D. F., DeArmond, S. J., and Prusiner, S. B. (1990) *Science* **250,** 1587-1590

108. Hsiao, K., Scott, M., Foster, D., DeArmond, S. J., Groth, D., Serban, H., and Prusiner, S. B. (1991) *Ann.NY Acad.Sci.* **640,** 166-170

109. Bueler, H., Fischer, M., Lang, Y., Bluethmann, H., Lipp, H.-P., DeArmond, S. J., Prusiner, S. B., Aguet, M., and Weissmann, C. (1992) *Nature* **356,** 577-582

110. Bueler, H., Fischer, M., Lang, Y., Bluthmann, H., Lipp, H.-P., DeArmond, S. J., Prusiner, S. B., Aguet, M., and Weissmann, C. (1993) *Nature*

111. Bueler, H., Aguzzi, A., Sailer, A., Greiner, R. A., Autenried, P., Aguet, M., and Weissmann, C. (1993) *Cell* **73,** 1339-1347

112. Legname, G., Baskakov, I. V., Nguyen, H. O., Riesner, D., Cohen, F. E., DeArmond, S. J., and Prusiner, S. B. (2004) *Science* **305,** 673-676

113. Legname, G., Nguyen, H., Baskakov, I. V., Cohen, F. E., DeArmond, S., and Prusiner, S. B. (2005) *Proc Natl Acad Sci USA* **102,** 2168-2173

114. Riek, R., Hornemann, S., Wider, G., Billeter, M., Glockshuber, R., and Wuthrich, K. (1996) *Nature* **382,** 180-182

115. Zahn, R., Liu, A. Z., Lührs, T., Riek, R., Von Schroetter, C., García, F. L., Billeter, M., Calzolai, L., Wider, G., and Wüthrich, K. (2000) *Proc.Natl.Acad.Sci.USA* **97,** 145-150

116. Riek, R., Wider, G., Billeter, M., Hornemann, S., Glockshuber, R., and Wuthrich, K. (1998) *Proc Natl Acad Sci U.S.A.* **95,** 11667-11672

117. James, T. L., Liu, H., Ulyanov, N. B., Farr-Jones, S., Zhang, H., Donne, D. G., Kaneko, K., Groth, D., Mehlhorn, I., Prusiner, S. B., and Cohen, F. E. (1997) *Proc.Natl.Acad.Sci.USA* **94,** 10086-10091

118. Liu, H., Farr-Jones, S., Ulyanov, N. B., Llinas, M., Marqusee, S., Groth, D., Cohen, F. E., Prusiner, S. B., and James, T. L. (1999) *Biochemistry* **38,** 5362-5377

119. Hosszu, L. L. P., Baxter, N. J., Jackson, G. S., Power, A., Clarke, A. R., Waltho, J. P., Craven, C. J., and Collinge, J. (1999) *Nature Struct.Biol.* **6,** 740-743

120. Stahl, N. and Prusiner, S. B. (1991) *FASEB J.* **5,** 2799-2807

121. Rudd, P. M., Wormald, M. R., Wing, D. R., Prusiner, S. B., and Dwek, R. A. (2001) *Biochemistry* **40,** 3759-3766

122. Stahl, N., Borchelt, D. R., Hsiao, K., and Prusiner, S. B. (1987) *Cell* **51,** 229-240

123. Caughey, B. W., Dong, A., Bhat, K. S., Ernst, D., Hayes, S. F., and Caughey, W. S. (1991) *Biochemistry* **30,** 7672-7680

124. Gasset, M., Baldwin, M. A., Fletterick, R. J., and Prusiner, S. B. (1993) *Proc.Natl.Acad.Sci.U.S A.* **90,** 1-5

125. Pan, K.-M., Baldwin, M. A., Nguyen, J., Gasset, M., Serban, A., Groth, D., Mehlhorn, I., Huang, Z., Fletterick, R. J., Cohen, F. E., and Prusiner, S. B. (1993) *Proc Natl Acad Sci USA* **90,** 10962-10966

126. Jackson, G. S., Hill, A. F., Joseph, C., Hosszu, L. L. P., Clarke, A. R., and Collinge, J. (1999) *Biochimica et Biophysica Acta* **1431,** 1-13

127. Jackson, G. S., Hosszu, L. L. P., Power, A., Hill, A. F., Kenney, J., Saibil, H., Craven, C. J., Waltho, J. P., Clarke, A. R., and Collinge, J. (1999) *Science* **283,** 1935-1937

128. Baskakov, I. V., Legname, G., Baldwin, M. A., Prusiner, S. B., and Cohen, F. E. (2002) *J.Biol.Chem.* **277,** 21140-21148

129. Baskakov, I. V. (2003) *J Biol.Chem*

130. Yanagihara, R. T., Asher, D. M., Gibbs, C. J. Jr., and Gajdusek, D. C. (1980) *Proc.Soc.Exp.Biol.Med.* **165,** 298-305

131. Clarke, M. C. and Haig, D. A. (1970) *Res Vet Sci.* **11,** 500-501

132. Gajdusek, D. C., Gibbs, C. J. Jr., Rogers, N. G., Basnight, M., and Hooks, J. (1972) *Nature* **235,** 104-105

133. Rubenstein, R., Carp, R. I., and Callahan, S. M. (1984) *J Gen.Virol.* **65,** 2191-2198

134. Butler, D. A., Scott, M. R., Bockman, J. M., Borchelt, D. R., Taraboulos, A., Hsiao, K. K., Kingsbury, D. T., and Prusiner, S. B. (1988) *J Virol.* **62,** 1558-1564

135. Caughey, B., Ernst, D., and Race, R. E. (1993) *J Virol.* **67,** 6270-6272

136. Caughey, B. and Raymond, G. J. (1993) *J Virol.* **67,** 643-650

137. Enari, M., Flechsig, E., and Weissmann, C. (2001) *Proc.Natl.Acad.Sci.USA* **98,** 9295-9299

138. Kocisko, D. A., Morrey, J. D., Race, R. E., Chen, J., and Caughey, B. (2004) *J Gen Virol* **85,** 2479-2483

139. Bosque, P. J. and Prusiner, S. B. (2000) *Journal of Virology* **74,** 4377-4386

140. Klohn, P. C., Stoltze, L., Flechsig, E., Enari, M., and Weissmann, C. (2003) *Proc.Natl.Acad.Sci U.S.A*

141. Weissmann, C. (2004) *Nat Rev.Microbiol.* **2,** 861-871

142. Ma, J., Wollmann, R., and Lindquist, S. (2002) *Science*

143. Ma, J. and Lindquist, S. (2002) *Science*

144. Harris, D. A. (1999) *Clin.Microbiol.Rev.* **12,** 429-444

145. Wegner, C., Roemer, A., Schmalzbauer, R., Lorenz, H., Windl, O., and Kretzschmar, H. A. (2002) *J.Gen.Virol.* **83,** 1237-1245

146. Raeber, A. J., Borchelt, D. R., Scott, M., and Prusiner, S. B. (1992) *J Virol.* **66 (10),** 6155-6163

147. Kocisko, D. A., Come, J. H., Priola, S. A., Chesebro, B., Raymond, G. J., Lansbury, P. T., and Caughey, B. (1994) *Nature* **370,** 471-474

148. Kocisko, D. A., Priola, S. A., Raymond, G. J., Chesebro, B., Lansbury, P. T., Jr., and Caughey, B. (1995) *Proc.Natl.Acad.Sci.U.S A.* **92,** 3923-3927

149. Caughey, W. S., Raymond, L. D., Horiuchi, M., and Caughey, B. (1998) *Proc Natl Acad Sci USA* **95,** 12117-12122

150. Chabry, J., Caughey, B., and Chesebro, B. (1998) *J Biol chem* **273,** 13203-13207

151. Bessen, R. A., Kocisko, D. A., Raymond, G. J., Nandan, S., Lansbury, P. T., and Caughey, B. (1995) *Nature* **375,** 698-700

152. Hill, A. F., Antoniou, M., and Collinge, J. (1999) *J.Gen.Virol.* **80,** 11-14

153. Saborio, G. P., Permanne, B., and Soto, C. (2001) *Nature* **411,** 810-813

154. Bieschke, J., Weber, P., Sarafoff, N., Beekes, M., Giese, A., and Kretzschmar, H. (2004) *Proc.Natl.Acad Sci U.S.A*

155. Deleault, N. R., Lucassen, R. W., and Supattapone, S. (2003) *Nature* **425,** 717-720

156. Lucassen, R., Nishina, K., and Supattapone, S. (2003) *Biochemistry* **42,** 4127-4135

157. Nishina, K., Deleault, N. R., Lucassen, R. W., and Supattapone, S. (2004) *Biochemistry* **43,** 2613-2621

158. Prusiner, S. B. (1991) *Science* **252,** 1515-1522

159. Jarrett, J. T. and Lansbury, P. T. J. (1993) *Cell* **73,** 1055-1058

160. Cohen, F. E., Pan, K.-M., Huang, Z., Baldwin, M., Fletterick, R. J., and Prusiner, S. B. (1994) *Science* **264,** 530-531

161. Come, J. H., Fraser, P. E., and Lansbury, P. T. J. (1993) *Proc.Natl.Acad.Sci.U.S A.* **90,** 5959-5963

162. Wickner, R. B. (1994) *Science* **264,** 566-569

163. Uptain, S. M. and Lindquist, S. (2002) *Annu.Rev.Microbiol.*

164. Patino, M. M., Liu, J. J., Glover, J. R., and Lindquist, S. (1996) *Science* **273,** 622-626

165. Lindquist, S., DebBurman, S. K., Glover, J. R., Kowal, A. S., Liu, J. J., Schirmer, E. C., and Serio, T. R. (1998) *Biochem.Soc.Trans.* **26,** 486-490

166. Serio, T. R., Cashikar, A. G., Kowal, A. S., Sawicki, G. J., Moslehi, J. J., Serpell, L., Arnsdorf, M. F., and Lindquist, S. L. (2000) *Science* **289,** 1317-1321

167. Chernoff, Y. O., Lindquist, S. L., Ono, B., Inge Vechtomov, S. G., and Liebman, S. W. (1995) *Science* **268,** 880-884

168. Grimminger, V., Richter, K., Imhof, A., Buchner, J., and Walter, S. (2003) *J Biol.Chem*

169. DebBurman, S. K., Raymond, G. J., Caughey, B., and Lindquist, S. (1997) *Proc.Natl.Acad.Sci.USA* **94,** 13938-13943

170. Schirmer, E. C. and Lindquist, S. (1997) *Proc.Natl.Acad.Sci.USA* **94,** 13932-13937

171. Jin, T. C., Gu, Y. P., Zanusso, G., Sy, M. S., Kumar, A., Cohen, M., Gambetti, P., and Singh, N. (2000) *Journal of Biological Chemistry* **275,** 38699-38704

172. Tanaka, M., Chien, P., Naber, N., Cooke, R., and Weissman, J. S. (2004) *Nature* **428,** 323-328

173. King, C. Y. and Diaz-Avalos, R. (2004) *Nature* **428,** 319-323

174. Stefani, M. and Dobson, C. M. (2003) *J Mol.Med.*

175. DuBay, K. F., Pawar, A. P., Chiti, F., Zurdo, J., Dobson, C. M., and Vendruscolo, M. (2004) *J Mol.Biol* **341,** 1317-1326

176. Wildegger, G., Liemann, S., and Glockshuber, R. (1999) *Nature Struct.Biol.* **6,** 550-553

177. Kayed, R., Head, E., Thompson, J. L., McIntire, T. M., Milton, S. C., Cotman, C. W., and Glabe, C. G. (2003) *Science* **300,** 486-489

178. Bucciantini, M., Giannoni, E., Chiti, F., Baroni, F., Formigli, L., Zurdo, J., Taddei, N., Ramponi, G., Dobson, C. M., and Stefani, M. (2002) *Nature* **416,** 507-511

179. Kretzschmar, H. A., Stowring, L. E., Westaway, D., Stubblebine, W. H., Prusiner, S. B., and DeArmond, S. J. (1986) *DNA* **5,** 315-324

180. Wopfner, F., Weidenhöfer, G., Schneider, R., Von Brunn, A., Gilch, S., Schwarz, T. F., Werner, T., and Schätzl, M. (1999) *Journal of Molecular Biology* **289,** 1163-1178

181. Manson, J., West, J. D., Thomson, V., McBride, P., Kaufman, M. H., and Hope, J. (1992) *Development* **115,** 117-122

182. Harris, D. A., Huber, M. T., Van Dijken, P., Shyng, S.-L., Chait, B. T., and Wang, R. (1993) *Biochemistry* **32,** 1009-1016

183. Jackson, G. S., Murray, I., Hosszu, L. L. P., Gibbs, N., Waltho, J. P., Clarke, A. R., and Collinge, J. (2001) *Proc.Natl.Acad.Sci.U.S.A* **98,** 8531-8535

184. Brown, D. R. (2001) *Brain Res.Bull.* **55,** 165-173

185. Brown, D. R., Qin, K., Herms, J. W., Madlung, A., Manson, J., Strome, R., Fraser, P. E., Kruck, T., von Bohlen, A., Schulz-Schaeffer, W., Giese, A., Westaway, D., and Kretzschmar, H. (1997) *Nature* **390,** 684-687

186. Jackson, G. S. and Clarke, A. R. (2000) *Curr.Opin.Struct.Biol.* **10,** 69-74

187. Stahl, N., Baldwin, M. A., Hecker, R., Pan, K. M., Burlingame, A. L., and Prusiner, S. B. (1993) *Biochemistry.1992 Jun 2* -53

188. Alberts, B., Johnson, A., Lewis, J., Raff, M., Roberts, K., and Walter, P. (2002) Intracellular vesicle traffic. Garland, New York

189. Vey, M., Pilkuhn, S., Wille, H., Nixon, R., DeArmond, S. J., Smart, E. J., Anderson, R. G. W., Taraboulos, A., and Prusiner, S. B. (1996) *Proc.Natl.Acad.Sci.USA* **93,** 14945-14949

190. Gorodinsky, A. and Harris, D. A. (1995) *J Cell Biol* **129,** 619-627

191. Madore, N., Smith, K. L., Graham, C. H., Jen, A., Brady, K., Hall, S., and Morris, R. (1999) *EMBO* **18,** 6917-6926

192. Shyng, S.-L., Huber, M. T., and Harris, D. A. (1993) *J Biol.Chem.* **268 (21),** 15922-15928

193. Shyng, S.-L., Heuser, J. E., and Harris, D. A. (1994) *J.Cell Biol.* **125,** 1239-1250

194. Colling, S. B., Khana, M., Collinge, J., and Jefferys, J. G. R. (1997) *Brain Res* **755,** 28-35

195. Colling, S. B., Collinge, J., and Jefferys, J. G. R. (1996) *Neurosci.Lett.* **209,** 49-52

196. Collinge, J., Whittington, M. A., Sidle, K. C. L., Smith, C. J., Palmer, M. S., Clarke, A. R., and Jefferys, J. G. R. (1994) *Nature* **370,** 295-297

197. Huber, R., Deboer, T., and Tobler, I. (2002) *Neuroreport* **13,** 1-4

198. Tobler, I., Gaus, S. E., Deboer, T., Achermann, P., Fischer, M., Rulicke, T., Moser, M., Oesch, B., McBride, P. A., and Manson, J. C. (1996) *Nature* **380,** 639-642

199. Tobler, I., Deboer, T., and Fischer, M. (1997) *Neuroscience* **17,** 1869-1879

200. Brown, D. R. (1999) *J.Neurosci.Res.* **58,** 717-725

201. Pauly, P. C. and Harris, D. A. (1998) *J Biol chem* **273,** 33107-33110

202. Brown, D. R. (2003) *J Neurochem.* **87,** 377-385

203. Brown, D. R., Schmidt, B., and Kretzschmar, H. A. (1997) *Int.J Dev.Neurosci.* **15,** 961-972

204. Brown, D. R. and Besinger, A. (1998) *Biochem J* **334,** 423-429

205. Brown, D. R., Wong, B. S., Hafiz, F., Clive, C., Haswell, S. J., and Jones, I. M. (1999) *Biochemical Journal* **344,** 1-5

206. Kuwahara, C., Takeuchi, A. M., Nishimura, T., Haraguchi, K., Kubosaki, A., Matsumoto, Y., Saeki, K., Yokoyama, T., Itohara, S., and Onodera, T. (1999) *Nature* **400,** 225-226

207. Hutter, G., Heppner, F. L., and Aguzzi, A. (2003) *Biol.Chem* **384,** 1279-1285

208. Mange, A., Milhavet, O., Umlauf, D., Harris, D., and Lehmann, S. (2002) *FEBS Lett.* **514,** 159-162

209. Schmitt-Ulms, G., Legname, G., Baldwin, M. A., Ball, H. L., Bradon, N., Bosque, P. J., Crossin, K. L., Edelman, G. M., DeArmond, S. J., Cohen, F. E., and Prusiner, S. B. (2001) *Journal of Molecular Biology* **314,** 1209-1225

210. Schmitt-Ulms, G., Hansen, K., Liu, J., Cowdrey, C., Yang, J., DeArmond, S. J., Cohen, F. E., Prusiner, S. B., and Baldwin, M. A. (2004) *Nat Biotechnol.*

211. Rieger, R., Edenhofer, F., Lasmézas, C. I., and Weiss, S. (1997) *Nat.Med.* **3,** 1383-1388

212. Oesch, B., Teplow, D. B., Stahl, N., Serban, D., Hood, L. E., and Prusiner, S. B. (1990) *Biochemistry* **29,** 5848-5855

213. Mouillet-Richard, S., Ermonval, M., Chebassier, C., Laplanche, J. L., Lehmann, S., Launay, J. M., and Kellermann, O. (2000) *Science* **289,** 1925-1928

214. Ma, J. Y. and Lindquist, S. (2001) *Proc.Natl.Acad.Sci.USA* **98,** 14955-14960

215. Yedidia, Y., Horonchik, L., Tzaban, S., Yanai, A., and Taraboulos, A. (2001) *EMBO J.* **20,** 5383-5391

216. Bence, N. F., Sampat, R. M., and Kopito, R. R. (2001) *Science* **292,** 1552-1555

217. Stahl, N., Borchelt, D. R., and Prusiner, S. B. (1990) *Biochemistry* **29,** 5405-5412

218. Narwa, R. and Harris, D. A. (1999) *Biochemistry* **38,** 8770-8777

219. Merz, P. A., Somerville, R. A., Wisniewski, H. M., Manuelidis, L., and Manuelidis, E. E. (1983) *Nature* **306,** 474-476

220. Govaerts, C., Wille, H., Prusiner, S. B., and Cohen, F. E. (2004) *Proc.Natl.Acad.Sci U.S.A*

221. Cohen, F. E. and Prusiner, S. B. (1998) *Annu.Rev.Biochem* **67,** 793-819

222. Hill, A. F. and Collinge, J. (2001) *Contrib.Microbiol.* **7:48-57.,** 48-57

223. Collinge, J., Sidle, K. C. L., Meads, J., Ironside, J., and Hill, A. F. (1996) *Nature* **383,** 685-690

224. Safar, J., Wille, H., Itri, V., Groth, D., Serban, H., Torchia, M., Cohen, F. E., and Prusiner, S. B. (1998) *Nat.Med.* **4,** 1157-1165

225. Jackson, G. S. and Collinge, J. (2001) *J.Clin.Pathol.Mol.Pathol.* **54,** 393-399

226. Caughey, B., Raymond, G. J., and Bessen, R. A. (1998) *Journal of Biological Chemistry* **273,** 32230-32235

227. Petkova, A., Leapman, R., Guo, Z., Yau, W., Mattson, M. P., and Tycko, R. (2005) *Science* **307,** 262-265

228. Rubenstein, R., Scalici, C. L., Papini, M. C., Callahan, S. M., and Carp, R. I. (1990) *J Gen.Virol.* **71,** 825-831

229. Schätzl, H. M., Laszlo, L., Holtzman, D. M., Tatzelt, J., DeArmond, S. J., Weiner, R. I., Mobley, W. C., and Prusiner, S. B. (1997) *J.Virol.* **71,** 8821-8831

230. Lehmann, S. and Harris, D. A. (1996) *Proc.Natl.Acad.Sci.USA* **93,** 5610-5614

231. Glatzel, M. and Aguzzi, A. (2000) *Microbe.Infect.* **2,** 613-619

232. Wadsworth, J. D. F., Joiner, S., Hill, A. F., Campbell, T. A., Desbruslais, M., Luthert, P. J., and Collinge, J. (2001) *Lancet* **358,** 171-180

233. Bosque, P. J., Ryou, C., Telling, G., Peretz, D., Legname, G., DeArmond, S. J., and Prusiner, S. B. (2002) *Proc.Natl.Acad.Sci.U.S.A* **99,** 3812-3817

234. Hunter, G. D., Millson, G. C., and Meek, C. (1964) *Journal of General Microbiology* **34,** 319-325

235. Clarke, M. C. and Millson, G. C. (1976) *J Gen.Virol.* **31,** 441-445

236. Taraboulos, A., Serban, D., and Prusiner, S. B. (1990) *J Cell Biol.* **110,** 2117-2132

237. Borchelt, D. R., Taraboulos, A., and Prusiner, S. B. (1992) *J Biol.Chem.* **267,** 16188-16199

238. Ivanova, L., Barmada, S., Kummer, T., and Harris, D. A. (2001) *Journal of Biological Chemistry* **276,** 42409-42421

239. Chiesa, R. and Harris, D. A. (2001) *Neurobiol.Dis.* **8,** 743-763

240. Brandner, S., Isenmann, S., Raeber, A., Fischer, M., Sailer, A., Kobayashi, Y., Marino, S., Weissmann, C., and Aguzzi, A. (1996) *Nature* **379,** 339-343

241. Mallucci, G., Dickinson, A., Linehan, J., Klohn, P. C., Brandner, S., and Collinge, J. (2003) *Science* **302,** 871-874

242. Arrasate, M., Mitra, S., Schweitzer, E., Segal, M., and Finkbeiner, S. (2004) *Nature* **341,** 805-810

243. Singh, N., Gu, Y., Bose, S., Kalepu, S., Mishra, R. S., and Verghese, S. (2002) *Front Biosci.* **7,** a60-a71

244. Ettaiche, M., Pichot, R., Vincent, J. P., and Chabry, J. (2000) *Journal of Biological Chemistry* **275,** 36487-36490

245. Forloni, G., Angeretti, N., Chiesa, R., Monzani, E., Salmona, M., Bugiani, O., and Tagliavini, F. (1993) *Nature* **362,** 543-546

246. Caughey, B. and Lansbury, P. T., Jr. (2003) *Annu.Rev.Neurosci.*

247. Lashuel, H. A., Hartley, D. M., Petre, B., Walz, T., and Lansbury-PT, J. (2002) *Nature* **418,** 291

248. Goldfarb, L. G., Brown, P., Goldgaber, D., Asher, D. M., Strass, N., Graupera, G., Piccardo, P., Brown, W. T., Rubinstein, R., Boellaard, J. W., and Gajdusek, D. C. (1989) *Am.J Hum.Genet.* **45,** A189

249. Owen, F., Poulter, M., Collinge, J., and Crow, T. J. (1990) *Nucleic.Acids.Res.* **18,** 3103

250. Owen, F., Poulter, M., Collinge, J., and Crow, T. J. (1990) *Am.J Hum.Genet.* **46,** 1215-1216

251. Palmer, M. S. and Collinge, J. (1993) *Human Mutation* **2,** 168-173

252. Furukawa, H., Kitamoto, T., Tanaka, Y., and Tateishi, J. (1995) *Brain Res Mol Brain Res* **30,** 385-388

253. Brandel, J. P., Preece, M., Brown, P., Croes, E., Laplanche, J. L., Agid, Y., Will, R., and Alperovitch, A. (2003) *Lancet* **362,** 128-130

254. Andrews, N. J., Farrington, C. P., Ward, H. J., Cousens, S. N., Smith, P. G., Molesworth, A. M., Knight, R. S., Ironside, J. W., and Will, R. G. (2003) *Lancet* **361,** 751-752

255. Dlouhy, S. R., Hsiao, K., Farlow, M. R., Foroud, T., Conneally, P. M., Johnson, P., Prusiner, S. B., and Ghetti, B. (1992) *Nature Genetics* **1,** 64-67

256. Hainfellner, J. A., Parchi, P., Kitamoto, T., Jarius, C., Gambetti, P., and Budka, H. (1999) *Annals of Neurology* **45,** 812-816

257. Hill, A. F., Joiner, S., Wadsworth, J. D., Sidle, K. C., Bell, J. E., Budka, H., Ironside, J. W., and Collinge, J. (2003) *Brain* **126,** 1333-1346

258. Prusiner, S. B., Scott, M., Foster, D., Pan, K. M., Groth, D., Mirenda, C., Torchia, M., Yang, S. L., Serban, D., Carlson, G. A., and Raeber, A. J. (1990) *Cell* **63,** 673-686

259. Schaetzl, H. M., Wopfner, F., Gilch, S., Von Brunn, A., and Jaeger, G. (1997) *Lancet* **349,** 1603-1604

260. Grantham, R. (1974) *Science* **185,** 862-864

261. Come, J. H., Fraser, P. E., and Lansbury, P. T., Jr. (1993) *Proc.Natl.Acad.Sci.USA* **90,** 5959-5963

262. Come, J. H. and Lansbury, P. T., Jr. (1994) *J.Am.Chem.Soc.* **116,** 4109-4110

263. Singleton, A., Myers, A., and Hardy, J. (2004) *Hum Mol.Genet*

264. Singleton AB, Farrer M, Johnson J, Singleton A, Hague S, Kachergus J, Hulihan M, Peuralinna T, Dutra A, Nussbaumm R, Lincoln S, Crawley A, Hanson M, Maraganore D, Adler C, Cookson MR, Muenter M, Baptista M, Miller D, Blancato J, Hardy J, and Gwinn-Hardy K (2004) *Science* **302,** 841

265. Shtilerman M, Ding T, and Lansbury-PT, J. (2002) *Biochemistry* **41,** 3855-3860

266. Goldberg m and Lansbury-PT, J. (2002) *Nature Cell Biology* **2,** E115-E119

267. Jimenez, J. L., Nettleton, E., Bouchard, M., Robinson, C. V., Dobson, C. M., and Saibil, H. R. (2002) *Proc.Natl.Acad.Sci.USA* **99,** 9196-9201

268. Jimenez, J. L., Tennent, G., Pepys, M., and Saibil, H. R. (2001) *J Mol.Biol* **311,** 241-247

269. Wong, B. S., Clive, C., Haswell, S. J., Jones, I. M., and Brown, D. R. (2000) *Biochemical and Biophysical Research Communications* **269,** 726-731

270. Hart, T. Mapping the folding nucleus of the prion protein. 2005. Imperial College.
Ref Type: Thesis/Dissertation

271. Petchanikow, C., Saborio, G. P., Anderes, L., Frossard, M. J., Olmedo, M. I., and Soto, C. (2001) *FEBS Letters* **509,** 451-456

272. Tahiri-Alaoui, A., Gill, A. C., Disterer, P., and James, W. (2004) *J Biol.Chem*

273. Tahiri-Alaoui, A. and James, W. Rapid formation of amyloid from alpha-monomeric recombinant human PrP in vitro. Protein Science 14, 1-6. 2005.
Ref Type: Journal (Full)

274. Hosszu, L. L., Jackson, G. S., Trevitt, C. R., Jones, S., Batchelor, M., Bhelt, D., Prodromidou, K., Clarke, A. R., Waltho, J. P., and Collinge, J. (2004) *J Biol.Chem*

275. Hosszu, L. L., Jackson, G. S., Trevitt, C. R., Jones, S., Batchelor, M., Bhelt, D., Prodromidou, K., Clarke, A. R., Waltho, J. P., and Collinge, J. (2004) *J Biol chem* **279,** 28515-28521

276. Liemann, S. and Glockshuber, R. (1999) *Biochemistry* **38,** 3258-3267

277. Bocharova, O., Breydo, L., Parfenov, A., Salnikov, V., and Baskakov, I. V. (2005) *J Mol Biol* **346,** 645-659

278. Lee, S. and Eisenberg, D. (2003) *Nat Struct.Biol.*

279. Haire, L. F., Whyte, S. M., Vasisht, N., Gill, A. C., Verma, C., Dodson, E. J., Dodson, G. G., and Bayley, P. M. (2004) *J Mol.Biol.* **336,** 1175-1183

280. Knaus, K. J., Morillas, M., Swietnicki, W., Malone, M., Surewicz, W. K., and Yee, V. C. (2001) *Nat.Struct.Biol.* **8,** 770-774

281. Adler, A., Greenfield, N., and Fasman, G. (1973) *Methods Enzymol.* **27,** 675-735

282. Woody, R. W. (1995) *Methods Enzymol.* **246,** 34-71

283. Chen, Y., Yang, J., and Chau, K. (1974) *Biochemistry* **13,** 3350-3359

284. Chen, Y. H., Yang, J. T., and Martinez, H. M. (1972) *Biochemistry* **11,** 4120-4131

285. Greenfield, N. and Fasman, G. (1969) *Biochemistry* **8,** 4108-4116

286. Staniforth, R. A., Burston, S. G., Smith, C. J., Jackson, G. S., Badcoe, I. G., Atkinson, T., Holbrook, J. J., and Clarke, A. R. (1993) *Biochemistry* **32,** 3842-3851

287. Lehmann, S. and Harris, D. A. (1996) *J.Biol.Chem.* **271,** 1633-1637

288. Bennhold, H. (1922) *Muenchen Med.Wochenschr.* **69,** 1537

289. Svedberg, T. and Pederson, K. (1940) *The Ultracentrifuge*, Oxford University Press,

290. van Holde, K., Johnson, W., and Ho, P. (1998) *Principles of Physical Biochemistry*, Prentice Hall,

291. Stokes, G. (1851) *Trans.Camb.Phil.Soc.* **9,** 6-106

292. Teller, D., Swanson, E., and DeHaen, C. (1979) *Methods Enzymol.* **61,** 103-124

293. Lebowitz, J., Lewis, M., and Shuck, P. (2002) *Prot.Sci.* **11,** 2067-2079

294. Shuck, P. (2003) *Analytical Biochemistry* **320,** 104-124

295. Weinreb, P. H., Zhen, W., Poon, A., Conway, K., and Lansbury, P. (1996) *Biochemistry* **35,** 13709-13715

296. Budka, H. (2003) *Br.Med.Bull.* **66,** 121-130

297. Kaneko, K., Zulianello, L., Scott, M., Cooper, C. M., Wallace, A. C., James, T. L., Cohen, F. E., and Prusiner, S. B. (1997) *Proc.Natl.Acad.Sci.USA* **94,** 10069-10074

298. Telling, G. C., Scott, M., Mastrianni, J., Gabizon, R., Torchia, M., Cohen, F. E., DeArmond, S. J., and Prusiner, S. B. (1995) *Cell* **83,** 79-90

299. Guijarro, J. I., Sunde, M., Jones, J., Campbell, I., and Dobson, C. M. (1998) *PNAS* **95,** 4224-4228

300. Sanger, F., Nicklen, S., and Coulson, A. R. (1977) *Proc Natl Acad Sci* **74,** 5463-5467

301. Sanger, F. (1981) *Science* **214,** 1205-1210

302. Low, M. G. (1987) *Biochem J* **244,** 1-13

303. Englund, T. (1993) *Annu.Rev Biochem* **62,** 121-138

304. Vidugiriene, J. and Menon, A. K. (1994) *J.Cell Biol.* **127,** 333-341

305. Thomas, J. R., Dwek, R. A., and Rademacher, T. W. (1990) *Biochemistry* **29,** 5413-5422

306. Rebecchi, M. and Pentyala, S. (2000) *Physiological Reviews* **80,** 1291-1335

307. Borchelt, D. R., Rogers, M., Stahl, N., Telling, G., and Prusiner, S. B. (1993) *Glycobiology.* **3,** 319-329

308. Caughey, B., Neary, K., Buller, R., Ernst, D., Perry, L. L., Chesebro, B., and Race, R. E. (1990) *J Virol.* **64,** 1093-1101

309. Rogers, M., Yehiely, F., Scott, M., and Prusiner, S. B. (1993) *Proc.Natl.Acad.Sci.U.S A.* **90,** 3182-3186

310. Taraboulos, A., Scott, M., Semenov, A., Avraham, D., Laszlo, L., and Prusiner, S. B. (1995) *J.Cell Biol.* **129,** 121-132

311. Hao, M., Mukherjee, S., and Maxfield, F. (2001) *Proc Natl Acad Sci (USA)* **98,** 13072-13077

312. Morandat, S., Bortolato, M., and Roux, B. (2002) *Biochem Biophys Acta* **1564,** 473-478

313. Chesebro, B. Direct and Indirect Mechanisms of Pathogenesis In TSE Diseases. Keystone Symposia Molecular Mechanisms of the TSEs , 19. 1-12-2005.
Ref Type: Abstract

314. Kishida, H., Sakasegawa, Y., Watanabe, K., Yamakawa, Y., Nishijima, M., Kuroiwa, Y., Hachiya, N. S., and Kaneko, K. (2004) *Amyloid.* **11,** 14-20

315. Kitamoto, T., Iizuka, R., and Tateishi, J. (1993) *Biochem and Biophys Res Commun* **192 (2),** 525-531

316. Ghetti, B., Piccardo, P., Spillantini, M. G., Ichimiya, Y., Porro, M., Perini, F., Kitamoto, T., Tateishi, J., Seiler, C., Frangione, B., Bugiani, O., Giaccone, G., Prelli, F., Goedert, M., Dlouhy, S. R., and Tagliavini, F. (1996) *Proc.Natl.Acad.Sci.U.S.A.* **93,** 744-748

317. Tagliavini, F., Prelli, F., Porro, M., Rossi, G., Giaccone, G., Farlow, M. R., Dlouhy, S. R., Ghetti, B., Bugiani, O., and Frangione, B. (1994) *Cell* **79,** 695-703

318. Tateishi, J. and Kitamoto, T. (1995) *Brain Pathol.* **5,** 53-59

319. Tateishi, J., Kitamoto, T., Hoque, M. Z., and Furukawa, H. (1996) *Neurology* **46,** 532-537

320. Stryer, L. (1995) Exploring Proteins. In Stryer, L., editor. *Biochemistry*, Freeman, New York

321. Cunningham, m. and Tang, J. (1976) *J Biol.Chem* **251,** 4528-4536

322. Erickson, A., Conner, G., and Blobel, G. (1981) *J Biol chem* **256,** 11224-11231

323. Dean, R. and Barret, A. (1976) *Essays Biochem.* **12,** 1-40

324. Sakai, H., Saku, T., Kato, Y., and Yamamoto, K. (1989) *Biochem Biophys Acta* **991,** 367-375

325. Baldwin, E., Bhat, T., Gulnik, S., Hosur, M., Sowder, R., Cachau, R., Collins, J., Silva, A., and Erickson, J. (1993) *PNAS* **90,** 9796-6800

326. Connor, G. (1998) Cathepsin D. In Banet, A., awlings, N., and oessner, J., editors. *The Handbook of Proteolytic Enzymes*, Elsevier,

327. Lee, A., Gulnik, S., and Erickson, J. Cathepsin D at pH 7.5. (MMDB 10875 PDB 1LYW). 1998.
Ref Type: Data File

328. Scarborough, P. and Dunn, B. (1994) *Protein Eng.* **7,** 495-502

329. Scarborough, P., Guruprasad, K., Topham, C., Richo, G., Connor, G., Blundell, T., and Dunn, B. (1993) *Prot.Sci.* **2,** 264-276

330. Offermann, M. K., Chlebowski, J. F., and Bond, J. S. (1983) *Biochem.J* **211,** 529-534

331. van Noort, J. M. and van der Drift, A. C. (1989) *J Biol chem* **264,** 14159-14164

332. Imoto, T., Okazaki, K., Koga, H., and Yamada, H. (1987) *J Biochem* **101,** 575-580

333. Faust, P., Kornfeld, S., and Chirgwin, J. (1985) *PNAS* **82,** 4910-4914

334. Takahashi, T. and Tang, J. (1981) *Methods Enzymol.* **80,** 565-581

335. Rochefort, H. (1990) *Breast Cancer Res.Treat.* **16,** 3-13

336. Siman, R., Mistretta, S., Durkin, J., Savage, M., Loh, T., Trusko, S., and Scott, R. (1993) *Journal of Biological Chemistry* **268,** 16602-16609

337. Higaki, J., Catalano, R., Guzzetta, A. W., Quon, D., Nave, J. F., Tarnus, C., D'Orchymont, H., and Cordell, B. (1996) *J Biol chem* **271,** 31885-31893

338. Hossain, S., Alim, A., Takeda, K., Kaji, H., Shinoda, T., and Ueda, K. (2001) *J Alzheimers.Dis.* **3,** 577-584

339. Kenessey, A., Nacharaju, P., Ko, L. W., and Yen, S. H. (1997) *J Neurochem.* **69,** 2026-2038

340. Cataldo, A. M., Barnett, J. L., Berman, S. A., Li, J., Quarless, S., Bursztajn, S., Lippa, C., and Nixon, R. A. (1995) *Neuron* **14,** 671-680

341. Hoffman, K., Bi, X., Pham, J., and Lynch, G. (1998) *Neurosci Letts* **250,** 75-78

342. Hamazaki, H. (1996) *FEBS Lett.* **396,** 139-142

343. Cataldo, A. M. and Nixon, R. A. (1990) *Proc-Natl-Acad-Sci-U-S-A.* **87,** 3861-3865

344. Papassotiropoulos, A., Bagli, M., Kurz, A., Kornhuber, J., Forstl, H., Maier, W., Pauls, J., Lautenschlager, N., and Heun, R. (2000) *Ann Neurol* **47,** 399-403

345. Crawford, F. C., Freeman, M. J., Schinka, J., Abdullah, L. I., Richards, D., Sevush, S., Duara, R., and Mullan, M. J. (2000) *Neurosci.Lett.* **289,** 61-65

346. Mateo, I., Sanchez-Guerra, M., Combarros, O., Llorca, J., Infante, J., Gonzalez-Garcia, J., Molino, J., and Berciano, J. (2002) *Am.J.Med.Genet.* **114,** 31-33

347. Diedrich, J. F., Minnigan, H., Carp, R. I., Whitaker, J. N., Race, R., Frey, W., and Haase, A. T. (1991) *J Virol* **65,** 4759-4768

348. Brown, A. R., Webb, J., Rebus, S., Williams, A., and Fazakerley, J. K. (2004) *Neuropathol.Appl.Neurobiol.* **30,** 555-567

349. Roelke, D. and Uhr, M. (1969) *Z Med Mikribiol Immunol* **155,** 156-170

350. Parkin, E. T., Watt, N. T., Turner, A. J., and Hooper, N. M. (2004) *J Biol.Chem*

351. Hill, A. F. and Collinge, J. (2004) *Contrib.Microbiol.* **11,** 33-49

352. Wadsworth, J. D. F., Hill, A. F., Joiner, S., Jackson, G. S., Clarke, A. R., and Collinge, J. (1999) *Nature Cell Biology* **1,** 55-59

353. Hooper, N. M., Cook, S., Lainé, J., and LeBel, D. (1997) *Biochem J* **324,** 151-157

354. Bordier, C. (1981) *J-Biol-Chem.* **256,** 1604-1607

355. Fischer, M., Rulicke, T., Raeber, A., Sailer, A., Moser, M., Oesch, B., Brandner, S., Aguzzi, A., and Weissmann, C. (1996) *EMBO J.* **15,** 1255-1264

356. Nishina, K., Jenks, S., and Supattapone, S. (2004) *J Biol chem*

357. Deleault, N. R., Geoghegan, J, Klohn, P. C., Mahal, S., Nishina, K., sheikh, R., Solstad, T, Supattapone, S., and Weissmann, C. biochemical studies of prion protein conformation and conversion. Keystone Symposia Molecular Mechanisms of the TSEs , 33. 1-11-2005.
Ref Type: Abstract

358. Gibbs, C. J. Jr. and Gajdusek, D. C. (1969) *Science* **165,** 1023-1025

359. Klebe, R. and Ruddle, F. (1969) *J-Cell-Biol.* **43,** 69

360. Weissmann, C. (2004) *Nat.Rev.Microbiology* **2,** 1-11

361. Jimenez, J. L., Guijarro, J. I., Orlova, E., Zurdo, J., Dobson, C. M., Sunde, M., and Saibil, H. R. (1999) *EMBO J.* **18,** 815-821

362. Tattum, M. H., Jackson, G. S., Clarke, A. R., Saibil, H. R., and Collinge, J. A 3-D reconstruction from electron microscopy images of PrP fibrils. In Preparation . 2003.
Ref Type: Journal (Full)

363. Ban, T., Hamada, D., Hasegawa, K., Naiki, H., and Goto, Y. (2003) *J Biol.Chem* **278,** 16462-16465

PAPERS SUBMITTED FOR PUBLICATION

"The codon 129 polymorphism of the human prion protein controls its ability to form amyloid fibrils" Patrick A. Lewis, Samantha Jones, Howard Tattum, Daljit Bhelt, Mark Batchelor, Anthony R. Clarke, John Collinge, and Graham S. Jackson *submitted to the journal of biological chemistry*

"Removal of the GPI anchor from PrP^{Sc} does not reduce prion infectivity" Patrick A. Lewis, Francesca Properzi, Kanella Prodromidou, Anthony R. Clarke, John Collinge, and Graham S. Jackson *submitted to the journal of biological chemistry*

THE CODON 129 POLYMORPHISM OF THE HUMAN PRION PROTEIN CONTROLS ITS ABILITY TO FORM AMYLOID FIBRILS

Patrick A. Lewis, Samantha Jones, Howard Tattum, Daljit Bhelt, Mark Batchelor, Anthony R. Clarke, John Collinge, and Graham S. Jackson
From the MRC Prion Unit, Department of Neurodegenerative Disease, Institute of Neurology, University College London, Queen Square, London, WC1N 3BG, United Kingdom

Running Title : Amyloid formation from PrP polymorphs

Address correspondence to : Graham S. Jackson, MRC Prion Unit, Department of Neurodegenerative Disease, Institute of Neurology, University College London,

; Email:

The human prion protein has a common polymorphism at residue 129 which can be valine or methionine. This polymorphism has a strong influence on susceptibility to prion diseases and on prion strain properties. Previous work has shown that this amino acid variation has no effect on the α-helical PrP^C structure and does not influence its stability. Here we show that the polymorphism also does not change the efficiency of conversion to the β-PrP conformation and has no effect on stability or protease resistance. However, in a partially denatured conformation the polymorphic variation has a profound influence on the ability of the protein to form amyloid fibrils.

The prion diseases or transmissible spongiform encephalopathies (TSEs) are a group of closely related neurodegenerative disorders characterised by spongiform degeneration of the brain. They include scrapie of sheep, BSE in cattle, chronic wasting disease affecting deer and elk and the human disorders CJD, GSS, FFI and vCJD (1). A unique and defining feature of diseases in humans is that they can be inherited, arise sporadically or be acquired through infection (1). According to the protein-only hypothesis, the central event in the pathogenesis of prion diseases is the conversion of the normal, cellular form of the prion protein (PrP^C) into an aberrantly folded, disease associated form known as PrP^{Sc} (2;3).

Inherited forms of prion disease are caused by mutations in the PRNP gene located on human chromosome 20 (4). Many pathogenic mutations in PrP have now been described, along with two polymorphisms: methionine or valine at codon 129 (M129V) and glutamine or lysine at codon 219 (E219K) (5;6). These polymorphisms, although not pathogenic, have a complex interaction with the disease process. Heterozygosity at either of these codons is associated with resistance to sporadic CJD (7;8). In addition to this, differences in codon 129 status result in phenotypic variation within pedigrees also carrying a pathogenic mutation in PrP (9-12), and homozygosity at this codon is a significant risk factor for the acquisition of transmissible forms of CJD, such as Kuru, vCJD and iatrogenic CJD (13-17). Whilst there is a great deal of genetic and clinical evidence supporting the role of the codon 129 polymorphism in prion disease, no obvious biochemical basis for this affect has so far been uncovered.

Based upon the nucleated seeding model of prion propagation (18), it has been suggested that the phenotypic impact of the codon 129 polymorphism may be due to incompatibilities between the nucleated growth of the two variants (19). The fact that all cases of vCJD thus far recorded are methionine homozygotes, that bovine PrP contains methionine at the homologous codon and that sequence complementarily has been shown to be important for the propagation of scrapie in *in vitro* and *in vivo* models (20-24) provides some evidence to support this. The methionine-valine variation is, however, relatively conservative with respect to the volume and hydrophobicity of the side chains (25), and NMR studies comparing the three dimensional structures of the two forms in the PrP^{C} conformation failed to find any difference in structure or global stability (26).

From these observations it seems likely that the influence of residue-129 on prion disease results from its effect on the physical properties of the PrP^{Sc} isoform. While there is no reliable, high-resolution information on the structure of this disease-associated conformer, the purified infectious material is aggregated, insoluble and has a predominantly β-sheet secondary structure. We have previously shown that acidification and disulphide reduction of the PrP^{C} species switches the conformation to one that is dominated by β-sheet and is capable of forming ordered fibrils. Given that it is a β-sheet form of the prion protein that is involved in the formation of prion aggregates *in vivo*, we wanted to look at the behaviour of this β-PrP species to see whether the switch between valine and methionine at codon 129 had any influence on its physical properties. Here we present an analysis of the prion protein codon 129 polymorphism and its affect on several aspects of the behaviour of recombinant human PrP comprising residues 91-231. Using a variety of techniques, the stability, structural plasticity, aggregation properties, protease resistance and amyloid formation of the methionine and valine forms of human PrP have been investigated.

EXPERIMENTAL PROCEDURES

Strict biosafety protocols were followed and all work with recombinant human prion protein was carried out in a microbiological containment level 3 facility.

Protein Production

Recombinant prion protein residues 91-231 containing either methionine or valine at codon 129 was produced as described elsewhere (27). The conversion of recombinant α-PrP to β-PrP was carried out at pH 4.0 and in reducing conditions using the protocol of Jackson *et al* (28). Total protein was calculated by UV absorption using a calculated molar extinction coefficient of 19632 M^{-1} cm^{-1} at 280nm in order to determine refolding yield. The conversion reactions were independently repeated 5 times and the mean yields with standard deviations calculated.

Circular Dichroism and Unfolding Analysis

Spectra were recorded with a Jasco J715 spectropolarimeter and measured at a protein concentration of 1mg/ml with a 0.01cm pathlength. Equilibrium unfolding analysis of protein stability was carried out with a protein concentration of 0.1mg/ml and a 1cm pathlength (measurements were taken over a 10nm bandwith centred around λ220nm). Protein denaturation was carried out by addition of aliquots of either 10M Urea or 6M Guanidine Hydrochloride (GuHCl). The ellipticity signal (θ) was converted to proportion of

molecules in the native state α_N according to the relationship $\alpha_N = (\theta - \theta_U)/(\theta_N - \theta_U)$, where θ_U and θ_N are the ellipticity signals for the unfolded and native states respectively. Data were fitted to the function:

$$\alpha_N = (K_{(N/U)}.\exp(m.D))/(1+K_{(N/U)}.\exp(m.D))$$

where m represents the sensitivity of the unfolding transition to denaturant and D is the denaturant activity (29).

Protease Resistance

10µl aliquots of 1mg/ml protein of the appropriate codon 129 status and predominant fold (either α or β) were digested with proteinase K at 0.1, 1, 10 or 100 µg/ml final concentration. Reactions were terminated by the addition of 2x SDS-loading buffer buffer [125 mM Tris–HCl (pH 6.8), 20% v/v glycerol, 4% w/v sodium dodecyl sulphate, 4% v/v 2-mercaptoethanol, 0.02% (w/v) bromophenol blue] containing 8 mM 4-(2-aminoethyl)-benzene sulfonyl fluoride (AEBSF; Pefabloc SC, Roche, Lewes, UK). Samples were heated to 100°C for 10mins and then subjected to centrifugation in a microfuge (15,000 g) for 1 minute. 20µl of each supernatant was applied to a 16% Tris-glycine gel (Novex; Life Technologies, Paisley, UK) according to the manufacturer's instructions. Gels were washed with distilled water and then stained with Coomassie blue (Coomassie brilliant blue 0.025% w/v, methanol 40% v/v, acetic acid 7% v/v in ddH_2O) for 1 hour followed by destaining with 40% v/v methanol, 7% v/v acetic acid in ddH_2O.

Fibril Formation

Fibril formation was analysed using a protocol adapted from that of Baskakov *et al* (30;31). Briefly, recombinant α-PrP of both M and V 129 status was transferred into 20mM Sodium Acetate pH 3.7 and denatured by the addition of 10M Urea. The protein was then dialysed into 1.3M Urea, 1M GuHCl pH 6. To stimulate assembly of monomeric PrP into fibrils, 800µl of 0.8mg/ml protein was aliquoted into a 1.5ml microfuge tube and shaken at 37°C and 600rpm. An identical reaction was also performed with twice the concentration V129 PrP (1.6mg/ml). Monitoring of fibril formation was carried out by determination of Thioflavin T fluorescence. 10µl of sample was removed from the shaking aliquots and diluted 1 in 20 into 5mM Sodium Acetate pH 5.5. Thioflavin T was then added to a final concentration of 50µM and fluorescence measured on a Jasco FP-750 spectrofluorimeter (excitation 450nm, emission 485nm) with 5nm band widths. All experiments were performed at 20°C.

RESULTS

α-PrP Structure and Stability

To examine the impact of the codon 129 polymorphism on α-PrP, recombinant PrP residues 91-231 with either methionine or valine at position 129 were examined by using circular dichroism (CD) for differences in structure or stability. Spectra in the far UV range (λ 190-250nm) were recorded (Figure 1A), with both M129 and V129 exhibiting spectra characteristic of a predominantly α-helical fold with no significant difference between the spectra, agreeing with data from NMR studies of the two variants. To assess whether the polymorphism has any impact on the stability of α-PrP, both M and V forms were subjected to equilibrium unfolding using GuHCl as described in the previous section. Both M and V containing proteins exhibited profiles characteristic of a single domain undergoing a co-operative unfolding event (Figure 1B). The free energy of folding in water calculated for both polymorphs were 6.62 kcal mol^{-1}

(M129) and 6.52 kcal mol^{-1} (V129) demonstrating that the polymorphism has no significant impact on the global stability of the α-PrP fold.

β-PrP Conversion, Structure and Stability

The lack of significant differences between the NMR solution structure of the two polymorphic variants in the α-conformation suggests that, if there is a structural difference between the two forms, it lies either in partly folded intermediates or in the β-sheet state. To investigate this, both polymorphs were converted to β-PrP and the yield for conversion calculated. No significant difference was found between the two as regards their propensity to form the β-sheet conformer (Figure 2). Circular dichroism spectra recorded in the far UV range for both β-PrP M129 and β-PrP V129 were qualitatively compared. Again, no significant difference was revealed, with both forms exhibiting spectra indicative of predominantly β-sheet structure with a minimum at λ 217nm (Figure 3A). Following this, equilibrium unfolding was carried out on to analyse the stability of the β-conformers (Figure 3B). Both showed none co-operative unfolding profiles, consistent with the view that β-PrP has characteristics similar to that of a molten globule folding intermediate (32) with no significant difference between their respective stabilities (M129 2.36 kcal mol^{-1} and V129 2.73 kcal mol^{-1}).

Protease Resistance

Both M and V variants of α-PrP digested for 1 hour at pH 8 with a variety of concentrations of proteinase K exhibited similar levels of protease resistance and fragmentation patterns. Both forms were completely digested by treatment with 10μg/ml proteinase K for 1 hour. β-PrP was digested at pH 4, with α-PrP digested at the same pH to act as a control for the pH dependent reduction in proteinase K activity. M and V β-PrP were more resistant to proteinase K treatment than their α-PrPcounterparts, but no difference in fragment pattern or resistance to digestion between the M and V polymorphs could be discerned (Figure 4).

Fibril Formation

Using the conditions described, human recombinant PrP^{91-231}, containing methionine at codon 129 formed amyloid material after a lag phase of approximately 35 hours. In contrast, recombinant PrP containing valine at codon 129 did not form amyloid material after a period exceeding 200 hours with twice the protein concentration (Figure 5).

DISCUSSION

This study of the physical behaviour of the methionine and the valine forms of human prion protein was stimulated by the dramatic effect of the codon 129 variations both on susceptibility to and phenotype of human prion disease. It has long been observed that individuals with an MV genotype are highly protected against developing sporadic and acquired prion diseases. This effect can be explained by the principle of molecular complementarity combined with a gene-dosage effect. That is, if there is a spontaneous conversion of PrP^{C} to PrP^{Sc} and only identical molecules can be recruited in the propagation process owing to structural complementarity, then a homozygote will have a double dose of available substrate hence the probability of initiation and and the rate of propagation will be enhanced. Moreover, recent work has demonstrated that BSE and vCJD prion infection in transgenic mice can result in the propagation of distinct molecular and neuropathological phenotypes dependent on host PrP

residue 129 status. These data were interpreted as revealing a critical role for codon 129 in governing the thermodynamic balance between human PrP^{Sc} conformations that determine strain type and gave rise to a conformational selection model of prion transmission barriers in which there is no overlapping preferred conformation for the valine and methionine forms of human PrP that can be generated as a result of exposure to the BSE prion strain.

Such effects on the propagation of the scrapie agent mean that the methionine-valine change must affect the structure and stability of either the □-helical PrP^{C} species or the PrP^{Sc} state of the protein or indeed both. Alternatively, the polymorphic state could influence the efficiency or kinetics of the PrP^{C}-to-PrP^{Sc} conversion or alter the interactions that stabilize the latter form. The ready availability of recombinant human PrP enables detailed experimental study of the physical effect of this amino acid variation on the physical properties of the PrP molecule in a variety of conformations and assembly states and some behavioural differences have been claimed.

For instance, binding studies performed on mouse PrP engineered to contain methionine and valine at the equivalent position in the murine sequence (murine PrP does not contain a homologous polymorphism) revealed that when both were refolded in the presence of copper there was a difference in their secondary structure content as determined by circular dichroism (33). This must, however, be qualified by the fact that there is 12% variation between the primary sequence of human and mouse PrP (34), raising questions as to how representative of the *in vivo* human situation this is.

Other studies have examined the possibility that differences in the ability of M and V codon 129 PrP to form ordered amyloid aggregates underlie the phenotypic variation seen in these diseases. Using a 30 amino acid peptide fragment of human PrP (residues 106-136), Petchanikow co-workers showed that the methionine form had a greater ability to form a β-sheet conformation in a variety of biochemical environments (35). More recently, Tahiri-Alaoui and colleagues showed that human PrP 90-231 containing methionine at position 129 has a greater propensity to form β-rich oligomers than the equivalent valine-containing protein (36).In addition, previous work from our laboratory has shown that the methionine-valine variation has no measurable effect on the global structure, dynamics, or stability of the normal cellular conformer (the PrP^{C} conformation) and we concluded that the powerful effect of residue 129 on prion strain selection is likely to be mediated by its effect on the conformation of PrP^{Sc} or its precursors or on the kinetics of their formation.

This finding has prompted us to examine the effect of the polymorphism on an alternative α-sheet-dominated fold of the human PrP protein chain, known as β-PrP, comprising residues 91-231. At low ionic strength, the β-PrP species is a soluble monomer composed almost entirely of β-sheet as determined by CD spectroscopy and, more recently, infra-red absorption. NMR measurements show this species to be molten globule-like with respect to the dynamics of the side chains. At higher ionic strength or on prolonged incubation in acid conditions this conformer assembles into fibrils with partial resistance to digestion with proteinase K, characteristic dseterminants of PrP^{Sc}.

The results we present here show that there is no difference in the propensity of the M or the V forms to convert from the α-helical PrP^C conformation to β-PrP at low pH and in reducing conditions. Further, an examination of CD spectra and protease resistance of β-PrP in the methionine and valine forms failed to reveal any difference in global conformation or accessibility to enzymatic cleavage. Also the two polymorphic forms of β-PrP had the same conformational stability when subjected to denaturation using chaotropic agents.

However, the polymorphic forms showed a striking difference in their propensity to form ordered fibrils. Using the protocol developed by Baskakov and co-workers, the methionine-129 version of partially denatured α-PrP readily formed fibrils with a lag time of 35-40 hours as measured by thioflavin T fluorescence; a finding which was in agreement with previous work (37). In stark contrast, the valine-129 version did not form amyloid even after more than 200-hours of incubation. This finding is consistent with previous work detailing the greater propensity of PrP with methionine at codon 129 to form aggregates (38;39).

REFERENCES

1. Collinge, J. (2001) *Annu.Rev Neurosci.* **24,** 519-550
2. Prusiner, S. B. (1982) *Science* **216,** 136-144
3. Prusiner, S. B. (1998) *Proc Natl Acad Sci U.S.A.* **95,** 13363-13383
4. Hsiao, K., Baker, H. F., Crow, T. J., Poulter, M., Owen, F., Terwilliger, J. D., Westaway, D., Ott, J., and Prusiner, S. B. (1989) *Nature* **338,** 342-345
5. Owen, F., Poulter, M., Collinge, J., and Crow, T. J. (1990) *Nucleic.Acids.Res.* **18,** 3103
6. Petraroli, R. and Pocchiari, M. (1996) *Am J Hum.Genet.* **58,** 888-889
7. Shibuya, S., Higuchi, J., Shin, R. W., Tateishi, J., and Kitamoto, T. (1998) *Ann.Neurol.* **43,** 826-828
8. Palmer, M. S., Dryden, A. J., Hughes, J. T., and Collinge, J. (1991) *Nature* **352,** 340-342
9. Dlouhy, S. R., Hsiao, K., Farlow, M. R., Foroud, T., Conneally, P. M., Johnson, P., Prusiner, S. B., and Ghetti, B. (1992) *Nature Genetics* **1,** 64-67
10. Monari, L., Chen, S. G., Brown, P., Parchi, P., Petersen, R. B., Mikol, J., Gray, F., Cortelli, P., Montagna, P., Ghetti, B., Goldfarb, L. G., Gajdusek, D. C., Lugaresi, E., Gambetti, P., and Autilio-Gambetti, L. (1994) *Proc.Natl.Acad.Sci.USA* **91,** 2839-2842
11. Hainfellner, J. A., Parchi, P., Kitamoto, T., Jarius, C., Gambetti, P., and Budka, H. (1999) *Annals of Neurology* **45,** 812-816
12. Goldfarb, L. G., Petersen, R. B., Tabaton, M., Brown, P., LeBlanc, A. C., Montagna, P., Cortelli, P., Julien, J., Vital, C., Pendelbury, W. W., Haltia, M., Wills, P. R., Hauw, J. J., McKeever, P. E., Monari, L., Schrank, B., Swergold, G. D., Autilio-Gambetti, L., Gajdusek, D. C., Lugaresi, E., and Gambetti, P. (1992) *Science* **258,** 806-808
13. Mead, S., Stumpf, M. P., Whitfield, J., Beck, J. A., Poulter, M., Campbell, T., Uphill, J., Goldstein, D., Alpers, M., Fisher, E. M., and Collinge, J. (2003) *Science*

14. Collinge, J., Palmer, M. S., and Dryden, A. J. (1991) *Lancet* **337,** 1441-1442
15. Zeidler, M., Stewart, G., Cousens, S. N., Estebeiro, K., and Will, R. G. (1997) *Lancet* **350,** 668
16. Lee, H. S., Brown, P., Cervenáková, L., Garruto, R. M., Alpers, M. P., Gajdusek, D. C., and Goldfarb, L. G. (2001) *Journal of Infectious Diseases* **183,** 192-196
17. Hill, A. F., Butterworth, R. J., Joiner, S., Jackson, G., Rossor, M. N., Thomas, D. J., Frosh, A., Tolley, N., Bell, J. E., Spencer, M., King, A., Al-Sarraj, S., Ironside, J. W., Lantos, P. L., and Collinge, J. (1999) *Lancet* **353,** 183-189
18. Come, J. H., Fraser, P. E., and Lansbury, P. T., Jr. (1993) *Proc.Natl.Acad.Sci.USA* **90,** 5959-5963
19. Come, J. H. and Lansbury, P. T., Jr. (1994) *J.Am.Chem.Soc.* **116,** 4109-4110
20. Kocisko, D. A., Come, J. H., Priola, S. A., Chesebro, B., Raymond, G. J., Lansbury, P. T., and Caughey, B. (1994) *Nature* **370,** 471-474
21. Kocisko, D. A., Priola, S. A., Raymond, G. J., Chesebro, B., Lansbury, P. T., Jr., and Caughey, B. (1995) *Proc.Natl.Acad.Sci.U.S A.* **92,** 3923-3927
22. Chien, P., DePace, A. H., Collins, S. R., and Weissman, J. S. (2003) *Nature* **424,** 948-951
23. Scott, M., Foster, D., Mirenda, C., Serban, D., Coufal, F., Wälchli, M., Torchia, M., Groth, D., Carlson, G., DeArmond, S. J., Westaway, D., and Prusiner, S. B. (1989) *Cell* **59,** 847-857
24. Scott, M., Groth, D., Foster, D., Torchia, M., Yang, S. L., DeArmond, S. J., and Prusiner, S. B. (1993) *Cell* **73,** 979-988
25. Grantham, R. (1974) *Science* **185,** 862-864
26. Hosszu, L. L., Jackson, G. S., Trevitt, C. R., Jones, S., Batchelor, M., Bhelt, D., Prodromidou, K., Clarke, A. R., Waltho, J. P., and Collinge, J. (2004) *J Biol chem* **279,** 28515-28521
27. Hosszu, L. L., Jackson, G. S., Trevitt, C. R., Jones, S., Batchelor, M., Bhelt, D., Prodromidou, K., Clarke, A. R., Waltho, J. P., and Collinge, J. (2004) *J Biol chem* **279,** 28515-28521
28. Jackson, G. S., Hosszu, L. L. P., Power, A., Hill, A. F., Kenney, J., Saibil, H., Craven, C. J., Waltho, J. P., Clarke, A. R., and Collinge, J. (1999) *Science* **283,** 1935-1937
29. Parker, M. J., Spencer, J., and Clarke, A. R. (1995) *J Mol Biol* **253,** 771-786
30. Baskakov, I. V., Legname, G., Baldwin, M. A., Prusiner, S. B., and Cohen, F. E. (2002) *J.Biol.Chem.* **277,** 21140-21148
31. Baskakov, I. V. (2003) *J Biol.Chem*
32. Jackson, G. S., Hosszu, L. L. P., Power, A., Hill, A. F., Kenney, J., Saibil, H., Craven, C. J., Waltho, J. P., Clarke, A. R., and Collinge, J. (1999) *Science* **283,** 1935-1937
33. Wong, B. S., Clive, C., Haswell, S. J., Jones, I. M., and Brown, D. R. (2000) *Biochemical and Biophysical Research Communications* **269,** 726-731
34. Wopfner, F., Weidenhöfer, G., Schneider, R., Von Brunn, A., Gilch, S., Schwarz, T. F., Werner, T., and Schätzl, M. (1999) *Journal of Molecular Biology* **289,** 1163-1178
35. Petchanikow, C., Saborio, G. P., Anderes, L., Frossard, M. J., Olmedo, M. I., and Soto, C. (2001) *FEBS Letters* **509,** 451-456
36. Tahiri-Alaoui, A., Gill, A. C., Disterer, P., and James, W. (2004) *J Biol.Chem*
37. Baskakov, I. V. (2003) *J Biol.Chem*

38. Petchanikow, C., Saborio, G. P., Anderes, L., Frossard, M. J., Olmedo, M. I., and Soto, C. (2001) *FEBS Letters* **509,** 451-456
39. Tahiri-Alaoui, A., Gill, A. C., Disterer, P., and James, W. (2004) *J Biol.Chem*

FOOTNOTES

This work was funded by the Medical Research Council. We are grateful to Ray Young for his assistance in preparation of figures for this manuscript.

The abbreviations used are CD, circular dichroism; CJD, Creutzfeldt-Jakob disease; GSS, Gerstmann-Sträussler-Scheinker disease; PrP, Prion Protein; PrP^{C}, cellular PrP isoform; PrP^{Sc}, pathogenic (scrapie) PrP isoform; HuPrP(129M/V), methionine/valine forms of human prion protein (residues 91-231); GuHCl, Guanidine Hydrochloride; TSE, transmissible spongiform encephalopathy; AEBSF, 8 mM 4-(2-aminoethyl)-benzene sulfonyl fluoride

FIGURE LEGENDS

Figure 1 **CD analysis of recombinant human α–PrP^{91-231}.** **(A)** Overlaid far UV spectra of M129 (blue) and V129 PrP (red), each compiled from an average of 50 scans. **(B)** Equilibrium denaturation curves of 129M (blue) and 129MV (red), as measured by amide CD absorption at 222nm. The lines superimposed upon the data are fits to the function:

$$\alpha_N = (K_{(N/U)}.\exp(m.D))/(1+K_{(N/U)}.\exp(m.D))$$

Figure 2 **Conversion efficiency of α-PrP to β-PrP.** The yield of folded soluble, monomeric protein in a beta-sheet conformation is shown for for M129 (blue) and V129 (red) polymorphs of human PrP^{91-231}. Black bars indicate the standard deviation from an average of 5 independent experiments.

Figure 3 **CD spectra of recombinant human PrP^{91-231} folded in a β-PrP confromation.** **(A)** Overlaid far UV spectra of M129 (blue) and V129 (red) PrP, compiled from an average of 50 scans. **(B)** Equilibrium denaturation curves of human β-PrP 129M (blue) and 129MV (red), as measured by amide CD absorption at 222nm. The lines superimposed upon the data are fits to the function:

$$\alpha_N = (K_{(N/U)}.\exp(m.D))/(1+K_{(N/U)}.\exp(m.D))$$

Figure 4 **Protease resistance of α and β conformational isoforms of the M and V human polymorphs.** Using identical conditions for digestion, soluble β-PrP has increased resistance to proteinase K when compared to α-PrP. The M and V polymorphs have identical levels of resistance and display similar patterns of cleavage products. The concentrations of PK indicated are the final concentrations in the digestion reactions.

Figure 5 **Amyloid fibril formation by the M and V forms of recombinant human PrP.** The formation of amyloid fibrils as determined by Thiofalvin T fluorescence is

shown as a function of time. Fibrillogenesis of M129 PrP (blue) occurs after a lag time of 35 hours, whereas V129 PrP at the same concentration (red), and twice the concentration (green) shows no evidence of fibril formation.

FIGURES

Figure 1

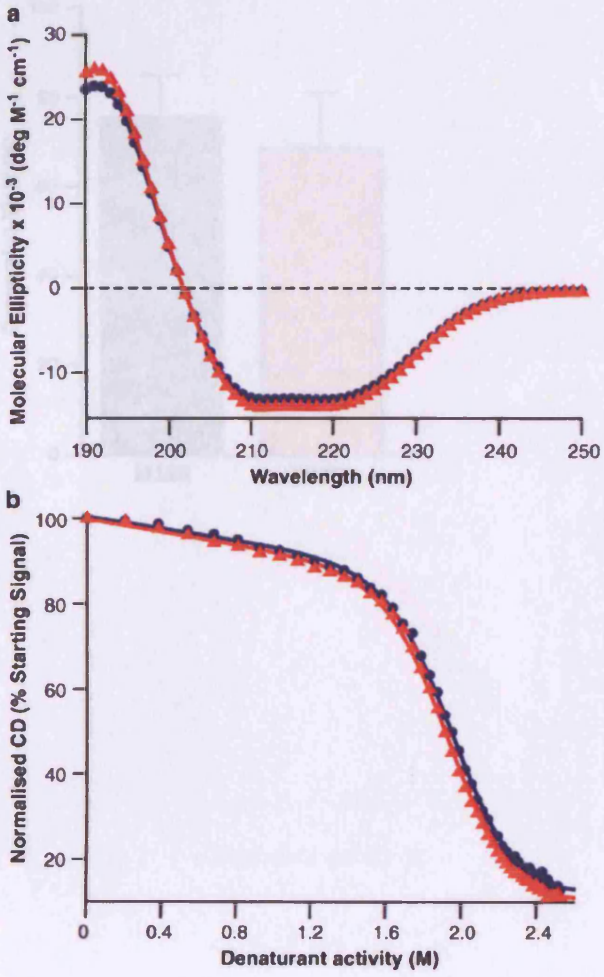

Figure 2

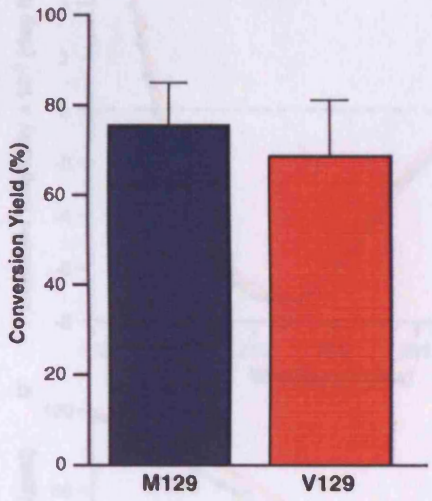

Figure 3

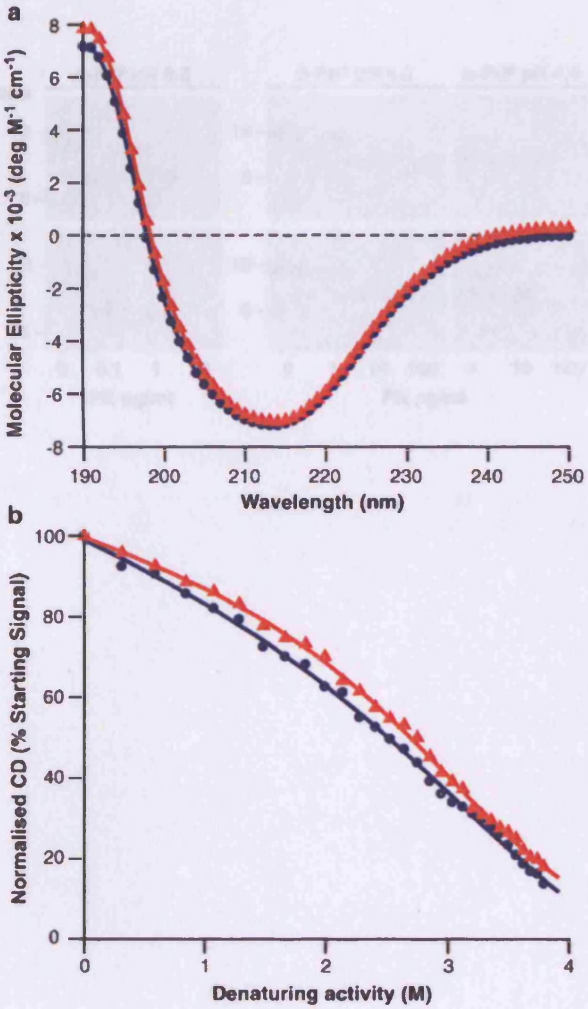
a
Molecular Ellipticity x 10-3 (deg M-1 cm-1)
8
6
4
2
0
-2
-4
-6
-8
190
200
210
220
230
240
250
Wavelength (nm)
b
Normalised CD (% Starting Signal)
100
80
60
40
20
0
0
1
2
3
4
Denaturing activity (M)

Figure 4

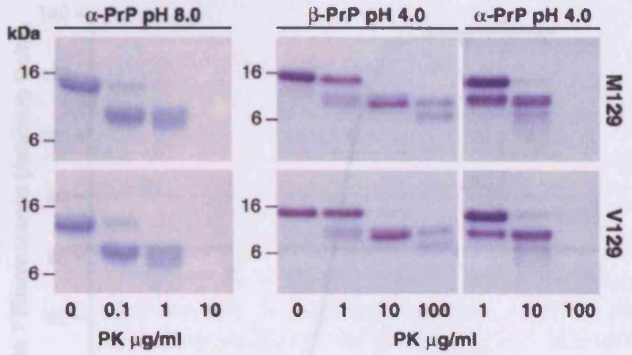
α-PrP pH 8.0
β-PrP pH 4.0
α-PrP pH 4.0
kDa
16
6
M129
V129
0 0.1 1 10
0 1 10 100 1 10 100
PK μg/ml
PK μg/ml

Figure 5

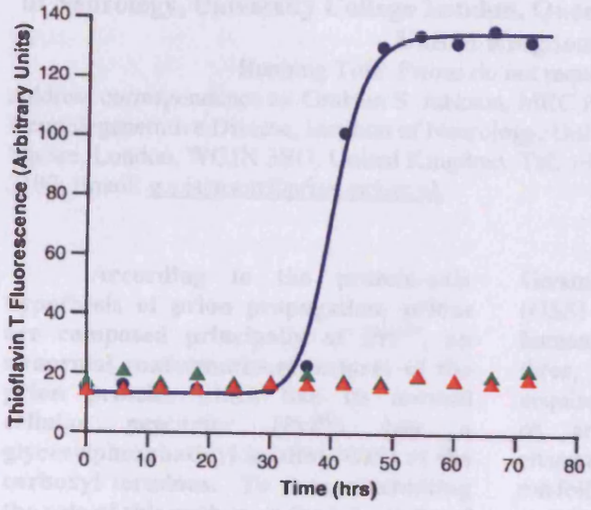
Thioflavin T Fluorescence (Arbitrary Units)
140
120
100
80
60
40
20
0
0
10
20
30
40
50
60
70
80
Time (hrs)

REMOVAL OF THE GPI ANCHOR FROM PRP^{Sc} DOES NOT REDUCE PRION INFECTIVITY

Patrick A. Lewis, Francesca Properzi, Kanella Prodromidou, Anthony R. Clarke, John Collinge, and Graham S. Jackson

From the MRC Prion Unit, Department of Neurodegenerative Disease, Institute of Neurology, University College London, Queen Square, London, WC1N 3BG, United Kingdom.

Running Title: Prions do not require a GPI anchor

Address correspondence to: Graham S. Jackson, MRC Prion Unit, Department of Neurodegenerative Disease, Institute of Neurology, University College London, . Tel: ; Fax: ; Email:

According to the protein-only hypothesis of prion propagation, prions are composed principally of PrP^{Sc}, an abnormal conformational isoform of the prion protein, which like its normal cellular precursor (PrP^{C}) has a glycosylphosphatidyl inositol (GPI) at the carboxyl terminus. To date, elucidating the role of this anchor on the infectivity of prion preparations has not been possible due to the resistance of PrP^{Sc} to the activity of phosphoinositol specific phopholipase C (PIPLC), an enzyme which removes the GPI moiety from PrP^{C}. Removal of the GPI anchor from PrP^{Sc} requires denaturation prior to treatment with PIPLC, a process that also abolishes infectivity. To circumvent this problem we have removed the GPI anchor from PrP^{Sc} in RML prion-infected murine brain homogenate using the aspartic endoprotease Cathepsin D. This enzyme eliminates a short sequence at the carboxyl terminal end of PrP to which the GPI anchor is attached. We find that this modification has no effect upon (1) an *in vitro* amplification model of PrP^{Sc}, (2) the prion titre as determined by a highly sensitive N2a-cell based bioassay, or (3) in a mouse bioassay. These data show that the GPI anchor has little or no role in either the propagation of PrP^{Sc} or on prion infectivity.

The prion diseases of humans and animals are a group of closely related, fatal neurodegenerative disorders that include scrapie in sheep, bovine spongiform encephalopathy (BSE) in cattle and Creutzfeldt Jakob disease (CJD), kuru, Gerstmann-Straüssler-Scheinker syndrome (GSS) and fatal familial insomnia (FFI) in humans (1). Prion diseases in humans have three, distinct aetiologies, being inherited, acquired by exposure to infectious material or arising sporadically. They are characterised by accumulation of a misfolded endogenous protein (the prion protein (PrP) (2)) and the protein-only hypothesis (3;4) states that the central event in the pathogenesis of these diseases is the conversion of the normal host prion protein, PrP^{c}, into an aberrantly folded infectious form denoted PrP^{Sc} (5). Although much research has been directed at unravelling the mechanism whereby this conversion occurs, very little is known about the molecular basis of PrP^{Sc} formation.

Human PrP is a 253 amino acid protein produced from a single exon located on chromosome 20 (6). Following translation, PrP is modified by the formation of an internal disulphide bond between residues 179 and 214 (7), glycosylation at asparagines residues 181 and 197, which has now been characterised (8) and, following the removal of 22 carboxyl terminal amino acids, the addition of a glycosylposphatidyl inositol (GPI) anchor to the C–terminal serine residue (9). Cellular PrP is attached to the plasma membrane via this GPI-anchor and localized, along with other GPI-anchored proteins, to cholesterol rich lipid rafts within the membrane (10). The GPI anchor attached to PrP^{C} can be cleaved by treatment of the protein with phosphoinositide specific phospholipase C (PIPLC), resulting in the release of the protein from the cell surface of intact cells (11). This also results in an apparent

increase in the molecular mass of PrP, as analyzed by SDS-PAGE, due to the extremely hydrophobic nature of the lost anchor (12;13). It has been shown in cell-culture models that location of PrP^{C} at the cell membrane is crucial for both infection of cells with PrP^{Sc} and for the continued propagation of the scrapie isoform. Treatment of cell cultures with PIPLC prior to addition of infectious homogenates has a protective effect and treatment following establishment of infection cures the cells (14). Analysis of the impact of GPI loss on the infectivity of PrP^{Sc} has, to date, not been possible due to the resistance of the scrapie isoform to the enzymatic activity of PIPLC, thought to be due to steric exclusion of the enzyme by the altered conformation of PrP (15). It has also been shown that mutations found in inherited prion disease, when introduced into PrP expressed in cultured cell lines, increase the resistance to cleavage with PIPLC (12). Removal of the GPI anchor from PrP^{Sc} requires denaturation prior to treatment with PIPLC, a process that also abolishes infectivity; it has thus been impossible to ascertain whether the GPI anchor is an essential component of prion infectivity. Answering this question has several consequences regarding our understanding of prion diseases. From a mechanistic point of view, the impact of GPI removal on the ability of PrP^{Sc} to infect cells may shed light both on the site of the conversion event and on the route that the scrapie isoform takes into the cell. Also, should the absence of a GPI anchor decrease the infectivity of PrP^{Sc}, this has implications for attempts to generate infectious prions *in vitro* from recombinant material, since the majority of recombinant prion protein is generated from bacterial sources and lacks a GPI anchor.

In this study, we describe the removal of the GPI anchor from PrP^{Sc} in RML-infected murine brain homogenate using the aspartic endoprotease Cathepsin D. This enzyme eliminates a short sequence at the carboxyl terminal end of PrP to which the GPI anchor is attached. We have used this phenomenon as a tool to probe the impact of removal of the GPI anchor upon an *in vitro* amplification model of PrP^{Sc} (16), and have assayed prion infectivity using both a highly sensitive N2a-cell based bioassay, the scrapie cell assay (17) and a mouse bioassay (18). We find that, in these systems, removal of the GPI anchor has no impact on either amplification of protease-resistant PrP or prion infectivity.

EXPERIMENTAL PROCEDURES

Source of homogenates

Whole mouse brains from normal and RML-infected CD-1 mice were homogenised as a 10% w/v preparation in Dulbecco's phosphate-buffered saline (PBS) without calcium and magnesium ions using a Dounce homogeniser. Homogenates were then split into aliquots and stored at -80°C.

Protease Treatment

Cathepsin D digests were carried out using Cathepsin D purified from bovine spleen (Merck), freshly made up in 1x PBS. Standard digest conditions were as follows: 10% infectious brain homogenates were thawed and centrifuged at 100g for 1 minute. 10µl aliquots of 10% homogenate supernatant were then digested with 100 units of Cathepsin D for 4 hours at 37°C with shaking at 450 rpm. Following this, samples were digested with Proteinase K (Sigma) at a final concentration of 50µg/ml for 1 hour at 37°C. Digests were terminated by the addition of 2x SDS sample buffer buffer [125 mM Tris.HCl (pH 6.8), 20% v/v glycerol, 4% w/v sodium dodecyl sulphate, 4% v/v 2-mercaptoethanol, 0.02% (w/v) bromophenol blue] containing 8 mM 4-(2-aminoethyl)-benzene sulfonyl fluoride (AEBSF; Pefabloc SC, Roche, Lewes, UK). In the case of Cathepsin D digests carried out in the presence of ethylenediaminetetraacetic acid (EDTA), 20mM EDTA (Sigma) was added to the reaction mixture and RML control samples.

Western Blot Analyses

Following the addition of 20µl of 2 x SDS-loading buffer, samples were heated to 100°C for 10mins and then subjected to centrifugation in a microfuge (15,000 g) for 1 minute. 20µl of each supernatant was applied to a 16% Tris-glycine gel (Novex; Life Technologies, Paisley, UK) according to the manufacturer's instructions. Gels were electroblotted onto PVDF membrane (Immobilon-P; Millipore, Watford, UK) and subsequently blocked in PBS containing

0.05% (v/v) Tween-20 (PBST) and 5% (w/v) non-fat milk powder for 60 min. After washing in PBST, the membranes were incubated with anti-PrP monoclonal antibody ICSM35 (D-Gen Ltd, UK) diluted to 0.2μg/ml in PBST for at least 60 min before washing in PBST (30 min) and incubation with an alkaline phosphatase-conjugated goat anti-mouse antibody (Sigma, Dorset, UK) diluted 1:10,000 in PBST for 60 min. Following washing in PBST (30 min), the membranes were developed using AttoPhos reagent (Promega Corp., USA) and visualized on a Molecular Dynamics Storm 840 (Amersham, UK).

Cell Culture

The murine neuroblastoma cell line, N2a, was used throughout. Cells were cultured in OPTI-MEM with 10% fetal calf serum (OFCS) and 100U/ml of both penicillin and streptomycin (Invitrogen Corp.). PIPLC treatment of cells was carried out by removal of growth media from confluent cells in a 10cm dish and addition of PBS containing either 200mUnits PIPLC (Sigma) or 100Units Cathepsin D. Cells were incubated for 3hrs and the culture supernatant harvested. 300μl of culture supernatant was mixed with 4 volumes of ice-cold methanol and centrifuged for 30 minutes at 25,000g and 4°C. The precipitated protein was then re-suspended in 20 μl of PBS and analysed by western blot as described above.

In vitro Amplification

Analysis of *in vitro* amplification of PrP^{Sc} was carried out using a modification of the protocol from Lucassen *et al* (16). 10% w/v brain homogenates were produced in PBS from RML infected CD-1, wild type CD-1 and PrP knock-out (FVB/N $Prnp^{0/0}$) mouse brains. RML homogenates were produced in the presence of 1% Triton X-100 (Sigma), with the wild type and PrP null homogenates containing 1x Complete protease inhibitors (Roche). 20μl of RML homogenate was digested with 200Units of Cathepsin D for 2 hours and then, in parallel with undigested RML control, diluted 1 in 25 into 1x PBS with 1% Triton X-100. These were then diluted 1:1 with CD-1 wild type or PrP null brain homogenate and incubated for 16 hours at 37°C with shaking at 450 rpm. Following incubation, homogenates were digested with PK at a final concentration of 50μg/ml for 1 hour at 37°C and analysed by western blotting. Each condition was repeated in triplicate.

Scrapie Cell Assay

High sensitivity cell culture assays for prion infectivity were carried out as described by Klöhn *et al* (17). Briefly, PK1 cells, a highly scrapie susceptible N2a sub clone, were exposed for three days in 96 well plates to serial dilutions (10^{-4}, 10^{-5}, 10^{-6} and 10^{-7}) of infectious RML homogenate either treated with Cathepsin D or untreated as a control. The cells were then grown to 80% confluence and split twice before finally being grown to confluence and re-suspended in OFCS. 25,000 cells per well were transferred to an enzyme-linked immunospot plate (ELISPOT, Millipore). The cells were then treated for one hour with 0.5μg/ml Proteinase K in lysis buffer (50mM Tris.HCl, 150mM NaCl, 0.5% Deoxycholate, 0.5% Triton X-100. pH 8.0), washed and denatured by treatment with 3M guanidine isothiocyanate (Sigma). Wells were then washed and blocked prior to probing with ICSM18 (D-Gen Ltd., UK), washing with TBST and probing with alkaline phophatase conjugated anti-IgG1. Scrapie positive cells were identified after treatment with alkaline phosphatase conjugate substrate (Bio-rad) using the Zeiss KS ELISPOT system (Carl Zeiss, Welwyn Garden City UK).

Mouse Bio-assay of Cathepsin D Treated PrP^{sc}

Cathepsin D treated RML was bio-assayed using Tg20 transgenic mice, which over-express the murine *Prn-p* gene (18). 10% RML was treated with 20u/μl Cathepsin D for 2hrs at 37°C or mixed with PBS and then diluted with PBS to 0.1% final concentration. RML, Cathepsin D treated RML, PBS and Cathepsin D-only controls were then inoculated intra-cerebrally into anaesthetised Tg20 mice (18). Animal care adhered to institutional guidelines and mice were examined daily for clinical signs of prion disease. Brain samples were taken from all groups following death, analysed by western blot for the presence of PrP^{Sc} and for neuropathological evidence of prion disease.

RESULTS

Cathepsin D digest of PrP^{Sc} strains

Treatment of 10% brain homogenate from RML infected mice with Cathepsin D resulted in the proteinase K resistant PrP in these homogenates running at an apparently higher molecular mass than those in control homogenates as analysed by SDS PAGE (Figure 1A). While proteolytic digestion should decrease relative molecular mass (RMM) due to the loss of polypeptide material, it has been shown previously that apparent increases in RMM occur upon removal of GPI anchors by the enzyme PIPLC. This effect is caused by the disproportionate amount of SDS that associates with the acyl chains of the GPI anchor on treatment compared with the polypeptide component (12;13). Hence, removal of the anchor results in a significant loss of SDS-associated charge and a slower migration in the electric field. Given this observation, the only plausible explanation for result derived from cathepsin D treatment is that the enzyme cleaves the chain close to the carboxy-terminus, so removing only a small mass of polypeptide along with the anchor.

To discover if this was a prion strain-specific phenomenon, PrP^{Sc} in brain homogenates isolated from hamster (strain 263K) and human (molecular strain types 1, 2 and 4 (19;20)) were subjected to proteolysis by cathepsin D. All exhibited the same apparent increase in molecular mass (Figure 1A). Using murine RML prions as a model system, the concentration and time-dependence of this affect was examined (Figure 1B and 1C), with the apparent RMM increase showing dependence upon both digestion time and concentration of Cathepsin D.

Cathepsin D mediated release of PrP from intact cell membranes

If treatment with Cathepsin D removes the GPI anchor, it would be expected that treatment of intact cells in culture with the enzyme would result in release of membrane anchored PrP^{C} into the cell media. To examine this, wild type N2a cells were treated with either Cathepsin D or PIPLC, with the incubation media analysed for the presence of released PrP^{C}. Under these conditions, treatment with either Cathepsin D or PIPLC resulted in the release of PrP^{C}, as measured by an increase in the PrP^{C} collected from the media (Figure 2).

Change in strain profile is independent of metal ion binding

An alternative explanation for this alteration in electrophoretic properties following digestion with cathepsin D is that there is a change in conformation of the PrP^{Sc} dependent upon the inadvertent introduction of metal ions during the experimental process (21). To eliminate this possibility, cathepsin D digests were carried out in the presence or absence of the metal chelating agent EDTA and the affect of increasing concentrations of Cu^{2+} upon the strain profile of RML were investigated (Figure 3A). The presence of EDTA did not affect the retardation of PrP in SDS gel electrophoresis following Cathepsin D digestion, not did the addition of copper to RML result in any prion strain-specific alteration in electrophoretic mobility (Figure 3B).

Loss of GPI anchor has no effect on in vitro amplification of PrP^{Sc}

To investigate the impact that GPI anchor loss has on the ability of PrP^{Sc} to replicate, cathepsin D treated RML was examined for its ability to seed amplification in an *in vitro* PrP^{Sc} replication model. Using the technique of Lucassen *et al* (16), cathepsin D-digested RML exhibited no significant difference in its ability to produce an amplified signal as compared to untreated RML (Figure 4).

Loss of GPI anchor has no effect on prion infectivity measured by Scrapie Cell Assay

To determine whether the loss of its GPI anchor alters prion infectivity, cathepsin D-treated RML prions were assayed for infectivity using a cell-culture assay based upon a highly susceptible line of N2a cells, the scrapie cell assay. Using a range of dilutions, cathepsin D-treated RML prion-infected brain homogenate was compared to untreated RML homgenate, along with cathepsin D-only controls and CD-1 homogenate digested with cathepsin D (no cellular toxicity was observed with control treatments, data not shown). As RML alone exhibits a slight decrease in infectious titre upon incubation at 37°C, Cathepsin D treated homogenates were compared with either RML added to the assay immediately

following thawing or incubated in parallel with the cathepsin D digest. There was no significant reduction in prion titre following RML digest of Cathepsin D (Figure 5).

Loss of GPI anchor has no effect on prion infectivity measured using mouse bioassay

Cathepsin D-treated RML was then compared with untreated RML by bioassay in Tg20 transgenic mice, which over-express mouse PrP^C (18). Mice were inoculated with untreated RML, cathepsin D-treated RML, PBS control, or with cathepsin D alone. Mice inoculated with cathepsin D-treated RML and with untreated RML developed clinical scrapie after 9 weeks, with no significant difference between the incubation periods (Figure 6A) Homogenates from both groups were examined for protease-resistant PrP, and were positive in both cases (Figure 6B). Mice were also examined for neuropathological hallmarks of scrapie infection and both groups showed classical signs of prion disease.

DISCUSSION

Despite decades of research, the precise molecular mechanism of both pathological injury and the nature of the infectious agent in the prion disorders remains elusive. One of the areas of prion disease biology that is not clearly understood is the role of the post-translational modifications of PrP. The presence of altered glycoform ratios in different prion strains suggests that glycosylation may play a role in the propagation of strain properties (19;22), and studies using PIPLC to remove the GPI anchor from PrP in infected cells indicate that perhaps this also plays a role in cell-to-cell propagation of infection (23).

In this study, Cathepsin D has been used to remove a short carboxyl terminal sequence from infectivity-associated PrP^{Sc}. In doing so, three major technical difficulties prevented the precise characterisation of the nature and location of the cleavage event. Firstly, PrP^{Sc} is difficult to purify without denaturation, secondly, its hydrophobicity prevents direct sequencing of the cleavage products (20), thirdly, Cathepsin D has a poorly defined cleavage consensus sequence (characterised only as a preference to cleave between two hydrophobic residues) (24;25). However, the evidence of retarded migration of PrP in SDS gel electrophoresis and the release of PrP from the cell membrane following digestion with Cathepsin D indicate that Cathepsin D removes a segment of the C terminus of the protein and, with those amino acids, the GPI anchor. This provided an alternate approach to the use of PIPLC treatment, and therefore denaturing conditions, as a means of evaluating the role of the GPI in the infective process.

It should be noted that the concentrations of Cathepsin D used to digest PrP^{Sc} were greatly in excess of physiologically relevant levels. It is intriguing, however, that Cathepsin D has been implicated in the proteolytic processing of amyloid β, alpha synuclein and Tau (26-28). Cathepsin D is also upregulated both in mouse models of scrapie (29;30) and in the brains of Alzheimer's disease patients (although this may reflect a general upregulation of lysosomal degradation in these disorders rather than a substrate-specific effect) (31). A polymorphism in the human Cathepsin D gene has also been identified as a risk factor for late onset Alzheimer's disease, providing a potential link with other neurodegenerative protein folding diseases (32).

The impact of the removal of the GPI from infective PrP^{Sc} was studied in three systems: a model *in vitro* amplification system, the *ex vivo* scrapie cell prion assay and mouse bioassay. No significant effect was observed with any of these techniques. The relationship of the first system to the *in vivo* situation remains a subject of debate. Several systems for the *in vitro* amplification of PrP^{Sc}, have been reported to generate an amplification of signal but no categorical proof of a concomitant increase in infectivity has been produced and so these systems may reflect an increase in protease resistant PrP rather than amplification of infectivity (33-36). However, data from the *in vivo* assay of cathepsin D-treated RML agrees with that from both the *in vitro* amplification and from the highly sensitive cell-culture analysis.

The evidence presented from these three systems demonstrates that the removal of the GPI from PrP^{Sc} does not affect the

infective properties of the scrapie agent. This is particularly well demonstrated by the scrapie cell assay which is capable of detecting just a two-fold change in infective titre. This finding has two major implications. Firstly, since endogenous proteolytic release of PrP^C has been reported (37), this may provide a mechanism whereby infectious PrP^{Sc} could spread from cell to cell and throughout the body of an infected host. Secondly, the fact that prion infectivity does not require a GPI anchor means that this is not a factor preventing the production of *de novo* prion infectivity using recombinant protein from bacterial sources. This is in agreement with the recent demonstration by Legname et al. (38) that PrP generated in E. coli cells by recombinant expression is capable of inducing prion disease in transgenic mice with high levels of overexpression of a truncated PrP.

REFERENCES

1. Collinge, J. (2001) *Annu.Rev Neurosci.* **24,** 519-550
2. Jackson, G. S. and Collinge, J. (2001) *J.Clin.Pathol.Mol.Pathol.* **54,** 393-399
3. Griffith, J. S. (1967) *Nature* **215,** 1043-1044
4. Prusiner, S. B. (1982) *Science* **216,** 136-144
5. Prusiner, S. B. (1998) *Proc Natl Acad Sci U.S.A.* **95,** 13363-13383
6. Liao, Y. C., Lebo, R. V., Clawson, G. A., and Smuckler, E. A. (1986) *Science* **233,** 364-367
7. Stahl, N. and Prusiner, S. B. (1991) *FASEB J.* **5,** 2799-2807
8. Rudd, P. M., Wormald, M. R., Wing, D. R., Prusiner, S. B., and Dwek, R. A. (2001) *Biochemistry* **40,** 3759-3766
9. Stahl, N., Borchelt, D. R., Hsiao, K., and Prusiner, S. B. (1987) *Cell* **51,** 229-240
10. Vey, M., Pilkuhn, S., Wille, H., Nixon, R., DeArmond, S. J., Smart, E. J., Anderson, R. G. W., Taraboulos, A., and Prusiner, S. B. (1996) *Proc.Natl.Acad.Sci.USA* **93,** 14945-14949
11. Caughey, B. and Raymond, G. J. (1991) *J Biol.Chem.* **266 No 27,** 18217-18223
12. Narwa, R. and Harris, D. A. (1999) *Biochemistry* **38,** 8770-8777
13. Englund, P. T. (1993) *Annu.Rev.Biochem.* **62,** 121-138
14. Enari, M., Flechsig, E., and Weissmann, C. (2001) *Proc.Natl.Acad.Sci.USA* **98,** 9295-9299
15. Stahl, N., Borchelt, D. R., and Prusiner, S. B. (1990) *Biochemistry* **29,** 5405-5412
16. Lucassen, R., Nishina, K., and Supattapone, S. (2003) *Biochemistry* **42,** 4127-4135
17. Klohn, P. C., Stoltze, L., Flechsig, E., Enari, M., and Weissmann, C. (2003) *Proc.Natl.Acad.Sci U.S.A*
18. Fischer, M., Rulicke, T., Raeber, A., Sailer, A., Moser, M., Oesch, B., Brandner, S., Aguzzi, A., and Weissmann, C. (1996) *EMBO J.* **15,** 1255-1264
19. Collinge, J., Sidle, K. C. L., Meads, J., Ironside, J., and Hill, A. F. (1996) *Nature* **383,** 685-690
20. Hill, A. F., Joiner, S., Wadsworth, J. D., Sidle, K. C., Bell, J. E., Budka, H., Ironside, J. W., and Collinge, J. (2003) *Brain* **126,** 1333-1346
21. Wadsworth, J. D. F., Hill, A. F., Joiner, S., Jackson, G. S., Clarke, A. R., and Collinge, J. (1999) *Nature Cell Biology* **1,** 55-59
22. Hill, A. F., Desbruslais, M., Joiner, S., Sidle, K. C. L., Gowland, I., and Collinge, J. (1997) *Nature* **389,** 448-450
23. Liu, T., Li, R., Pan, T., Liu, D., Petersen, R. B., Wong, B. S., Gambetti, P., and Sy, M. S. (2002) *J.Biol.Chem.*
24. Offermann, M. K., Chlebowski, J. F., and Bond, J. S. (1983) *Biochem.J* **211,** 529-534
25. van Noort, J. M. and van der Drift, A. C. (1989) *J Biol chem* **264,** 14159-14164
26. Higaki, J., Catalano, R., Guzzetta, A. W., Quon, D., Nave, J. F., Tarnus, C., D'Orchymont, H., and Cordell, B. (1996) *J Biol chem* **271,** 31885-31893
27. Hossain, S., Alim, A., Takeda, K., Kaji, H., Shinoda, T., and Ueda, K. (2001) *J Alzheimers.Dis.* **3,** 577-584
28. Kenessey, A., Nacharaju, P., Ko, L. W., and Yen, S. H. (1997) *J Neurochem.* **69,** 2026-2038

29. Brown, A. R., Webb, J., Rebus, S., Williams, A., and Fazakerley, J. K. (2004) *Neuropathol.Appl.Neurobiol.* **30,** 555-567
30. Diedrich, J. F., Minnigan, H., Carp, R. I., Whitaker, J. N., Race, R., Frey, W., and Haase, A. T. (1991) *J Virol* **65,** 4759-4768
31. Cataldo, A. M., Barnett, J. L., Berman, S. A., Li, J., Quarless, S., Bursztajn, S., Lippa, C., and Nixon, R. A. (1995) *Neuron* **14,** 671-680
32. Crawford, F. C., Freeman, M. J., Schinka, J., Abdullah, L. I., Richards, D., Sevush, S., Duara, R., and Mullan, M. J. (2000) *Neurosci.Lett.* **289,** 61-65
33. Kocisko, D. A., Come, J. H., Priola, S. A., Chesebro, B., Raymond, G. J., Lansbury, P. T., and Caughey, B. (1994) *Nature* **370,** 471-474
34. Saborio, G. P., Permanne, B., and Soto, C. (2001) *Nature* **411,** 810-813
35. Lucassen, P. J., Williams, A., Chung, W. C. J., and Fraser, H. (1995) *Neurosci.Lett.* **198,** 185-188
36. Hill, A., Antoniou, M., and Collinge, J. (1999) *J.Gen.Virol.* **80,** 11-14
37. Parkin, E. T., Watt, N. T., Turner, A. J., and Hooper, N. M. (2004) *J Biol.Chem*
38. Legname, G., Baskakov, I. V., Nguyen, H. O., Riesner, D., Cohen, F. E., DeArmond, S. J., and Prusiner, S. B. (2004) *Science* **305,** 673-676

FOOTNOTES

This work was funded by the Medical Research Council. We are grateful to Ray Young for his assistance in preparation of figures for this manuscript.

The abbreviations used are: CJD, Creutzfeldt-Jakob disease; GSS, Gerstmann-Sträussler-Scheinker disease; EDTA, Ethylene Diamine Tetra acetic Acid; FFI, fatal familial insomnia; PrP, Prion Protein; PrP^{C}, cellular PrP isoform; PrP^{Sc}, pathogenic (scrapie) PrP isoform; SDS-PAGE, Sodium Dodecyl Sulphate Polyacrylamide Gel Electrophoresis; RMM, Relative molecular mass; GPI, Glycosylphosphatidyl Inositol; Cat D, Cathepsin D; RML, Rocky Mountain Laboratory; ECF, Enhanced ChemiFluorescence; AEBSF, 4-(2-aminoethyl)-benzene sulfonyl fluoride.

FIGURE LEGENDS

Figure 1 Cathepsin D digestion of mouse RML, hamster 263K and human types 1, 2, 3 and 4 PrP^{Sc} visualised by western blot (A). Samples were digested with 20U cathepsin D per µl of 10% w/v brain homogenate and exhibit retarded migration in SDS PAGE as compared to untreated controls, indicative of C-terminal truncation and loss of GPI. Concentration (B) and time (C) dependence of gel retardation following digestion with cathepsin D are also shown, exemplifying the enzymatic nature of the cleavage.

Figure 2 Release of PrP from the cell membrane of wild type N2a cells by PIPLC (A) and cathepsin D (B). Cells were treated with the indicated concentration of enzyme for three hours, with the supernatant collected and analysed by western blotting. The presence of PrP^{C} in the supernatant, recognised by ICSM 35, signifies release of the protein from the cell membrane upon either GPI cleavage (PIPLC) or C-terminal truncation (cathepsin D)

Figure 3 Impact of EDTA on cathepsin D digestion of RML (A) and of increasing Cu^{2+} on RML strain profile (B). The presence of the metal chelator EDTA has no effect on cathepsin D digest of RML, nor does the presence of Cu^{2+} alter the apparent RMM of RML, indicating that the gel retardation following cathepsin D treatment is not metal ion dependent.

Figure 4 *In vitro* amplification of cathepsin D treated and normal RML. Treated or untreated RML infected brain homogenate diluted into wild type CD-1 brain homogenate both exhibited amplification of protease resistant signal (compared to RML diluted into $PrP^{0/0}$ brain homogenate) as quantified by band intensity following western blot analysis. Data shown is the mean of 3 separate reactions with

standard deviations indicated. No significant difference was observed between treated and untreated samples

Figure 5 Scrapie cell assay analysis of RML infectivity. RML was incubated for 4 hours at 37°C and RML digested with cathepsin D for 4 hours at 37°C. A range of dilutions of RML brain homogenates from 10^{-4} to 10^{-7} were used to allow estimation of any impact of cathepsin D digestion on the infectivity of RML, with no significant difference between digested and undigested samples. Data shown is the mean number of cells that contain detectable PrP^{RES} per 25,000 viable cells from 3 independent experiments with standard deviations as indicated.

Figure 6 *In vivo* analysis of the infectivity of cathepsin D treated RML (A) and the presence of protease resistant material in the brains of mice inoculated with both RML and cathepsin D treated RML (B). TG20 transgenic mice were inoculated intra cerebrally with 0.1% w/v RML brain homogenate and monitored for clinical signs of prion disease. Groups of mice inoculated with either cathepsin D treated RML or native RML exhibited similar incubation times shown in days post-inoculation. The presence of protease resistant material in the brains of both experimental groups was confirmed by western blotting. Control groups (PBS and cathpepsin D alone) showed no evidence of prion disease.

Figure 1

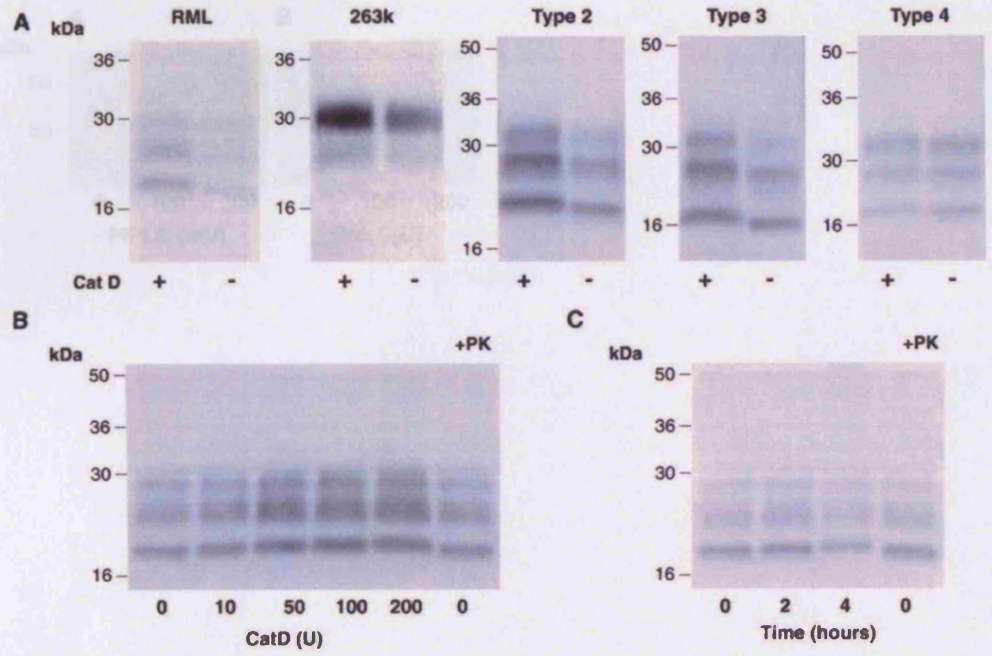
A
kDa
RML
263k
Type 2
Type 3
Type 4
36
30
16
50
Cat D
+
-
B
kDa
+PK
50
36
30
16
0
10
50
100
200
0
CatD (U)
C
kDa
+PK
50
36
30
16
0
2
4
0
Time (hours)

Figure 2

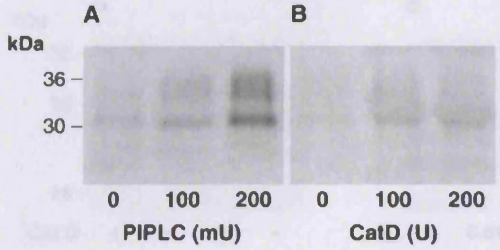

Figure 3

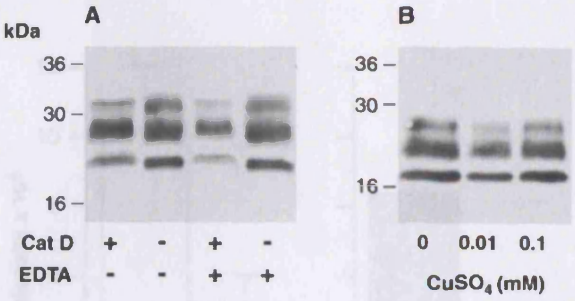

Figure 4

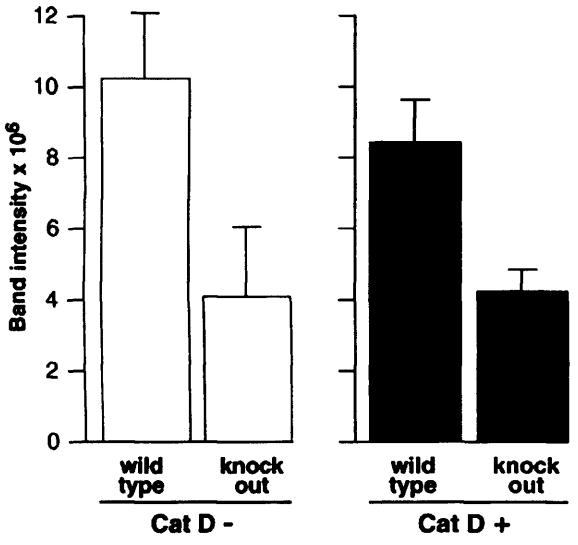
12
10
8
6
4
2
0
Band intensity x 10⁶
wild type
knock out
Cat D -
wild type
knock out
Cat D +

Figure 5

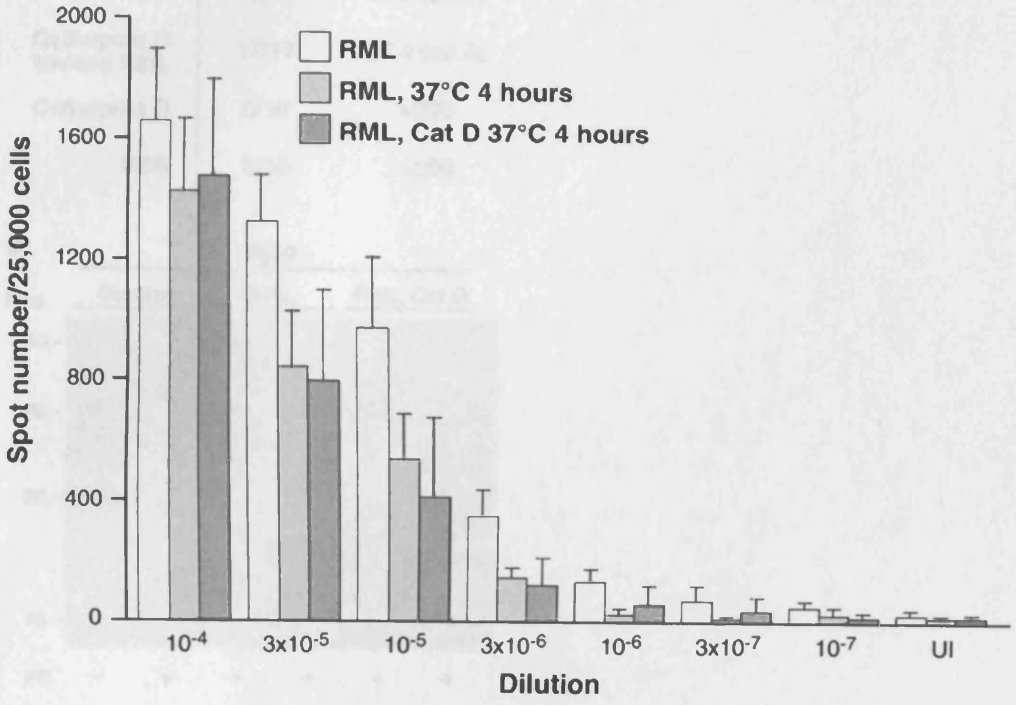
2000
1600
1200
800
400
0
Spot number/25,000 cells
RML
RML, 37°C 4 hours
RML, Cat D 37°C 4 hours
10-4
3x10-5
10-5
3x10-6
10-6
3x10-7
10-7
UI
Dilution

Figure 6

A

Treatment	Clinically affected	Average incubation (SE)
RML	17/17	67.5 (±2.2)
Cathepsin D treated RML	17/17	67.4 (±2.5)
Cathepsin D	0/10	>200
PBS	0/10	>200

B